UNIVERSITY OF
LIVERPOOL

Assessing the response of deep-marine macrofauna to the early Palaeogene hyperthermal events: An integrated ichnological, geochemical and stratigraphical approach in the Basque Basin, northern Spain

Thesis submitted in accordance with the requirements of the University of Liverpool for degree of Doctor in Philosophy by

John Paul Cummings

September 2011

ABSTRACT

To understand the response of bathyal macrofauna to long-term climate change requires a multi-disciplinary approach (ichnology, sedimentology, stratigraphy, geochemistry), and an extensive integrated dataset. The deep-marine Basque Basin in northern Spain preserves a wide range of submarine fan-related environments of deposition in well exposed and easily accessible Cretaceous and Palaeogene outcrops. These outcrops contain exceptionally preserved deep-marine trace fossil assemblages, including the Zumaia section, one of the most expanded/continuous sections of early Palaeogene deposits in the world.

In a detailed investigation to understand the control exerted by the environment of deposition on trace fossil assemblages in submarine fan related environments, an increase in ichnodiversity and an increase in the ratio of pre- versus post-depositional forms occurs from lobe complex axis to lobe complex off-axis and fringe positions. In channel-related environments, diverse pre-depositional dominated assemblages are prevalent in marginal and overbank settings. These are replaced by low diversity post-depositional dominated assemblages in more axial positions within the system. Diverse pre- and post-depositional assemblages are common in fan fringe deposits, with less diverse assemblages dominated by post-depositional ichnotaxa in basin floor deposits. The use of sub-ichnofacies is shown to have limited use in high resolution environmental interpretation in submarine fan related environments of deposition, but is still of value as an informal way of categorising a general position within the submarine fan system (e.g. proximal *versus* distal). Instead, it is proposed that ethology and colonisation styles are the most powerful tool in complementing sedimentary facies and element geometry in the interpretation of depositional environments.

The deep-water submarine fan deposits also span several major environmental perturbations associated with ancient episodes of climate change, namely the Danian-Selandian (D/S) transition, the mid-Palaeocene biotic event (MPBE), the Palaeocene Eocene Thermal Maximum and the early Eocene Climatic Optimum (EECO). This permits investigation into ichnological changes across major environmental perturbations. Low diversity, deep-tier fodinichnial dominated assemblages prevail throughout the Palaeocene, with the D/S transition and the MPBE having little impact on ichnodiversity and preserved ethologies. The extinction event that affected benthic microfauna at the PETM is found to have also affected macrofauna communities recorded in the ichnological record. Following the PETM, a gradual return to a tiered trace fossil community occurs but ichnodiversity remains relatively low. A vast increase in ichnodiversity, largely driven by diversification of the graphoglyptids is coincident with sedimentation in the basin becoming dominantly siliciclastic well into the early Eocene. Occurrences of *Ophiomorpha* (a crustacean trace) and *Scolicia* (an echinoid trace) also increase dramatically at this time.

Analysis of clay minerals (utilising XRD) across the PETM, which represents a global highstand, and from EECO sediments, reveals several spikes of kaolinite. This is a phenomena recorded across the Atlantic, and is interpreted to represent the global increase in delivery of terrigenous material into the ocean over a prolonged period. Delivery of this material is associated with degradation of a mature regolith during elevated PETM and EECO temperatures. The incipient Pyrenean orogeny enhanced delivery of siliciclastic material into the basin. Benthic macrofauna were able to gradually adjust to fundamental changes in sediment delivery to the deep basin, and eventually were able to exploit this increase in terrigenous material. Several examples of *Ophiomorpha* group trace fossils are

discussed in detail, including agrichnial forms, which are interpreted to represent an ethological response to climatically-driven changes in sediment supply.

ACKNOWLEDGEMENTS

I made a very strange decision four years ago to give up financial stability and a good job to go and look at squiggles in rocks (they told me it was called 'ichnology'). Little did I know that it would become such a big (dominant?) part of my life! Now is the time to thank the people who helped steer me along the way during the last four years. Firstly, I must thank my beautiful wife Nichola for inspiring me to never accept my 'lot' in life and to always try to aspire to achieve better things. And for also providing me with the most perfect, wonderful daughter who is the only motivation anybody could ever need to get through the difficult times. Clara, Daddy is very sorry for being a rubbish dad these last few months but we will definitely make up for it now the nasty PhD is (nearly) gone! Both my mum and mother in law deserve special thanks for child care duties along the way with particular thanks going to Aileen and her recent Saturday job as childminder! Also to my mam for providing financial assistance that a grown man should no longer rely on! And thanks to my dad for inspiring a curiosity in the natural world from a very young age. Also, special thanks to my sister Jackie, whose childcare provision over the last 2-3 years went way beyond what anybody could expect from a sister.

From an academic perspective, the biggest thanks must go to Hodgson for his tireless enthusiasm, thought provoking discussions, tolerance of my naive geological skills at the start of the PhD and for always encouraging moderation when it comes to anything alcohol related. Charlotte Jeffery-Abt and Richard Worden are also thanked for their increasing contributions towards the end of this research. James Utley proved invaluable in not only providing XRD advice, guidance and access to his instrument (ahem...) but also in thought provoking discussions concerning all things clay. Paddy and Gemma's tea making fuelled many a productive day (but many more unproductive days...particularly when the drinks were prepared at Casa!). The Welsh one (Jerrett) must also be acknowledged for letting some of his tireless (annoying) enthusiasm for rocks rub off on me. Other members of the STRAT group are also acknowledged for their company and geological discussions over the past few years.

The main source of funding for this PhD project was the UK Natural Environment Research Council (NERC) who are gratefully acknowledged. Further financial assistance was provided by the Steve Farrell Memorial Fund (BSRG) and the IAS postgrad scheme.

Special thanks go to Amendine Prelat and Emma Morris for not only providing logistical/logging support during field seasons but also for thought provoking ideas on deep-water sedimentology. Also for impromptu, expensive Jack Daniels sessions! And Jimmy Santangeli for SGR assistance and keeping me company for 5 hours on a cliff top after narrowly escaping death...

I must thank everybody at Ichron. Firstly, Andy Taylor and Stuart Gowland for being daft enough to give me a job (sorry for being approximately a year late finishing the PhD!) and also for being incredibly patient during the longest finishing stages of a PhD. Also, I sincerely thank Ichron for allowing me to pursue ichnology as a profession. John Cater is thanked for being the world's biggest ichno cynic, making talking about trace fossils at him for hours on end, endless fun (and also for teaching me a bit about deep water sed and logging core along the way). In the last few days of this project, Vicky Howard and Chris Shaw have not only provided drafting assistance but also remained patient with my increasingly stupid requests! As has Rob Raine.

Finally, I must thank the tireless efforts of the brewers at Leuven, Belgium. Often, their work goes un-praised. However, particularly during the last few months, they have provided me with endless support during the really trying times and without them, I would have struggled even more than I did! I need to submit this thing in 12 hours time so sorry to anybody that I have forgotten!

"How many years can a mountain exist before it is washed to the sea? How many years can some people exist before they're allowed to be free...the answer my friend, is blowing in the wind, the answer is blowing in the wind". Bob Dylan, 1963

"True knowledge lies in knowing that we know nothing. That's us dude!" Bill S. Preston esquire and Ted Theodore Logan (via Socrates), 1989

TABLE OF CONTENTS

		Page
Abstract		**ii**
Acknowledgements		**iv**
Chapter 1		
INTRODUCTION		
1.1	**Background**	**1**
1.2	**Thesis aims and key research questions**	**3**
1.3	**Thesis layout**	**8**
1.3.1	Thesis chapters	8
Chapter 2		
A SCIENTIFIC OVERVIEW OF THE PETM AND SOME GENERAL ICHNOLOGICAL PRINCIPLES		
2.1	**The Palaeocene Eocene Thermal maximum**	**12**
2.1.1	Introduction	12
2.1.2	Geochemical and climatic effects	13
2.1.3	Trigger mechanisms	17
2.1.4	Biotic response to the PETM	17
2.1.5	Duration and recovery of climate system back to a 'normal' state	18
2.1.6	Palaeogene hyperthermal events	20
2.2	**An introduction to ichnology**	**23**
2.2.1	The development of early ichnology	23
2.2.2	Ichnotaxonomy	24
2.2.3	Toponomy	25
2.2.4	Pre- versus post-depositional trace fossils	27
2.2.5	Ethology	28

2.2.6 The ichnofacies concept 33

2.2.7 Ichnofabric 37

2.2.8 Infaunal tiering 38

2.2.9 Ichnology in core versus outcrop 40

Chapter 3

GEOLOGICAL BACKGROUND

3.1 Study area 43

3.1.1 Introduction 43

3.1.2 Palaeogeographic and tectonic setting 44

3.1.3 Stratigraphy 46

3.1.4 Lithostratigraphy 48

3.1.5 Sedimentary facies and depositional environments 51

Chapter 4

AN AGRICHNIAL FEEDING STRATEGY FOR DEEP-MARINE PALEOGENE *OPHIOMORPHA* GROUPTRACE FOSSILS

4.1 Introduction 67

4.2 Deep-water ichnology – Temporal change 68

4.2.1 *Nereites* ichnofacies 68

4.2.2 *Ophiomorpha;* A shallow marine trace? 69

4.2.3 An agrichnial feeding strategy for *Ophiomorpha?* 72

4.3 Geological setting 72

4.3.1 Stratigraphy and sedimentary facies associations 75

4.4 Exceptionally organised Y-shaped burrows 75

4.4.1 Morphotype morphologies 78

4.4.2 Morphotype occurrences and association with other trace fossils 82

4.4.3 Identification, interpretation, and comparison to similar forms 85

4.5 Discussion 88

4.5.1 An agrichnial feeding strategy for *Ophiomorpha*? 88

4.5.2 Implications for *Paleodictyon* type networks 90

4.5.3 An Eocene peak in deep-marine *Ophiomorpha* 91

4.6 Conclusions 93

Chapter 5

ASSESSING CONTROLS ON THE DISTRIBUTION OF ICHNOTAXA IN SUBMARINE FAN ENVIRONMENTS OF DEPOSITION, THE BASQUE BASIN, NORTHERN SPAIN

5.1 Introduction 96

5.2 Study area 99

5.2.1 Depositional environments 101

5.3 Data acquisition 105

5.3.1 Methodology 105

5.3.2 Ethological interpretation 110

5.4 Results 110

5.4.1 Channel related environments of deposition 112

5.4.2 Lobe related environments of deposition 114

5.4.3 Distal fan environments of deposition 115

5.4.4 Results summary 116

5.5 Discussion 118

5.5.1 Comparison to previous studies 118

5.5.2 Taphonomy in submarine fan deposits 123

5.5.3 Palaeoecology and sediment supply 124

5.5.4 Does age matter? Global ecological change as a control on trace fossil assemblages 129

5.6 Conclusions 133

Chapter 6

AN INTEGRATED ICHNOLOGICAL AND GEOCHEMICAL ASSESSMENT OF THE EARLY PALAEOGENE HYPERTHERMAL EVENTS IN THE BASQUE COUNTRY, NORTHERN SPAIN

6.1 Introduction **136**

6.1.1 The Basque Basin as a natural ichnological laboratory 138

6.2 Geological setting **140**

6.3 Clay minerals as a palaeoclimate proxy **143**

6.3.1 Kaolinite as a diagnostic indicator of the PETM 144

6.3.2 Spectral Gamma Ray data as a proxy for weathering in the Continental hinterland 146

6.4 Methodology **147**

6.4.1 Sedimentology and ichnology 147

6.4.2 Analaytical methods 147

6.4.2.1 X-Ray Diffraction 147

6.4.2.2 Field based SGR 150

6.5 Results **150**

6.5.1 Disordered illite in Basque PETM/EECO assemblages 150

6.5.2 Clay mineralogy results 152

6.5.2.1 Zumaia 152

6.5.2.2 Ermua 153

6.5.2.3 Gorrondatxe 154

6.5.3 Spectral Gamma Ray signatures across the PETM 156

6.5.4 Ichnology 158

6.5.4.1 Danian-Selandian to MPBE 160

6.5.4.2 MPBE to PETM 161

6.5.4.3 Latest Palaeocene to PETM recovery 163

6.5.4.4 Early Eocene transitional system 165

6.5.4.5 Early Eocene siliciclastic system 167

6.6 Discussion 167

6.6.1 Palaeoclimatic signal in Basque Basin clay mineral assemblages 168

6.6.2 Spectral Gamma Ray response to the PETM 172

6.6.3 Ichnological changes across environmental perturbations 173

6.6.4 The PETM as a maximum flooding surface? 176

6.6.5 Oligotrophy as a driver of ichnological change? 179

6.7 Conclusions 181

Chapter 7

CONCLUSIONS

7.1 Responses to key research questions 183

7.2 General conclusions 195

7.3 Suggestions for further research 198

7.3.1 Core based environmental interpretation utilising ichnology 198

7.3.2 Collaboration between neoichnologists and palaeoichnologists 200

7.3.3 Constraining the PETM kaolinite spike 201

Chapter 8

REFERENCES 204

APPENDICES

Appendix 1 Tabulated ichnotaxonomy, ethology and morphological groupings 229

Appendix 2 Photographic plates 230

Appendix 3 Sedimentary logs and ichnodata 238

Appendix 4 Raw clay mineral data 261

LIST OF FIGURES

Figure 2.1 Compilation of PETM geochemical curves 15

Figure 2.2 Compilation of PETM clay mineral curves 16

Figure 2.3	Stratigraphic position of Palaeogene Hyperthermals	21
Figure 2.4	Zumaia photo panel	22
Figure 2.5	Toponomic classification diagram	26
Figure 2.6	Figure illustrating concept of pre- and post deposition	28
Figure 2.7	Common ethologies	32
Figure 2.8	Ichnofacies in the context of a 'source to sink' block diagram	36
Figure3.1	Geographic map of study area	44
Figure 3.2	Palaeogeographic map	46
Figure 3.3	Biochronostratigraphic framework	48
Figure 3.4	Geological setting of the study area	51
Figure 3.5	Photo panel of facies in the Hondaribbia area	55
Figure 3.6	Photo panel of facies near Orio	59
Figure 3.7	Photo panel of facies in the Geteria – Zumaia area	64
Figure 4.1	Simple geological map of study area	74
Figure 4.2	Sedimentary logs preserving *Ophiomorpha* group morphotypes	77
Figure 4.3	Turbidite bed preserving *Ophiomorpha* group morphotypes	79
Figure 4.4	*Ophiomorpha* group morphotype 1	80
Figure 4.5	*Ophiomorpha* group morphotype 2	81
Figure 4.6	*Ophiomorpha* group morphotype 2	83
Figure 4.7	Schematic representation of agrichnial *Ophiomorpha*	90
Figure 4.8	Histogram illustrating occurrences of *Ophiomorpha* in deep marine Settings since Upper Jurassic	92
Figure 5.1	Location/simple geological maps of study area	100
Figure 5.2	Stick logs and photos of depositional interpreted depositional environments	104
Figure 5.3	Sedimentary logs from a proximal to distal transect	106
Figure 5.4	Sedimentary log and quantitative trace fossil data from a lobe	

	complex setting, Gorrondatxe Beach	107
Figure 5.5	Sedimentary log and quantitative trace fossil data from a distal fan setting, Zumaia	108
Figure 5.6	Toponomic classification system	109
Figure 5.7	Pie charts displaying ethologies per environment	111
Figure 5.8	Quantitative trace fossil data per environment (bar charts)	113
Figure 5.9	Idealised sedimentary log displaying sub-ichnofacies distribution	126
Figure 5.10	Model displaying depth of erosion and resultant trace fossil assemblages Per environment of deposition	132
Figure 6.1	Photo panel showing stratigraphic position of hyperthermals at Zumaia	137
Figure 6.2	Map of study area	142
Figure 6.3	XRD diffractograms from PETM intervals at Zumaia and Ermua	149
Figure 6.4	Geochemical curves from Zumaia (PETM)	153
Figure 6.5	Geochemical curves from Ermua (PETM)	155
Figure 6.6	Geochemical curves from Gorrondatxe (EECO)	157
Figure 6.7	Ichno-tiering model across key environmental perturbations	159
Figure 6.8	Quantitative ichnodata from D/S and MPBE intervals	162
Figure 6.9	High resolution ichnolog across the PETM	164
Figure 6.10	Quantitative ichnodata from early Eocene transitional system and Siliciclastic system (EECO)	166
Figure 6.11	Bar charts displaying occurrences of key environmental indicator taxa	178
Figure 7.1	XRD diffractograms of samples obtained from ODP Leg 174AX	204

LIST OF TABLES

Table 2.1	Ichnofacies and their environmental significance	35
Table 4.1	UTM co-ordinates and lithofacies of studied localities	76
Table 5.1	UTM co-ordinates and age of studied localities	102

Table 5.2 Sedimentary facies, facies associations and depositional environments 103

Table 5.3 Complete list of ichnotaxa, plus abundances per locality 120

CHAPTER 1

INTRODUCTION

1.1 BACKGROUND

A catastrophic increase in global temperatures resulting from huge input of carbon into the atmosphere is a scenario that most people are familiar with. Today's 'globally warming' world is widely attributed to be the result of ever increasing amounts of anthropogenic greenhouse gas (GHG) emissions, leading to an enhanced greenhouse effect. Since the Kyoto summit, and subsequent Kyoto Agreement few areas of science have received as much media attention (and contention) as that of climate change. However, catastrophic environmental consequences associated with rapid input of GHGs into the atmosphere is a not a scenario that is unique to the modern world.

At the Palaeocene-Eocene boundary (55.5 Ma), a rapid, high magnitude, yet transient episode of global warming occurred that witnessed sea surface temperature increases of around 5-10°C (e.g. Kennett and Stott, 1991; Koch *et al.*, 1992; Dickens *et al.*, 1995, 1997: Zachos *et al.*, 2001, 2003, 2005). These increases occurred perhaps in as little as 1000 years (Zachos *et al.*, 2005) and were triggered by massive input of methane, a powerful GHG, into the atmosphere. This event is now known as the Palaeocene-Eocene Thermal Maximum (PETM). Dickens *et al.* (1995, 1997) calculate that somewhere in the region of 2000 Gt of methane was responsible for this episode of global warming. Dickens (1999) suggests that somewhere in the region of 2000-4000Gt will have been emitted due to anthropogenic activity within 1000 years of the onset of the industrial age. As such, PETM is arguably the most suitable analogue available to understand and mitigate against the possible consequences of continuing GHG emissions.

The most prominent biotic effect of this major environmental perturbation was the extinction of up to 50% of benthic foraminifera taxa (e.g. Thomas and Zachos, 2000; Thomas *et al.*, 2000; Thomas, 2007; Alegret *et al.*, 2009), making the event the most significant benthic extinction event of at least the last 65 million years. Extensive literature on the trigger mechanism, biotic effects and geochemical effects (see Chapter 2 for discussion) of the PETM has been published since the early 1990s. However, one factor that has still not been satisfactorily resolved is the effect of the PETM on benthic macrofauna communities. Studies investigating the effects of environmental perturbations on macrofauna communities traditionally utilise body fossils (e.g. Smith and Jeffery, 1998, Smith *et al.*, 1999). However, the activity of benthic macrofauna communities is often recorded in sedimentary successions by trace fossil associations (see Chapters 2 and 4-6 for detailed discussion). Trace fossils are often not subject to the same taphonomic factors as body fossils, so often preserve a more complete record of benthic response to environmental perturbations than a traditional body fossil investigation affords.

Studies investigating the effect of the Cretaceous-Tertiary (K/T) mass extinction on deep marine trace fossil assemblages rarely record any significant changes in diversity or abundances (e.g. Rodrìguez-Tovar and Uchman, 2004, 2006; Uchman, 2004). The benthic extinction event that occurred at the PETM is also devoid in trace fossil assemblages from this period. In fact, the Early Eocene displays the highest trace fossil diversity throughout the whole of the Phanerozoic (Uchman 2003, 2004), largely contributed to by diversification of the graphoglyptids. The graphoglyptids are regular meander, net or star shape trace fossils (e.g. Seilacher, 1977a, 1977b; Uchman, 2003) that are representative of lower bathyal- abyssal water depth trace fossil communities (known as the Nereites ichnofacies, see chapter 2). The graphoglyptids reach a peak in diversity and in overall contribution to deep sea trace fossil assemblages during the Early

Eocene (Uchman 2003), immediately following the PETM. The early Eocene also witnesses a peak contribution of crustacean (*Ophiomorpha*) and echinoid (*Scolicia*) traces to deep marine assemblages, both of which are more generally associated with shallow marine conditions in older successions (Tchoumatchenco and Uchman, 2001; Uchman, 2004).

Climatic changes associated with the PETM likely had profound effects on weathering cycles, terrestrial runoff and sediment supply to the deep marine realm (e.g. Schmitz *et al.,* 2001; Egger *et al.,* 2002; Crouch *et al.,* 2003; Schmitz and Pujalte, 2003, 2007) as well as impacting the dispersal and distribution of terrestrial flora (e.g. Wing *et al.,* 2003; Wing *et al.* 2005). However, few studies have attempted to link climatic changes on the continental hinterland with sediment supply to the deep ocean and any associated palaeoecological changes in the deep marine realm.

1.2 THESIS AIMS AND KEY RESEARCH QUESTIONS

This research project has utilised a multidisciplinary approach in order to investigate the effects of the PETM on benthic macrofauna communities on a basin-wide scale in the Basque Basin, northern Spain. High resolution sedimentary logging and facies analysis, ichnological (trace fossil) logging, analysis of clay mineral assemblages utilising X-ray Diffraction (XRD) and recording of Spectral Gamma Ray (SGR) data at outcrop are presented and synthesised into a format to answer the following key scientific questions:

Question 1: ***How do trace fossil assemblages respond to severe environmental perturbations such as the PETM in terms of;***

i.) ***Changes in abundances and diversity?***

ii.) ***Changes in the contribution of 'key environmental indicator' taxa to deep marine trace fossil assemblages?***

iii.) ***Changes in tiering relationships?***

Rationale: It has been noted that deep marine trace fossil assemblages remained largely unaffected by the K/T mass extinction (e.g. Rodríguez-Tovar and Uchman, 2004, 2006) but experienced a significant diversity burst following the PETM (e.g. Uchman, 2003, 2004). This seems to be contrary to the benthic extinction event that occurred at the onset of the PETM and implies favourable conditions for macrofauna in the benthic realm. Occurrences of *Ophiomorpha* and *Scolicia* in the deep marine realm experience a peak during the earliest Eocene (e.g. Tchoumatchenco and Uchman, 2001; Uchman, 2004, 2009), suggesting that shallow water fauna were able to successfully colonise deeper settings. Trace fossil data concerning diversity, abundances and different associations (ichnofacies and ichnofabrics, see chapter 2 for discussion), collected quantitatively across the PETM and other key environmental perturbations in the Basque country are to be analysed to assess and quantify this key research question.

Question 2: ***How do trace making organisms respond ethologically in response to palaeoecological changes?***

Rationale: It has been suggested that the crustacean trace *Ophiomorpha* was able to adapt to surviving in the deep marine realm by adopting an agrichnial (microbe cultivating) trophic strategy (e.g. Uchman, 2009). During preliminary visits to the Basque Basin, and subsequent field seasons, several specimens closely associated with *Ophiomorpha* were observed. These specimens appeared to mimic complex geometric shaped burrow networks such as *Paleodictyon*, the archetypal agrichnial trace fossil (e.g. Seilacher, 1977a, 1977b). Also, occurrences of

Ophiomorpha in distal environments, away from the influx of terrestrial organic matter, are common in the Basque Basin (Crimes, 1977; Leszcyznski, 1991; Cummings and Hodgson, 2011a, 2011b). This seems to be incompatible with the infaunal sediment feeding strategy of *Ophiomorpha*, suggesting that this particular taxon adapted ethologically to palaeoenvironmental changes. A change in the ethological behaviour of a trace making organism can be used as direct evidence of adaption to short-term environmental change. The adaption can be maintained after the perturbation.

Question 3: ***Is it possible to utilise trace fossil assemblages as a diagnostic tool in discriminating between sub-environments within submarine fans?***

Rationale: The ichnofacies concept (Seilacher, 1964, 1967) provided a rudimentary depositional environment control model for trace fossil assemblages, primarily controlled by bathymetry. It has long been recognised that bathymetry is only one of the parameters controlling trace fossil assemblages and that a given ichnofacies may occur across a broad range of bathymetries that display similar characteristics such as salinity, hydrodynamic energy and food supply etc. Seilacher (1974) proposed that the Nereites ichnofacies could be subdivided into sub-ichnofacies based on proximal (Paleodictyon sub-ichnofacies) – distal (Nereites sub-ichnofacies) positions within submarine fans. Uchman (2001) went on to propose the Ophiomorpha rudis sub-ichnofacies for thick bedded channel and lobe related environments. However, Heard and Pickering (2008) explicitly documented the (interpreted) depositional environments that their quantitative trace fossil data was compiled in, meaning that it is possible to test the applicability of their findings in a similar setting and a basin of broadly contemporaneous age and palaeogeography. This will provide an invaluable dataset that may establish certain associations of trace fossils and/or ethologies as being diagnostic of particular sub-environments within

submarine fans. Also, to fully constrain the effect of palaeoecological changes brought about by the PETM, it is first necessary to measure the effect that the depositional environment has on trace fossil assemblages. Similarly, it is also important to assess whether trace fossil assemblages preserved in similar depositional environments, are comparable when they are hosted in sediments preserved on both sides of major environmental perturbations.

Question 4: ***Is it possible to determine if the large influx of kaolinite during the PETM was the result of climatically influenced pedogenetic processes on the continental hinterland or was the kaolinite derived from erosion of older regolith?***

Rationale: A key geochemical feature of the PETM is a prominent spike in the abundance of the clay mineral kaolinite. This has frequently been ascribed to an increase in warmth and humidity at the PETM. However, it still remains unclear whether the kaolinite spike represents a true climatic signal or represents erosion of older kaolinite rich regolith delivered to the deep marine realm. Previous studies in the Basque Basin have identified this spike in kaolinite at the onset of the PETM (e.g. Knox, 1998; Pujalte *et* al., 1998; Gawenda *et al.*, 1999; Winkler and Gawenda, 1999). These authors interpret this increase in kaolinite to represent the onset of warm humid conditions associated with the PETM. However, Schmitz *et al.* (2001) challenge this interpretation due to strong evidence of arid/semi-arid conditions in the Basque Basin at the PETM including; prominent evaporites and caliche soil palaeosols in coeval continental deposits and a strongly evaporated $\delta^{18}O$ signature in the nearby Paris Basin. It has been suggested (e.g. Thiry, 2000; Schmitz *et al.*, 2001) that the predominance of kaolinite in early Eocene deposits may be due to enhanced erosion and runoff, delivering kaolinite that formed in warm humid regions prior to the break-up of Gondwana, to the deep marine realm. Approximately 150 samples were taken at a 20-50cm resolution across key intervals in the Basque Basin and

analysed using XRD. Approximately 500 SGR readings were also taken to test the applicability of using SGR as a proxy for clay mineral assemblages (see chapter 6). As part of a pilot study, samples were also obtained from core related to ODP Leg 174ax (onshore NJ, USA), with the objective of analysing clay composition on the West Atlantic margin during the PETM.

Question 5: ***Can changes in terrestrially derived sediment supply be tied with palaeoecological effects in deep marine trace fossil assemblages through analysis of changes in the composition and abundance of clay mineral assemblages?***

Rationale: Recent work in the Basque country (Rodríguez-Tovar *et al.*, 2010) has suggested that trace fossil assemblages in the basin are largely controlled by nutrient/benthic food supply, which in turn is strongly influenced by sea level. However, sea level inferences were largely made from siliciclastic versus carbonate sedimentation rates. The PETM in the Basque country is generally represented by a sand starved, clay dissolution interval suggesting a sea-level highstand. Yet sedimentation rates are higher than the latest Palaeocene and early Eocene (e.g. Schmitz *et al.*, 2001). This suggests that the PETM experienced a high sediment flux from the continental hinterland, albeit in the form of fine grained sediments rather than coarse grained siliciclastic turbidites that dominate in the early Eocene. By analysing changes in clay mineral composition and abundances, coupled with changes in quartz:calcite ratios this study aims to investigate the control that terrestrial input of sediment into the basin exerts on trace fossil assemblages. This may be particularly important if certain trace fossil taxa adapted their trophic strategies to exploit terrestrially derived food sources (see key research question 2).

1.3 THESIS LAYOUT

1.3.1 Thesis chapters

Below is a summary of the chapters included in this thesis. This thesis contains three chapters that have (or are intended to be) submitted to international geoscience journals. As such, these chapters have been constructed as independent manuscripts. Chapters 2 and 3 provide a scientific overview of the PETM, plus a geological background to put the independent manuscripts into context. Methodologies are detailed within the individual manuscript chapters. Chapter 7 summarises the three independent manuscripts and synthesises them into broader conclusions.

Chapter 2: This chapter provides a scientific background to the PETM, documenting the causes and consequences of this period in the Earth's history. This chapter also details the development of modern ichnology, and outlines the major ichnological concepts. The primary aim of this is to provide the reader (who is assumed to have a basic grasp of geological and palaeontological concepts) with an introduction to the terminology and nomenclature of ichnology.

Chapter 3: This chapter provides a brief overview of the geological setting and stratigraphy of the main study area (the Basque Basin, northern Spain).

Chapter 4: This chapter constitutes an independent manuscript, submitted to Palaios (July 2010, resubmitted December 2010, Published April 2011. DOI: 10.2110/palo.2010.p10-098r). The manuscript documents morphotypes of *Ophiomorpha* group trace fossils that are interpreted to represent a trophic adaptation by *Ophiomorpha* trace makers, whereby the tracemaker constructs regular, polygonal network type traces indicative of an agrichnial feeding strategy. The trophic adaptations by *Ophiomorpha* are postulated to have been driven by changes in food/nutrient

availability in the benthic realm, and by increased supply of terrigenous derived material driven by global climatic changes.

Chapter 5: This chapter constitutes an independent manuscript submitted to the Journal Sedimentary Geology (submitted February 2011, published August 2011, DOI: 10.1016/j.sedgeo.2011.06.009). The manuscript contains detailed ichnological data including diversity, abundances and ethologies of trace fossil assemblages explicitly tied down to carefully documented interpreted environments of deposition. The manuscript concludes that trace fossil assemblages are intrinsically controlled by the environment of deposition in which they are preserved but that an appreciation/evaluation of palaeoecological changes is necessary if comparing assemblages that span major environmental perturbations.

Chapter 6: This chapter constitutes an independent manuscript to be submitted to Palaeogeography, Palaeoclimatology, Palaeoecology (submission pending). The manuscript presents a multi-disciplinary approach to investigating the palaeoecological effects of the PETM in the deep marine realm while also assessing the connection between climatic changes on the continental hinterland with delivery of sediment to the deep marine realm.

Chapter 7: This chapter summarises the thesis and brings together the three independent manuscripts and synthesises them into conclusions that address the five key research questions posted in chapter 1. This chapter also presents ideas and recommendations for further work.

1.3.1 Status of manuscripts at time of thesis submission

Below is a summary of the status of the manuscripts submitted (or to be submitted) to geological journals.

Chapter 4: Cummings, J.P., Hodgson, D.M. *'An agrichnial feeding strategy for Palaeogene Ophiomorpha group trace fossils'.* Submitted to *Palaios* in August 2010, Published April 2011 (DOI: 10.2110/palo.2010.p10-098r).

Contributions of authors: Cummings, J.P: Principal investigator and author.

Hodgson, D.M: Detailed discussion and reviews of initial and final manuscripts, plus modification of some figures.

Chapter 5: Cummings, J.P., Hodgson, D.M. '*Assessing the controls on the distribution of ichnotaxa in submarine environments*'. Submitted to Sedimentary Geology, April 2011, published August, 2011 (DOI: 10.1016/j.sedgeo.2011.06.009).

Contributions of Authors: Cummings, J.P: Principal investigator, data collection, data analysis, principal author.

Hodgson, D.M: Detailed discussion and reviews of initial and final manuscripts.

Chapter 6: Cummings, J.P., Hodgson, Jeffery-Abt, C.H., D.M., Worden, R.J. '*An Integrated Ichnological and Geochemical assessment of the early Palaeogene hyperthermal events in the Basque Country, Northern Spain.'* Submission pending to Palaeogeography, Palaeoclimatology, Palaeoecology.

Contributions of authors:

Cummings, J.P: Principal investigator, data collection, sample collection, sample preparation, sample analysis, data processing and analysis and principle author.

Hodgson, D.M: Detailed discussion and reviews of initial and final manuscripts.

Jeffery-Abt, C.H: discussion and reviews of initial and final manuscripts.

Worden, R.W: Analytical guidance plus review of final manuscript.

CHAPTER 2

A SCIENTIFIC OVERVIEW OF THE PETM AND SOME GENERAL ICHNOLOGICAL PRINCIPLES

2.1 THE PALAEOCENE-EOCENE THERMAL MAXIMUM (PETM)

2.1.1 Introduction

It has long been recognised that a major environmental perturbation occurred at the Palaeocene-Eocene (P/E) boundary. Beckmann (1960) and von Hillebrandt (1962) both noted an extinction affecting benthic foraminifera at the P/E boundary. However, work by Thomas (1989, 1990) established the severity and rapid nature of the benthic extinction event that occurred at the P/E boundary. Between 30-50% of benthic foraminifera species became extinct during this event (Thomas, 2007; Alegret *et al.*, 2009), making the benthic extinction event the most significant of at least the last 65 million years as benthic forams were largely unaffected by the K/T mass extinction (e.g. Thomas, 1989, 1990, 1998, Thomas *et al.*, 2006).

Interest in the Palaeocene-Eocene boundary was renewed in the early-mid 1990s when first, Kennett and Stott (1991), Koch *et al.* (1992) and then Dickens *et al.* (1995, 1997) identified significant oxygen and carbon isotope anomalies during the latest Palaeocene/earliest Eocene that were interpreted to be the result of major episodes of global warming. Initially, a myriad of terms were applied to the PETM due to uncertainty associated with the precise timing of the event, including the Initial Eocene Thermal Maximum (IETM, e.g. Wing *et al.*, 2003) and the

Late Palaeocene Thermal Maximum (LPTM, eg. Dickens *et al.*, 1995, 1997). However, the onset of the PETM is now widely acknowledged to coincide with the start of a negative carbon isotope excursion (CIE) that is coincident with the benthic extinction event. The Global Stratotype Section Point (GSSP) is located at Dababiya Quarry, Egypt (e.g. Schmitz *et al.,* 2004).

2.1.2 Geochemical and climatic effects.

The onset of the PETM is characterised primarily by a negative CIE of between 2-5‰ in the oceanic realm (e.g. Kennett and Stott, 1991; Dickens *et al.,* 1995, 1997, Zachos *et al.,* 2001, 2005), and c.5-6‰ in the terrestrial realm (e.g. Koch *et al.*, 2003, Bowen *et al.*, 2004). It is largely accepted that the CIE resulted from the input of 1400-2800gt of CH_4 into the atmosphere (e.g.Dickens *et al.*, 1995, 1997; Zachos *et al.*, 2005), probably released from destabilised oceanic clathrates. This input of isotopically light carbon (in the form of methane) led to an enhanced greenhouse effect and a subsequent episode of rapid, high magnitude global warming. Sea surface temperatures increased by 5-6°C in equatorial regions and by as much as 10°C at high latitudes, with bottom waters in the deep oceans also experiencing temperature increases of up 5°C (e.g. Kennett and Stott, 1991; Zachos *et al.*, 2003; Tripati and Elderfeld, 2004, 2005: Zachos *et al.*, 2005; Thomas, 2007).

The nature of the CIE (rapid, 10^3 years, Zachos *et al.*, 2005) suggests that isotopically light CH^4 with a $\delta^{13}C$ of c.-60‰ was the source (Dickens *et al.* 1995, 1997). This mass input of isotopically light carbon into the carbon cycle led to rapid acidification of ocean waters leading to a rapid (<30 000 years) shoaling of the calcite compensation depth (CCD). The CCD shoaled by at least 2 km and took more than 100 000 years to recover to a normal state (Zachos *et al.* 2005). This led to extensive carbonate dissolution in the deep oceans that contributed to (but

does not solely account for) the benthic extinction event that occurred at the onset of the PETM (e.g. Thomas, 2007; Alegret *et al.*, 2009).

Commonly, detrital clay mineral assemblages in PETM marine sediments display a prominent spike in the abundance of the clay mineral kaolinite (e.g. Robert and Chamley, 1991; Robert and Kennet, 1994; Pujalte *et* al., 1998; Cramer *et al.,* 1999; Gawenda *et al.*, 1999; Winkler and Gawenda, 1999; Bolle and Adatte, 2000; Cramer and Kent, 2005; Harrington and Kemp, 2005; Dypvik *et al.,* 2011). Detrital clay minerals form during pedogenesis on the continental hinterland and are influenced by the prevailing climate and associated weathering conditions (e.g. Chamley, 1989; Thiry, 2000). As such, they are often used as a palaeoclimate proxy (e.g. Gawenda *et al.*, 1999; Winkler and Gawenda, 1999; Ruffell and Worden, 2000; Ruffel *et al.*, 2002). The kaolinite spike associated with the PETM is usually ascribed to an increase in warm, humid conditions on the hinterland (see chapter 6 for detailed discussion of PETM Kaolinite).

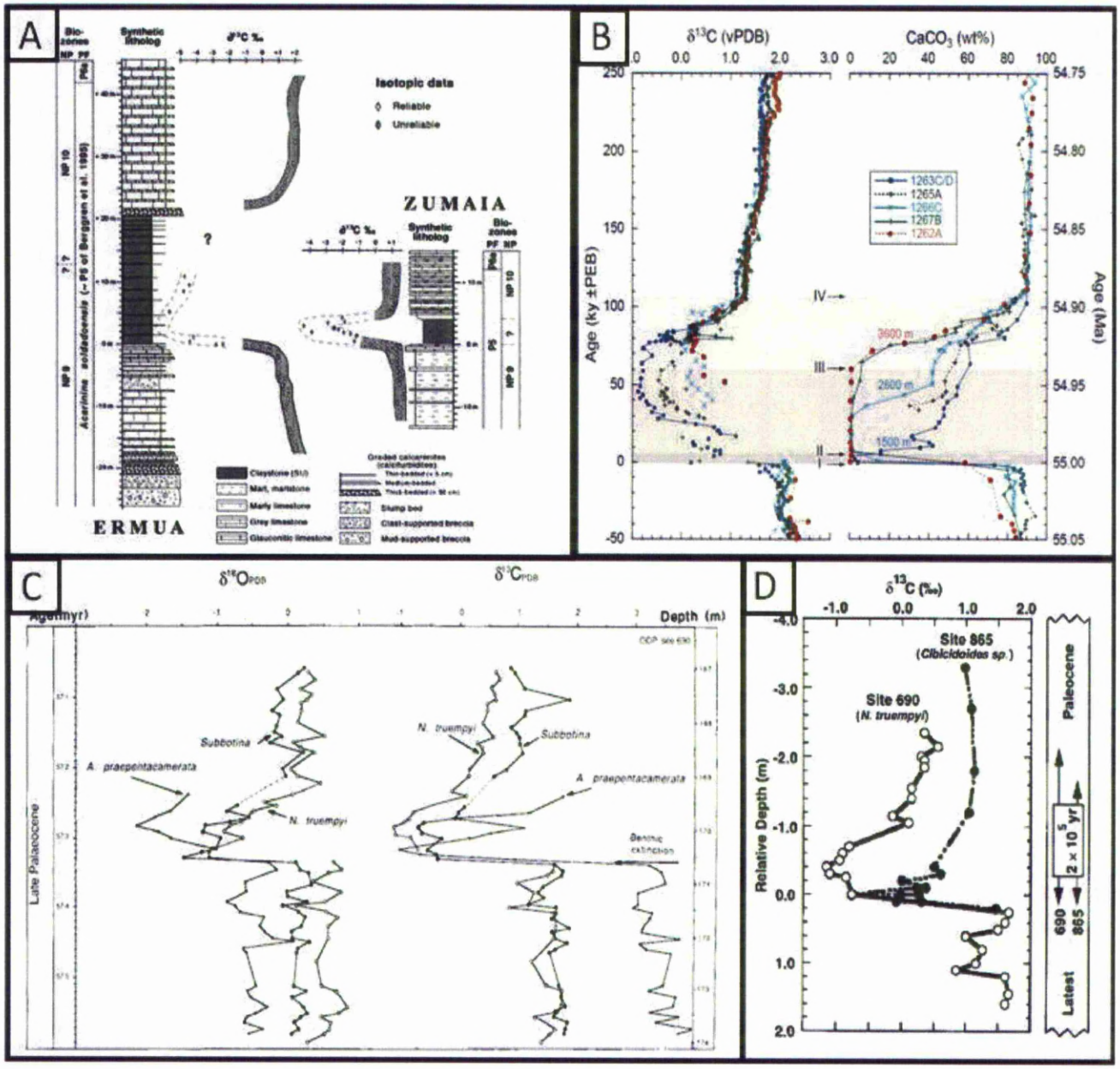

Fig. 2.1 Compilation of PETM geochemical curves from: A.) The Basque Basin, northern Spain. $\delta^{13}C$ (bulk rock) obtained from well exposed outcrops of deep marine sediments (from Schmitz *et al.*, 2001). B.) $\delta^{13}C$ and carbonate ($CaCO_3$) by weight % (bulk rock) from ODP drill holes 1263CD, 1265A, 1266C, 1267B, 1262A, Walvis Ridge, South Atlantic (from Zachos *et al.*, 2005). C.) $\delta^{18}O$ and $\delta^{13}C$ (planktonic foraminifera) from ODP drill hole 690B, Maud Rise, Antarctica (from Kennet and Stott, 1991). D.) $\delta^{13}C$ (from benthic foraminifera) from Maud Rise, Antarctica and ODP Site 865, Equitorial Pacific (from Dickens *et al.*, 1997). This figure highlights the global scale and contemporaneous nature of the PETM/CIE.

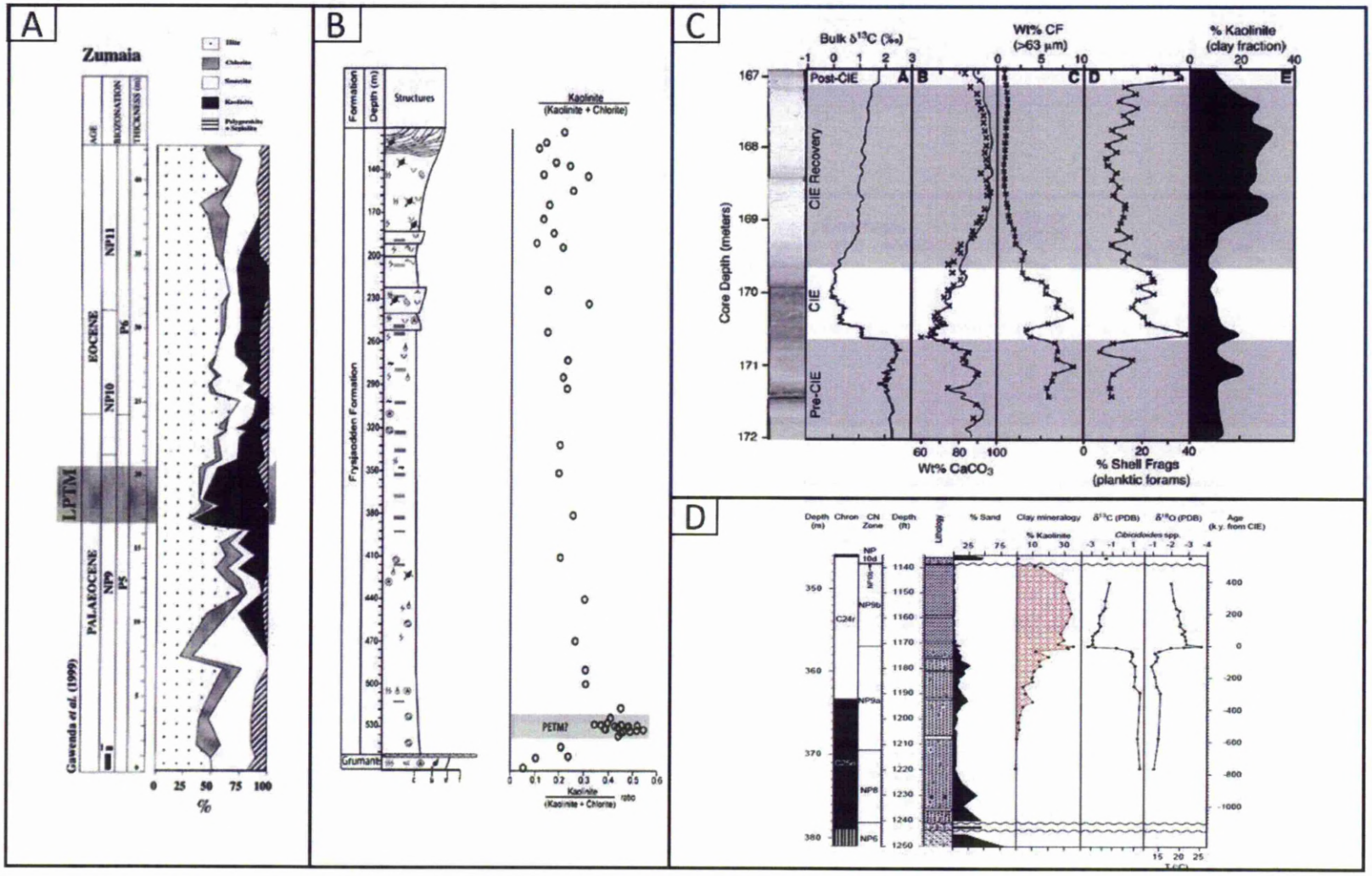
A
Zumaia
Illite
Chlorite
Smectite
Kaolinite
Polygorskite + Sepiolite
AGE
BIOZONATION
THICKNESS (m)
EOCENE
PALAEOCENE
NP11
NP10
NP9
P6
P5
LPTM
Gawenda et al. (1999)
0 25 50 75 100
%
B
Formation
Depth (m)
Structures
Fryjasodden Formation
Grumant
Kaolinite
(Kaolinite + Chlorite)
PETM?
0 0.1 0.2 0.3 0.4 0.5 0.6
Kaolinite / (Kaolinite + Chlorite) ratio
C
Bulk δ13C (‰)
-1 0 1 2
Wt% CF (>63 μm)
3 0 5 10
% Kaolinite (clay fraction)
0 20 40
Post-CIE
A
B
C
D
E
CIE Recovery
CIE
Pre-CIE
Core Depth (meters)
167
168
169
170
171
172
60 80 100
Wt% CaCO3
0 20 40
% Shell Frags (planktic forams)
D
Depth (m)
Chron
CN Zone
Depth (ft)
Lithology
% Sand
Clay mineralogy
% Kaolinite
Cibicidoides spp.
δ13C (PDB)
δ18O (PDB)
Age (k.y. from CIE)
NP10
NP9b
NP9a
NP8
NP6
C24r
C24n
350
360
370
380
1140
1150
1160
1170
1180
1190
1200
1210
1220
1230
1240
1250
25 75
10 30
-3 -1 1
-1 -2 -3 -4
400
200
0
-200
-400
-600
-800
-1000
15 20 25
T (°C)

Fig. 2.2 (previous page) Compilation of PETM clay mineral curves. A.) Clay mineral composition across the Palaeocene Eocene boundary (and therefore the PETM) at Zumaia (from Bolle and Adatte, 2000). B.) Kaolinite/kaolinite + chlorite across the PETM at Svalbard, Norway (from Dypvik *et al.*, 2011). C.) Kaolinite (as a % of clay fraction) across the PETM at ODP Site 690, Maud Rise, Antarctica (from Kelly *et al.*, 2005). D.) Kaolinite (as % of clay fraction), IODP Leg 150ax, onshore New Jersey, USA.

2.1.3 Trigger mechanisms

Whilst it may be largely accepted that the environmental perturbations experienced during the PETM were largely as a result of the massive input of CH^4 into the atmosphere, the trigger mechanism of the methane release is still highly contentious. It has been suggested that changes in oceanic circulation patterns may have been the trigger (e.g. Thomas, 1998; Thomas *et al.*, 2000; Tripati and Elderfeld, 2005). Continental slope failure (e.g. Katz *et al.*, 2001), bolide impact (Kent *et al.*, 2003; Cramer and Kent, 2005) and sea-level fall (e.g. Speijer and Wagner, 2002) have also been proposed as trigger mechanisms to explain the event. However, the PETM was broadly synchronous with North Atlantic Igneous Province (NAIP) volcanism (e.g. Svensen *et al.*, 2004, 2010). A volcanic trigger is strongly suggested by Schmitz *et al.* (2004) who observed 3 distinct ash layers in Danish PETM sediments, located close to an area of explosive basaltic volcanism in the North Atlantic. Furthermore, Svensen *et al.* (2010) utilised Zircon U-PB dating to confirm that emplacement of magmatic sills in the Vøring basin, offshore Norway occurred synchronously with the PETM. However, an implication of this is that the GHG release

that caused the PETM was due to carbon released from organic rich sediments contacted by the intrusions rather than from destabilized clathrates.

2.1.4 Biotic response to the PETM

The biotic effects of the PETM were not limited to the benthic realm. Oceanic surface waters witnessed the *Apectodinium* dinoflagellate acme, whereby shelfal waters witnessed blooms of *Apectodinium* at latitudes normally higher than the range inhabited by this taxa (e.g. Crouch *et al.*, 2003), coincident with a high latitude expansion of other thermophilic marine and terrestrial organisms (e.g. Crouch *et al.*, 2001; Wing *et al.*, 2005). Calcareous nannoplankton experienced significant turnover (e.g. Angori *et al.*, 2007), with planktonic foraminifera establishing a unique 'excursion' fauna characteristic of the PETM (e.g. Kelly *et al.*, 1996) and diversification of shallow water larger benthic foraminifera (e.g. Pujalte *et al.*, 2003). Also, in the terrestrial realm, dispersal and diversification of land mammals occurred (e.g. Clyde & Gingerich 1998; Bowen *et al.*, 2002), with archaic mammals being replaced by fauna similar to that which can be seen today. This included evolution of the first true primates (Gingerich, 2003). Floral impacts due to the PETM were also significant with shifts in relative abundances and higher latitude shifts in ranges characterising the effect of this climatic event (Wing *et al.* 2003).

2.1.5 Duration and recovery of the climate system back to a 'normal' state

In geological terms, the PETM was a short transient event. Initially, the duration of the PETM was poorly constrained with estimates generally in the range of between 100 ka to 250 ka (e.g Kennett and Stott, 1991, Koch *et al.*, 1992). Recent work e.g. (Lourens *et al.*, 2005) has suggested that Milankovitch climate cycles may have paced the climate around the time of the PETM, with the eccentricity cycle (100 ka and 405 ka) being the driver of the PETM. However, Röhl *et al.* (2007) used a multi-proxy approach utilising analysis of extraterrestrial helium, X-ray fluorescence (XRF) core analysis, and cycle stratigraphy. They calculated that the duration of the PETM lasted c. 170 ka based on the number of complete precession cycles detected by their XRF analysis. They also illustrate that the 100 ka eccentricity cycle seems to modulate the

precession cycle with the PETM onset occurring halfway between two precession cycles within the 100 ka eccentricity cycle.

Zachos *et al.* (2005) estimate that the full extent of warming associated with the PETM was reached within 30 ka (albeit with the most severe warming in the first 1 ka). The recovery of ^{13}C isotopes to pre excursion levels took at least 100 ka. Rapid acidification of ocean waters resulting from elevated atmospheric CO_2 will likely have been buffered by weathering of silicate rocks during the PETM. The aforementioned spike in kaolinite at the onset of the PETM does seem to hint at increases in weathering (and runoff) in the terrestrial realm. Zachos *et al.* (2005) and Torfstein *et al.* (2009) propose this as being the main recovery mechanism as it will have allowed the oceans to sequester atmospheric CO_2 upon the CCD and lysocline recovering to pre-PETM depths.

Another key mechanism that possibly aided the recovery of the climate system back to a normal state is that of an increase in surface productivity of the oceans, enabling uptake of atmospheric CO_2. Specifically, it has been proposed that significant coccolithophore blooms contributed to increase surface productivity, suppressing the lysocline and CCD, thereby providing an important positive feedback mechanism in reducing atmospheric CO_2 (e.g. Kelly *et al.*, 2005; Stoll *et al.*, 2007). It is probable that a number of feedback mechanisms contributed to the recovery of the system to a normal state. For example, an increase in silicate weathering of rocks would lead to an increase in terrestrially derived organic matter and nutrients to the deep oceans, which in turn would increase surface productivity, suppressing the lysocline and CCD, and allowing further sequestration of atmospheric CO_2 by the oceans.

2.1.6 Palaeogene hyperthermal events

It has been suggested that the PETM was in fact one of a series of abrupt high magnitude, transient episodes of global warming that occurred throughout the early Palaeogene. These events, termed 'hyperthermals' (e.g. Thomas and Zachos, 2000; Thomas *et al.*, 2000) are all characterised by significant oxygen and carbon isotope excursions, extinctions and/or significant turnover of benthic microfauna, dissolution of carbonate in the deep marine realm, and significant increases in global temperature. These events include the Mid-Palaeocene Biotic Event (MPBE, Bernaola *et al.*, 2006a, 2007), the Danian-Selandian transition (D/S transition, e.g. Bernaola *et al.*, 2009) the ELMO event (e.g. Lourens *et al.,* 2005), the X-event (e.g. Roehl *et al.*, 2005) and the Palaeocene-Eocene Thermal Maximum (PETM, e.g. Kennet & Stott 1991; Koch *et al.* 1992; Dickens, 1995, 1997; Zachos *et al.*, 2001; Zachos *et al.*, 2005). The PETM was the highest magnitude of these events (e.g. Lourens *et al.*, 2005; Thomas, 2007). Lourens *et al.* (2005) suggest that all of these events were actually intrinsic to the Earth's climate system (albeit perhaps modulated and/or amplified by internal feedback mechanisms such as GHG concentrations) and were paced astronomically by variations in the Earth's orbit around the sun (i.e. Milankovitch cycles). Temperatures remained elevated throughout most of the early Eocene following the PETM (following the recovery of the climate from hyperthmal conditions). This period is often referred to as the early Eocene climatic optimum (EECO) which is defined as the $\delta^{18}O$ minima which persisted throughout the early Eocene from 53-c.49Ma (Zachos *et al.*, 2001; Hollis *et al.*, 2009).

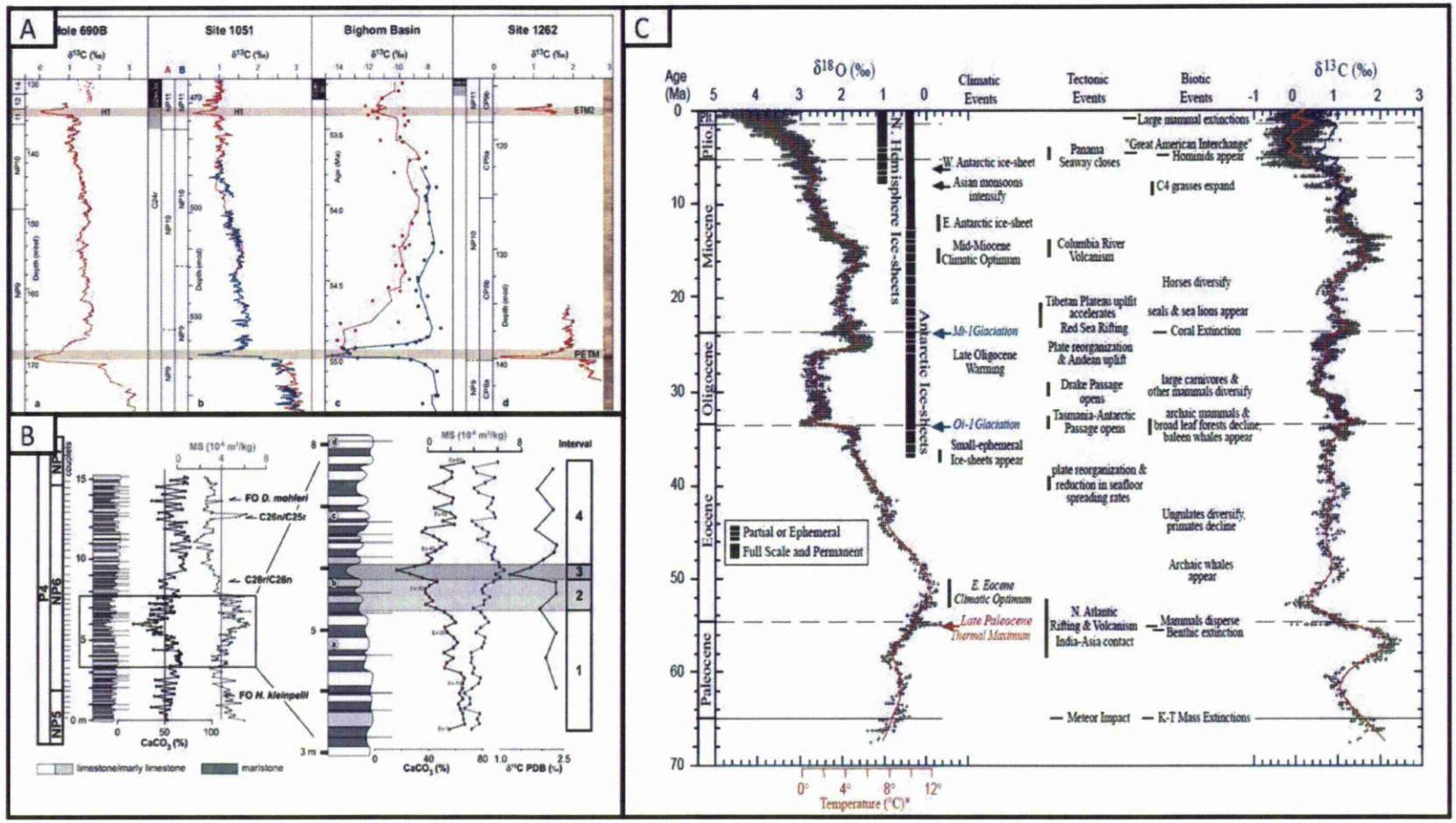

Fig. 2.3 Figure displaying stratigraphic position of Palaeogene hyperthermal events. A.) $\delta^{13}C$ curves from ODP Site 690B, Site 1051, Site 1262 and The Bighorn Basin (terrestrial strata, Wyoming, USA). A 2nd, younger negative CIE is shown relative to the PETM. The interval is named the H1 event at Sites 690B and 1051 and ETM2 (Eocene thermal maximum 2) at Site 1262. Lourens *et al.* (2005) correlate all of these events, and show its presence in the terrestrial realm (Bighorn Basin) and rename it the Elmo horizon. They show it to be a synchronous event in the terrestrial and marine realm just as the PETM was. B.) Position of the mid-Palaeocene biotic event (MPBE) at Zumaia (Bernaola *et al.*, 2007). C.) Cenozoic $\delta^{13}C$ and $\delta^{18}O$ curves highlighting major climatic, tectonic and biotic events. Note the position of the EECO, coincident with the $\delta^{18}O$ minima throughout the whole of the Cenozoic (from Zachos *et al.*, 2001).

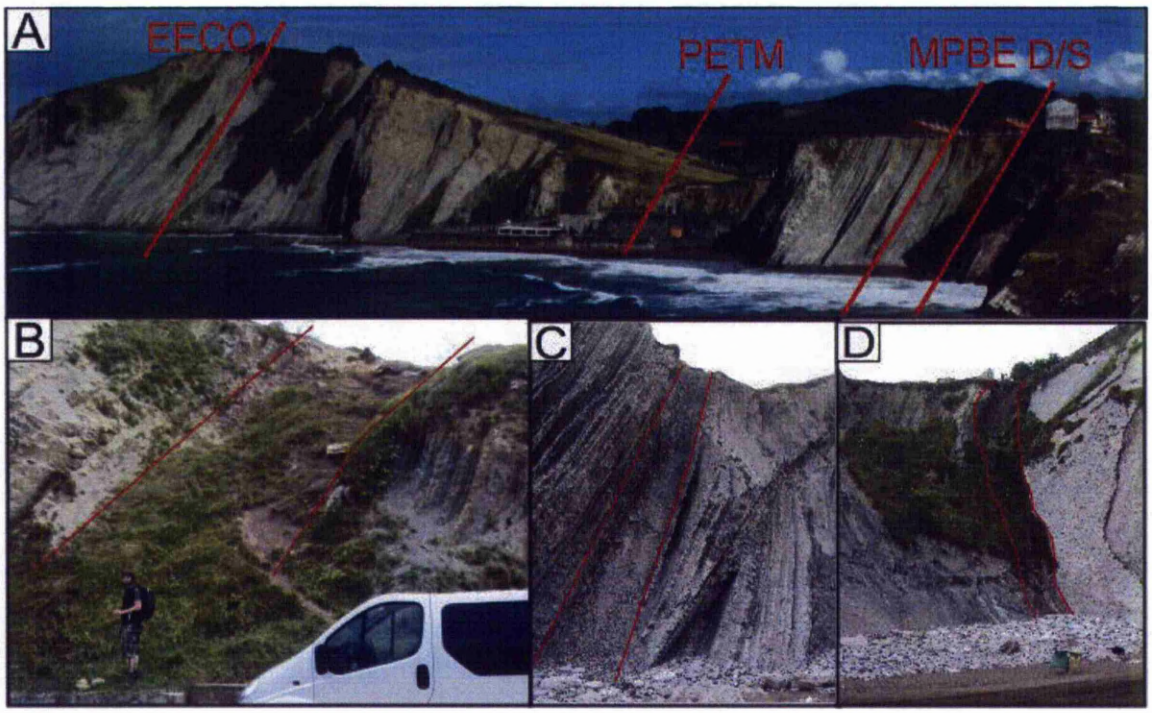

Fig. 2.4 Annotated photos from Zumaia showing position of hyperthermals. A.) Photo taken from the Aitzgorri Headland. D/S = Danian-Selandian transition. This event marks the first carbon isotope anomaly following the K/T boundary. This study encompasses Stratigraphy from the uppermost Danian (i.e. just below the D/S line). MPBE = mid-Palaeocene Biotic event. PETM = Palaeocene Eocene thermal maximum. EECO = approximate zone of transition from mixed siliciclastic/carbonate sedimentation to dominantly siliciclastic. This is approximately concurrent with the NP11/NP12 biozone boundary (Martini, 1971). Note that the EECO is not a formally defined unit and relates to a prolonged (c. 2Ma) period of elevated temperatures. The EECO line therefore represents the onset of this period. B.) Close up view of the PETM interval. CIE = glauconitic limestone in which the CIE initiated. Rec = marlstone recovery interval where carbon isotope values begin to return towards pre-excursion values. C.) Close up of theMPBE interval. The black dashed line shows a fault zone. D.) Close up of the red marlstone overlying the D/S that represents the recovery interval following the minor CIE at the D/S boundary.

2.2 AN INTRODUCTION TO ICHNOLOGY

2.2.1 The development of early ichnology

Heer (1877) published an extensive monograph on Flysch Lebensspuren (see section 2.2.2) in which trace fossils were described as plants. Heer's work was published during a period known as 'the age of the fucoids' (e.g. Osgood, 1975; Cadée and Goldring, 2003). The period 1828-1881, (Osgood, 1975) is so called due to the widespread belief that most marine trace fossils were in fact fossil algae (or fucoids). Brongiart (1828) subdivided the genus *Fucus* into 'sections' (essentially taxa). This work was subsequently continued into the late 19th century with further taxonomic work into fucoids being carried out, most notably by Fischer-Ooster (1858) as well as the aforementioned work by Heer (1877). Most of this taxonomic work on 'fucoids' had been conducted in flysch deposits. This created a legacy that has been carried through to modern day deep-marine ichnology, as many taxonomic names are still in use (Uchman, 2003b). Perhaps the most well known of these, and indeed the trace fossil genus that bears the closest resemblance to fucoids is *Chondrites* (Sternberg, 1833).

Cadée and Goldring (2003) credit Nathorst (1873, 1881) as being the founder of ichnology as a scientific discipline. Nathorst's early experiments showed that worms were able to construct branching burrows that had a similar appearance to fucoid algae. Nathorst (1873, 1881) was therefore the first ichnologist to recognise that 'fucoids' were in fact trace fossils produced by marine invertebrates. Fuchs (1895) went onto describe regular meander, spiral and net shaped trace fossils as graphoglyptids, a term still widely employed today to describe such traces (e.g. Uchman, 2001, 2003; Heard and Pickering, 2008; Rodríguez-Tovar *et al.*, 2010). He attributed most of these traces to the activity of gastropods (Uchman, 2007c).

2.2.2 Ichnotaxonomy

Perhaps as a legacy from 'the age of the fucoids' trace fossil taxonomy (or ichnotaxonomy) is derived from zoological taxonomy and is governed by the International Congress on Zoological Nomenclature (ICZN, e.g. Bromley, 1996, Uchman, 2007c, Knaust, 2009b). An important step in establishing a workable ichnotaxonomic framework was Hantzschel's (1975) contribution to the Treatise on Invertebrate Palaeontology, a framework that still underpins modern ichnotaxonomy.

Following on from Hantzschel's (1975) work, Książkiewicz (1977) implemented a deep marine (or flysch), morphological based classification scheme with ten subdivisions based purely on morphological appearance. Uchman (1998) modified this scheme and erected 8 divisions as follows:

1.) Circular and elliptical structures

2.) Simple and branched structures

3.) Radial structures

4.) Spreite structures

5.) Winding and meandering structures

6.) Spiral structures

7.) Branched, winding and meandering structures

8.) Networks.

Uchman's (1998) scheme was devised by revising the taxonomy on over 1800 specimens from the Marian Książkiewicz collection, housed at Jagiellonian University, Krakow, Poland. The collection comprises specimens collected from Tithonian-Miocene flysch deposits in the Polish Carpathians and probably represents the most complete collection of deep marine trace fossils in the world. As such, Uchman's (1998) taxonomy is followed in this thesis. All of the taxa referred to throughout this study have been the subject of extensive taxonomic investigation in recent years (see Uchman, 1992, 1995, 1998, 1999, 2001, 2007a, 2007b; Tunis and Uchman, 1996a, 1996b, 1998; Tchoumatchenco and Uchman, 2001 for detailed systematic ichnology/taxonomy of discussed taxa). As such, a detailed taxonomical review is beyond the scope of this research and deemed unnecessary. However, all taxa are tabulated in Appendix 1, including type specimen reference, their morphological group and their interpreted ethology. Photographic plates of the most commonly occurring taxa are included in Appendix 2.

Trace fossils are subdivided into the ranks of ichnogenus (igen.) and ichnospecies (isp.).

2.2.3 Toponomy

Toponomy represents the morphological expression of a trace fossil relative to its casting medium (Bromley, 1996) or the mode of occurrence and preservation/alteration of a trace (Pemberton *et al.*, 2001). A variety of toponomic classification schemes have been devised over the years, most notably by Simpson (1957), Seilacher, (1964a, 1964b) and Chamberlain (1971). However, the most widely used scheme in deep marine ichnology is that of Martinsson (1965, 1970). This scheme is a stratinomic classification whereby trace preservation is described in terms of its relationship to its casting medium.

Hypichnia relates to structures that are preserved on the lower surface of the casting medium.

Epichnia relates to structures preserved on the upper surface of the casting medium.

Endichnia relates to structures that are preserved within the casting medium.

Exichnia relates to structures that are preserved predominantly outside of the casting medium.

See over page for graphic representation of these terms.

Some authors (e.g. Monaco *et al.*, 2007; Monaco *et al.*, 2010) also propose using ***crossichnia*** as a descriptive term for deep tier trace fossils that penetrate several beds (*Ophiomorpha* being an example).

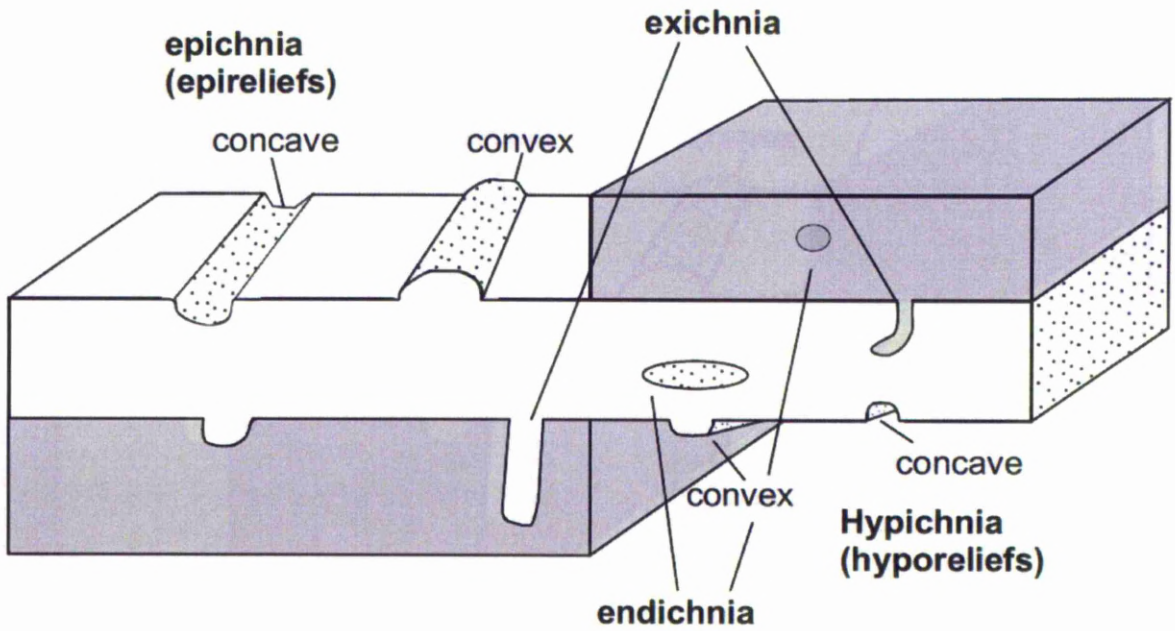

Fig 2.5 Toponomic classification system used in this study (after Martinsson, 1970, modified from Savrda, 2007). There is room for ambiguity with this stratinomic/toponomic scheme as many endichnial traces may express themselves not only within a bed but also on upper and lower surfaces of a bed. Here, endichnial is only applied to trace fossils preserved in cross section. Epichnial and hypichnial are retained for traces preserved on upper and lower surfaces respectively. The terms 'semi relief' and 'full relief' are applied to discriminate between traces that are preserved within their host sediment and traces cast at lithological interfaces, respectively.

2.2.4 Pre- versus post-depositional trace fossils

Perhaps one of the most important concepts in deep-marine ichnology is the recognition of pre- versus post-depositional trace fossil communities. Identifying traces as semi relief or full relief goes part way in doing this but is only of toponomic significance. However, pre- versus post-depositional trace fossil communities represent two very different communities, ecologically. Turbidite settings provide an ideal natural laboratory to investigate this concept.

In quiescent, pelagic/hemipelagic sedimentation regimes, stable, equilibrium communities develop that comprise organisms that are able to thrive in such stable conditions. However, such equilibrium communities tend to have very narrow environmental tolerances as they usually rely on highly specialised feeding strategies (e.g. microbe cultivation/agrichnia) which allow them to exploit niches. Such organisms are referred to as 'K-selected taxa' (*sensu* Ekdale, 1985). They are characterised by low population densities and low individual taxa abundances but with very high species diversity. The graphoglyptids (Fuchs, 1885) are the archetypal K-selected taxa.

However, in turbidite settings, the background quiescent hemipelagic regime is punctuated by delivery of sand into the basin via turbidity currents. Turbidites are taphonomically important for the 'background' K-selected community, as gently erosive turbidity currents will exhume the delicate graphoglyptid burrow systems and cast them on the sole of the turbidite (Seilacher, 1977a, 1977b). However, pre-depositional K-selected communities on the soles of turbidites are often cross cut by a different community that was able to exploit the newly delivered sediment. This post-depositional community represents the 'r-selected' strategists (*sensu* Ekdale, 1985), opportunistic taxa that are able to adapt to rapidly fluctuating environmental conditions. R-

selected taxa are characterised by low diversity, high population communities, partly as a result of higher reproductive rates than K-selected taxa (Ekdale, 1985; Bromley, 1996).

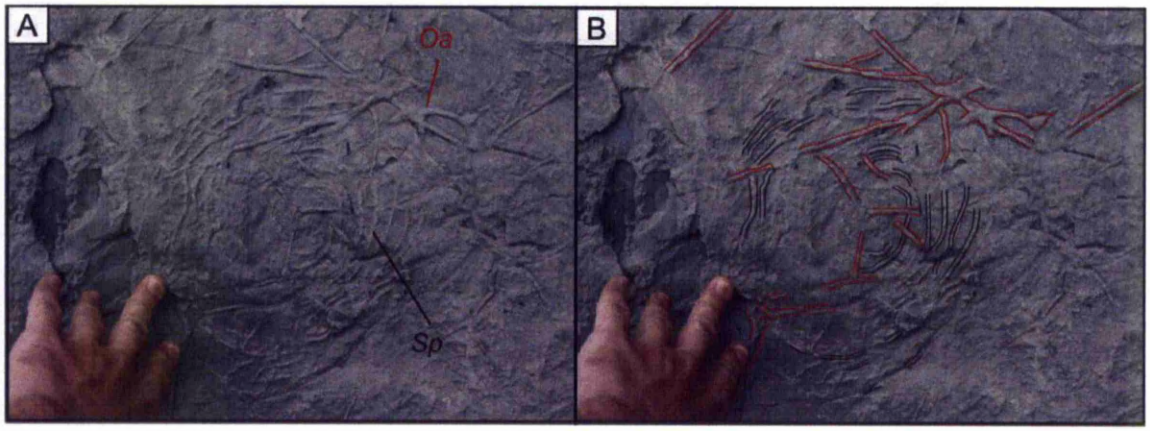

Fig 2.6 A.) Sole of an 8cm thick low concentration turbidite preserving *Spirorhapha involuta (Sp)* and *Ophiomorpha annulata (Oa).* B.) Burrow margins of both taxa highlighted. *Spirorhaphe* burrow margins, whilst showing distinct relief in places, lithologically are identical to the host sediment. This infers that the trace is pre-depositional (i.e. it was exhumed and cast by the turbidity current). The *Ophiomorpha* burrows can be seen to taper in and out of the bed rather than just display sporadic preservation as the *Spirorhaphe* burrow does. The burrow margin of the *Ophiomorpha* burrows displays a distinct contrast to the host sediment due to the presence of a burrow lining (muddy pellets). The preservation of the burrow lining is an indicator of the post depositional nature of this trace. It can also be clearly seen to cross-cut the pre-depositional *Spirorhaphe* burrow, indicating that it was emplaced later. Again, this re-enforces the post depositional diagnosis of this trace.

2.2.5 *Ethology*

Trace fossils are formed via the interaction of organisms with sediment. What is primarily recorded by this interaction is the behaviour of the trace maker. As such, many ichnologists feel that the most logical way to classify trace fossils is by their behaviour (e.g. Seilacher, 1964, 1967; Bromley, 1996). The study of animal behaviour is called ethology. Seilacher (1964)

initially recognised 5 ethological groups. These 5 groups have subsequently been extended many times. There are now at least 11 ethological categories commonly in use in ichnology:

Calichnia *(breeding structures)* are structures built predominantly to raise juveniles or larvae (Bromley, 1996). *Hormosiroidea* may represent a calichnial structure (e.g. Uchman, 1998).

Cubichnia *(resting traces)* are structures created by organisms that have settled in a stationary position within the substrate. Commonly, the organism has some kind of 'anchor' to fix it to the substrate e.g. a bivalves foot leaves behind a resting trace assignable to *Lockeia.* This trace is usually preserved as a convex hyporelief on the soles of event beds.

Domichnia *(domicile/dwelling traces)* are structures whose primary function is to act as a semi-permanent domicile for the trace maker. Often, these structures have wall linings that act to strengthen the burrow (e.g. *Ophiomorpha*). Most domichnia are later passively filled with sediments (Frey and Pemberton, 1985), although *Ophiomorpha* with distinct pelletted wall linings occasionally preserve a meniscate backfill (pers. Observation).

Equilibrichnia *(equilibrium traces)* are structures that record the response of an organism to changes in sedimentation rates in dynamic environments (e.g. Frey and Pemberton, 1985). For example, in rapidly aggrading sediments, most organisms need to maintain an open connection to the sea floor so will correspondingly adjust their burrow upwards. In erosive environments, animals may adjust their burrows downwards (to avoid predation for instance). A classic example of equilibrichnia is *Diplocraterion* .

Agrichnia *(farming/microbe cultivation traces)* are structures that have a primary function of either trapping meiobenthos or cultivating microbes within the burrow system. Seilacher (1977a, 1977b) was the first to suggest that the graphoglyptids were in fact agrichnia, due to their complex burrow networks being constructed in a manner that enabled revisiting of the burrow

system by the tracemaker, whilst always maintaining an open connection to the sea floor to aid irrigation/aeration. The archetypal graphoglyptid (and therefore agrichnium) is the hexagonal network trace, *Paleodictyon.*

Chemichnia *(chemosymbiotic traces)* are structures that facilitate chemosymbiosis between the trace maker and a symbiont. It has been postulated that *Chondrites* acts as a 'sulphide pump' possibly linked to hydrothermal vents, cultivating sulphate reducing bacteria as symbionts (e.g. Seilacher, 1990; Uchman, 2011). However, Bromley (1996) questions the validity of chemichnia as an ethology based on the fact that there is limited difference between cultivating microbes for food and cultivating them for symbiosis.

Fodinichnia *(feeding traces)* are characterised by structures that serve a dual purpose of a semi-domicile but where the primary function is feeding (Bromley, 1996). A good example of a fodinichnial structure is *Thalassinoides* which differs from *Ophiomorpha* in that the lack of burrow re-enforcement means exploiting the substrate as a food source supersedes dwelling within it as an ethology.

Pascichnia *(grazing traces)* often may be inter-gradational with locomotion traces (see *Repichnia*), however, the path may follow a tightly meandering course where it is clear that the trace maker was exploiting nutrient/food rich areas of the sea floor (Bromley, 1996). Classic *Pascichnia* include *Nereites* and *Phycosiphon.*

Repichnia *(locomotion/grazing traces)* are largely distinguished from pascichnia in that the morphology of the trace does not reflect any organised path that may be exploiting a food source, rather the animal is just progressing from one point to another. One of the best known repichnia is *Cruziana* (Bromley, 1996).

Praedichnia *(predation traces)* are structures relating to predatory behaviour (Ekdale, 1985). Praedichnia is particularly prevalent in hardgrounds where shells are often penetrated by predatory organisms (e.g. the trace *Oichnus*; Bromley, 1996).

Fugichnia *(escape traces)* represent the escape of an organism from substrate, usually following rapid burial. These are easily differentiated from more systematic equilibrichnia in that fugichnia are usually preserved in the form of collapsed laminations within substrate rather than coherent trace fossils (e.g. Bromley, 1996, Taylor *et al.*, 2003). As such, fugichnia are not usually assigned to any particular genus but merely described as fugichnia.

Aedifichnia *(edifices constructed above substrate)* are structures constructed from sediment that has been cemented by the trace maker. Common examples include wasps nest and termite mounds. In the marine realm, sand reefs formed by sabellarid polychaetes may be considered aedifichnia (Bromley, 1996).

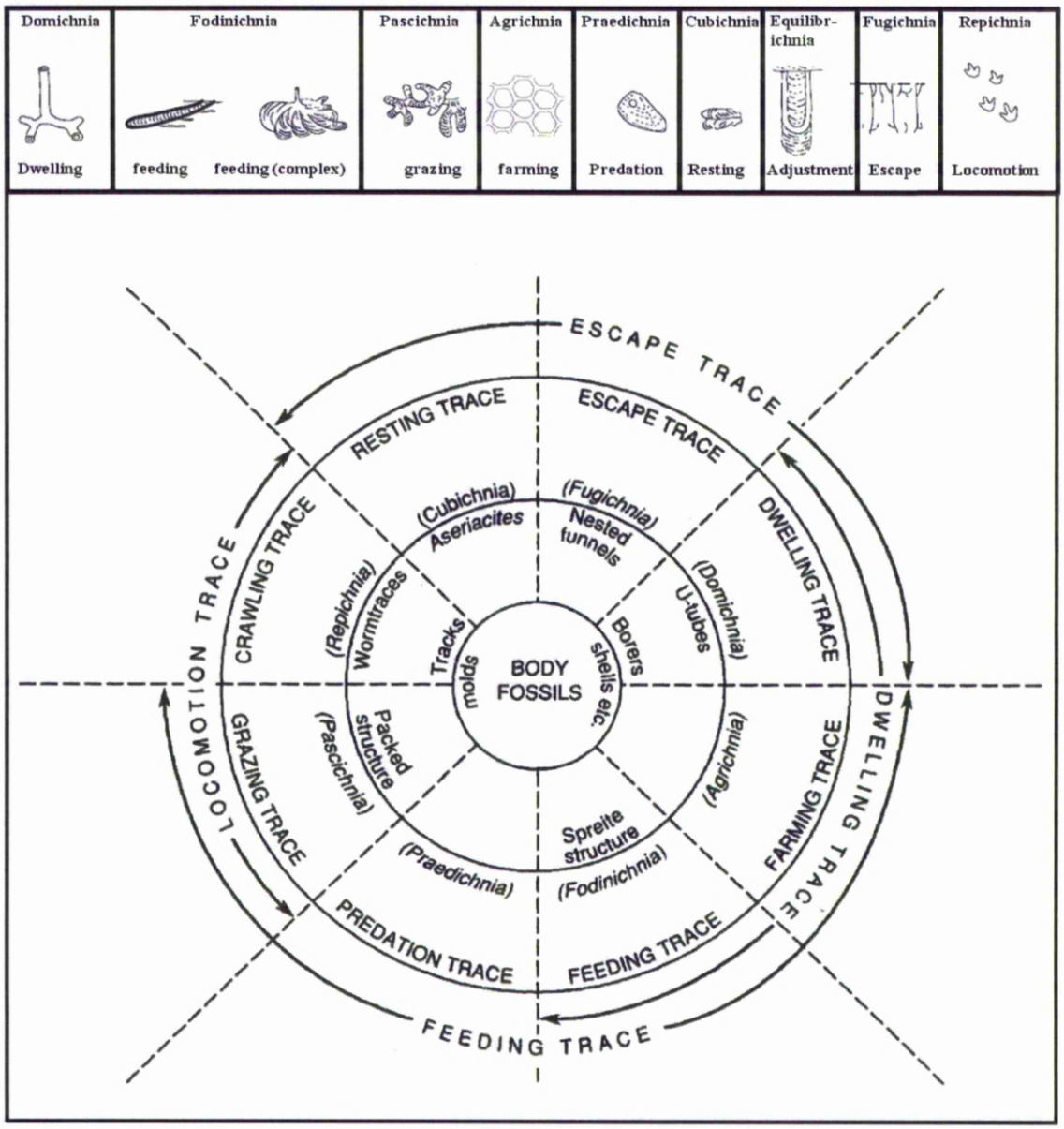

Fig 2.7 List of commonly used ethologies and typical expression when preserved as trace fossils. 'Ethological wheel' at base of figure illustrates how ethologies may often overlap and/or be intergradational. Figure has been modified from Pemberton *et al.* (1992) from which the ethological wheel was taken plus also contains redrawn elements from Bromley (1996).

2.2.6 The ichnofacies concept

Seilacher (1964, 1967) noted certain reoccurrences of trace fossil assemblages that appeared to be at least passively controlled by bathymetry. Initially, six ichnofacies were erected. These ichnofacies were named after the archetypal ichnogenus and placed within a bathymetric gradient (excluding the Glossifungites ichnofacies, representative of hard grounds formed during periods of depositional hiatus or erosion, and the Trypanites ichnofacies, representative of trace fossil assemblages preserved in continental red beds). Seilacher (1967) also noted variations in the types of spreiten burrows that similarly seemed to be controlled by a bathymetric gradient. It was inferred that the variations in these spreiten burrows were driven by food availability. Shallow, high energy environments are dominated by vertical burrows due to the trace makers seeking shelter from the high energy conditions at the sediment-water interface, plus feeding through suspension due to nutrients/food being stripped from the sediment by wave action. Moving progressively basinward, energy levels decrease and horizontal burrowing and deposit feeding increases.

It has long been recognised that trace fossil assemblages, and therefore ichnofacies are controlled by a number of environmental gradients, of which water depth is only one. Other factors that influence trace fossil assemblages include:

- Substrate consistency
- Hydrodynamic energy
- Food/nutrient availability
- Water turbidity

- Oxygenation
- Salinity
- Sedimentation rates

Frey *et al.* (1990) go as far to question whether or not water depth actually ever governs ichnofacies. Rather, they imply that bathymetry only passively controls trace fossil assemblages by any influence it may have on the above factors (see also, Pemberton *et al.*, 1992; MacEachern, 2007 for reviews of ichnofacies).

Table 2.1 (see over) List of commonly used ichnofacies and their environmental significance. A comprehensive review of ichnofacies is beyond the scope of this research and readers are guided to the references above.

Marine softground ichnofacies			
Ichnofacies	**typical environments**	**Substrate**	**Comments**
Nereites	Deep-marine (generally in turbiditic settings)	Soupground-softground pelagic muds punctuated by siliciclastic turbidite deposition	Characterised by regular meander, star and net shaped trace fossils (the graphoglyptids; e.g. *Paleodictyon, Lorenzinia, Megagrapton),* and efficient grazing traces (e.g. *Nereites*).
Zoophycos	Slope to basin floor muds	Soupground-softground, occasional firmground muddy substrate	Not restricted to slope environments as inferred by original Seilacherian ichnofacies. Predominates over *Nereites* in bathyal to abyssal zones beyond the reach of turbidity currents. One of the least well defined ichnofacies (i.e. Accessory ichnotaxa to *Zoophycos* itself not widely published). Often linked to low oxygen conditions.
Cruziana	Shelfal zone (below FWWB, above FWWB), lagoonal settings, some estuarine environments	Shifting to stable substrates, generally softground sea floors.	Perhaps the widest ranging of the Seilacherian ichnofacies. Crawling traces (repichnia) particularly abundant. Horizontal *Thalassinoides* and *Ophiomorpha* a common component. Horizontal spreiten burrows (e.g. *Rhizocorallium*) common.
Skolithos	High energy near shore environments, ?submarine canyons/channels	Shifting, loosely consolidated substrate	Dominated by vertical (*Skolithos*), often U-shaped (*Arenicolites*) burrows plus equilibrichnia in response to aggradation/degradation. Escape traces common. Vertically inclined *Ophiomorpha* more representative than *Skolithos* in post late- Mesozoic sediments.
Psilonichnus	Sandy backshore (generally supra-littoral)	Shifting, loosely consolidated substrate	J, Y and occasional U-shaped domicile burrows (e.g. *Polykladichnus, Psilonichnus*). May also preserve rhizoliths.
Continental ichnofacies			
Scoyenia	Lake margins, fluvial channel margins/overbank, wet interdunes	Looseground substrates subject to dessication	Low energy, periodically sub-aerially exposed continental settings characterise this ichnofacies. Mobile deposit feeders producing meniscate back filled traces (e.g. *Taenidium, Scoyenia, Beaconites*), plus repichnia (*Diplichnites, Cochlichnus*).
Mermia	Lacustrine environments (including lacustrine turbidites)	Soupground-softground substrate in permanently subaqueous settings	Characterised by non-specialised grazing trails such as *Mermia* and *Gordia,* plus occasional cubichnia (e.g. *Lockeia*).
Coprinisphaera	Subarial continental settings	Looseground-firmground in permanently subarial settings	Assemblages dominated by dwelling structures (domichnia) such as *Termitichnus* and *Coprinisphaera.* Rhizoliths and palaeosol concretions are commonly preserved.
Substrate controlled ichnofacies			
Glossifungites	n/a	**Stiffground-firmground**	This ichnofacies is charcterised by vertical to sub-vertical sharp walled, unlined burrows that often crosscut soupground/sofground assemblages.As such, the ichnofacies is interpreted to have a sequence stratigraphic significance as it is usually associated with erosional events (e.g. sequence boundaries, TSEs etc). Scratchmarks are common due to firmness of the substrate. Typical genera; *Arenicolites, Skolithos, Diplocraterion, Thalassinoides.*
Teredolites	n/a	**Woodground (xylic substrate)**	Characterised by clavate boring structures (i.e. *Teredolites* igen.). Note: This only represents a true ichnofacies when preserved in fossilised peat swamps (i.e. Coal beds) exposed by erosion. *Teredolites* burrows are often preserved in woody/coal clasts but this does NOT represent an ichnofacies.
Trypanites	n/a	**Hardground substrates**	This ichnofacies is characterised by borings and rasping gnawings of algal grazers. May be inter-gradational with *Glossifungites* ichnofacies as *Trypanites* predominates in hardgrounds associated with omission surfaces.

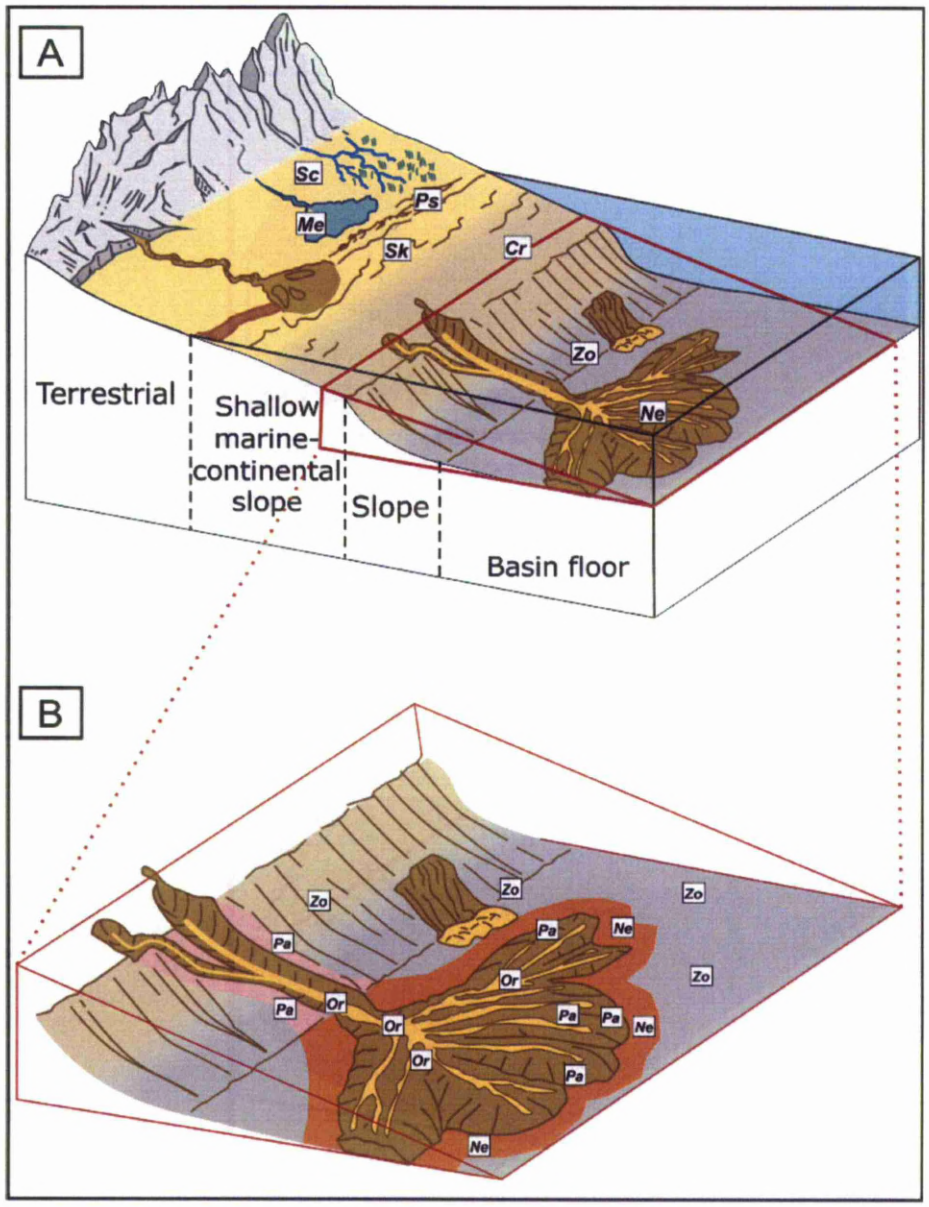

Fig 2.8 A.) Ichnofacies distribution on a continental to deep marine block diagram (see table 2.1 for details of each ichnofacies. *Ne* = Nereites, *Zo* = Zoophycos, *Cr* = Cruziana, *Sk* = Skolithos, *Me* = Mermia, *Sc* = Scoyenia. B.) Detail of slope to basin floor (bathyal to abyssal zone) showing distribution of sub-ichnofacies of the Nereites ichnofacies (see chapter 5 for significance of these sub-ichnofacies). *Ne* = Nereites, *Or* = Ophiomorpha rudis, *Pa* = Paleodictyon sub-ichnofacies.

2.2.7 Ichnofabric

Bromley and Ekdale (1983) define ichnofabrics as the aspect of a sediments texture and internal structure that is modified by bioturbation and/or bioerosion. One factor that separates ichnofabrics from ichnofacies is that the primary sedimentary texture (whether it be completely preserved or completely obliterated) is an equally important factor to any trace fossils that may be preserved (Taylor and Goldring, 1993; Taylor *et al.*, 2003). An ichnofabric is therefore a record of:

- Primary sedimentary conditions
- The original endobenthic tiered community structure
- Taphonomic history of the tiered community (Taylor and Goldring, 1993).

An ichnofacies study primarily relies on the recognition of individual ichnotaxa and associations of such ichnotaxa, often independently of sedimentary observations. A comprehensive ichnofabric investigation relies on the recognition of many more parameters including:

- Primary sedimentology (including lithology, grain size, sedimentary structures)
- A measurement of ichnodiversity
- A measurement of bioturbation intensity
- Tiering patterns
- Ethology
- Style of colonisation (Taylor and Goldring, 1993; Taylor *et al.*, 2003).

Unlike ichnofacies, ichnofabrics have no kind of formal definition and generally are named after the dominant ichnotaxa, with associated ichnotaxa attached to a particular ichnofabric. The key difference between assigning ichnofabrics and ichnofacies is that an ichnofabric is never named after a trace fossil that is not present in the assemblage, which is contrary to ichnofacies where this is often normal procedure! However, no attempt is made to constrain these ichnofabrics within an environmental gradient as with ichnofacies. Rather they are tied down to particular sedimentary facies, as the sedimentary facies goes part way in determining which ichnofabric is ascribed. As such, the number of potential ichnofabrics runs not into the tens but into at least the hundreds (e.g. Bromley, 1996).

Critics of the ichnofabric method may feel that the near limitless potential ichnofabrics severely limits their use in environmental interpretation (e.g. MacEachern *et al.*, 2007). However, Taylor *et al.* (2003) propose that the ichnoataxa *per se* are not of importance. Rather it is the changes in environmental conditions that determine the overall style of colonisation that determines an ichnofabric. As such, rather than attempt to constrain a particular depositional environment, ichnofabrics can be utilised to recognise *key stratal surfaces* such as omission surfaces, sediment bypass surfaces and hiatal surfaces.

2.2.8 Infaunal tiering

Animals (and plants) penetrate to various depths in sediment, depending on their respiratory and/or feeding strategies (Taylor, 2003). This creates a vertical sequence that is referred to as 'tiering' (Ausich and Bottjer, 1982). In muddy substrates, Bromley (1996) demonstrates that sediments can be subdivided into three distinct zones:

1. *The mixed layer:* This layer comprises the uppermost few centimetres of sediment beneath the sediment-water interface. In well oxygenated settings, this layer is thoroughly to completely bioturbated.

2. *The transition layer:* This layer is much thicker and can range from 10s of centimetres to several metres in inter-tidal/upper shoreface sands. However, in truly mobile sandy substrates, this layer does not exist (Taylor *et al.*, 2003). The ichnofabric of this layer is largely determined by the ability of burrowing organisms to respond to changing physical and geochemical properties of the sediment (Bromley, 1996; Taylor *et al.*, 2003).

3. *The historical layer:* This represents the deepest layer where most active burrowing activity has ceased. The deepest burrowing (or deep tier) animals tend to overprint shallower burrowing (or shallow tier) communities, meaning that the historical layer has a taphonmical bias towards preserving deep tier burrowers.

The mixed layer tends to preserve a mottled fabric with few distinct trace fossils (e.g. Rodríguez Tovar *et al.*, 2011) when viewed in cross section. However, trace fossil communities preserved in turbidite depositional systems often preserve the mixed layer (or shallow tier) community on the sole of turbidite beds. Such communities are cast and exhumed from the pelagic muds by mildly erosive turbidity currents (e.g. Seilacher, 1977a, 1977b; Wetzel and Uchman, 1998). This background community are known as 'single layer colonisers' *sensu* Uchman (1995).

'Multi-layer colonisers' are deep tier burrowers that are the first to exploit newly deposited turbidite deposits and also exploit historical (i.e. buried) turbidites. These taxa represent the r-selected opportunistic taxa (e.g. Uchman, 1995; Tunis and Uchman 1996). These taxa are sometimes also referred to as crossichnia (e.g. Monaco *et al.*, 2007; Monaco *et al.*, 2010).

2.2.9 Ichnology in core versus ichnology at outcrop

There are many benefits and disadvantages of utilising ichnology in core based studies versus outcrop based studies, and vice versa (see Bromley, 1996; Knaust 2009b for a review).

Core based ichnological studies offer:

- Generally extensive vertical continuity that may offer a greater resolution of assessing facies successions than outcrop.
- Core is largely unweathered offering a freshly cut, often polished surface.
- Core is often obtained from wells that have been strategically drilled (by the oil industry for instance), allowing intra-well correlations to be made.
- Cored wells usually have large amounts of supplementary geophysical data (e.g. wireline logs) available, meaning that ichnology can act as a powerful supplementary tool in broad scale, multi-proxy environmental interpretations, rather than as a supplementary tool to support sedimentological observations alone.

Outcrop based studies offer:

- Much greater lateral continuity than the narrow (c. 15cm) window offered when viewing core. This enables lateral changes in trace fossil assemblages (abundances diversity, bioturbation intensity etc) to be quantified rather than inferred.
- Horizontal/bedding plane views of trace fossils can largely only be observed at outcrop. In the rare instances where a trace fossil is preserved at a section of broken core, only taxa that are smaller than the diameter of the core can be accurately represented.

- Outcrop studies allow both vertical and horizontal ichnodata to be obtained. However, it should be noted that vertical ichnological observations (i.e. bed cross sections) are often limited at outcrop. This is particularly true of mudstones that characteristically display fissile weathering profiles.

The limited vertical resolution of outcrop ichnological studies means that one of the primary limitations is accurate recognition of tiering profiles. It is often difficult to assess tiering profiles beyond the differentiation of 'shallow versus deep tier' (see section 2.2.7). Recognising cross-cutting relationships is largely limited to observations made when analysing bedding planes. The most valuable ichnological observations that can be made at outcrop therefore are the presence/absence and/or variations in the relative abundance of ichnotaxa. This approach largely falls within the ichnofacies method.

The ichnofabric approach offers a much greater resolution than ichnofacies in the analysis of tiering profiles and the recognition of key stratal surfaces, such as omission, hiatus and sediment bypass surfaces. However, these factors, particularly tiering profiles, are much easier to recognise in core than in outcrop based studies. As such, the ichnofabric method is arguably more effective in core than at outcrop.

This brief review of ichnofacies and ichnofabrics goes some way to highlighting the seemingly bipartite world of modern ichnology. However, ichnofacies and ichnofabrics often overlap in their approach. While it may be true that ichnofacies are much more dependent upon specific trace identification than ichnofabrics, both techniques still recognise key taxa as being of environmental significance. Perhaps the biggest area of overlap is ethology. Given that trace

fossils essentially represent 'fossil behaviour', both techniques are heavily reliant upon interpreting the ethology of preserved trace fossils to aid in environmental interpretations.

Cummings and Hodgson (2011b, see chapter 5) do not explicitly use either an ichnofacies or an ichnofabric approach, when using deep-water trace fossil assemblages to aid in the discrimination between sub-environments preserved within submarine fans. However, comprehensive taxa lists per environment are presented (ichnofacies but without assigning a specific ichnofacies!), combined with ethological data per environment (ichnofacies and ichnofabric), tiering and cross cutting relationships (ichnofabric, although this element is limited in vertical profile) and identifying potential ichnoguilds (ichnofabric).

Recent work by Rodríguez-Tovar *et al.* (2011) utilised a traditional ichnofabric approach (without explicitly erecting various ichnofabrics) by sampling bedding planes at outcrop and then polishing the slabs in a laboratory. They then documented ichnological data based on these polished cross sections. This potentially provides an exciting way of truly exploiting the potential of ichnofabrics at outcrop. However, the logistics of collecting enough samples to evaluate ichnological changes on a long temporal scale may limit this approach. However, Philips *et al.* (2011) successfully use an ichnofabric approach at outcrop, in interpreting palaeoenvironmental and depositional changes. Unlike Rodríguez Tovar *et al.* (2011), Philips *et al.* (2011) use ichnofabrics without the need to take samples to polish.

CHAPTER 3

GEOLOGICAL BACKGROUND

3.1 STUDY AREA

3.1.1 Introduction

The study area is in the Basque Country, northern Spain. Extensive coastal outcrops of Upper Jurassic to mid-Eocene age crop out between Bilbao in the west and Hondaribbia (on the French border) in the east. Overall, the outcrops record late Mesozoic to early Cenozoic deposition of sediments in a deep-marine trough, the Basque Basin, with an approximate ESE - WNW orientation (e.g. Crimes, 1976; Van Vliet, 1978, 2007; Hodgson and Wild, 2007). Early benthic foraminiferal studies suggested a water depth of 1000-4000m (e.g. Kruit *et al.*, 1975). More recently, Alegret *et al.* (2009) estimated a palaeobathymetry of c.1000m (middle-lower bathyal environment) for the basin during the earliest Eocene, based on benthic foraminifera. This is consistent with sedimentological estimates made by Pujalte *et al.* (1998) and micropaleontological estimates made by Orue-Etxebarria *et al.* (1996). Palaeocurrent measurements, stacking patterns and geographic distribution of thicker bedded sandstone units suggest a general east-west, proximal-distal relationship in the basin (Van Vliet, 1978, 2007; Pujalte *et al.*, 1995; Winkler and Gawenda, 1999; Hodgson and Wild, 2007).

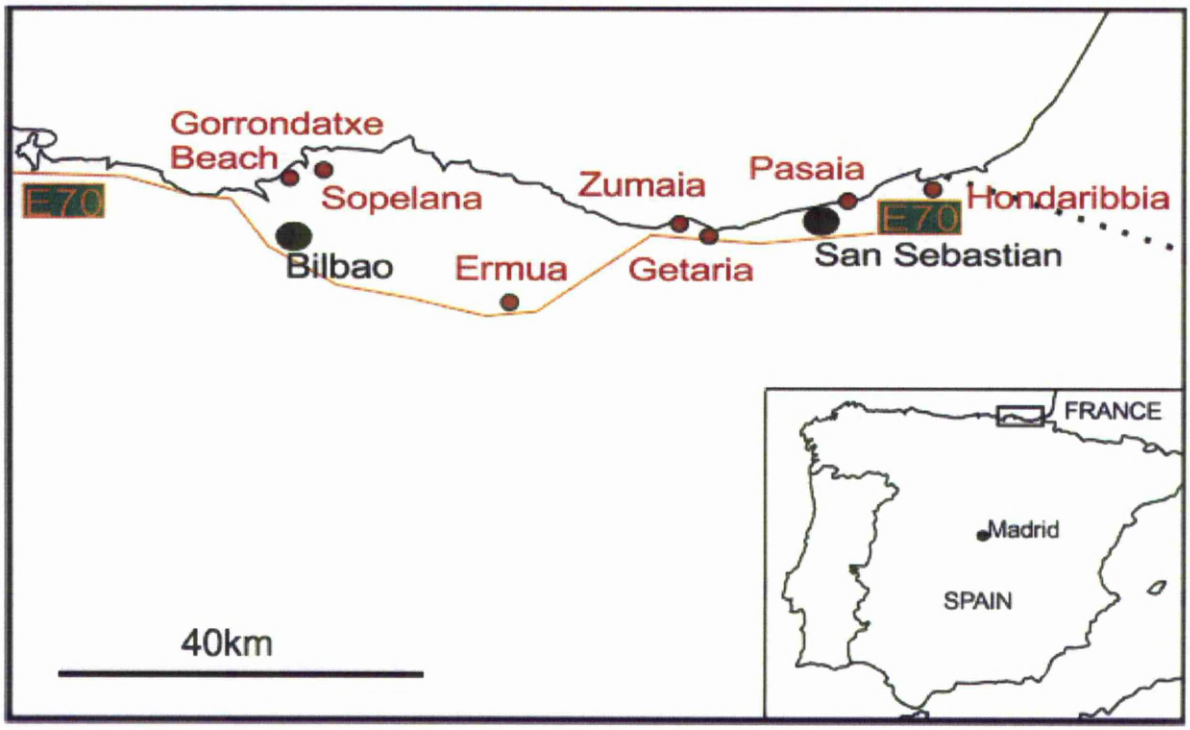

Fig. 3.1 Geographical map displaying location of Basque Country on northern Spanish coast (inset). Studied localities are marked by red dots. Major urban centres are represented by larger black dots. E70 is the major motorway that runs through the provinces of Guipuzkoa and Bizkaia. More detailed maps included geological context and actual outcrop locations are included in individual chapters.

3.1.2 Palaeogeographic and tectonic setting

During the late Mesozoic/early Cenozoic, the Basque Basin was located at c. 35°N (Plaziat *et al.*, 1981; Smith *et al.*, 1994), farther south than it is today. The elongate deep marine trough that comprises the study area was surrounded by pene-contemperaneous shallow water carbonate platforms (e.g. Pujalte *et al.*, 1995; Pujalte *et al.*, 1998). Sediments delivered to the deep basin were shed from the Aquitanian basin to the north-east and the South Pyrenean foreland basin to the south-east (Van Vliet, 1978; Hodgson and Wild, 2007). The Basque Basin was initiated through rifting in the Bay of Biscay during the early Cretaceous. By the early Eocene the basin

had been incorporated into the fold and thrust belt/foreland basin complex associated with the Pyrenean orogeny. This orogenic episode was driven by collision of the European and Iberian plates, creating two foreland basins located on the north and south sides of the main thrust zone (Verges *et al.*, 1995).

The South Pyrenean foreland basin comprised flanking shallow water carbonate depositional systems with the foredeep being infilled by approximately 4000m of siliciclastic turbidites sourced from fluvio-deltaic systems to the south (e.g. Pickering and Corregidor, 2000, 2005; Heard and Pickering, 2008). The north Pyrenean foredeep (i.e. the Basque Basin) was infilled by approximately 2500m of (predominantly) siliciclastic turbidites and hemipelagites. Typically, this depositional system is referred to as the Higuer-Getaria Formation (e.g. Pujalte *et al.*, 2000; Alonso-Zarza *et al.*, 2002; Hodgson and Wild, 2007; see chapter 3.1.3 for detailed stratigraphic discussion).

The Basque Basin sits on a metamorphic and plutonic basement. The oldest sediments are Permo-Triassic red beds and evaporites, with shallow water carbonates dominating from the Jurassic to the earliest Cretaceous (Van Vliet, 1978). Deep-marine (lower bathyal – upper abyssal depths) sedimentation commenced in the earliest Cretaceous and persisted until at least the mid-Eocene (e.g. Winkler and Gawenda, 1999; Gawenda *et al.*, 1999; Bernaola *et al.*, 2006a, 2006b; Rodríguez Tovar *et al.*, 2010). Continued compressional tectonics during the latest Eocene to the mid Miocene led to basin inversion, meaning sediments of mid-Eocene to younger are not exposed along the coastline (Alonso-Zarza *et al.*, 2002).

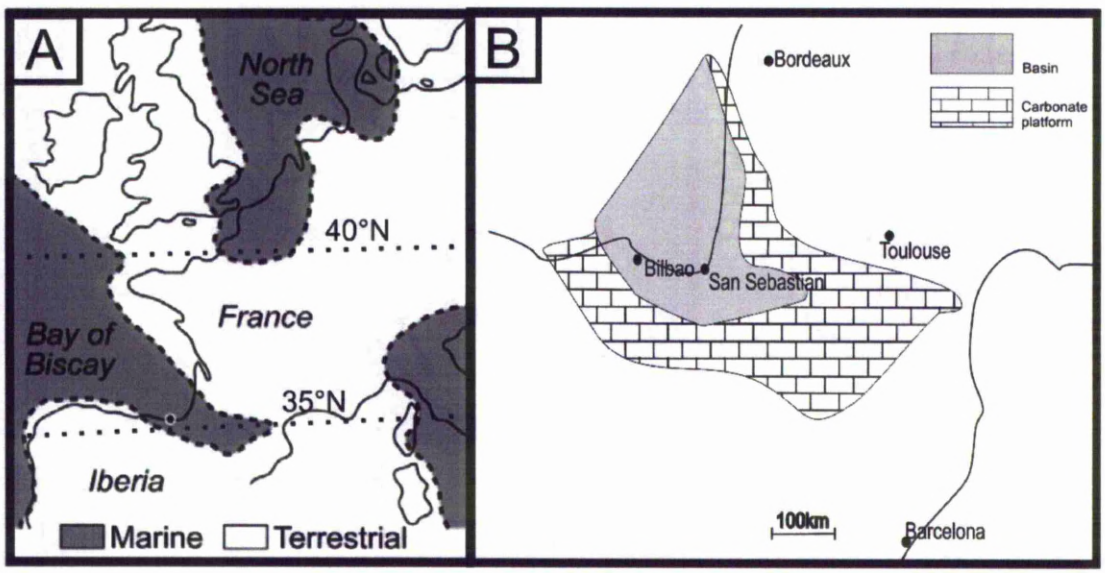

Fig 3.2 A.) Palaeographic map of Western Europe (early Palaeogene) showing continental versus marine deposition (modified from Bernaola *et al.*, 2009; Palaeolatitudes inferred from Plaziat *et al.*, 1981; Smith *et al.*, 1994). B.) Palaeogeographic map showing the extent of the carbonate platform bounding the Basque Basin (modified from Schmitz *et al.*, 2001).

Overall, the outcrops exposed in the Basque region represent a broadly northward-dipping (20° - 50°) monocline that is locally interrupted by diapirism of Triassic evaporites in the Zarautz area (e.g. Hanisch, 1974; Van Vliet, 1978; Hodgson and Wild, 2007). This disturbance has led to a regional divergence of strike being diverted to the north, with dips increasing or even overturning (e.g. at Orio, see also Van Vliet, 1978).

3.1.3 Stratigraphy

Due to the excellent outcrop exposure and largely continuous stratigraphy from the Santonian to the Lutetian/Thanetian (e.g. Winkler and Gawenda, 1999; Gawenda *et al.*, 1999) the Zumaia succession is of world renown and as such has been extensively studied. Studies include:

- Multiple studies on late Cretaceous ammonites and inoceramids (e.g. Wiedmann, 1988; Ward *et al.*, 1991; Ward & Kennedy, 1993; Smith *et al.*, 1999; Smith and Jeffery, 1999).

- Late Maastrichtian to lower Paleogene calcareous nannoplankton (e.g. von Hillebrandt, 1965; Orue-Etxebarria, 1983; Bernaola *et al.*, 2009).

- Magnetostratigraphy and cyclostratigraphy (Roggenthen, 1976; Ten Kate & Sprenger, 1993; Pujalte *et al.*, 1995; Dinarès-Turell *et al.*, 2002; Payros *et al.*, 2007).

- Chronostratigraphic boundaries such as the Cretaceous/Paleogene (Lamolda *et al.* 1988; Lamolda & Gorostidi, 1992; Apellaniz *et al.*, 1997; Arenillas *et al.*, 1998), the Danian/Selandian (Schmitz *et al.*, 1998; Bernaola *et al.*, 2009), and the Palaeocene/Eocene (Canudo *et al.*, 1995; Schmitz *et al.*, 1997; Baceta *et al.* 2000; Dinarès-Turell *et al.*, 2002; Alegret *et al.*, 2009).

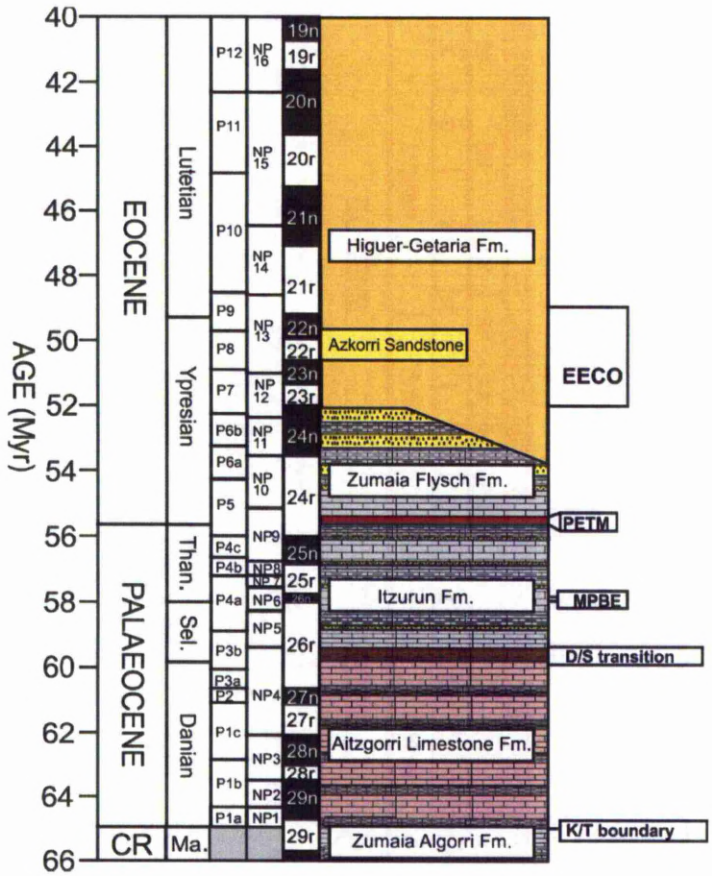

Fig 3.3 Biochronostratigraphic framework of the Basque Basin (modified from Bacetta *et al.*, 2004). Planktic foraminifera biozones (P) after Berggren *et al.* (1995), Calcareous nannofossil zones (NP) after Martini (1971), Polarity chrons after Bacetta *et al.* (2004), Payros *et al.* (2007), and refs therein.

3.1.4 Lithostratigraphy

The Danian Limestone Formation (Appelaniz* et al. *1983)/ Aitzgorri Limestone Formation (e.g. Bernaola* et al., *2009)

This formation spans the base Danian to the Danian-Selandian transition and comprises intercalated indurated limestones and marlstones. The limestones predominate over the marlstones throughout the Danian. Turbidites form only a minor component of the formation and

are predominantly calcareous although a minor siliciclastic component occurs. This formation is age equivalent to Rosell *et al.* (1985) San Telmo Red Carbonate Sequence. (see Fig. 3.4)

The Itzurun Formation (Baceta* et al., *2004)

The base of the Itzurun Fm. is marked by a sharp transition from rhythmic couplets of limestone/marlstones of the Danian Limestone Fm. to a red marl/clay rich interval at the base Selandian. The formation is dominantly carbonate but is much more variable than the underlying Danian limestones in that some intervals are more marl rich than limestone rich. Also, turbidites form a more significant component of the deposits. Calcareous turbidites are still the dominant type but from the mid-late Palaeocene (Thanetian onwards) siliciclastic turbidite deposition becomes much more frequent (e.g. Crimes, 1973; Winkler and Gawenda, 1999; Gawenda *et al.*, 1999; Baceta *et al.*, 2004). The top of the Itzurun Fm. is marked by a green glauconitic limestone that marks the base of the CIE at the onset of the PETM (i.e. the Palaeocene-Eocene boundary). This is approximately age equivalent to Rosell *et al.*, (1985) Lower San Telmo Sequence (see also Fig. 3.4). However, the lower San Telmo Sequence overlaps into the overlying Zumaia Flysch.

The Zumaia flysch (e.g. Bernaola* et al., *2009)

At Zumaia, the stratigraphy overlying the PETM is informally referred to as the Zumaia flysch. Alternations of hemipelagic limestones/marlstone dominate in the earliest Eocene. However, as the Eocene progresses, an increase in siliciclastic sedimentation is recorded. Winkler and Gawenda (1999) refer to this as the 'transitional system'. By the onset of the NP12 biozone (Martini, 1971, see also Winkler and Gawenda, 1999; Gawenda *et al.*, 1999), sedimentation becomes exclusively siliciclastic (the siliciclastic system of Winkler and Gawenda, 1999). Thin

bedded low-concentration turbidites and hemipelagic claystones and siltstones are the dominant deposits, with an increasing amount of thicker bedded (upper dm-scale) turbidites also evident as the Eocene progresses. Occasional m-scale high-concentration turbidites are also present towards the top of the Zumaia succession. The lower most Zumaia Flysch Fm. is age equivalent to Rosell *et al.* (1985) Lower San Telmo Sequence. The influx of siliciclastic turbidites towards the top of Winkler and Gawenda's (1999) transitional system marks the boundary between the Lower San Telmo and Upper San Telmo Sequence (see Also Fig. 3.4).

The Higuer Getaria Formation (Pujalte* et al., *2000)

The Higuer-Getaria Fm. comprises c. 2000 - 2500m of siliciclastic turbidites and hemipelagites (Pujalte *et al.*, 2000; Hodgson and Wild, 2007). The deposits comprise proximal base of slope (channel-lobe transition, proximal lobe), lobe (lobe axis, lobe off-axis, lobe fringe) and distal fan fringe – basin plain deposits. Van Vliet (1978, 2007) and Hodgson and Wild (2007) recognise the presence of at least five 'lobe megacycles'. The base of each of these megacycles is marked by an abrupt increase in sandstone bed thickness from upper cm-scale beds to metre scale beds. Each megacycle ranges in thickness from 20 – 70m thick. Sandstones become increasingly amalgamated upwards and individual beds (that probably represent rapidly deposited, amalgamated units) may reach up to 15m thick at the top of each megacycle. These units are interpreted to represent progradational stacking of depositional lobes. The top of each megacycle is marked by an abrupt decrease in bed thickness (back down to cm-scale) and increase in mud content. The basal beds and heterolithic units overlying the tops of megacycles can be used as marker beds for correlation purposes. The Higuer-Getaria Fm. can be subdivided into the Sarikola Sequence (oldest), The Hondaribbia Sequence and the Jaitzkibel Sequence (youngest; Rosell *et* al., 1985).

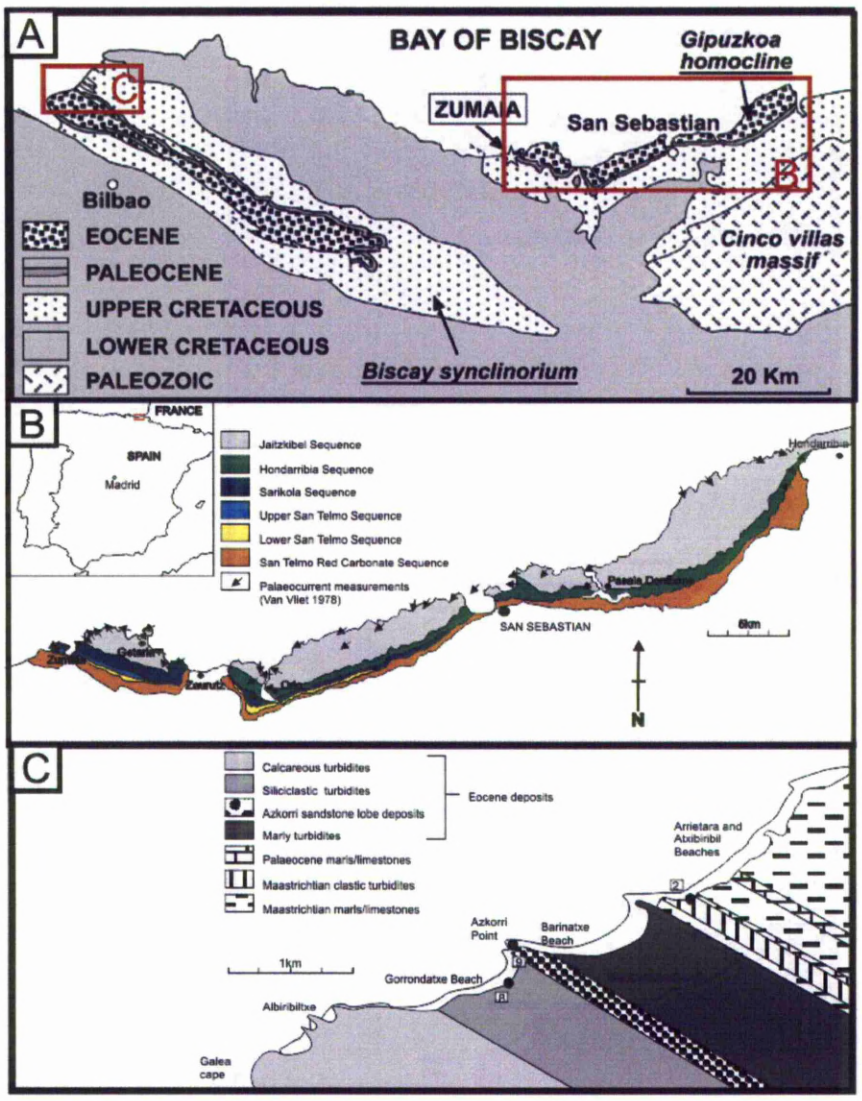

Fig 3.4 Geological setting of the study area. A.) General geological map of the Basque Country (Bizkaia and Guipuzkoa regions, from Bernaola *et al.*, 2009). B.) Geological map of Guipuzkoa (Zumaia to Hondaribbia) showing exposures of sequences defined by Rosell *et al.* (1985, after Hodgson and Wild 2007, Palaeocurrents from Van Vliet, 1978). C.) Simplified geological map of the Sopelana area (modified from Bernaola *et al.*, 2006).

3.1.5 Sedimentary facies and depositional environments

The Basque Basin can broadly be divided into proximal lobe related environments of deposition and more distal fan fringe and basin floor related environments of deposition. Palaeocurrent

measurements and stacking patterns of thicker bedded sandstone units suggest a general east-west, proximal-distal relationship in the basin (Van Vliet, 1978, 2007; Hodgson and Wild, 2007). Below is a summary of the main sedimentary facies associations and their interpreted environments of deposition along an approximate east to west transect along the present-day coastline.

Hondaribbia – San Sebastian (Channel-lobe transition and proximal lobe deposits)

Sedimentary facies associations alternate between poorly exposed thin-bedded successions and well exposed thick-bedded successions. Typically, thin-bedded successions are 15-40 m-thick. The tops of thin-bedded packages are marked by a sharp transition into overlying thick-bedded packages. Thick-bedded intervals range in thickness from 20-80 m-thick. From east to west, the proportion of thick-bedded sandstone units decreases. Paleocurrent measurements (Hodgson and Wild, 2007) support the interpretation of Van Vliet (1978) that this reflects a general proximal to distal down dip trend

Thin-bedded sedimentary facies association:

Description: Typically, thin-bedded (0.05 - 1 m-thick) sandstone successions form overall coarsening-and thickening-upward packages. Sandstones are interbedded with marlstones and mudstones. Typically, at the base of thin-bedded successions is a mudstone-prone unit with normally graded sharp-based very fine-grained sandstone and siltstone beds, with basal tool markings and common parallel to ripple cross laminated divisions. As the coarsening-and thickening-upward trend continues, normally graded medium- to fine-grained sandstone beds, up to 1 m-thick, with parallel and ripple laminated upper divisions become common. Thin sandstone beds are continuous at the scale of the outcrop.

Interpretation: Normally graded bedding, bed base flutes and grooves and parallel- ripple laminated divisions indicate that the thin-beds were deposited from low-density turbidity currents. Thin-bedded successions are interpreted to accumulate towards the fringe of a lobe complex (*sensu* Prélat *et al.*, 2009). The common coarsening- and thickening-upward packing of beds suggests overall basinward stepping of the deep-water system with increasing sediment supply. The sedimentary facies, stacking pattern, and package geometry is not consistent with an external levee or channel margin interpretation.

Thick-bedded sedimentary facies association:

Description: Hodgson and Wild (2007) identified two types of thick-bedded sandstones. Type A are sharp based and weakly erosive (rare flutes) 0.5-5 m-thick fine- to medium- grained sandstone beds. Normal grading is observed at bed bases, which are locally loaded, and at bed tops. Although the beds are dominantly structureless, the upper parts preserve parallel to convolute lamination. The geometry of the beds is tabular, with individual beds traced on a kilometre-scale. Locally, beds preserve concentrations of de-watering phenomena, in particular dish and pipe structures, which mark amalgamation surfaces forming sand-on-sand contacts. Commonly, laterally persistent thin (0.05-0.15 m-thick) mudstone layers can separate amalgamated sandstone sheets for 100's m down dip and along-strike (Hodgson and Wild, 2007).

In contrast, Type B thick-bedded sandstones are thick (0.5-9.0 m-thick) fine- to granule-grained sandstones with metre-scale erosive or loaded bed bases that are locally associated with mudstone clast conglomerates and large flakes of biotite mica. Type B units are generally structureless in appearance, with cross-lamination locally observed, and contain numerous

internal grain-size breaks and pervasive de-watering phenomena that highlight common amalgamation surfaces. Granular grade material is dominantly composed of angular and sub-angular quartz grains and mica flakes, with subordinate amounts (5-10%) sub-rounded to well rounded quartz grains. Amalgamated units are traced for kilometres, although individual beds can be highly lenticular due to erosion and amalgamation. Towards the extreme east of the study area (sea cliffs close to Cabo Higuer/Hondaribbia), m-scale cross bedding is evident in beds of medium to very coarse sand grade. Scour/incision surfaces up to 2-3 m deep are evident within amalgamated units but beds still generally maintain tabular geometries.

Interpretation: In Type A beds, the basal normal grading, flutes and grooves, and upper parallel laminated divisions indicate that Type A beds were deposited from turbidity currents. Convolute lamination indicates de-watering processes, and regular amalgamation surfaces suggest high frequency emplacement of multiple turbidity current events. The low amounts of erosion, the common coarsening- and thickening-upward signature, and their sheet-like geometry indicate that the beds were deposited in a lobe complex off-axis setting (*sensu* Prélat *et al.*, 2009). Bed grading, common erosion and amalgamation surfaces, and pervasive dewatering structures indicate that Type B beds were deposited from high-density turbidity currents. The coarse grain-size and low textural maturity of Type B beds indicate limited time spent in the sediment transport system from erosion in the hinterland to deep-water deposition. Lenticular bed geometries and laterally discrete packages of this sedimentary facies indicate erosional confinement, and support a proximal (base-of-slope?) lobe complex axis setting (*sensu* Prélat *et al.*, 2009). Coarse grained, cross-stratified units seem to imply channelling but no true channel geometries are observed. This suggests that incision was limited to ephemeral scour surfaces incised within the main axial zone of lobe deposition. The commonly observed coarsening and

thickening up stacking pattern of such deposits suggest a progradational lobe complex stacking. Mudstone clast conglomerates that mantle erosion surfaces indicate some sediment bypass to the deeper basin.

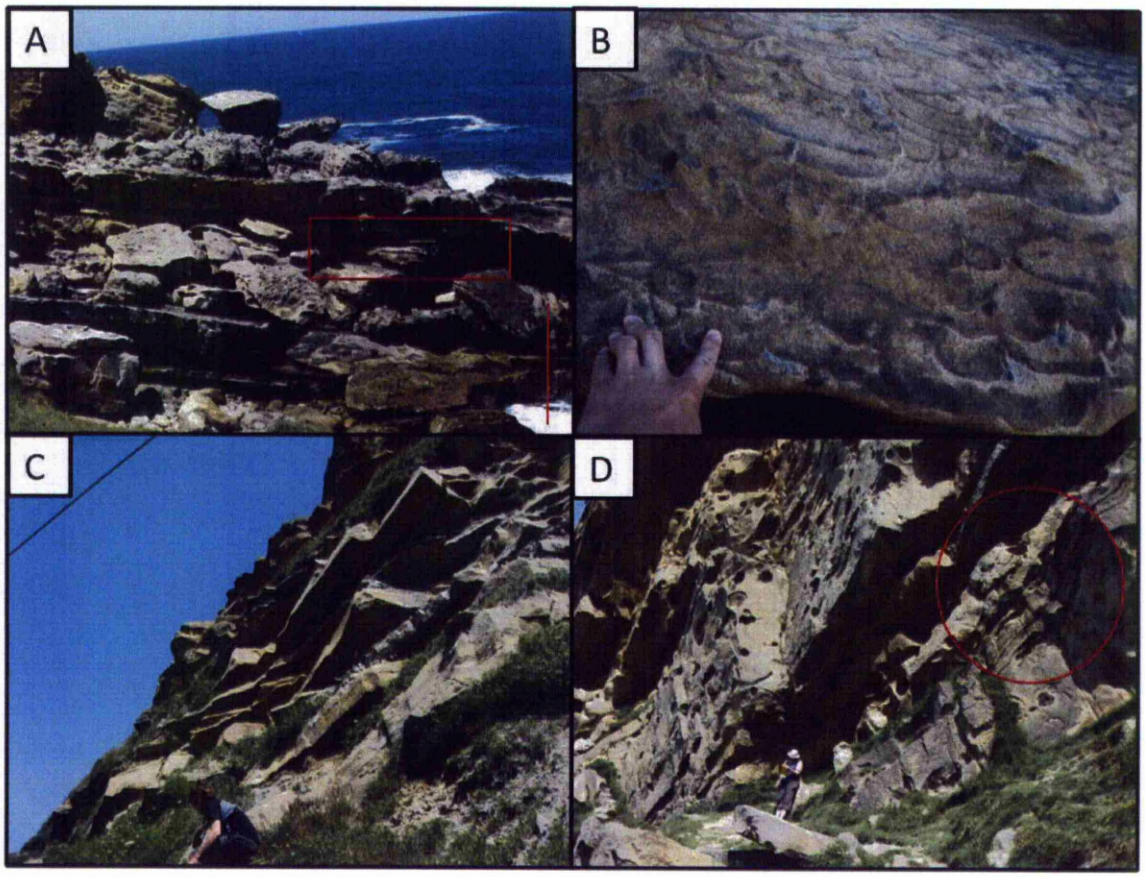

Fig 3.5 Photo panel of facies in the Hondaribbia area. A.) Upper dm- to m-scale beds of medium to coarse grade sandstone preserving crude stratification and localised cross bedding (highlighted, scale bar = 2m). These represent tractional grain flows. This environment was interpreted as the channel-lobe transition. B) Well developed dish structures (fluid escape) highlighted by variations in silt content, in a m-scale, medium grained, lobe complex axis sandstone. C.) Base of a lobe complex. The vegetated area preserves cm-scale heteroliths that can be seen to abruptly coarsen and thicken up into massive based sandstones with crude horizontal stratification in their upper portions D.) Upper part of the same lobe complex. Beds are now up to granular grade and the uppermost beds

exceed 5m in thickness. Note how the c. 3m thick sandstone (highlighted) preserves stratification in its upper portion. This is a characteristic feature of such beds throughout the basin.

Orio - Zauratz (including external levee complex)

The deposits on the western bank of the Orio River comprise some of the more complicated stratigraphy encountered throughout this study. The main studied section is overturned, in contrast to the generally northward dipping Guipuzkoa monocline. It is possible that the overturned beds resulted from diapirism of Permo-Triassic evaporites. These deposits onlap abruptly onto the same diapiric structure. Hansich (1974) suggested that the deposits in this area result from shedding of material from the incipient diapir. However, Van Vliet (1978) challenges this on the basis of the presence of well rounded pebbles in coarser beds that could not have formed in a diapiric salt mass, concluding that a shallow marine source for the pebbles is the most satisfactory explanation.

Thin bedded distal fan/lobe fringe deposits can be seen to abruptly coarsen and thicken up in a similar manner to the progradational lobe megacycles identified in the east of the Basin by Van Vliet (1978, 2007) and Hodgson and Wild (2007). Thicker bedded units display massive bases but often are crudely planar stratified at their tops. Units display an upward increase in amalgamation and dewatering phenomena (dish and pipe structures). The main succession of interest in this area overlies the uppermost thick bed of such a coarsening and thickening up package.

Description: Upper cm- to lower dm-scale beds of very fine to fine-grained sandstones rhythmically interbedded with mudstones of a similar thickness. Sandstones are predominantly planar to ripple laminated and grade up into overlying siltsones (Tbcd). Commonly, ripple sets

are climbing with stoss-side preserved laminae. Mud drapes are occasionally preserved in the ripple sets. Sole marks are rare with only occasional minor flute casts that co-occur on bed bases with pre-depositional graphoglyptid trace fossils. Minor scouring (cm-scale) is rarely observed. The overturned nature of these beds means that their most characteristic feature is the diverse pre-depositional trace fossil communities preserved on the soles of the beds. Mudstone interbeds are predominantly siliciclastic with occasional marlstones. Bed thicknesses appear quasi-rhythmic with no obvious thickening/thinning profiles. The thin bedded succession is underlain by a coarsening and thickening up sandstone succession similar to such sequences in the San Sebastian – Hondaribbia area. The uppermost bed of this coarsening and thickening up package is a c. 2m thick high concentration turbidite. However, unlike most high concentration thick bedded turbidites, this one lacks a crudely stratified (low concentration) cap. Instead, pebble to cobble (and locally boulder) grade mudstone clasts are concentrated towards the top of the bed. Common carbonaceous clasts are also evident in the top of the bed.

Interpretation: Ripple cross lamination forms by deposition from strongly depositional flows. Such deposits often occur when a flow breaches its confinement, in an overbank setting for instance. However, increasing rates of climb within ripple trains indicates rapidly increasing rates of sediment fallout. Such deposits are commonly recorded in external channel levee settings (*sensu* Kane and Hodgson, 2011). The rhythmic, thin bedded nature with minimal erosion is also consistent with (but not exclusive to) a channel levee setting (e.g. Kane *et al.*, 2007; Kane and Hodgson, 2011).

The thick bedded, coarser grained deposits are more ambiguous than the thin bedded unit. The thick bed underlying the basal bed of the thin bedded succession preserves mudstone clasts up to cobble grade and common coaly debris concentrated towards the top of the bed. This bed represents an attached debrite. Turbidites with linked debrites are thought to predominate in confined depositional settings (e.g. Haughton *et al.*, 2003; Amy and Talling, 2006), although have been identified in channelised settings (e.g. Haughton et al. 2009). In unconfined settings, they have been reported as occurring in the fringe of submarine lobes (e.g. Hodgson, 2009). The tabular nature of even the thickest beds observed in this study suggest a sheet like, and therefore unconfined, depositional setting. The thick (c. 2m) nature of the bed would seem to suggest that it was not deposited in a distal position within the fan/lobe. However, the overlying thin bedded succession interpreted as an external levee succession suggests that the underlying thick bedded succession may therefore represent the axis to a base-of-slope lobe complex. The significance of the linked debrite therefore remains enigmatic. Van Vliet (1978) suggests that some of the coarsening and thickening up packages, where tabular geometries may not be evident (due to limited exposure etc) may represent channel-fills. The thickening and coarsening up profile (as opposed to a classic fining and thinning up channel 'back-fill') may record channel migration with the thicker, coarser beds representing deposition in more axial zones of the channel.

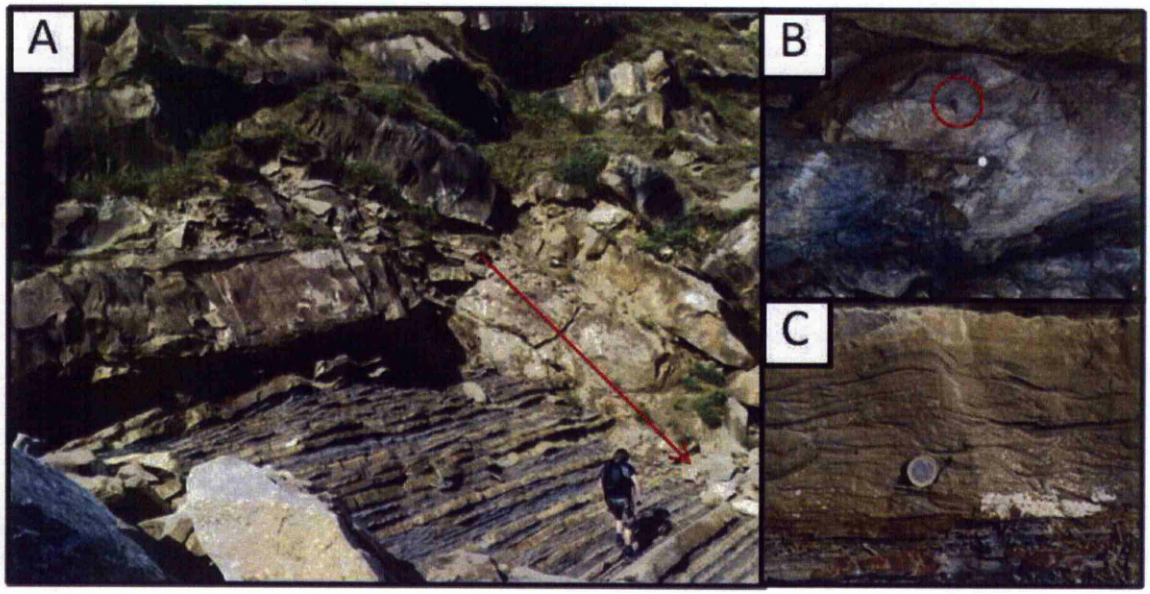

Fig. 3.6 Photo panel of facies located on western side of Orio estuary. A.) Abrupt transition from thick bedded (m-scale) high concentration turbidites to dm- to cm-scale low concentration turbidites, interpreted to represent an external levee (*sensu* Kane and Hodgson, 2011). Red arrow shows younging direction (i.e. overturned beds). Boulder grade siltstone clast preserved at the top of the uppermost thick bed in A. Note presence of coaly debris (highlighted), suggesting short residence time on the shelf (1€ coin for scale). C.) Climbing ripple lamination preserved in the levee facies (note photograph has been rotated so appears right way up).

Getaria – Zumaia (lobe off-axis/lobe fringe – fan fringe – basin floor)

The deposits preserved to the west of Getaria essentially represent the distal expression of those preserved in the eastern part of the basin around the Hondaribbia area (e.g. Van Vliet, 1978, 2007). Moving westwards from Getaria towards Zumaia, the same east-west proximal-distal relationship can be observed. However, to the east of Zumaia, coastal outcrops preserve exclusively Eocene aged deposits (e.g. Crimes, 1973, 1976: Van Vliet, 1978, 2007). The Zumaia section itself however preserves complete stratigraphy from the Santonian to the Lutetian/Thanetian. As such, a range of depositional settings/environments are preserved.

Thick bedded sedimentary facies association:

Description: Thick bedded facies are best preserved on the main coastal road between Getaria and Zumaia. They comprise stacks of coarsening and thickening up lobe megacycles (Van Vliet, 1978, 2007). Individual sandstone bed thickness range from dm-scale at the base of megacycles, upto 4-5m thick at the top of each megacycle. Bed amalgamation is absent in the basal parts of megacycles but occurs locally in thicker beds towards the top of each cycle. Some of the thicker beds also display significant m-scale scours at their bases but still retain an overall tabular geometry. Sandstones of upper dm-scale and above tend to have massive bases with planar laminated tops although ripple cross lamination is also common towards the base of each megacycle. Even the thicker beds (>1m) rarely exceed upper fine grained sand grade. Bed soles preserve flute casts and tool marks but most beds of a thickness of less than 1m also preserve diverse pre-depositional trace fossil assemblages. This suggests limited erosive capacity of the turbidity current. Mudstone interbeds are almost exclusively siliciclastic. Mudstone beds decrease in thickness up through each megacycle from 30-50cm thick at the base to 2-5cm thick at the top (where bed amalgamation is absent).

Interpretation: The low amounts of erosion, the common coarsening- and thickening-upward signature, and the sheet-like geometry of sandstones, in this succession indicate that the beds were deposited in a lobe complex off-axis setting (*sensu* Prélat *et al.*, 2009). However, some of the more amalgamated packages at the top of megacycles display scour surfaces at their base and are interpreted as a lobe complex axis (*sensu* Prelat *et al.*, 2009).

Thin bedded siliciclastic facies association:

Description: Cm- scale very fine to upper fine-grained sandstone beds, with rare medium-grained sandstone beds, which commonly preserve planar lamination with rippled tops. Some thinner beds only preserve ripples. Climbing ripple lamination is not observed. Many beds are normally graded with thin siltstone upper divisions. Locally, some of the coarser beds have erosive bases (minor scours) but generally the bed soles preserve either flute casts, tool marks, graphoglyptid rich trace fossil communities, or sometimes a combination of these. Locally, thicker medium-grained sandstone beds (upper dm- to lower m-scale) erode into the thin bedded units. Mudstone interbeds are dominantly siliciclastic with rare marlstones. No obvious coarsening/thickening up signatures are observed.

Interpretation: The predominance of Tbc and Tde turbidite divisions, the lack of any coarsening/thickening stacking patterns, lack of erosion and presence of significant mudstone interbeds is consistent with a fan fringe depositional setting.

Limestone/Marlstone sedimentary facies association:

Mid-Cretaceous to lowermost Eocene sediments preserved in the Basque Basin are predominantly carbonate in nature.

Description: From the Santonian to the Danian-Selandian transition, indurated micritic limestones (essentially pelagic ooze composed of forams and coccoliths e.g. Van Vliet, 1978; Bernaola *et al.*, 2009) dominate, with subordinate marls and marly limestones. Bed thicknesses (limestone and marlstone) vary between 5-60cm. A distinct red marlstone interval marks the Danian-Selandian transition. Above this unit, the ratio of limestone:marlstone becomes variable with some intervals being marlstone dominated rather than limestone dominated. Average bed

thickness is around 5-10cm although some limestone beds occasionally exceed 40cm thickness. The limestones lack stratification. The marlstones are highly fissile but appear to also lack stratification. Thin bedded (<5cm thick) turbidites are predominantly calcareous. They tend to have structureless bases and rippled tops although occasionally, planar laminated (Tb) divisions are evident. Towards the uppermost Palaeocene, siliciclastic turbidites become increasingly common. Grain size in both the calcareous and siliciclastic is predominantly very fine to fine sand.

Interpretation: The lack of sedimentary structures in the limestones means they are not characteristic of any particular depositional setting. However, the occasional intercalations of calcareous and/or siliciclastic turbidites suggests a basinal setting. The mixed nature (calcareous versus siliciclastic) of the turbidites is well constrained as representing differing provenence. The calcareous turbidites being sourced from collapse of pene-contemperaneous shallow water carbonate platforms, with the siliciclastic component being sourced from supply triggered by the incipient Pyrenean orogeny (e.g. Crimes, 1973, 1976; Van Vliet, 1978, 2007; Winkler and Gawenda, 1999).

Some slumping is evident in limestone dominated sections suggesting an unstable slope setting. However, the predominance of the limestone/marlstone beds in the basin display tabular geometries suggesting deposition on a low gradient (i.e. not the slope). Trace fossil assemblages typical of the *Zoophycos* ichnofacies also seem to suggest a slope setting. The *Zoophycos* ichnofacies in its original application was slotted into such a slope setting in Seilacher's (1967) original bathymetric model. However, in modern sediments, *Zoophycos* has been recorded at abyssal depths in basin plain settings (e.g. Bromley, 1996; Uchman, 2003). It is now widely accepted that trace fossils representative of the *Zoophycos* ichnofacies not only occur in slope

settings but are also characteristic of basin plain settings that are beyond the reach of turbidity currents (e.g. Uchman, 2003). No direct sedimentological observations corroborate Crime's (1973, 1976) inference that the transition from the *Zoophycos* to the *Nereites* ichnofacies records an increase in water depth in the basin. As such, a basin plain setting is preferred here.

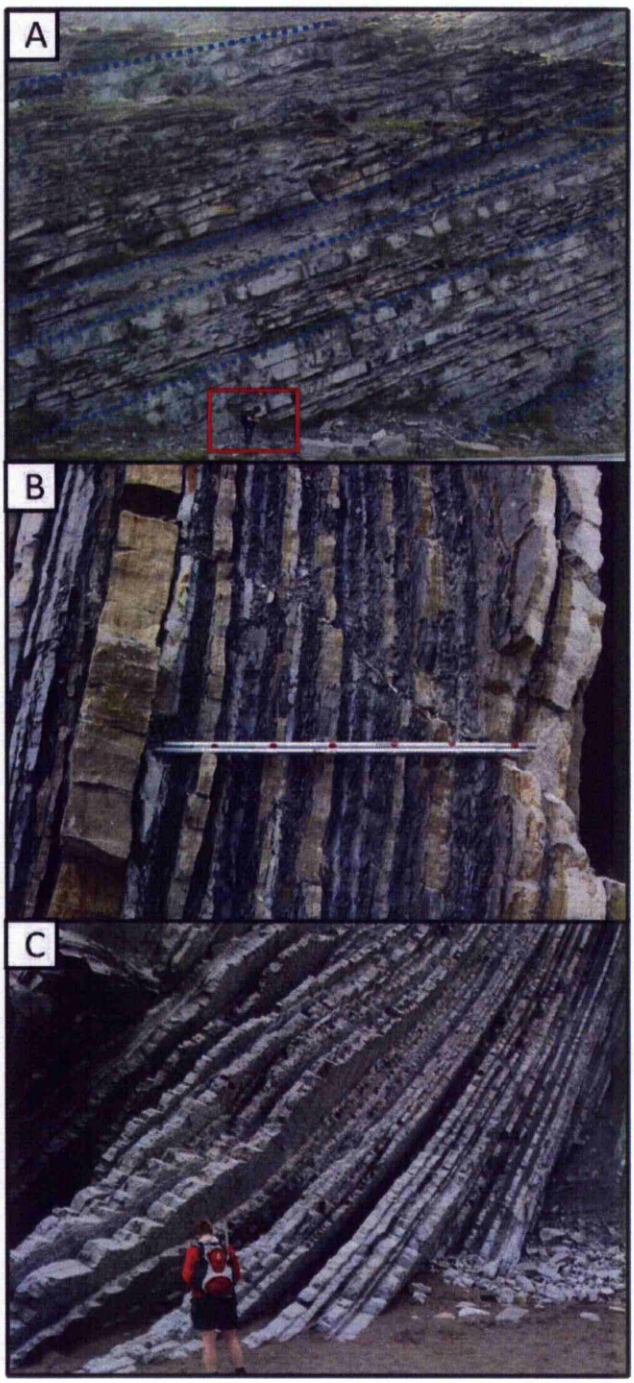

Fig 3.7 Photo panel of facies located between Zumaia and Getaria. A.) Early Eocene Lobe complex off-axis deposits located on the coast road between Zumaia and Getaria. Blue dashed line indicates tops and bases of coarsening and thickening up lobe complexes. B.) Fan fringe deposits located on Itzurun Beach, Zumaia (early Eocene). Note the light grey colour of the mudstone interbeds. These represent calcareous mudstones and marlstones. This is part of Winkler and Gawenda's (1999) transitional system. C.) Late Palaeocene basin plain carbonate deposits located on Itzurun Beach, Zumaia.

CHAPTER 4

AN AGRICHNIAL FEEDING STRATEGY FOR DEEP-MARINE PALEOGENE *OPHIOMORPHA* GROUP TRACE FOSSILS

ABSTRACT

Ophiomorpha group trace fossils occur abundantly in a range of Eocene-aged deep-marine environments of deposition in the Basque basin, northern Spain. The morphology and dimensions of several _Ophiomorpha_ group-related trace fossils observed in off-axis submarine lobe deposits are discussed. The reported specimens display a highly organised and systematic burrowing behaviour preserved on turbidite bed bases that display interconnecting 'Y'-shaped [hexagonal-polygonal] morphologies. This observation together with the cross-cutting relationship with tool marks suggests construction of post-depositional agrichnial burrow networks. The networks probably harvested microbes that broke down cellulose-based organic matter providing an exploitable nutrient source for crustacean trace makers of _Ophiomorpha_. Therefore, the _Ophiomorpha_ group-related traces discussed herein are postulated to represent an ethological response to changes in deep marine environmental conditions driven by global climate change during the early Paleogene including the early Eocene hyperthermal events.

4.1 INTRODUCTION

Paleontological analyses of body fossils are widely employed to infer the response of marine macrofauna to abrupt and transitional changes in past environmental conditions (e.g. Smith and Jeffery, 1998, Smith *et al.*, 1999). A detailed ichnological analysis, however, can potentially

provide a more powerful tool in quantifying the response of marine macrofauna to paleoenvironmental changes because trace fossil assemblages respond to many factors including variations in water temperature and salinity, benthic food supply and sedimentation rates (e.g. Frey *et al.*, 1990: Pemberton *et al.*, 1992). The habitats and bathymetric range that ichnotaxa are found in is not static through geological time. For example, in deep marine settings, the 'doomed pioneer' scenario (*sensu* Föllmi and Grimm, 1990) is less compelling when the number and organisation of ichnotaxa increases through time. When this is observed the implication is that such taxa were able to establish new habitats and behaviour in deeper marine settings rather than simply to survive transportation to deeper environments for a transient period.

Ichnology was included as part of a wider study investigating environmental change across the Paleocene Eocene Thermal Maximum (PETM) in the Basque basin, northern Spain. Several traces closely associated with *Ophiomorpha* bioturbation occur in early Eocene strata towards the east of the Basque basin (San Sebastián – Hondarribbia). Several sandstone beds that internally are bioturbated by sub-horizontal to sub-vertical *Ophiomorpha,* also preserve organised systematic network type burrows on the sole of the beds. The traces display interconnecting 'Y'-shaped burrows branched at ~120° that display partial hexagonal geometries suggesting a systematic feeding strategy that mimics *Paleodictyon* type networks in form. However, these traces are demonstrably post-depositional in origin and share many morphological/taxonomical features with *Ophiomorpha.*

4.2 DEEP-WATER ICHNOLOGY – TEMPORAL CHANGE

4.2.1 *Nereites* ichnofacies

The *Nereites* ichnofacies, representative of lower bathyal to abyssal water depth trace fossil communities (usually within turbiditic strata), only became established in the deep marine realm after the Cambrian (Crimes & Fedonkin, 1994; Orr, 2001). Agrichnial and pascichnial traces, typically associated with the *Nereites* ichnofacies, are important components of shallow marine strata of late Proterozoic – early Phanerozoic age, with vertical burrowing being limited until the early Ordovician. One hypothesis is that horizontal burrowers (including agrichnial and pascichnial taxa) migrated to deeper marine settings due to increased competition from vertical burrowing organisms. This would have necessitated biological adaptations through time to allow exploitation of deep marine ecological settings (Droser & Bottjer, 1993; Hagadorn & Bottjer, 1999; Orr, 2001). Taxa that later migrated to deep-marine environments actually developed behavioural optimisation (e.g. agrichnial feeding strategies) during the Cambrian whilst occupying the shallow marine realm (Crimes and Fedonkin, 1994). This suggests that such adaptations were governed more by benthic food supply and competition rather than water depth *per se.* Whilst significant colonization of the deep marine realm had occurred by the Ordovician (Crimes and Fedonkin (and refs. therein), 1994; Orr, 2001), this was not the end of deep-marine incursions by 'shallow' marine taxa.

4.2.2 *Ophiomorpha:* A shallow marine trace?

The *Ophiomorpha* group chiefly comprises *Ophiomorpha* Lundgren (1891), *Thalassinoides* Ehrenberg (1944) and *Spongeliomorpha* Saporta (1887). *Ophiomorpha*, a vertical to horizontal burrow displaying a distinct lining comprised of muddy pellets, first appeared in the Permian, where it exclusively exists in shallow water nearshore deposits (Bottjer *et al.*, 1987, 1988). Commonly, *Ophiomorpha* is considered one of the most reliable environmental indicators for this type of depositional setting (Frey *et al.,* 1978). Vertically inclined *Ophiomorpha* have been

proposed as being one of the major components of the *Skolithos* ichnofacies (e.g. Seilacher, 1967; Pemberton *et al.,* 1992; MacEachearn *et al.*, 2007) and are considered indicative of deposition above fair-weather wavebase (i.e. shoreface environments) according to the (passive) bathymetric scheme proposed by Seilacher (1967). Horizontally inclined *Ophiomorpha* are also included as major components of the *Cruziana* ichnofacies, representing the more distal, below fair-weather wavebase but above storm weather wavebase zone (shoreface-offshore transition zone) (e.g. MacEachearn *et al.,* 2007). However, *Ophiomorpha* is commonly identified in interpreted submarine slope and fan environments in Cretaceous and younger strata (Bottjer *et al.,* 1987, 1988; Tchoumatchenco & Uchman, 2001). *Ophiomorpha* is an important component of the *Nereites* ichnofacies in Paleogene strata leading to Uchman (2001) proposing the *Ophiomorpha rudis* sub-ichnofacies of the *Nereites* ichnofacies (see Uchman, 2009 for detailed discussion of the *O. rudis* sub-ichnofacies). This sub-ichnofacies is based on *Ophiomorpha rudis* and *O. annulata* being the most representative trace fossils of medium and thick-bedded sandstones in submarine channel, lobe axis and lobe fringe settings. This follows on from Książkiewicz's (1970, 1977) and Crimes' (1973) observations of differences within the *Nereites* ichnofacies based on proximal-to-distal relationships. This observation was also noted by Seilacher (1974) who proposed the *Nereites* (mud rich fan fringe – basin plain environment) sub-ichnofacies of the *Nereites* ichnofacies and the *Paleodictyon* (sand rich distal fan environments) sub-ichnofacies of the *Nereites* ichnofacies. Bottjer *et al.* (1987, 1988) investigated the onshore to offshore trends of *Ophiomorpha* (and *Zoophycos*) from Paleozoic to modern strata. They found that *Ophiomorpha* migrated to the deep marine realm by the Upper Cretaceous (c. 90Ma). However, Wetzel *et al* (2007) record *Ophiomorpha recta* in Late Triassic turbidites in Oman.

This is the oldest recorded occurrence of *Ophiomorpha* in an interpreted deep marine environment.

Tchoumatchenco & Uchman (2001) record occurrences of *Ophiomorpha* isp. and *Ophiomorpha annulata* in the Upper Jurassic-Lower Cretaceous sediments of the Kostel Formation (deep water turbidites) but the trace maker failed to establish a stronghold in the deep marine realm at this time. Tchoumatchenco & Uchman (2001) discussed whether the initial invasion was by 'doomed pioneers' (*sensu* Föllmi and Grimm, 1990) or whether the trace makers were only able to establish limited areas of refuge initially, but flourished later following improved oxygenation and/or benthic food supply to the deep-marine sea floor after the Cenomanian-Turonian anoxic event. By the early Eocene, *Ophiomorpha* had carved a niche in deep ocean environments, as it constitutes a major component of *Nereites* assemblages of this age (Uchman, 2003, 2004). However, it remains unclear what paleoenvironmental changes facilitated colonization of deeper settings. One hypothesis states that *Ophiomorpha* trace makers were able to exploit increases in terrigenous derived plant detritus, particularly angiosperm material (Uchman, 2003, 2004). However, little work has been undertaken to test this assertion. Another possibility is that *Ophiomorpha* simply exploited new food resources connected to increases in primary productivity associated with enhanced runoff and delivery of organic material to the oceanic realm. This may be a particularly pertinent point during the early Paleogene due to multiple extreme greenhouse warming events such as the Paleocene-Eocene Thermal Maximum (e.g. Kennett and Stott, 1991; Dickens *et al.*, 1995, 1997, Zachos *et al.*, 2001, 2005) that likely had profound effects on sediment supply to the oceans (e.g. Schmitz *et al.*, 2001; Egger *et al.*, 2002; Schmitz and Pujalte, 2003, 2007).

4.2.3 An agrichnial feeding strategy for *Ophiomorpha*?

An agrichnial feeding strategy for deep marine *Ophiomorpha* has been postulated previously (e.g. Uchman, 2004, 2009). Certain types of shallow marine *Thalassinoides* have also been identified as possible agrichnia (e.g. Ekdale and Bromley, 2003), along with the probable crustacean trace *Sinusichnus sinuosis* (de Gibert, 1996, de Gibert *et al.*, 1999) that has close affinity to *Ophiomorpha* group traces. Compelling modern analogues of this type of feeding are provided by several species of shrimp; *Callianassa, Callichirus* and *Upogebia,* who all construct *Ophiomorpha* type burrows (Ott *et* al., 1976; Frey *et al.*,, 1978; Bromley, 1996). Deep marine trace fossils representative of the *Nereites* ichnofacies are composed of complicated geometric patterns (star and net shapes) and elegant, regular meanders that have been interpreted as agrichnial trace fossils. These traces belong to the graphoglyptid group and are almost always pre-turbidity current deposition in origin (Seilacher, 1977a, 1977b; Miller, 1991; Uchman, 2003). The graphoglyptids form in stable, background pelagic and hemipelagic sediments in oligotrophic conditions (i.e. K-selected taxa *sensu* Ekdale, 1985) and are exhumed and cast onto the soles of weakly erosive turbidity current deposits (Wetzel & Uchman, 2001; Uchman, 2003). Possibly the most widely recognised graphoglyptid is *Paleodictyon* (see Uchman, 1995, 1998 for detailed taxonomic discussion), with its distinctive hexagonal mesh geometry.

4.3 GEOLOGICAL SETTING

Deep-marine sediments of Cretaceous to mid Eocene age are exposed along the coastline of the Guipuzcoa region, Basque Country, northern Spain. The sediments were deposited in an ESE to WNW oriented elongate deep marine trough (Van Vliet, 1978, 2007) at a paleolatitude of approximately 35°N (Plaziat , 1981; Smith *et al.,* 1994). The well-known Zumaia-San Telmo

section (43°18.00'N, 2°15.37'W) is a comprehensive record of sedimentation from the late Cretaceous through to the early Eocene, including the Cretaceous-Tertiary (K/T) boundary and the Paleocene-Eocene boundary sections. Late Cretaceous to late Paleocene sedimentation in the basin was predominantly carbonate in nature with alternations of hemipelagic marlstones and limestones, interspersed by thin, calcareous turbidites sourced from collapse of pene-contemporaneous surrounding shallow water carbonate platform with a dominantly axial east-to-west paleoflow (Crimes, 1976; Pujalte *et al.*, 1995; Winkler and Gawenda, 1999). Late Paleocene-to-early Eocene sedimentation is marked by an increase in siliciclastic sediment supply and has been termed the 'transitional system' (Winkler and Gawenda, 1999). Sedimentation became almost completely siliciclastic in nature during the early Eocene (Crimes, 1973, 1976; Van Vliet, 1978, 2007; Winkler and Gawenda, 1999), leading to the development of a submarine fan system (Kruit *et al.*, 1972; Van Vliet, 1978) with sediment derived predominantly from the north and east with a subordinate supply to the southeast (Van Vliet, 1978, 2007).

The Zumaia succession has previously been the subject of detailed ichnological studies (e.g. Crimes, 1973, 1977; Leszczynski, 1991; Gianetti and McCann, 2010). Crimes (1973) noted a gradual progression from distal *Cruziana* (based on the presence of *Rhizocorallium*) to *Zoophycos* to *Nereites* ichnofacies and inferred a gradual deepening of the basin. However, no direct sedimentological evidence corroborates this inference.

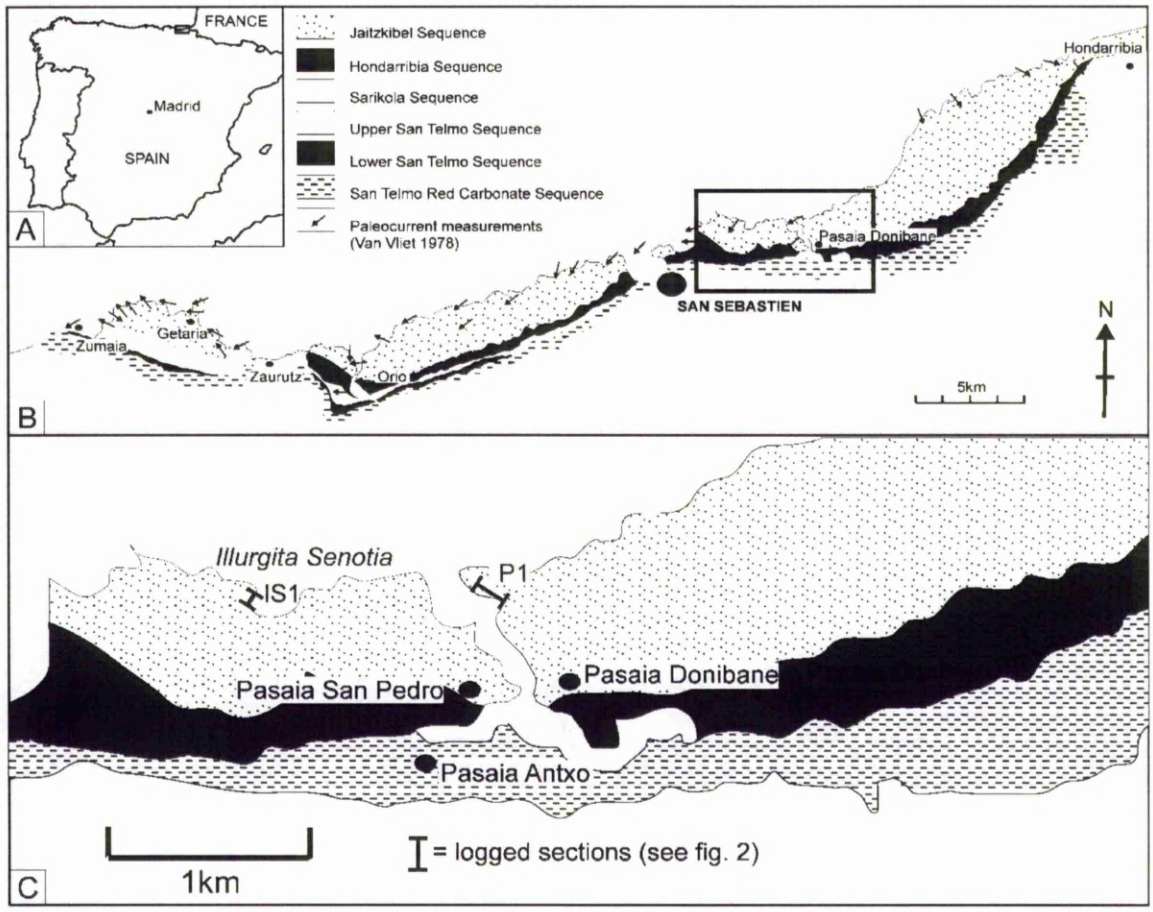

Fig 4.1 A.) Map of Spain with study area inset. B.) Simple geological map of Guipuzcoa region, Basque Country, northern Spain. C.) Detail of study area located to the east of San Sebastien (modified originally from Rosell *et al.*, 1985, after Hodgson and Wild, 2007).

Alegret *et al.* (2009) state a paleobathymetric depth of c.1000m (middle-lower bathyal environment) during the earliest Eocene, which is consistent with sedimentological estimates made by Pujalte *et al.* (1998) and micropaleontological estimates made by Orue-Etxebarria *et al.* (1996).

4.3.1 Stratigraphy and Sedimentary facies associations

Early Eocene siliciclastic depositional sequences in the Basque basin have been subdivided stratigraphically into the Sarikola, Hondaribbia and Jaizkibel Sequences (Rosell *et al.*, 1985). The outcrops studied here all fall within the Jaizkibel sequence (see Fig. 4.1), which is also referred to as the Higuer-Getaria Formation (e.g. Pujalte *et al.*, 2000; Hodgson & Wild, 2007). The Jaizkibel sequence is early Eocene in age and falls within the *T. orthostylus* biozone of Romein (1979), which is equivalent to zone NP12 of Martini (1971). This ages the sequence at c.53-51.5Ma (Ypresian). Sedimentary facies, sedimentary structures, facies associations and interpreted depositional environments of deposits hosting the trace fossils studied are summarised in table 4.1 and sedimentary logs from the studied sections are provided in Fig. 4.2. This scheme is based on more detailed facies associations presented by Van Vliet (1978, 2007) and Hodgson & Wild (2007), and uses the nomenclature of Prélat *et al.* (2009) for submarine lobe environments of deposition.

4.4 EXCEPTIONALLY ORGANISED Y-SHAPED BURROWS

Three examples of organised Y-shaped burrows, tied to sedimentary facies, and stratigraphic position are illustrated, described, and interpreted below. All traces are interpreted to belong to the *Ophiomorpha* group of trace fossils comprising *Ophiomorpha* Lundgren (1891), *Thalasinoides* Ehrenberg (1944) and *Spongeliomorpha* Saporta (1887). De Gibert (1996, also see de Gibert *et al.*, 1999) also assigned *Sinusichnus* (de Gibert, 1996) to the *Ophiomorpha* group. The discussed traces are initially assigned morphotypes, which are then put into the context of their ichnogenera/species in the subsequent discussion.

Locality/UTM	Sedimentary facies	Sedimentary structures	Depositional process	Depositional environment
Illurgita Senotia UTM: 585094 4798337	Thin (1-10cm) F sst beds w/ subordinate medium (0.5-1m) F-M sst beds intercalated w/ clastic mudstones (0.1-0.4m). Sandstone packages display overall coarsening and thickeng up trends.	Normally graded ssts w/ upper planar- ripple laminated divisions (Tbc) plus common convolute laminations and water escapestructures. Flutes and grooves common at bed bases.	Unconfined low density turbidity current deposits	Lobe complex fringe/off axis (*sensu* Prélat et al., 2009)
Pasaia UTM: 587040 4798593	Lower succession displays fine grained, thin bedded ssts (0.1-0.3m) interbedded w/ marlstones and clastic mudstones	Ssts normally graded w/ planar-ripple laminations (Tbc) and basal grooves.	Unconfined low density turbidity current deposits	Progradational trend from lobe complex fringe through off-axis to axis (*sensu* Prélat et al., 2009)
	Upper succession coarsens and thickens upward through medium to thick beded (1-5m thick) and coarse-grained (granule-pebble grade), w/ common bed amalgamation and rare intercalated thin (<10cm) mudstone units	Amalgamated beds are often structureless or contain abundant fluid escape features (dish and pipe structures) and are commonly erosive based. Some bed bases display grooves and flutes with upper parallel laminated divisions (Tb).	Thick amalgamated beds w/ erosive bases deposited by high density turbidity currents.	

Table 4.1 Localities, UTM co-ordinates, lithofacies and facies associations pertaining to the discussed traces. See Fig. 4.1 for map.

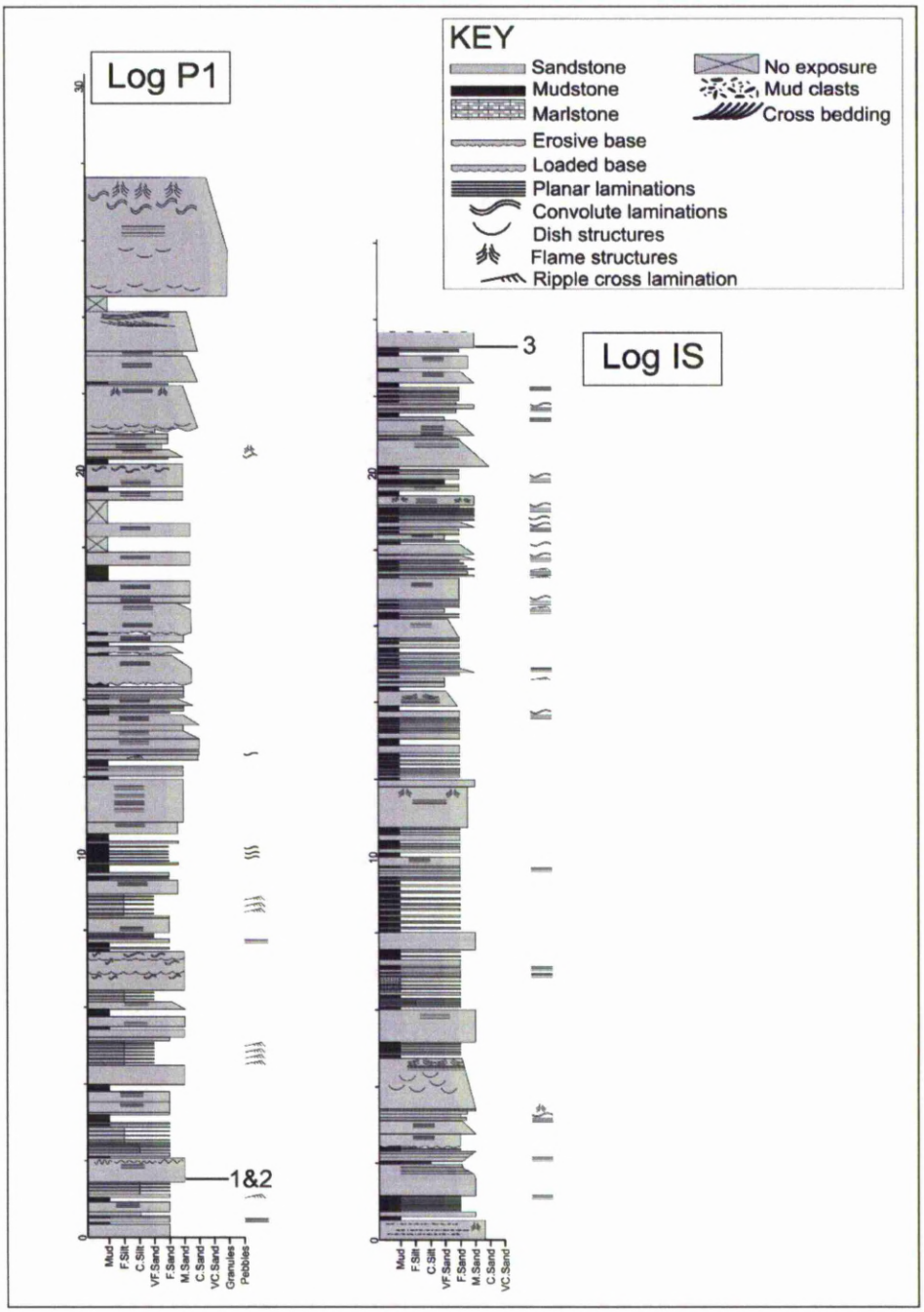

Fig. 4.2—Sedimentary logs from Pasaia (A). 1 & 2 denotes bed preserving examples 1 and 2. Illurgita Senotia (B). 3 denotes bed preserving example 3. See Fig. 1C for locations.

4.4.1 Morphotype morphologies

Morphotype 1.- This morphotype displays distinct Y-shaped branches that interconnect at the termination of each arm to form a slightly arcuate single axis of partial hexagons (three or four sides). Burrow diameter varies from 7 to 10 mm with the distance between the terminae of each Y-branch (or mesh width in terms of a true network such as *Paleodictyon*) averaging approximately 40-60 mm. The inter-branch angles of the Y-shaped burrows are not always even, with some examples displaying one open angle at ~140°, and two tighter angles at ~110°, forming a morphology closer to the interlimb angle of a pentagon rather than a true hexagon (see Fig. 4.3 and Fig. 4.4). The exterior of the burrow generally appears smooth.

Morphotype 2.- This trace also displays well developed partial hexagonal geometries. Burrow diameter ranges between 7-9 mm with the angle of Y-shaped branches at 110-130°, which is consistent with both the *Ophiomorpha* group and *Paleodictyon* networks (perfect hexagons display 120° inter-branch angles although these may be distorted by effects such as sediment compaction and tectonic strain etc.). However, no complete hexagonal mesh was observed, with only three or four sides of a hexagonal mesh constructed. The burrow comprises a number of Y-shaped branches that appear interconnected with slightly bulbous forms at connection points (i.e. connections of each individual Y is within the bed). This specimen appears to be physically connected with a single *Ophiomorpha annulata* burrow (see Fig. 4.5). Locally, burrow limbs steepen up and pass into the bed. The burrow exterior appears smooth.

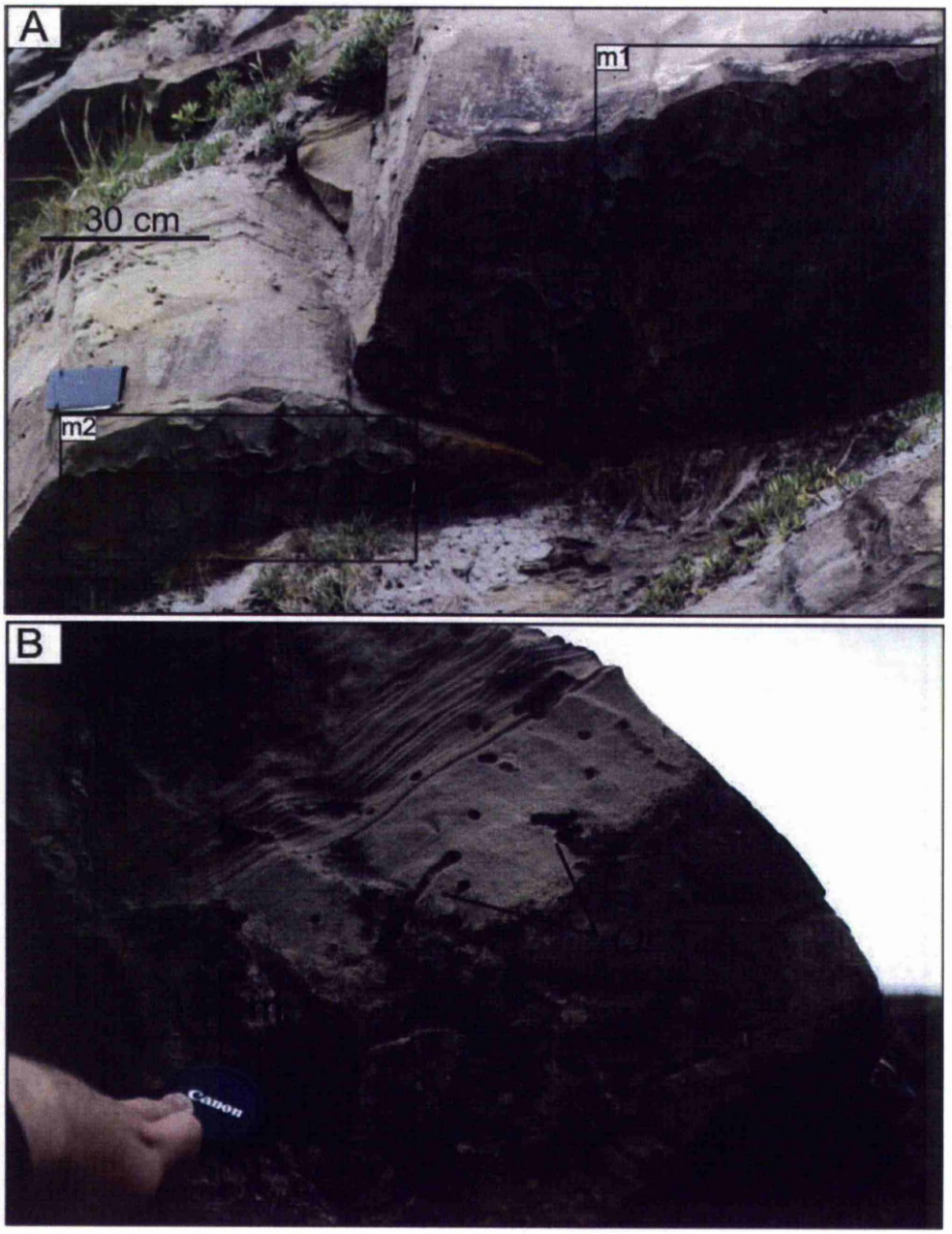

Fig. 4.3 Turbidite bed base preserving examples 1 and 2. A.) Displays location of both morhotypes (m1 = morphotype 1, m2 = morphotype 2). B.) Displays endichnial examples of *Ophiomorpha.* Note the sub-vertical to sub-horizontal nature of the endichnial *Ophiomorpha* bioturbation toward the base of the bed.

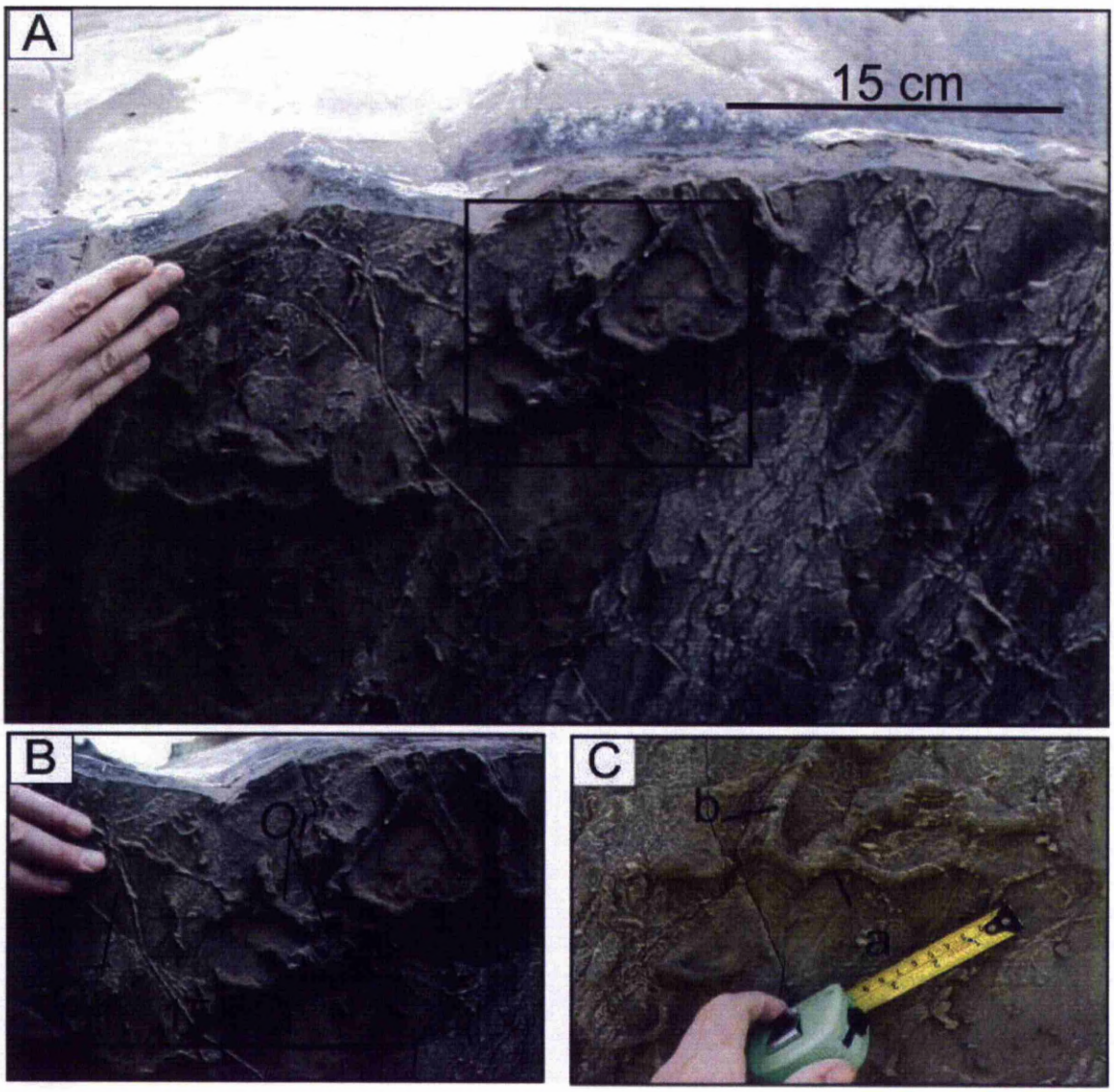

Fig. 4.4 A.) Morphotype 1. Hypichnial full relief (see Fig. 2 for sedimentary log). Highlighted area displays *Ophiomorpha rudis* either cannibalising the burrow network or forming an integral part of the network. B.) Detail of photo 1 highlighted area. *Oa* = *Ophiomorpha annulata, Or* = *O. rudis.* (C) Note obtuse Y shaped branches (a) typical of *Thalassinoides.* The top left of the burrow network is a regular meander burrow (b) that possibly represents a transition from domichnial/fodinichnial ethology to an agrichnial (farming) ethology.

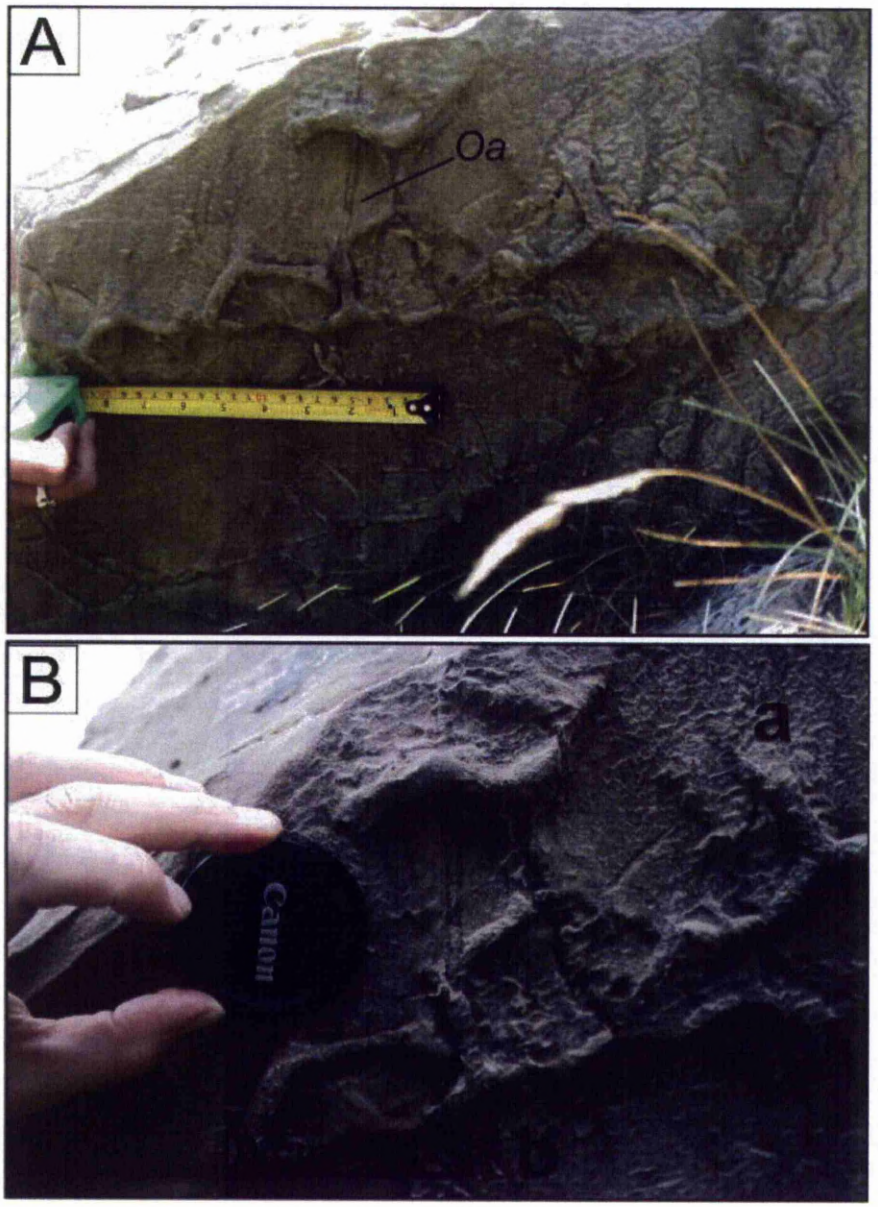

Fig. 4.5 Morphotype 2. A.) Hypichnial full relief (see Fig. 2 for sedimentary log). Y-shaped branches (a) indicative of *Thalassinoides* but constructed in a more organised and repeating form. This trace has previously been identified as *Paleodictyon* isp. (Crimes, 1977) and *Granularia* (Hodgson and Wild, 2007). Note how the indicated *Ophiomorpha annulata* (*Oa*) seems to be interconnected with the networked system. B.) Close up of area intersected by *O. annulata*. (a) Displays a limb of the network that appears welded to the bed suggesting that the trace may actually be pre-depositional in origin. (b) Displays a limb that seems to pass upwards into the bed. The lack of truncation by the turbidite seems to suggest a post-depositional origin.

Morphotype 3.- The diameter of the component burrows of morphotype 3 are ~10 mm, with the burrow system being arranged in a series of Y-shaped branches that form semi-hexagonal type geometries (inter-branch angle ~120°). Some of the bifurcation points are swollen and locally the trace appears to be reinforced with irregularly distributed pellets/granules (Fig. 4.6). The 'mesh' diameter is 45-50 mm, although usually, no more than three sides of a hexagonal mesh is constructed. Certain sections display a more pentagonal morphology where four limbs of a pentagon are constructed. The trace runs perpendicular to tool marks and is approximately 0.6 m in length along its main axis. A second axis runs sub-parallel to tool marks and is approximately 0.3 m in length.

4.4.2 Morphotype occurrences and association with other trace fossils

Morphotypes 1 and 2.- The eastern side of the port entrance at Pasaia Donibane, approximately 5km to the east of San Sebastián (Fig. 4.1) has an easily accessible, well exposed outcrop of multiple thick- and thin-bedded successions (UTM: 587040 4798593). Thin-bedded successions (0.5-1 m thick beds) intercalated with thin mudstones (usually less than 10cm thick with cm scale sandstone beds within) dominate the lower section and are interpreted as a turbidite lobe complex fringe to off-axis settings (*sensu* Prélat *et al.*, 2009). Upper amalgamated beds in the succession are up to 8m thick and are interpreted as a lobe complex axis setting. Morphotypes 1 and 2 are preserved on the sole of a single 0.6m thick medium-grained sandstone bed that has a lower weakly-graded structureless division and an upper planar-ripple laminated division, with water escape structures and convolute laminae (Fig. 4.2). The bed top is intensely bioturbated by *Scolicia*. Internally, the bed is moderately bioturbated by sub-horizontal *Ophiomorpha rudis* and *O. annulata*.

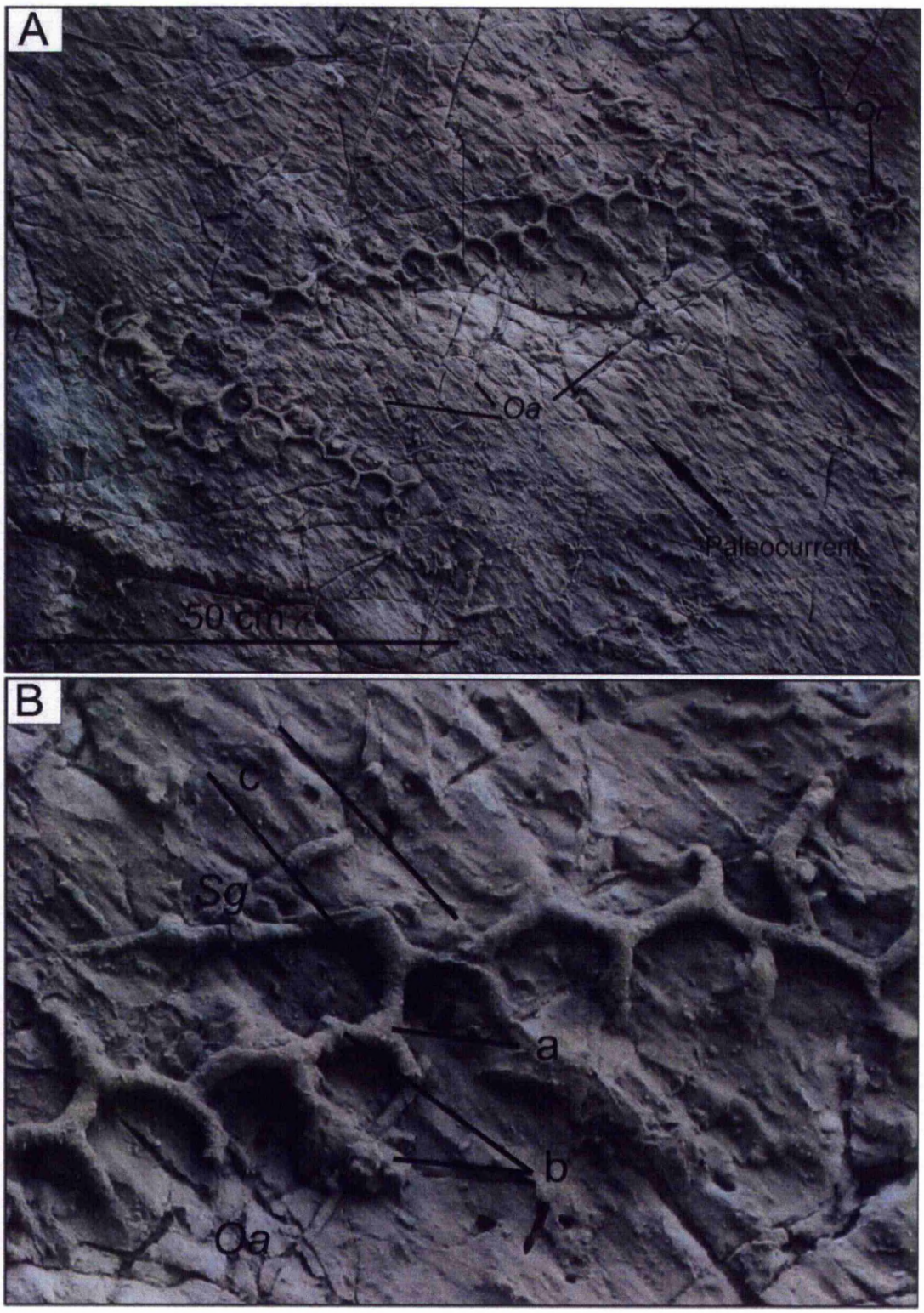
A
Oa
Paleocurrent
50 cm
B
c
Sg
a
b
Oa

Fig. 4.6 A.) Morphotype 3. Hypichnial full relief (see figure 2 for sedimentary log). Note well developed partial hexagonal type geometry similar in form to *Paleodictyon* but with no complete hexagonal mesh. (B) Note moderate-to-intense *Ophiomorpha rudis* (*Or*) and *O. annulata* (*Oa*) bioturbation and swellings at some branching points (a) and irregularly distributed granules within wall structure (b). The trace is parallel to the undulating bed base which is mantled by tool marks and common grooves which the trace clearly cross cuts (c). Certain limbs of the trace also clearly pass upward into the bed (d-note how trace again postdates grooves and tool marks). *Sg* = *Strobilorhaphe glandifer*, *Oa* = *Ophiomorpha annulata*.

The base of the bed preserving *morphotypes 1* and *2* is sharp. The swollen intersections may suggest that the burrows were welded to the bed upon its exhumation by the preserving turbidity current (A. Wetzel, *Pers. Comm.* 2010). However, burrows can be seen to steepen and pass upward into the overlying bed (i.e. not truncated), which suggests that the trace maker burrowed down from the parent sandstone and is therefore preserved in full relief. A similar trace to morphotype 1 (albeit constructed less systematically) is illustrated by Bromley (Fig 8.12, 1996) and assigned to *Thalassinoides suevicus.* The trace is preserved on the base of a non-erosive pelagic chalk bed, supporting a post-depositional origin.

Morphotype 3.- Illurgita Senotia is a small bay located approximately halfway between San Sebastián (Donostia) and the entrance to Pasaia Harbour (Fig. 4.1; UTM: 585094 4798337). The outcrop displays packages of c.1-2 m thick, normally graded coarse- to fine-grained sandstone beds, with structureless lower divisions and planar laminated upper divisions and common water escape structures (flames and convolute laminae). These alternate with thin-bedded and finer grained (fine sand to coarse silt), cm-to-dm scale sandstone beds that are intercalated with mudstones and marlstones. The depositional environment is interpreted to be a turbidite lobe complex off axis setting (*sensu* Prélat *et al.*, 2009). Example 3 occurs on the base of a 0.6m-thick, medium-fine-grained normally graded sandstone with planar to convolute laminae (Fig.

4.2, note top of bed was inaccessible). Physical correlation suggests that this example is slightly younger than the Pasaia examples (Hodgson and Wild 2007). The bed preserving morphotype 3 displays a moderately diverse ichnoassemblage comprising pre-depositional *Protopaleodictyon* and *Paleodictyon,* and post-depositional *Strobilorhaphe, Ophiomorpha annulata* and *O. Rudis.* The trace follows a slightly undulating bed base, and cuts tool marks (Fig. 4.6), thus clearly post-dating emplacement of the tool marks and associated bed.

4.4.3 Identification, interpretation, and comparison to similar forms

Association with Ophiomorpha.- The bed preserving morphotype 1 and 2 displays low-to-moderate *Ophiomorpha rudis* bioturbation. Morphotype 1 is cannibalised by *O. rudis* in the centre section (see Fig. 4.4). It is possible that *Ophiomorpha rudis* and morphotype 1 are intrinsically linked. Morphotype 2 is physically connected with a single, post depositional *Ophiomorpha annulata* burrow (see Fig. 4.5) suggesting that the trace maker of *Ophiomorpha annulata* may have been responsible for this trace. However, the *Ophiomorpha annulata* burrow is narrower at 4mm, typical of flysch *O. annulata* (Uchman, 1995, 1998). It is not unusual for *Ophiomorpha* burrow networks to comprise elements of varying diameter (de Gibert, 2006). Morphotype 3 is closely associated with endichnial forms of *Ophiomorpha rudis* and *O. annulata,* which occur commonly on upper and lower bedding planes, and at a range of orientations within the beds. The trace also shares morphological features with *Ophiomorpha rudis,* notably, swellings at branching points and local, irregularly distributed granules in the wall structure (see Fig. 4.6).

Taxonomic classification.- The substrate dependent, gradational relationship between *Ophiomorpha* and *Thalassinoides* is well established (e.g. Kerne and Warme, 1974; Frey *et al.*,

1978). Morphotype 1 and 2 both display morphological features of *Thalassinoides suevicus* but are also closely associated with *Ophiomorpha.* Morphotype 1 is tentatively assigned to *Thalassinoides suevicus* (see Howard and Frey, 1984 for discussion). Morphotype 2 is slightly more ambiguous. Crimes (1977, plate 4e) diagnosed the same specimen as *Paleodictyon,* however, no complete hexagonal mesh is preserved. Crimes (1973) reports a post-depositional form of *Paleodictyon* from the Basque basin based on the trace wrapping round a groove cast. It is possible that the reported trace may be similar to the example discussed here. The same trace has also been categorised as *Granularia* (which is a synonym of *Ophiomorpha annulata* (Uchman, 1998)) by Hodgson and Wild (2007). The trace could possibly be categorised as *Thalassinoides suevicus* (see Howard and Frey, 1984; Uchman, 1998 for morphological and taxonomic discussion of *Thalassinoides suevicus*) or a gradational specimen between *Thalassinoides suevicus* and *Ophiomorpha annulata.* In fact, it cannot be ruled out that the trace is a form of *Ophiomorpha annulata* as the granulated section of *Ophiomorpha annulata* burrows tend to be located in the less cohesive substrate (i.e. sand rather than mud). Frey *et al.* (1978, fig. 5) display specimens of *Ophiomorpha nodosa* that also display a pellet-lined wall limited to the upper section of the burrow. The ventral exterior is smooth walled and is morphologically similar to *Thalassinoides. Ophiomorpha* burrows constructed at the sand-mud interface tend to display smoother exteriors when preserved on the base of turbidites. However, both traces display a highly organised and much more systematic burrowing behaviour than previously considered for *Ophiomorpha* group traces.

Morphotype 3 shares more characteristics with *Paleodictyon* than the Pasaia specimens. However, the post depositional nature of the trace contradicts this diagnosis as graphoglyptids tend to live in the background pelagic sediment and are then cast onto the soles of turbidites (e.g.

Wetzel & Uchman, 2001; Uchman, 2003). Furthermore, although the trace displays distinctive partial hexagonal geometries, no complete hexagonal mesh has been constructed meaning the trace is not a true network (*sensu* Uchman, 1998). The lack of an interconnecting, complete hexagonal mesh precludes diagnosis of this trace as *Paleodictyon* (see Uchman, 1995, 1998; Wetzel, 2000 for diagnostic/taxonomic information relating to *Paleodictyon*). *Ophiomorpha irregulaire* and *O. nodosa* are commonly noted to construct regular polygonal, three-dimensional burrow maze networks (Frey *et al.*, 1978) that superficially may resemble large *Paleodictyon* networks.

Comparison with similar forms.- Wetzel (2000) reported a giant *Paleodictyon* from the Zumaia section that resembles the specimens reported here. Wetzel's giant *Paleodictyon* has a maximum string diameter of 6.5mm with mesh diameter averaging 85mm. Using Uchman's (1995) criteria this specimen was diagnosed as *Paleodictyon gomezi.* The key difference between the Zumaia specimen and those reported herein is the pre-depositional nature (Wetzel, 2000) compared with the post-depositional nature of the specimens reported here. Wetzel's specimen is a true network with the hexagonal mesh interlocking (albeit in an eroded state due to the pre-depositional nature of the trace). Several specimens of *Thalassinoides suevicus* were identified in this study that share characteristics with the preserved remnants of Wetzel's *Paleodictyon.* This again hints at a more systematic burrowing method than has previously been considered for the *Ophiomorpha* group. The uncertainty in identification of these traces necessitates further taxonomic investigation of these traces.

4.5 DISCUSSION

4.5.1 An agrichnial feeding strategy for *Ophiomorpha?*

Ophiomorpha is considered to be a classic example of a domichnion (i.e. dwelling burrow). Unlike many trace fossils, *Ophiomorpha* has a reliable modern analogue in the burrows of the crustaceans *Callianassa* and *Callichirus,* which share the pelleted wall structure of *Ophiomorpha* when constructed in sediments that lack cohesion (Frey *et al.*, 1978; Bromley, 1996). However, like *Ophiomorpha,* modern crustacean burrows display a wide range of morphologies. Bromley (1996) suggests that such variations in morphology of modern crustacean burrows are due to differing trophic strategies. *Ophiomorpha* trace makers are generally considered to be deposit feeders due to their infaunal nature. However, some *Upogebia* (a decapod crustacean) have been reported to construct Y-shaped vertical burrows that have been interpreted as microbial gardens due to the presence of decomposing plant matter in the deepest parts of the burrow, where the water is strongly reducing due to microbial activity (Ott *et al.,* 1976; Bromley, 1996). In such an environment, the animal may selectively feed on bacterial blooms that form on decomposing plant matter. Marine crustaceans are unlikely to be able to directly digest tough cellulose based organic material. Gastropods are the only marine invertebrate group known to be able to directly digest cellulose. Echinoids digest cellulose via a chemosymbiotic process utilising bacteria in their gut to break it down into digestible material, and also eventually consume the bacterial cultures in their gut as well (Kent Barnes *et al.*, 1991).

Modern crustaceans, such as *Upogebia,* exploit plant material by feeding on the microbes that break it down (Ott *et al.,* 1976; Bromley, 1996). Trace fossils that comprise the *Nereites* ichnofacies, particularly the graphoglyptid group which are characterised by regular meander,

star and net shaped trace fossils, are commonly interpreted to be microbial farms or agrichnia (Uchman, 2003). Networked trace fossils, such as *Paleodictyon* and *Megagrapton,* are archetypal agrichnial trace fossils. An agrichnial feeding strategy is beneficial in deep marine settings due to the relative lack of conventional food sources 100s-1000s of metres below the photic zone.

None of the three examples discussed herein display complete hexagonal mesh geometries such as those of *Paleodictyon.* However, the regular, systematic nature of the construction of these semi-hexagonal burrows does support development of an agrichnial strategy beneath the sand deposit. The area cannibalised by *O. rudis* in Morphotype 1 was most likely enriched in organic material. The organic material may have been harvested and redistributed throughout the burrow network to facilitate breakdown of the material by microbes. Although the burrows are preserved on the soles of sandstone beds, it is likely that an open connection to the sea floor was maintained, which would have facilitated irrigation of the burrow network while allowing organic material/detritus to enter. Subsequent decomposition of the organic material provided an exploitable food source for the trace maker. The variety of *Ophiomorpha* related specimens discussed herein supports the hypothesis that deep sea *Ophiomorpha* increasingly utilised an agrichnial strategy in the early Paleogene.

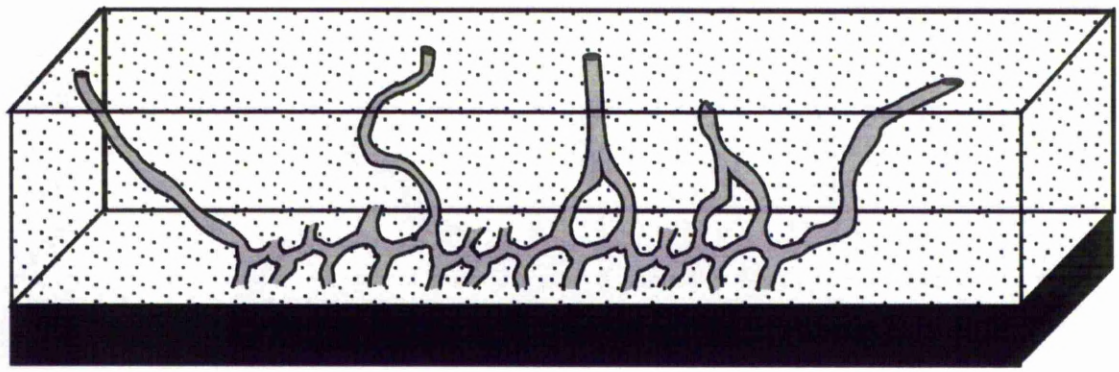

Fig. 4.7 Schematic representation of *Ophiomorpha* colonizing a sandstone turbidite and constructing a network type structure at the sand-mud interface at the bed base (based on morphotype 3).

4.5.2 Implications for Paleodictyon type networks

A recent study found sponge DNA in a hexagonal network structure formed on the sea floor that appears to be identical to the trace fossil *Paleodictyon nodosum* (Rona *et al.*, 2009). Although it is a possibility that the sponge DNA may possibly have been sourced from detritus, it was suggested by the authors that the structure may not even be a burrow at all but a form of hexactinellid sponge. All of the burrows discussed herein are interpreted to be *Ophiomorpha* group related traces and as such are interpreted to have been constructed by crustaceans. This study clearly shows that regular, geometrically shaped networks can be constructed by burrowing organisms, albeit in this case by crustaceans rather than the probable polychaete trace maker of *Paleodictyon*. The linear construction of morphotype 3 (see also Fig. 4.7 for schematic representation of this trace) may also shed some light on the construction technique of regular *Paleodictyon* burrows, which is often a source of speculation (e.g. Wetzel, 2000: Fig. 5).

4.5.3 An Eocene peak in deep marine *Ophiomorpha*

Outcrop studies suggest the Upper Cretaceous witnessed a rapid expansion of *Ophiomorpha* occurrences in deep marine environments, stabilising throughout the Paleocene and once again increasing dramatically in the Eocene, before a decrease through the Neogene (see Fig. 4.8). It has been postulated that *Ophiomorpha* trace makers were able to exploit an increase in terrigenous derived plant matter delivered to the deep marine realm following the evolution of angiosperms in the Cretaceous (Uchman, 2004). Lidgard and Crane (1988) show that angiosperms actually appear in the Upper Jurassic, then experience significant increases in diversity in the Albian and the Cenomanian. This is approximately coincident with the observed increases in deep-sea occurrences of *Ophiomorpha* (Fig. 4.8). The deeply burrowing *Ophiomorpha* trace makers may have developed the ability to exploit increases in plant matter delivered to the deep-sea realm by turbidity currents. Rising sea levels during the early Paleocene (Haq *et al.,* 1987, Miller *et al.*, 2005) may have hindered the deep-sea invasion of *Ophiomorpha,* possibly due to a decrease in angiosperm-derived detritus reaching deeper ocean basins. However, delivery of all terrestrially derived organic matter via turbidity currents to deeper ocean basins will have been reduced due to elevated sea levels. As such, a causal relationship between increases in *Ophiomorpha* and radiation of the angiosperms can only be inferred.

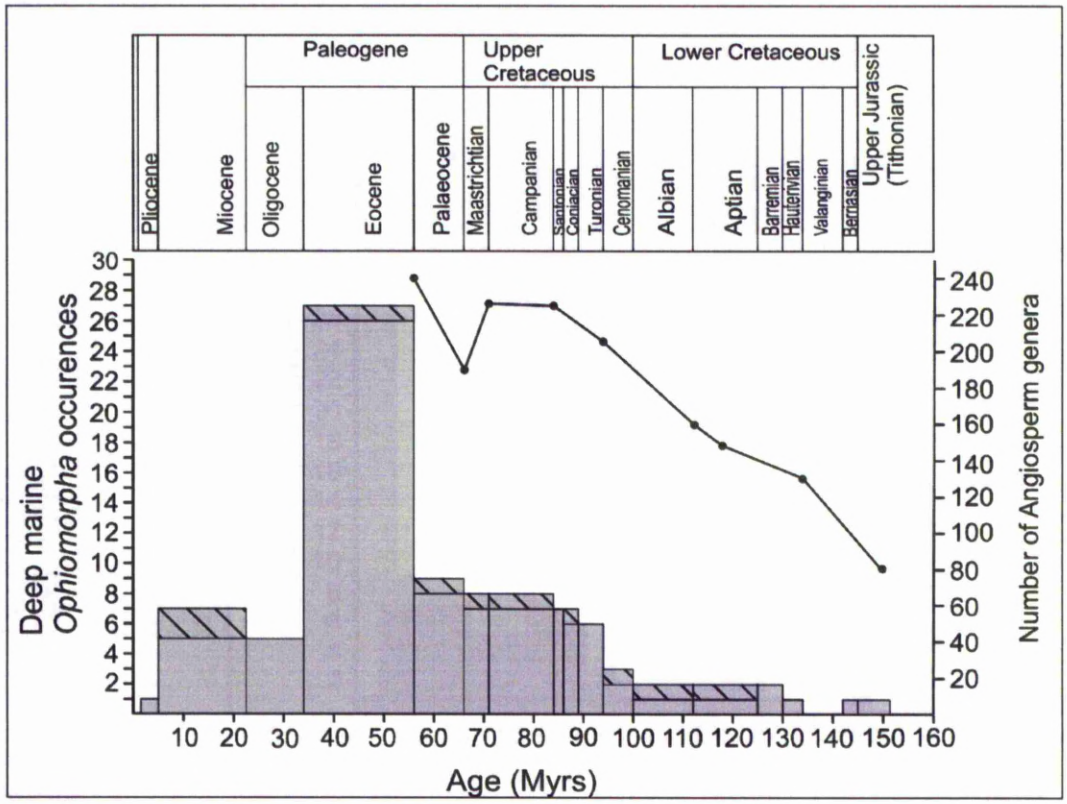

Fig. 4.8 Histogram displaying occurrences of *Ophiomorpha* in deep marine environments since Upper Jurassic (first occurrence in Triassic; Wetzel et al., 2007). Solid bars indicate certain occurrences, hatched bars indicate probable occurrences. Adapted from Uchman (2009). Solid black line illustrates radiation of angiosperm genera up to the Eocene (from Lidgard and Crane, 1988).

Globally, Eocene-aged turbidite deposits are common, notwithstanding the overall high sea levels of the time, which in part is due to the number of active plate margins during this tectonically active period, including the formation of the Pyrenees adjacent to the Basque Basin. The early Eocene also witnessed a number of abrupt, high magnitude global warming events such as the PETM (e.g. Kennett and Stott, 1991; Dickens *et al.,* 1995, 1997, Zachos *et al.,* 2001, 2005) that would have likely had profound effects on weathering cycles, terrestrial runoff and sediment supply to the deep marine realm (Schmitz *et al.,* 2001; Egger *et al.,* 2002; Crouch *et al.,*

2003; Schmitz and Pujalte, 2003, 2007) as well as impacting the dispersal and distribution of terrestrial flora (e.g. Wing *et al.*, 2003; Wing *et al.* 2005). The PETM resulted in the extinction of up to 50% of benthic foraminifera taxa (Alegret *et al.*, 2009) implying stressed conditions in the benthic realm. However, by the early Eocene, *Ophiomorpha* had adapted to the deep marine environment. *Ophiomorpha rudis* exists solely in deep marine environments (Uchman, 2009), therefore does not fit into the 'doomed pioneers' scenario (*sensu* Föllmi & Grimm, 1990). Both *Ophiomorpha annulata* and *O. rudis* occur frequently in Eocene deposits in the Basque basin and display a wide range of dimensions suggesting the presence of juveniles and adults. This is a reliable indicator of long-term colonisation of an environment. *Ophiomorpha* group trace makers seemingly exploited the increased delivery of terrestrially derived material to the deep oceans triggered by a combination of climatic perturbations and active tectonic activity. An increasingly organised agrichnial trophic strategy is interpreted as a response to these paleoenvironmental changes.

4.6 CONCLUSIONS

1. *Ophiomorpha* displays a quasi-progressive colonisation of deeper marine settings since the Permian, first appearing in the deep marine realm in the Late Triassic (Wetzel *et al.*, 2007). *Ophiomorpha* occurrences increase markedly in the Paleogene and experience a peak contribution to deep-sea trace fossil assemblages during the early Eocene (Uchman, 2004, 2009).
2. It is likely that the crustacean trace makers of *Ophiomorpha* will have had to make several biological adaptations to colonise new environmental niches such as deeper marine environments. Such adaptations most likely included developing new trophic strategies.

3. *Ophiomorpha* may have been able to exploit an increase in angiosperm derived plant detritus by developing an agrichnial feeding strategy and/or exploited increased influx of terrestrially derived organic matter associated with enhanced runoff due to climatic changes associated with the early Eocene hyperthermal events such as the PETM.
4. The examples discussed herein represent variations of *Ophiomorpha* group traces that display optimised agrichnial behaviour by constructing regular, irrigated burrow networks intended to harvest microbes breaking down such organic material. Morphotype 1 could almost certainly be assigned to *Thalassinoides suevicus*. Morphotypes 2 and 3 are closely associated with *Ophiomorpha annulata* and *O. rudis*. Morphotype 2 is devoid of any clear pellet/granulated lining so as with Morphtype 1, has more affinity to *Thalassinoides*. However, the fact that the trace is preserved in hypichnion with an underlying mudstone means a typical *Ophiomorpha* may not preserve pellets/granules on the underside, in contact with the cohesive mud. Morphotype 3 however, does display irregularly distributed pellets/granules, which are sometimes concentrated at swollen branching points. This associates the trace with *Ophiomorpha rudis*.
5. If these traces represent a macrofaunal response to global changes in deep marine conditions during the early Eocene then it is likely that similar traces occur in other contemporaneous outcrops/basins.

CHAPTER 5

ASSESSING CONTROLS ON THE DISTRIBUTION OF ICHNOTAXA IN SUBMARINE FAN ENVIRONMENTS, THE BASQUE BASIN, NORTHERN SPAIN

ABSTRACT

The Cretaceous to Eocene aged Basque Basin in northern Spain preserves a variety of submarine fan related environments of deposition in well exposed outcrops. Here, quantitative trace fossil data is calibrated to sedimentologically defined environments of deposition. Nine environments of deposition are assigned according to sedimentary facies associations, depositional architecture and stratigraphic context. The preserved trace fossil assemblages are interpreted in terms of extrinsic palaeoecological, and intrinsic taphonomical and depositional environment controls. In channel related environments, diverse pre-depositional dominated assemblages are prevalent in marginal settings. These are replaced by low diversity post-depositional dominated assemblages in more axial positions within the system. Lobe related environments display a higher level of diversity and bioturbation intensity in more distal/off axis (lobe fringe) environments compared to the most axial lobe environments that preserve low diversity, and exclusively post-depositional assemblages (dominated by *Ophiomorpha*). Diverse pre- and post-depositional assemblages are common in fan fringe deposits, with less diverse assemblages dominated by post-depositional ichnotaxa (particularly *Zoophycos*) in basin floor fan deposits. The use of 'sub-ichnofacies' is found to only aid characterisation of trace fossil assemblages based on a general (proximal-distal) position within a submarine fan system. Tier preservation of

trace fossil assemblages is almost exclusively determined by the depth of erosion that a substrate is subjected to. As such, colonisation style (pre- versus post depositional) and ethological groupings are proposed as being the most powerful tool in assisting sedimentological observations in assigning environments of deposition.

5.1 INTRODUCTION

Ichnology is an important complement to traditional sedimentological techniques in the interpretation of depositional environments and the record of environmental change. The ichnofacies concept (Seilacher, 1967) is based on the reoccurrence of certain trace fossil associations that are at least passively controlled by bathymetry (Frey *et al.*, 1990). This provided a rudimentary, depositional environment-controlled model for the distribution of trace fossils. It is widely recognised, however, that trace fossil assemblages are controlled by a wide range of environmental controls of which water depth is only one (e.g. Frey *et al.*, 1990; Pemberton *et al.*, 1992; Uchman and Wetzel, 2011). Nutrient supply, substrate consistency, salinity, sedimentation rates, temperature and hydrodynamic regime may all exert a control on the types and behaviour (ethology) of fauna able to thrive or survive in a given environment.

Taphonomic controls on trace fossil assemblages may vary considerably compared to taphonomic processes affecting micro/macrofossils (e.g. dissolution of carbonate would not affect trace fossil preservation to the same degree as calcareous body fossils). Commonly however, the preservation potential of trace fossils is influenced by different factors to those that affect body fossils. Perhaps the most important of these factors is the depth and style of erosion that benthic communities are subjected to. These factors may vary significantly between depositional environments within a given bathymetric range. For example, the *Cruziana*

ichnofacies in its original application was implied to be representative of the sublittoral zone or below fair weather wave base but generally above storm weather wave base (Seilacher, 1967; Pemberton *et al.*, 1992). The *Cruziana* ichnofacies, however, may also be representative of a wide range of environments that are characterised by low-to-moderate energy conditions that offer high preservation potential in the upper tiers (Bromley, 1996; Pemberton *et al.*, 2001). Examples of such environments include lagoonal, deltaic, lower shoreface, and mud prone tidal-subtidal environments (MacEachern *et al.*, 2007). While trace fossil assemblages in these environments may all fall within the *Cruziana* ichnofacies, each environment will preserve distinct trace fossil assemblages characteristic of the environment of deposition in which they are preserved.

Typically, submarine fan environments preserve trace fossils characteristic of the *Nereites* ichnofacies. It has been long recognised that *Nereites* assemblages have subtle differences within the ichnofacies largely controlled by proximal-distal relationships (e.g. Książkiewicz 1970, 1977; Crimes 1973). This observation was also noted by Seilacher (1974) who proposed the *Nereites* (mud rich fan fringe – basin plain environment) and the *Paleodictyon* (sand rich distal fan environments) sub-ichnofacies of the *Nereites* ichnofacies. The proliferation of *Ophiomorpha* in Cretaceous and younger submarine fan environments led Uchman (2001) to propose the *Ophiomorpha rudis* sub-ichnofacies based on *Ophiomorpha rudis* and *O. annulata* being the most representative trace fossils of medium and thick bedded channel, lobe and lobe fringe facies. However, a broader range of sub-environments occur within submarine fan systems.

This study focuses on the distribution, diversity and ethologies of trace fossils in the deep marine Basque basin, northern Spain. Previous studies (e.g. Crimes, 1973, 1977; Leszczynski, 1991;

Gianetti and McCann, 2010) yielded ichnological results broadly similar to a number of studies from basin successions of a similar Paleogene age (e.g. Uchman, 1995, 1999, 2001 Uchman and Demircan, 1999; Tunis and Uchman, 1996a, 1996b, 1998). However, Heard and Pickering (2008) highlighted the importance of considering a wide range of well documented depositional environments in the Ainsa-Jaca Basin, a broadly contemporaneous basin of early-mid Eocene age and palaeogeographically close to the Basque Basin. The main objectives of this study are:

- To test the exportability of the Heard and Pickering (2008) model of trace fossils as diagnostic indicators of submarine fan related environments, and provide an additional dataset of Paleogene deep water ichnology where depositional environment is carefully interpreted and documented.

- To compare trace fossil assemblages (diversity, abundances, and ethologies) with other published work of similar geological age (late Cretaceous-early Eocene) and similar environments of deposition.

- To discriminate between intrinsic palaeoenvironmental controls and extrinsic palaeoecological factors that may influence trace fossil assemblages.

The influence of extrinsic controls is important to consider during the early Paleogene, as the greenhouse climate was punctuated by a number of abrupt, high magnitude transient global warming episodes such as the Paleocene-Eocene Thermal Maximum (e.g. Kennett and Stott, 1991; Dickens *et al.*, 1995, 1997; Zachos *et al.*, 2001, 2005), which had profound effects on benthic microfaunal communities (e.g. Thomas, 2007; Alegret, 2009).

5.2 STUDY AREA: THE BASQUE BASIN, NORTHERN SPAIN

Deep-marine sediments of Cretaceous to mid-Eocene age are exposed along the coastline of the Guipuzcoa region, Basque Country, northern Spain (Fig. 5.1). The sediments were deposited in an ESE to WNW oriented elongate deep marine trough (Van Vliet, 1978, 2007) at a palaeolatitude of approximately 35°N (Plaziat *et al.,* 1981; Smith *et al.,* 1994). The well-known Zumaia-San Telmo section (Fig. 5.1D) is a comprehensive record of sedimentation from the late Cretaceous through to the early Eocene, including the Cretaceous-Tertiary (K/T) boundary (e.g. Mount and Ward, 1986; Kuhnt and Kaminski, 1993; Smith *et al.*, 1999) and the Paleocene-Eocene boundary (PETM) sections (e.g. Canudo *et al.*, 1995; Schmitz *et al.*, 1997; Gawenda *et al.*, 1999; Winkler and Gawenda, 1999; Alegret *et al.*, 2009; Rodríguez-Tovar *et al.* 2011). Late Cretaceous to late Paleocene sedimentation in the basin was predominantly carbonate in nature with alternations of hemipelagic marlstones and limestones, interspersed by thin, calcareous turbidites sourced from shedding of carbonate material from surrounding contemporaneous carbonate platforms with a dominantly axial WNW palaeoflow (Crimes, 1976; Pujalte *et al.,* 1995; Winkler & Gawenda, 1999). Late Paleocene-to-early Eocene sedimentation is marked by an increase in siliciclastic supply and has been termed the 'transitional system' (Winkler and Gawenda, 1999). During the early Eocene, sedimentation became almost completely siliciclastic in nature (Crimes, 1973, 1976; Van Vliet, 1978, 2007; Winkler and Gawenda, 1999), leading to the development of a submarine fan system (Kruit *et al.,* 1972; Van Vliet, 1978) with sediment derived predominantly from the north and east with a subordinate supply from the southeast (Crimes, 1976; Van Vliet, 1978, 2007).

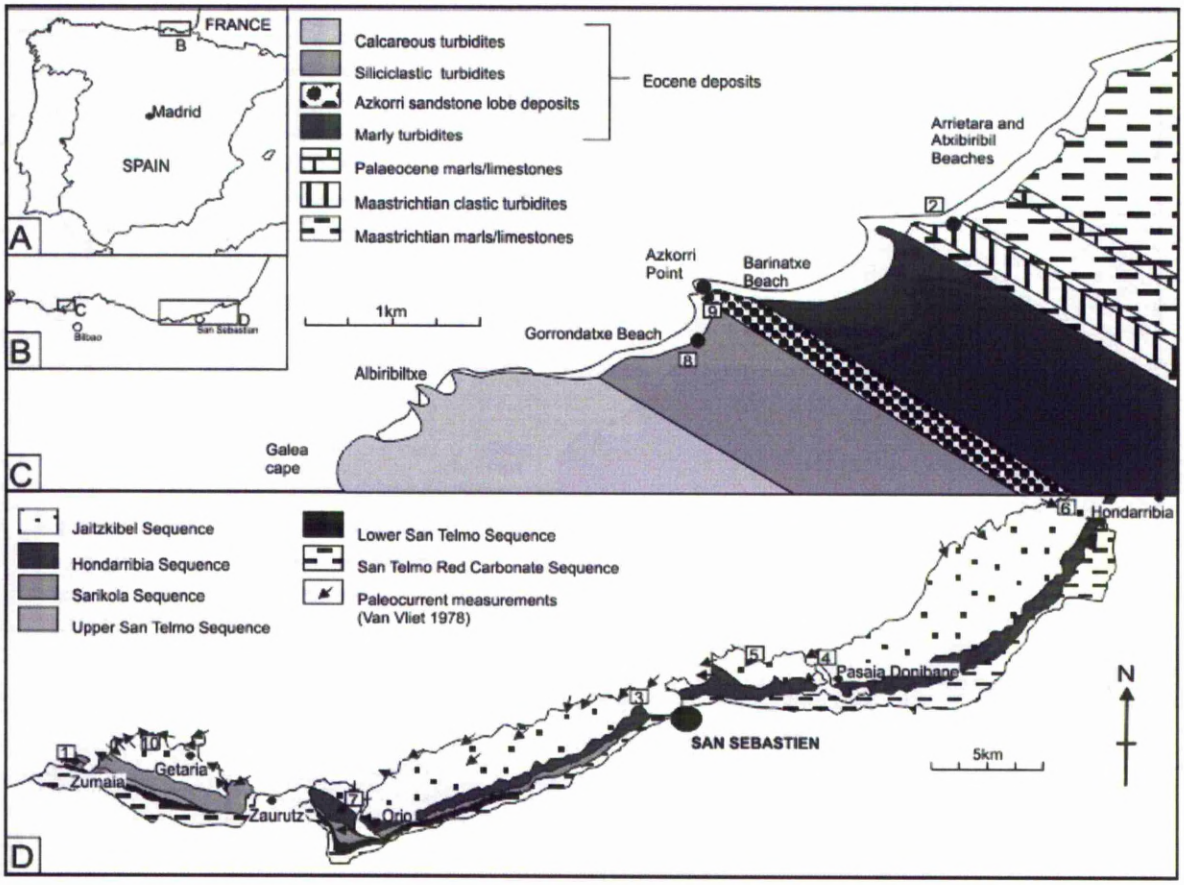

Fig. 5.1 A.) Location of study area on northern Spanish coastline. B.) Location of C and D within the Basque Country (Guipuzcoa and Bizkaia regions). C.) Simplified geological map of the Sopelana area (10km NE of Bilbao) with localities/logged sections indicated (modified from Bernaola *et al.* 2006). D.) Simplified geological map of the Guipuzcoa region with localities/logged sections indicated (modified from Rosell *et al.*, 1985).

Strata of Cretaceous-to-early Eocene age are also extensively exposed towards the western margin of the basin close to Bilbao in the Bizkaia region, but due to extensive post-depositional faulting, the stratigraphy is less continuous than that of Guipuzcoa. However, Arrietera beach (Fig. 5.1c) has a well constrained K/T boundary section (e.g. Lamolda *et* al., 1983, Kuhnt and Kominski, 1993) composed of alternations of hemipelagic marlstones and pelagic micritic limestones. The western end of the beach section also displays mid-to-late Cretaceous siliciclastic deposits. Much of the late Paleocene-early Eocene (including the PETM) is absent

due to faulting, but Barrinatxe beach (Fig. 5.1c) has good exposures of early Eocene hemipelagic marl and limestones interspersed with mixed siliciclastic-carbonate turbidites. Gorrondatxe beach (Fig 5.1c.) to the west also has around 700m of similar facies (but with dominantly siliciclastic turbidites) of Ypresian-Lutetian age (Bernaola, 2006; Payros, 2007).

The Zumaia succession has previously been subject to detailed ichnological studies (e.g. Crimes, 1973, 1977; Leszczynski, 1991; Gianetti and McCann, 2010; Rodríguez-Tovar *et al.* 2011). Crimes (1973) noted a gradual progression from distal *Cruziana* (based on the presence of *Rhizocorallium*) through *Zoophycos* to *Nereites* ichnofacies, and inferred a gradual deepening of the basin. However, no direct sedimentological evidence corroborates this inference. The Gorrondatxe section has been subject to a detailed study on the sequence stratigraphic control on ichnology (Rodríguez-Tovar *et al.*, 2010). Alegret *et al.* (2009) estimate a palaeobathymetry of c.1000m (middle-lower bathyal environment) for the basin during the earliest Eocene, which is consistent with sedimentological estimates made by Pujalte *et al.* (1998) and micropaleontological estimates made by Orue-Etxebarria *et al.* (1996). Palaeocurrent measurements and stacking patterns of thicker bedded sandstone units suggest a general east-west, proximal-distal relationship in the basin (Van Vliet, 1978, 2007; Hodgson and Wild, 2007).

5.2.1 Depositional environments

Nine submarine fan environments of deposition have been identified in this study based on sedimentary facies associations, depositional architecture, and stratigraphic context, and are made independent of ichnological observations (see Table 5.1, 5.2 and Fig. 5.2). The nomenclature and criteria of Prélat *et al.* (2009) is employed to describe and identify submarine lobe environments (sheet-like successions). Interpretation of submarine channel-levee and

proximal fan deposits use the criteria and nomenclature of Hodgson and Wild (2007), Heard and Pickering (2008) and Kane and Hodgson (2011). Trace fossil associations were analysed by depositional environment where multiple environments of deposition are identified along a stratigraphic section. This approach differs from previous studies (e.g. Uchman, 2001; Heard and Pickering, 2008) where a depositional environment is assigned per locality (see Table 5.1, 5.2).

Number	Locality	Age	UTM base section	UTM top section
1	Zumaia (Itzurun Beach)	Mid Paleocene-early Eocene	0559919 4794322	0560079 4794609
2	Sopelana (Arrieterra Beach)	Late Cretaceous	0500140 4803771	0500041 4803727
3	San Sebastian (Ondaretta Beach)	early Eocene	0580648 4796991	0580627 4797013
4	Pasaia	early Eocene	0587044 4798586	0587027 4798632
5	Illurgita Senotia	early Eocene	0585192 4798521	0585097 4798345
6	Hondaribbia (Jaizkibel)	early Eocene	0534334 4803866	0593868 4803444
7	Orio	early Eocene	0570224 4793509	0570119 4793549
8	Gorrondatxe Beach	early -mid Eocene	0498364 4802833	0498338 4802808
9	Azkorri Sandstone (Gorrondatxe Beach)	early Eocene	0498899 4803296	0498839 4803249
10	Getaria	early Eocene	0562238 4795377	0562347 4795448

Table 5.1: List of localities, ages and UTM co-ordinates (WGS84).

Heard and Pickering (2008) identified a total of sixteen fan and related environments in their study. The Ainsa-Jaca basin yielded more environments of deposition because it can be subdivided into the proximal Ainsa Basin (slope, channel and related environments, proximal base of slope apron etc.) and the more distal Jaca Basin (lobe, lobe fringe, fan fringe, basin plain etc.) (Das Gupta and Pickering, 2007; Heard and Pickering 2008 and references therein). The

Basque basin deposits west of San Sebastian (see Fig. 5.1D) are predominantly distal fan-fringe-to-basin plain environments. More proximal sedimentary facies to the east of San Sebastian have not been the focus of detailed study (with the exception of Van Vliet, 2007, 1978; Hodgson and Wild, 2007; Kruit *et al.*, 1972; Crimes, 1976) but mainly comprise base of slope, proximal, amalgamated lobe bodies. No channel axis deposits were recorded in this study.

Sedimentary facies	Sedimentary structures	Depositional process	Depositional environment	Localities
Basin plain -Fan fringe environments				
Interbedded pelagic micritic lsts (5-40cm thick) & hemipelagic marlstones (5-50cm thick). Thin bedded (1-10cm) F- & VF-calcareous ssts & silststone	Structureless lsts & marlstones. ssts normally graded to ripple cross laminated (Tc). Siltstones parallel laminated (Td)	(Hemi)pelagic carbonate mud deposition w/ rare dilute turbidity current deposits	**Basin floor**	1
Interbedded micritic pelagic lsts (5-20cm thick) & marlstones (5-15cm thick). Common thin (1-10cm) VF & F ssts.	Carbonate beds structureless. ssts graded to sub-parallel laminated (Tb) to ripple cross laminated (Tc) with rare convolute lams	(Hemi)pelagic carbonate mud deposition w/ dilute turbidity current deposits	**Fan fringe-basin floor transition**	1, 8,
Common thin bedded (1-10cm) ssts & m-scale clastic mudstone packages	Graded thin sst beds w/ planar (Tb) and ripple lam (Tc) divisions	Unconfined low concentration turbity current deposits locally dewatered	**Fan fringe**	1, 2
Submarine lobe environments				
Clastic mudstones interbedded with predominantly thin (1-10cm) F sst beds with subordinate medium (0.5-1m) f-m sst beds	Thin bedded ssts ripple laminated (Tc)and normally graded	Unconfined low concentration turbidity current deposits	**Lobe complex fringe**	5, 9
Predominantly medium bedded (10cm-1m) but w/ common thick (1-1.5m) FS-MS ssts	Medium sst beds normally graded w/ structureless, parallel & ripple laminated (Tbc) & common flames & convolute lams.	Unconfined low to high concentration turbidity current deposits	**Lobe complex off-axis**	3, 4, 9, 10,
Thick (1->5m) CS -GR ssts	Thick ssts commonly erosive base, w/ structureless or dewatered lower division & thin planar/wavy/ripple lam upper divisions	Amalgamated high concentration turbidity current deposits	**Lobe complex axis**	4
Channel related environments				
Medium bedded (10cm-1m) MS-CS ssts with thick (>1m) & very thick (>3-10m) MS-PB grade ssts.	Thick erosive based sst, structureless (clast-rich) & planar lam divisions, locally w/ dune forms on bed tops (>0.5m scale). Abundant flame & dish structures	Amalgamated and dewatered high concentration turbidity currents, with local reworking of bed tops	**Channel-lobe transition**	6
Interbedded marlstones (2-60 cm) w/ rare micritic lsts (10cm thick). Thin (<10cm) FS & medium (14-65cm) VFS-GR sst beds, w/ bioclastic material.	Carbonate beds structureless. Graded thin ssts structureless to planar (Tb) to ripple cross laminated (Tc). Bioclastic sst bed displays 10cm scale cross bedding.	Turbidity currents with tractional bedforms overlying erosional surfaces	**Channel margin**	2
Thin bedded (5-10cm) FS grading to silt, w/ rare MS ssts (10-30cm)	Normally graded ssts w/ structureless to planar-wavy laminated divisions, & stoss-preserved climbing ripple lamination (Tc) that grade to laminated silts (Td)	Waning turbidity currents that deposited rapdily	**External levee**	7

Table 5.2: Table documenting localities, sedimentary facies, facies associations and interpreted depositional environments based on Hodgson and Wild (2007), Heard and Pickering (2008), Prélat *et al.* (2009), and Kane and Hodgson (2011).

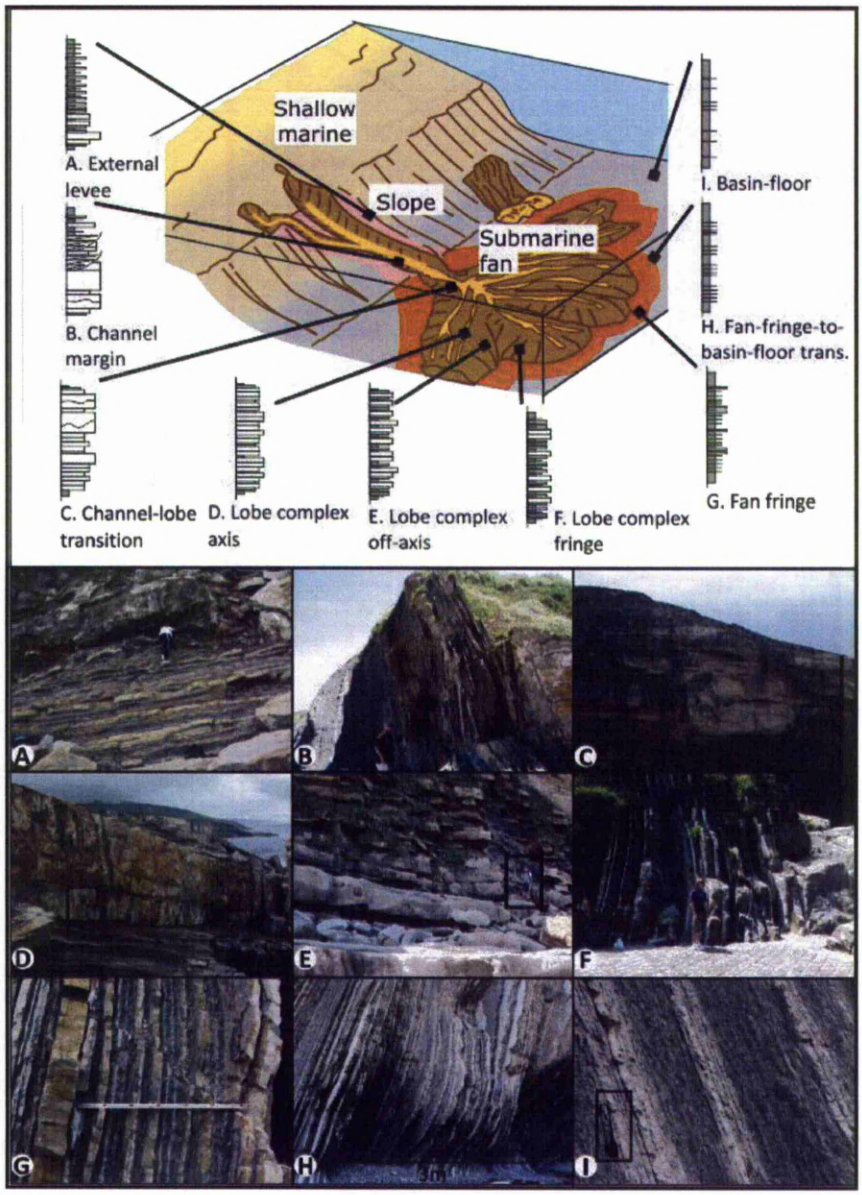

Fig. 5.2 Submarine fan model showing the relative position and a representative stick log of each interpreted depositional environment. A.) External Levee deposits at Orio (younging top to base) (locality 7, Table 1). B.) Channel margin deposits at Arrieterra Beach, Sopelana (locality 2). C.) Channel-lobe transition deposits at The Lezonabar Member at Erentzun Zabal (Hodgson and Wild, 2007). D.) Lobe complex axis deposits, Erentzun Zabal. E.) Lobe complex off-axis deposits at Getaria road section (locality 10). F.) Lobe complex fringe deposits at San Sebastian (locality 3). G.) Fan fringe deposits at Azkorri sandstone, Gorrondatxe (locality 9). H) Fan fringe-basin floor transition at Zumaia (locality 1). I.) Basin floor deposits at Zumaia (locality 1).

5.3 DATA ACQUISITION

5.3.1 Methodology

Detailed measured sections (e.g. Figs. 5.3, 5.4 and 5.5) and quantitative ichnological data (e.g. Figs. 5.4 and 5.5) were collected at 10 localities to capture a range of depositional environments (Fig. 5.1). Quantitative ichnological data collection methods followed a similar strategy to Heard and Pickering (2008). Bedding planes with at least $1m^2$ of largely unweathered surfaces were chosen to log trace fossil data. Trace fossils were identified to species level using Uchman's (1995, 1998) taxonomic classification system. The areal coverage of individual ichnotaxa was calculated as a percentage of the total trace fossil assemblage for each bedding plane sampled (see also Miller and Smail, 1997). The toponomy of each trace fossil assemblage was recorded using Martinsson's (1965, 1970) classification (see Fig. 5.6). Finally, bioturbation intensity of each sampled bedding plane was calculated using a $0.2m^2$ quadrat divided into a $2cm^2$ grid. The number of squares containing bioturbation translates directly to a percentage value and to a bioturbation index (B.I. e.g. Droser and Bottjer, 1991; Taylor *et al,*. 2003) as subdivisions within the B.I. are largely based on semi-quantitative estimates of percentage bioturbation overprinting the original sedimentary fabric. Ichnodiversity was calculated by counting the total number of ichnotaxa recorded per depositional environment.

A total of 900m of sedimentary logs were constructed (e.g. Fig. 5.3) with ichnological data collected at a c.2m stratigraphic spacing (e.g. Figs 5.4, 5.5). This equates to approximately 900 bedding planes (including bed soles and tops). Any bioturbation contained in cross section (endichnial traces, see Fig. 5.6) was also recorded.

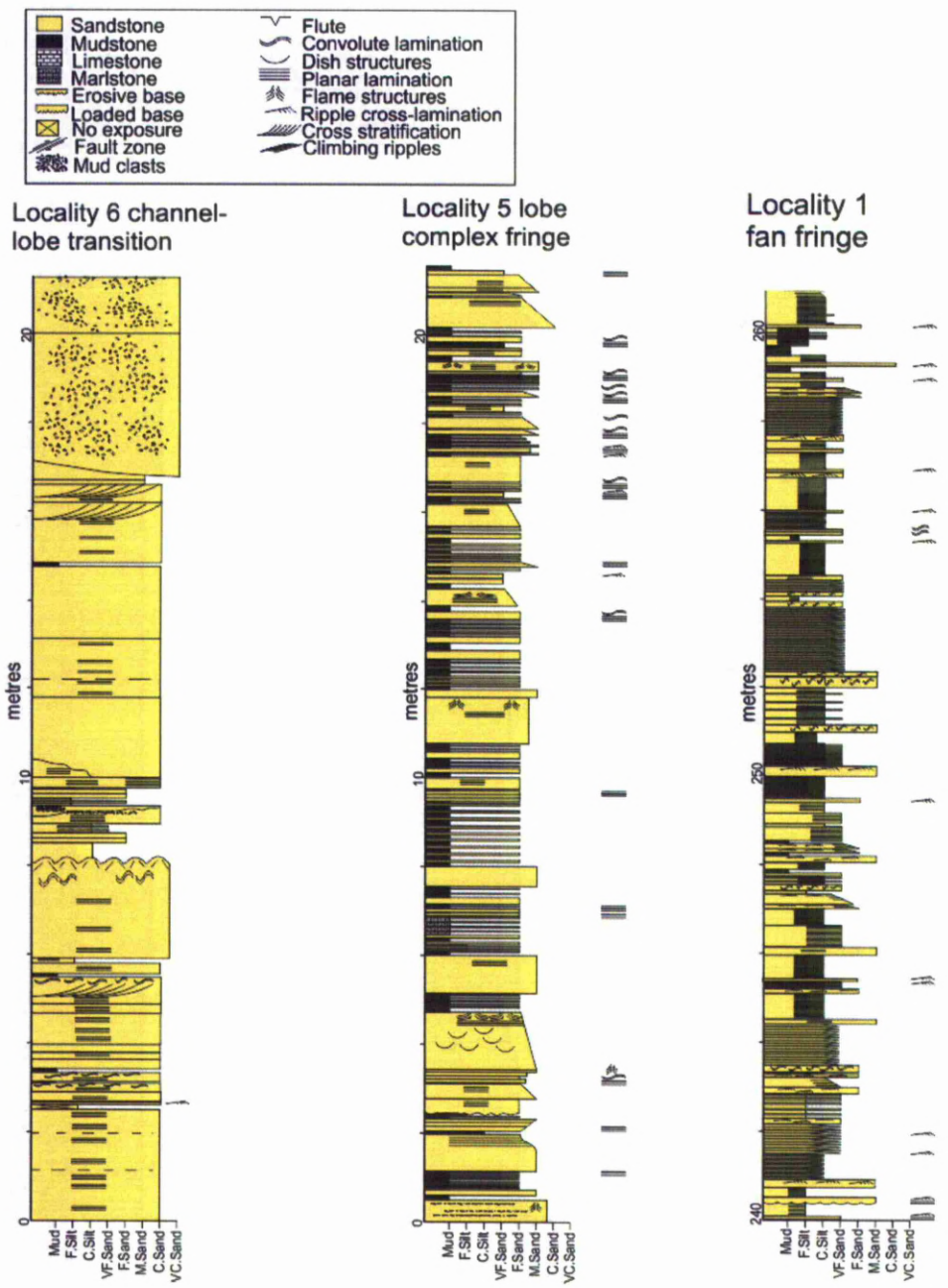

Fig. 5.3 Representative sedimentary logs of different ages in the Basque Basin showing a gross proximal-distal trend. A) Channel-lobe transition at Hondaribbia. B) Lobe complex fringe at Illurgita Senotia (near San Sebastian). C) Fan fringe deposits, Playa Itzurun, Zumaia.

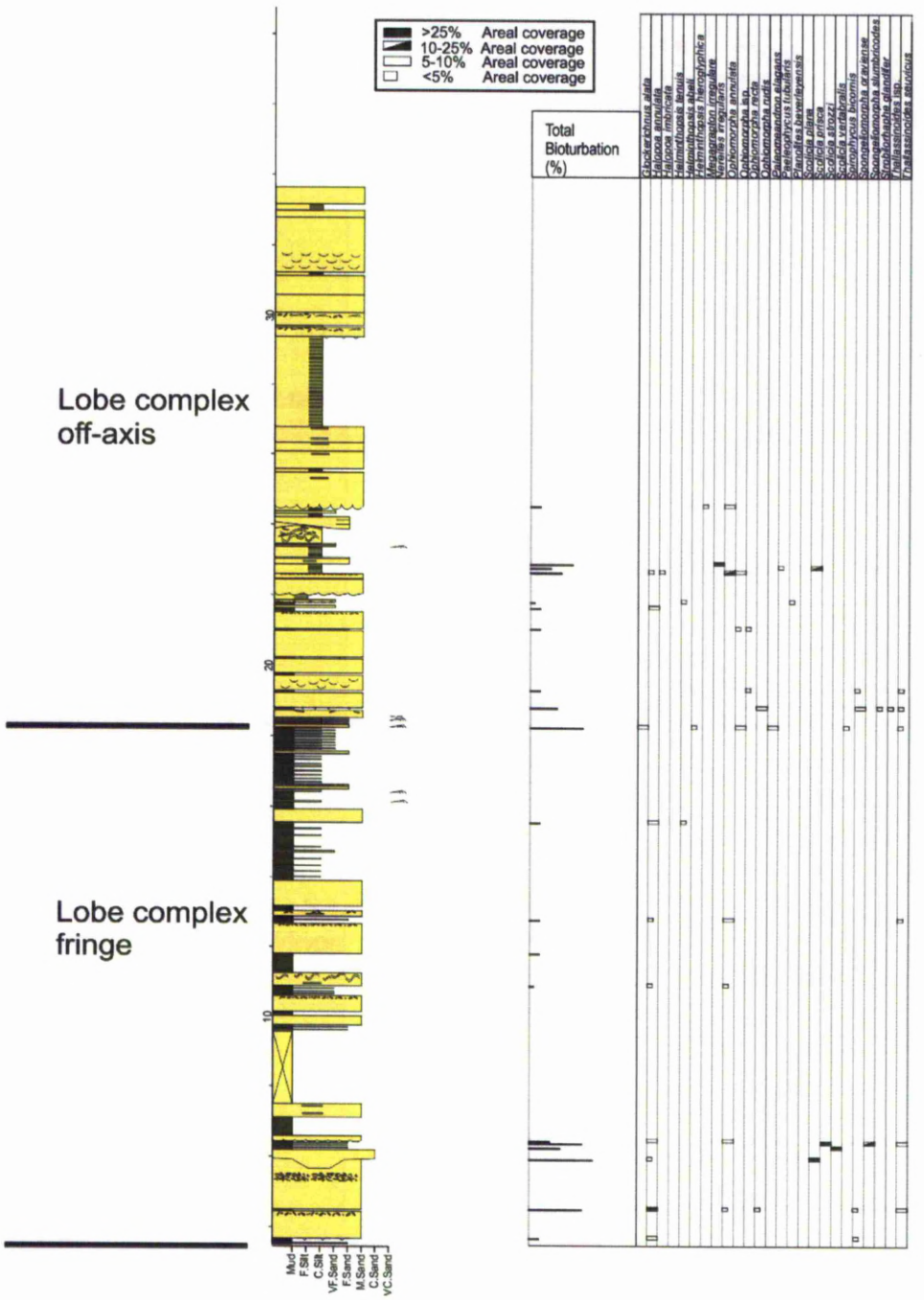

Fig. 5.4 Sedimentary log constructed at Azkorri Sandstone, Gorrondatxe Beach, displaying the trace fossil data capture method (after Heard and Pickering, 2008). Note the subdivision of lobe complex fringe to lobe complex off-axis at the same locality based on sedimentary facies.

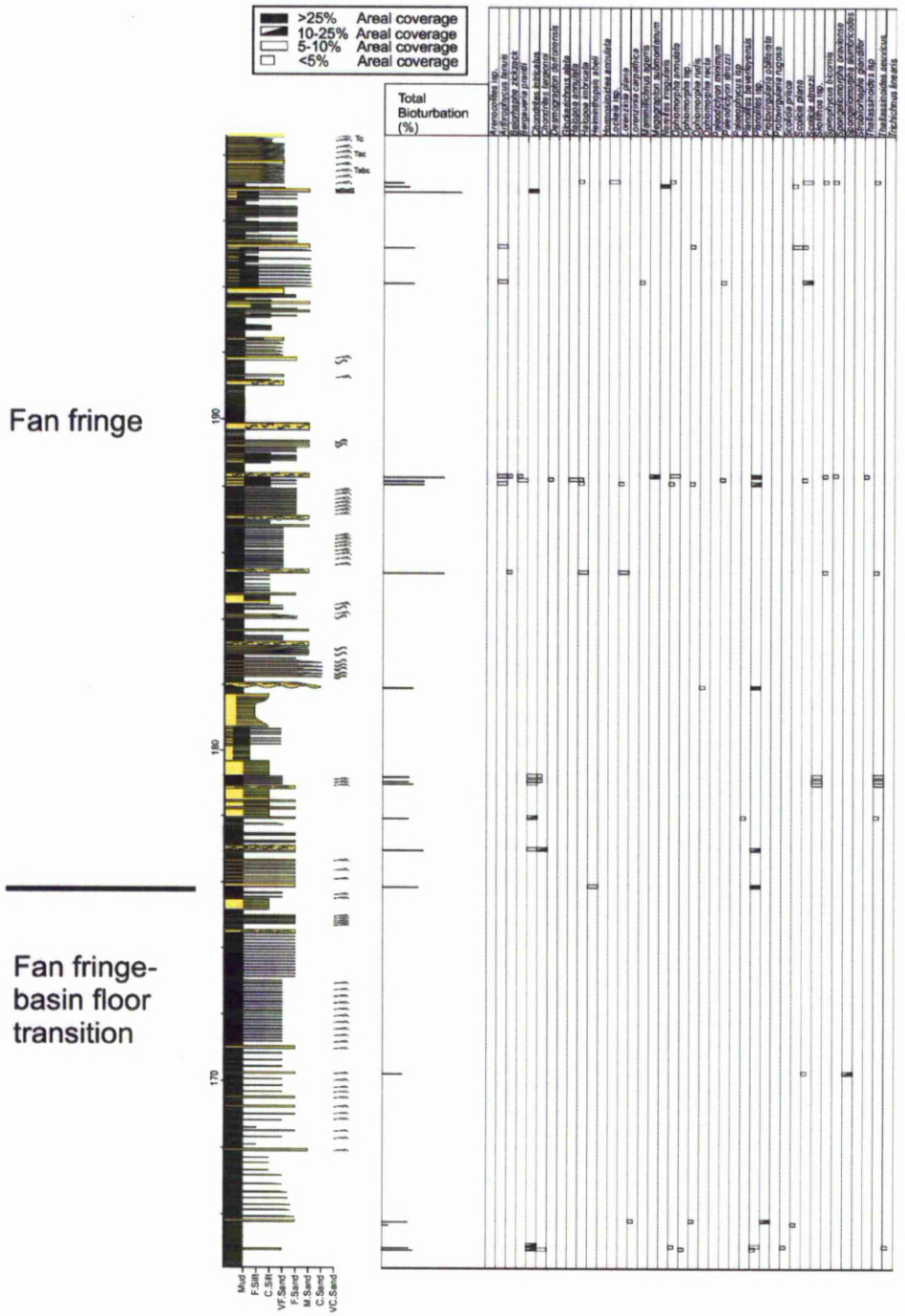

Fig. 5.5 Sedimentary log constructed at Zumaia displaying trace fossil assemblages preserved in the fan fringe-basin floor transition and fan fringe environments based on sedimentary facies.

Fig. 5.6 Toponomic classification system used in this study (after Martinsson, 1970, modified from Savrda, 2007). Description of ethologies referred to in text. Note, the list is not exhaustive as it only relates to discussed ethologies. Ethologies such as repichnia (locomotion) and fugichnia (escape traces) are omitted (see chapter 2.2 for discussion of these ethologies). Legend: Agrichnia; *Pa = Paleodictyon, Me = Megagrapton, Sp = Spirorhaphe.* Chemichnia; *Ch = Chondrites.* Cubichnia; *Ca = Cardioichnus, Be = Bergaueria.* Domichnia; *Oph = Ophiomorpha.* Fodinichnia; *Th = Thalassinoides, Zoo = Zoophycos.* Pascichnia; *Sc = Scolicia, Ne = Nereites.*

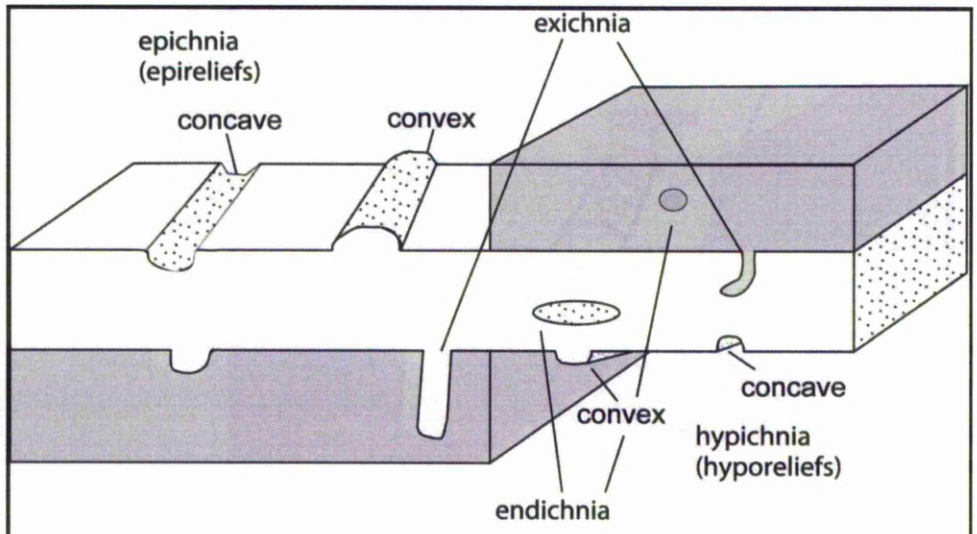

Ethology	Description	Typical genera
Agrichnia	Microbial farming/ gardening traces	Pa. Me. Sp.
Chemichnia	Chemosymbiotic feeding traces	Ch.
Cubichnia	Resting traces	Ca. Be.
Domichnia	Dwelling traces	Oph.
Fodinichnia	Feeding traces	Th. Zoo.
Pascichnia	Grazing traces	Sc. Ne.

5.3.2 Ethological interpretation

Trace fossils record the behaviour (ethology) of a trace maker. As such, a single trace may potentially be a composite of several different behaviours (and therefore ethologies). Here, only a single dominant ethology is applied to each trace fossil. For example, *Ophiomorpha* may represent domichnia, fodinichnia, or a combination (e.g. Frey and Howard, 1978). Recent work has also suggested that deep marine *Ophiomorpha* may represent agrichnia (e.g. Uchman, 2009; Cummings and Hodgson, 2011). *Ophiomorpha* is diagnosed by the presence of muddy pellets used to reinforce the burrow wall in loose, unconsolidated substrate (e.g. Frey *et al.*, 1978). As this reinforcement serves to create a semi-permanent domicile, the trace fossil is here treated to primarily represent domichnia. All graphoglyptid taxa are here interpreted to represent agrichnia (see Seilacher, 1977a, 1977b; Uchman, 2003 for further discussion). Uchman (1995, 1998, 2001) and Rodríguez-Tovar *et al.* (2010) also provide detailed information on ethology of deep sea trace fossils. Figure 5.6 displays a list of discussed ethologies and typical ichnogenera assigned to these ethologies. Appendix 1 lists type specimen references, morphological groupings (*sensu* Uchman, 1998) and interpreted ethologies of all trace fossils encountered in this study. Appendix 2 is a collection of photographic plates pertaining to all of the discussed traces.

5.4 RESULTS

Trace fossil distribution from proximal to distal environments in the Basque Basin

The distribution of ethologies across the various interpreted environments of deposition are summarised below and in Figure 5.7. Ichnodiversity, bioturbation intensity and graphoglyptid distributions are summarised in Figure 5.8. A full list of individual ichnotaxa per environment of deposition is given in Table 5.3.

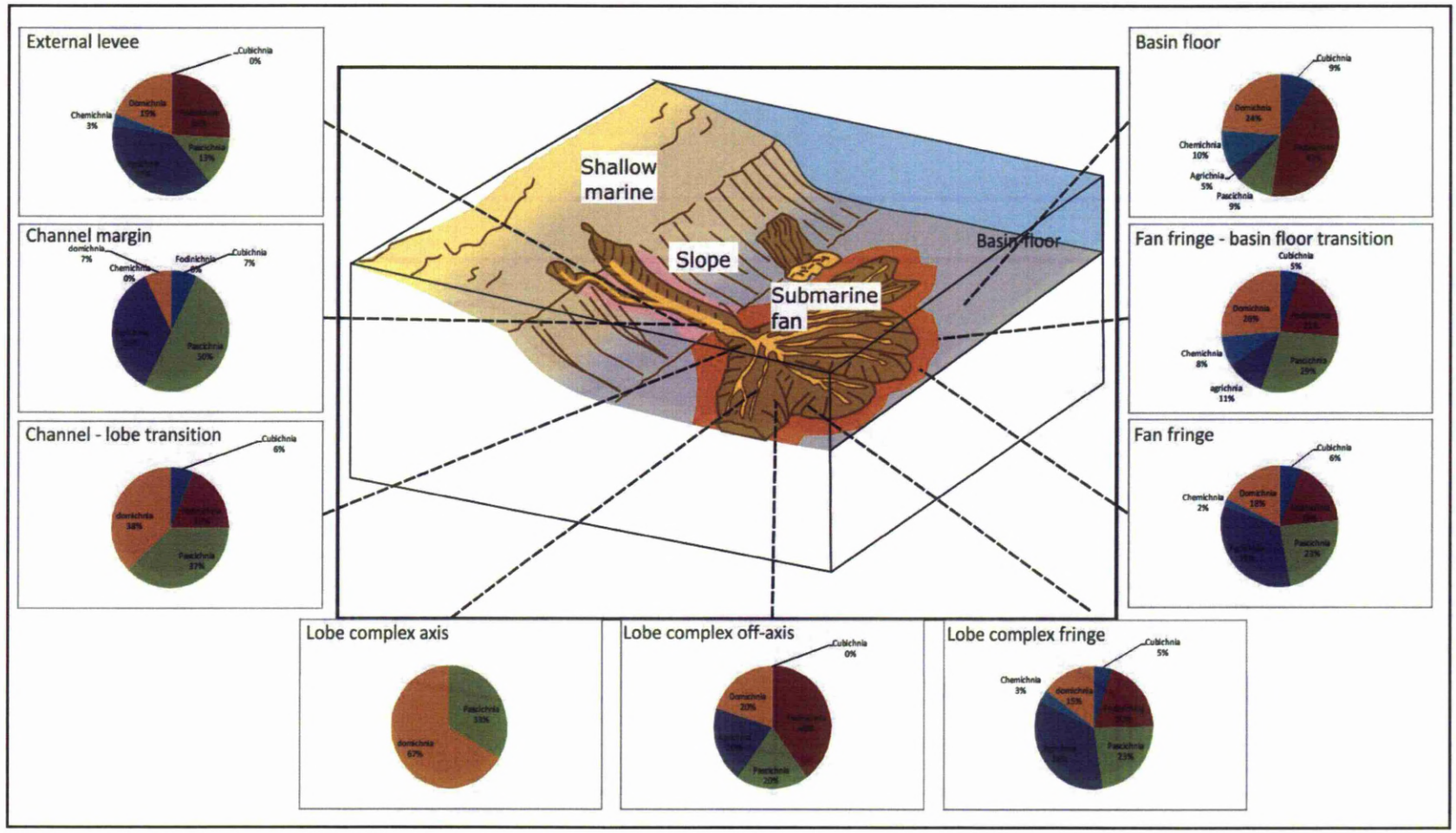

Fig. 5.7: Pie charts displaying distribution of ethologies throughout different sub-environments of the submarine fan. See text for discussion.

5.4.1 Channel related environments of deposition

Submarine external levee deposits (*sensu* Kane and Hodgson, 2011; Fig. 5.2A) preserve 19% domichnia, 24% fodinichnia and 13% pascichnia. Agrichnia is the dominant ethology, representing 39% of ichnotaxa present. Chemichnia (3%) are solely represented by the ichnogenus *Chondrites*. Cubichnia are absent. The average bioturbation intensity is 21% (Fig. 5.7, 5.8).

Channel margin deposits (thin-beds that thin above incision surfaces, see Fig. 5.2B) display very rare domichnia (7%) and fodinichnia are absent. Pascichnia are the dominant ethology (50%) with a total of 7 pascichnial ichnotaxa present. *Scolicia* is particularly abundant in this environment. Agrichnia represents 36% of ichnotaxa although this figure reflects the relatively low overall ichnodiversity (14 ichnotaxa of which 6 are agrichnia/graphoglyptids). Cubichnia are recorded at 7%, with absent chemichnia. The average bioturbation intensity is 39% (Fig. 5.7, 5.8).

Channel-lobe transition/base-of-slope deposits (Fig. 5.2C) are dominated by thick-bedded and amalgamated sandstones with widespread dewatering features. Deposition by high concentration turbidity currents means internal lamination is rare although locally, metre-scale cross bedding is present. This environment of deposition is dominated by domichnia (38%) with *Ophiomorpha rudis* particularly common. Fodinichnia are relatively common (19%). Pascichnia are common (37%) and is dominated by *Scolicia,* which routinely is preserved as intensely bioturbated monospecific assemblages on epichnial surfaces on thicker bedded sandstones. A single resting trace (*Cardioichnus planus*) provided the only example of cubichnia, with agrichnia and chemichnia being absent. The average bioturbation intensity is 36% (Fig. 5.7, 5.8).

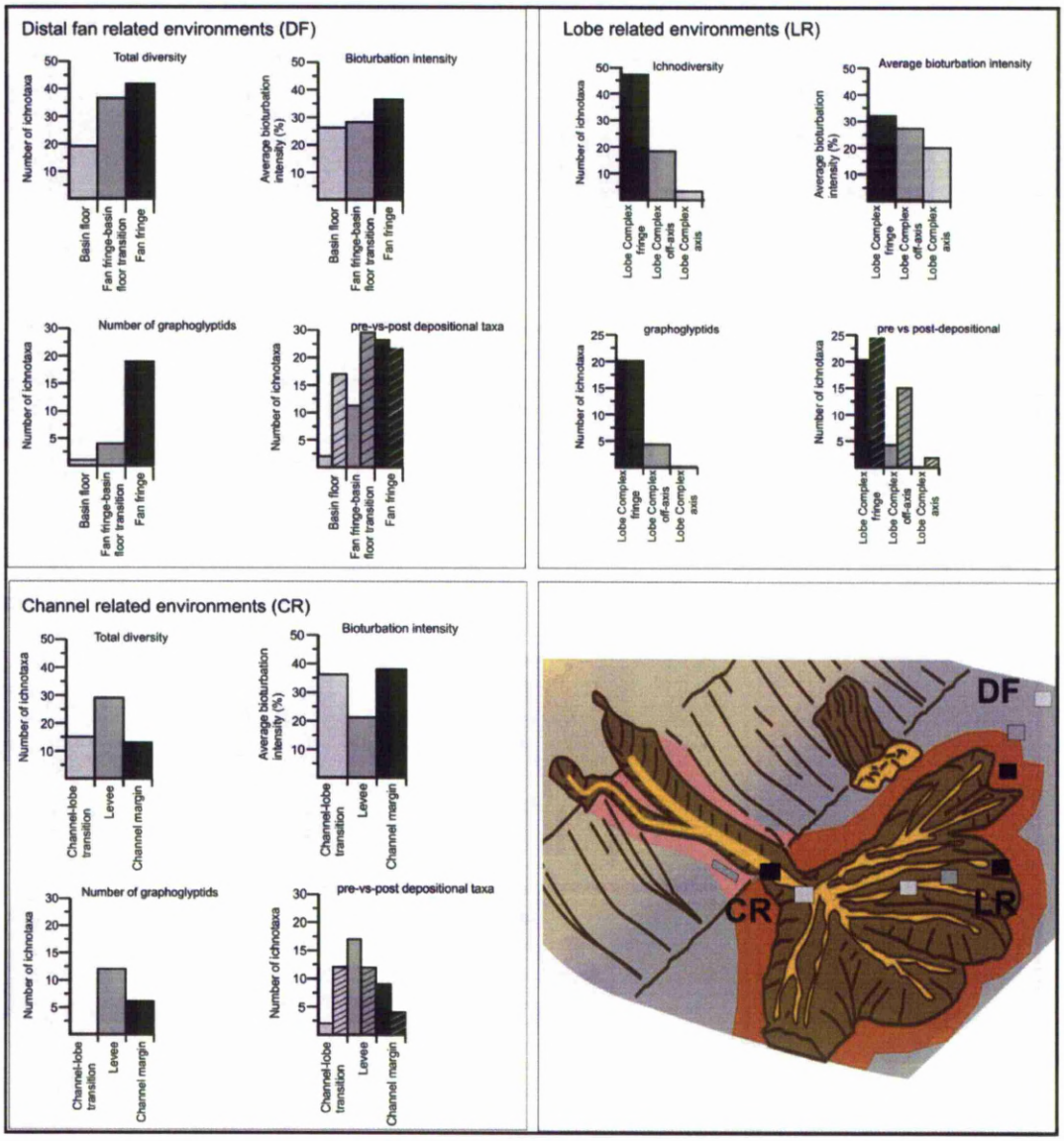

Fig. 5.8: Trace fossil data from sub-environments within the submarine fan. Bar charts are colour coded to their location within the submarine fan system (LR = lobe related, CR = channel related, DF = distal fan related). Pre-vs.-post-depositional ichnotaxa; solid bar = pre-depositional, crosshatch bar = post-depositional ichnotaxa.

5.4.2 Lobe related environments of deposition

Lobe complex axis deposits (*sensu* Prélat *et al.* 2009, see Fig. 5.2D) are dominated by thick amalgamated coarse-grained, high concentration turbidites with rare intercalated fine-grained deposits. The axial lobe complex deposits display a very low ichnodiversity assemblage dominated by endichnial *Ophiomorpha rudis* with rare *Ophiomorpha annulata.* Epichnial surfaces are moderately bioturbated by *Scolicia prisca* trace makers. As a consequence of the low recorded ichnodiversity, domichnia (67%) and pascichnia (33%) are the only recorded ethologies. The average bioturbation intensity is 20% (Fig. 5.7, 5.8).

Lobe complex off-axis deposits (*sensu* Prélat *et al.* 2009, see Fig. 5.2E) display similar sedimentary facies to the lobe fringe, but medium-to-thick (c.0.5-1 m) sandstone turbidites are more common and intercalated mud-prone packages are much thinner to absent (<20cm). This environment of deposition displays identical levels of domichnia, agrichnia and pascichnia (20%). The dominant ethology is fodinichnia (40%) due to a diverse assemblage of fodinichnial traces including the ichnogenera *Planolites*, *Palaeophycus, Thalassinoides, Fascichnium* and *Spongeliomorpha* (which here is classified as fodinichnia/domichnia). Cubichnia and chemichnia are both absent. The average bioturbation intensity is 27% (Fig. 5.7, 5.8).

Lobe complex fringe deposits (*sensu* Prélat *et al.* 2009, see Fig. 5.2F) display packages of fine-to-medium-grained sandstone turbidites that commonly display coarsening- and thickening-upward trends. Intercalated fine-grained sediments are almost exclusively siliciclastic mudstone with thin fine-grained turbidites. Lobe complex fringe successions on average preserve 15% domichnia and 20% fodinichnia. Pascichnia are common (29%), due to diverse pascichnial ichnotaxa with *Scolicia* (post-depositional *Scolicia plana, S. prisca, S. vertebralis* and pre

depositional *S. strozzi*) being the most abundant plus less commonly occurring *Halopoa annulata* and *H. imbricata,* with *Nereites irregularis*. Agrichnia is the dominant ethology in the lobe fringe (34%) with graphoglyptids being particularly common (20 ichnotaxa identified across approximately 60m of stratigraphy) in thinner (<1m) beds. Thicker beds (>1m) are rare but when present, are intensely bioturbated by *Ophiomorpha rudis* trace makers. Cubichnia (5%) and chemichnia (3%) comprise the remaining ethologies. The average bioturbation intensity is 32% (Figs. 5.7, 5.8).

5.4.3 Distal fan environments of deposition

The fan fringe deposits (Fig. 5.2G) preserved at Zumaia and Sopelana display thin bedded (1-15 cm) siliciclastic turbidites that are generally fine grained but occasionally up to medium-grained sandstone. Mudstones are dominantly siliciclastic although some units are rich in carbonate. Both localities display near identical ethological characteristics with fodinichnia (18%), agrichnia (33%), and pascichnia (23%) representing the dominant ethologies of ichnotaxa present. Domichnia are also common (18%), with chemichnia (2%) and cubichnia (5%) comprising the remaining ichnotaxa. The average bioturbation intensity is 38% (Figs. 5.7, 5.8).

Fan fringe-basin floor transition deposits (Fig. 5.2H) are dominated by mixed carbonate and siliciclastic mudstones rarely exceeding 1m thickness with more thin (1-5cm), fine-grained siliciclastic turbidites compared to the basin floor. Domichnia represents 26% of ichnotaxa identified in the fan fringe-basin floor transition. Fodinichnia are common (21%), with agrichnia being comparatively rare (11%). Pascichnia dominates this environment (29%), largely due to

diverse *Scolicia* (pre-depositional *Scolicia strozzi* and post depositional *S. plana, S. prisca* and *S. vertibralis*). and commonly occurring *Nereites irregularis. Halopoa imbricata* and *H. annulata*

occur less commonly and are largely restricted to siliciclastic turbidite beds. Chemichnia (8%) and cubichnia (5%) also occur infrequently as ethologies, although *Chondrites* (particularly *C. intricatus*) is of high abundance. The average bioturbation intensity is 29% (Figs. 5.7, 5.8).

Typically, distal basin floor deposits (Fig. 5.2I) in the Basque Basin are represented by carbonate or siliciclastic mudstones intercalated with rare thin-bedded fine-grained calcareous and sandstone turbidites. This environment preserves trace fossil assemblages that are dominated by fodinichnia (43%) and domichnia (24%). *Zoophycos brianteus*, *Zoophycos insignis* and *Chondrites intricatus* are the most common trace fossils. Overall, ichnodiversity is moderate with 19 ichnotaxa identified. Agrichnia are very rare (5%) with a single graphoglyptid recorded (*Paleomeandron elagans*). While *Chondrites* is abundant, only two ichnotaxa were identified (*Chondrites intricatus* and *C. targionni*) leading to chemichnia being a comparatively rare ethology along with Pascichnia and cubichnia (9% each). The average bioturbation intensity is 26% (Figs. 5.7, 5.8).

5.4.4 *Summary*

Overall, ichnodiversity is high in most of the studied lobe-related environments and displays an increase from the lobe complex off-axis (18 ichnotaxa) to the lobe complex fringe (47 ichnotaxa), the most diverse trace fossil assemblage of any of the studied depositional environments. Fan fringe settings display the next most diverse assemblage (42 ichnotaxa). The most proximal environments (channel-lobe transition) and axial environments (lobe complex

axis) yielded assemblages with low ichnodiversity (less than 15 ichnotaxa and 3 ichnotaxa respectively) where amalgamated beds indicate comparatively little time for colonization of substrate between emplacement of (high- concentration) turbidity currents. Also, bed amalgamations also imply significant/complete erosion of mudstone interlayers, and tops of sand beds, which reduces the preservation potential of pre-depositional trace fossil communities. The distal fan fringe-basin floor transition settings also yielded a low ichnodiversity assemblage. Fodinichnia are most prevalent in the distal basin floor where abundant *Zoophycos* is the dominant ichnogenus.

In lobe-related environments of deposition, fodinichnia display a general increase towards more proximal environments. Domichnia, which is dominated by *Ophiomorpha rudis* and *Ophiomorpha annulata,* displays a general increase both towards more proximal and more axial environments. However, both of these ichnotaxa occur abundantly throughout all depositional environments of the Basque Basin except the most distal basin floor setting. Graphoglyptids (and therefore agrichnia, see Seilacher, 1977; Uchman, 2003) increase from distal (basin floor) to proximal (fan fringe-basin floor transition, fan fringe, lobe complex fringe/lobe complex off-axis) settings, although they are absent in the most proximal/axial lobe environments, in part due to erosion and bed amalgamation.

Pascichnia are abundant in the fan fringe-basin floor transition zone (mainly *Nereites irregularis*). *Scolicia* ichnospecies are rare in the distal basin floor but are extremely common in fan fringe environments where they commonly completely bioturbate epichnial (*Scolicia plana* and *S. prisca*) and hypichnial surfaces (pre-depositional *S. strozzi* and post-depositional *S. plana* in *Subphyllochorda* preservation, see Uchman, 1995, 1998). Channel-related environment trace fossil assemblages display a wide range of pascichnia (channel-lobe transition 37%, channel

margin 50%, levee overbank 19%). *Halopoa* is common in channel margin and channel-lobe transition deposits, but is completely absent in the levee-overbank deposits where the only pascichnial traces are *Helminthopsis* and pre-depositional *Scolicia strozzi.*

Chemichnia are most prevalent in distal environments, particularly the fan fringe-basin floor transition zone and the distal basin floor. Chemichnia and cubichnia only occur sporadically throughout the other recorded depositional environments.

5.5 DISCUSSION

5.5.1 Comparison to previous studies

Heard and Pickering (2008) proposed trace fossil assemblages as being a supplementary diagnostic tool to the identification of submarine fan-related environments of deposition rather than only as a proxy for proximal-distal relationships (e.g. Seilacher 1974; Crimes 1977; Uchman 2001). This study broadly supports many findings of their study, particularly when viewed from an ethological perspective. That this case study, and the Heard and Pickering (2008) work, are from pene-contemporaneous and palaeogeographically close successions is important as the habitats of ichnotaxa do not remain stable over geological time (e.g. Bottjer *et al.*, 1987, 1988; Tchoumatchenco and Uchman, 2001; Cummings and Hodgson, 2011).

Heard and Pickering (2008) noted the greatest ichnodiversity in lobe and lobe fringe environments due to diverse graphoglyptid-enriched trace fossil assemblages, which is consistent with the findings presented here (Fig. 5.8, 5.10). A peak in overall deep-marine ichnodiversity during the earliest Eocene is largely due to diversification of graphoglyptid ichnotaxa (Uchman, 2003, 2004). Uchman (2001) recorded similar results in his study of the Hecho Group. This study also supports a higher proportion of graphoglyptids in fan fringe environments *versus*

basin plain environments. Studies on the Hecho Group (Uchman, 2001; Heard and Pickering, 2008) recorded higher levels of graphoglyptids in basin plain environments than this study, and also recorded lobe related facies as having the greatest average bioturbation intensity. However, bioturbation intensity as a quantitative measurement should be treated with caution as outcrops may bias hypichnial or epichnial surfaces and rarely do they give a true reflection of endichnial bioturbation (see Fig. 5.6).

A proximal-to-distal decrease in domichnia and increase in fodinichnia is consistent with observations of both Uchman (2001) and Heard and Pickering (2008). Similar axis-to-off axis-to-fringe trends in bioturbation were noted in this study. A distinct increase in graphoglyptids (and agrichnia) occurs towards more off axis environments, particularly the channel margin and levee overbank, combined with a decrease in domichnia and increase in pascichnia. It should be noted, however, that proximal/axial channel-lobe transition deposits in this study revealed an anomalously high proportion of pascichnia primarily due to abundant and intense bioturbation by *Scolicia* trace makers on epichnial surfaces. *Scolicia* is recorded as rare in distal lobe/fan fringe environments in Heard and Pickering's (2008) study which is contrary to the findings of this study where *Scolicia* routinely completely bioturbates beds in the fan fringe environments.

Uchman (2001) noted differences in the types of graphoglyptids preserved in different depositional environments. *Helminthorhaphe* and *Cosmorhaphe* displayed a relatively uniform distribution. *Helminthorhaphe* is largely confined to the fan fringe at Zumaia but *Cosmorhaphe* shows no strong environmental control. *Desmograpton* and *Urohelminthoida* are representative graphoglyptids of distal fan fringe deposits in both this study and those of Uchman (2001) and Heard and Pickering (2008).

		Distal Fan			Lobe related			Channel related		
Taxa	**Plate**	**BF**	**FF-BF**	**FF**	**LF**	**LO-A**	**LA**	**EL**	**CM**	**CLT**
Acanthorhaphe delicatula	4		R				R			
Acanthorhaphe incerta	4		R	C		R				
Arenocolites isp.	1			R						
Arthrophycus strictus	1			R				R		
Arthrophycus tenuis	1	R	C	C						
Beaconites capronus	2				R					
Belocosmorhaphe aculeata	3							R		
Belorhaphe zickzack	4		R	C	C					
Bergaueria prantli	2	C	C							
?Chondrohaphe isp.	3				R					
Cardioichnus planus	2			R	R					R
Chondrites intricatus	3	A	A	A	C			C		
Chondrites targionni	3	C	C							
Cosmorhaphe lobata	3			C	C			R		
Desmograpton alternum	5			C					R	
Desmograpton dertonensis	5			C	C			C		
Fascichnium extentum	5					R				
Glockerichnus alata	5			R	C					
Glockerichnus glockeri	5				R					
Gordia marina	5			C	R					
Halopoa annulata	6		C	C	C	C				C
Halopoa imbricata	6	R	R	C		R			A	C
Helminthopsis abeli	6		C	C	C			R	R	R
Helminthopsis granulata	6				R	C		R		
Helminthopsis tenuis	6				C	C				
Helminthopsis hyroglyphica	6		R	R	R					
Helminthorhaphe flexuosa	5			C	C				R	
Helminthorhaphe miocenica	5			R	C					
Hormosiroidea annulata	5		R	C	R	R		R		R
Lorenzinia carpathica	4				R	C				
Lorenzinia plana	4		C	A	C	C		C		
Mammillichnus aggeris	2			R	C				R	
Megagrapton irregulare	3			C	C	R			C	
Megagrapton submontanum	3			R	A					

		Distal Fan			Lobe related			Channel related		
Taxa	Plate	BF	FF-BF	FF	LF	LO-A	LA	EL	CM	CLT
Nereites irregularis	3		A	A	A	C			A	
Ophiomorpha annulata	1	R	A	A	A	A	C	C	C	A
Ophiomorpha rudis	1	R	C	A	A	A	A	C		A
Ophiomorpha recta	1	R	R	R		R				
Oscillorhaphe venzeloelana	4			R				R		
Paleodictyon gomezi	6				R					
Paleodictyon latum	6			R	R					
Paleodictyon majus	6				C			R		
Paleodictyon minimum	6			C					R	
Paleodictyon miocenicum	6			R						
Paleodictyon strozzi	6			C	R			C		
Paleomeandron elegans	4			R	R					
Paleomeandron robustum	4			R	R			R		
Palaeophycus tubularis	1	A	C	R	R	C				C
Planolites beverleyensis	1	A	A	C	C	C		C		C
Phycosiphon incertum	2		A	C	C				R	
Protovirgularia obliterata	5			R	R	R				
Protopaleodictyon incompositum	4			C	C			R		
Rhizocorallium iregulare	2	R								
Saerichnites isp.	5			R	C	R				
Saerichnites canadensis	5			R						
Scolicia plana	2		C	A	A	A			A	C
Scolicia prisca	2			C	A		C		C	A
Scolicia strozzi	2		A	A	A			C	A	
Scolicia vertabralis	2				R					C
?Skolithos linearis	2		R						C	
Spirorhaphe involuta	3				C				R	
Spirophycus bicornis	4		C	C	A	C		A		
Spirophycus involitimus	4				C					
oraviense	1			R	R					
slumbricoides	1		R	R	R	R		R		R
Strobilorhaphe clavatus	6			R				R		
Strobilorhaphe glandifer	6		R		C	C		R		
Taenidium isp.	2		R	R						
Thalassinoides suevicus	1	A	A	C	C	C		R		A
Trichichnus linearis	2		C							
Urohelminthoida dertonensis	4			R					C	
Zoophycos brianteus	3	A	R							
Zoophycos insignis	3	A	A	R						

Table 3: (page 120-121) Complete list of ichnotaxa identified at each locality. R = rare (less than 5 recorded occurrences). C = common (5-10 recorded occurrences). A = abundant (more than 10 recorded occurrences). Distal fan environments: BF = basin floor, FF-BF = fan fringe to basin floor transition, FF = fan fringe. Lobe related environments: LF=lobe fringe, L-OA = lobe off-axis, LA = lobe axis. Channel related environments: EL = external levee, CM = channel margin, CLT = channel-lobe transition. Scale bar =2 cm except where otherwise stated.

More regular patterned forms such as *Paleodictyon* seem dependent on regular input of sand under weakly erosive conditions and thus occur more frequently in off-axis lobe/lobe fringe environments and levee environments where low-concentration turbidity currents predominate over erosive high-concentration flows. Uchman (2001) challenged Książkiewicz's (1970, 1977) and Crimes' (1973) use of rosetted (and meandering) forms as indicators of distal environments. This study also confirms that rosetted forms (particularly *Lorenzinia*) show no real proximal-distal trends apart from displaying an absence in the most proximal lobe facies. However, *Lorenzinia* does occur frequently in medium-thick bedded, fine grained lobe fringe-off axis facies at Getaria and also in the external-levee deposits at Orio. Figure 5.10 summarises typical trace fossil assemblages across the interpreted depositional environments pertaining to this study.

The distribution of graphoglyptids, the frequency of *Nereites irregularis* (commonly assigned to *Helminthoida*), the preponderance of *Ophiomorpha* and *Scolicia* in sandier facies and the dominance of *Zoophycos* and *Chondrites* in carbonate and/or basin floor facies is consistent with many studies on Paleogene basin-fill successions (e.g. Crimes, 1973, 1977; Uchman, 1992, 1995, 1999, 2001; Tunis and Uchman, 1996a, b, 1998, Uchman and Demircan, 1999; Buatois *et al.*, 2001; Uchman *et al.*, 2004; Monaco *et al.*, 2010). Phillips *et al.* (2011) suggest that ichnodiversity in turbiditic settings may be overstated by a bias towards studying particularly enriched and famous sections such as the Hecho Group (Uchman, 2001; Heard and Pickering, 2008) or Zumaia (e.g. Crimes, 1977; Leszcyznski, 1991; Gianetti and McCann, 2010; this study).

The weight of previous literature seems to contradict this suggestion. However, the ichnofabric approach used by Phillips *et al.* (2011) does confirm the importance of *Ophiomorpha* as a normal component of Paleogene deep-marine trace fossil assemblages.

Knaust (2009) conducted a core and seismic based study on a Campanian deep sea fan system in the Norwegian Sea that revealed similar bioturbation patterns. Low ichnodiversity *Ophiomorpha* ichnofabrics dominate in proximal/channelized facies. Ichnodiversity increases distally and laterally off-axis, but decreases in the most distal mud-dominated environments where *Zoophycos, Chondrites* and *Phycosiphon* commonly occur with *Thalassinoides,* which was interpreted to represent transgression surfaces. *Scolicia* ichnofabrics dominate in heterolithic sediments that were interpreted as proximal overbank deposits. *Scolicia* was also a commonly occurring component of a *Phycosiphon* ichnofabric interpreted to represent a fan fringe depositional environment, again consistent with this study. However, it should be noted that core based ichnological analysis (both ichnofabric and ichnofacies) differs significantly to outcrop-based studies due to the vertical bias of core versus the bedding plane bias of outcrop data (for discussion see Bromley, 1996; Knaust, 2009).

5.5.2 Taphonomy in submarine fan deposits

To constrain the effects on trace fossil assemblages of any palaeoecological/environmental factors requires an understanding of taphonomical processes. Such processes vary significantly across the broad range of depositional environments preserved in a submarine fan so influence the types of trace fossil assemblages preserved. Perhaps the most important factor affecting the preservation of trace fossil assemblages is the depth of substrate erosion. Trace fossil

communities display distinct tiering (e.g. Bromley and Ekdale, 1986; Leszcyznski, 1991; Wetzel, 1991; Wetzel and Uchman, 2001). Endobenthic traces (i.e. below sediment water interface), particularly the shallow tier graphoglyptids, are reliant upon gently erosive turbidity currents to exhume and cast them (e.g. Seilacher, 1977). The depth to which a passing turbidity current incises into a substrate dictates the depth of tier that may be cast and preserved. Pre-depositional trace fossils such as the graphoglyptids are almost exclusively preserved on the soles of turbidites. Commonly, proximal/axial environments that experience frequent flow events form amalgamated beds. High concentration, coarse grained turbidity currents associated with such environments are likely to be too erosive to preserve shallow tier trace fossil communities. The Basque basin, particularly in the late Cretaceous-late Paleocene, also received input of calcareous turbidites of considerably different composition than the siliciclastic turbidites of the early Eocene. Uchman (1995) suggests the compositional differences of marly turbidites versus siliciclastic turbidites may affect the level of tiering revealed after erosion. Carbonate sediments are usually enriched in material with low weight to surface area ratios (e.g. foraminifera tests) and are thus less erosive than dense siliciclastic grains. This means that shallow tier communities such as the graphoglyptids are not exhumed by such low density flows.

5.5.3 Palaeoecology and sediment supply

There are a number of factors that can contribute to the dramatic differences in trace fossil assemblages across a relatively narrow range of depositional environments. Firstly, the late Paleocene basin floor environment is dominanted by carbonate muds (micritic limestone and marlstones) interspersed with dominantly calcareous turbidites with subordinate siliciclastic turbidites, increasing in frequency as the *Paleocene* progresses. Previous studies (e.g. Uchman, 1999, 2007a, 2007b and references therein) have shown that mixed carbonate-siliciclastic deep

marine deposits generally yield lower diversity trace fossil assemblages than exclusively siliciclastic deposits. This is in part due to the monotonous nature of sedimentation in limestone/marlstone alternations that is likely depleted of organic matter compared to siliciclastic sediments that receive pulses of nutrients/organic matter from shallower water and the terrestrial realm. It is also probable that oxygenation is lower in the more distal basin floor due to the lack of turbidity currents importing well oxygenated waters. Carbonate sediments will also display a lower contrast in colour between bioturbated and non-bioturbated fabrics, hindering the identification of ichnotaxa and the quantification of bioturbation intensity.

Ichnodiversity is almost certainly affected by oxygen levels with shallow tier burrowers typically the first to disappear under disoxic/anoxic conditions (e.g. Wetzel, 1991). The *Chondrites-Zoophycos* ichnoguild (groups of ichnofauna that thrive in particular environments) for deep basinal settings (e.g. Bromley, 1996) is recognized in the late Paleocene basin floor of Zumaia (see also Gianetti and McCann, 2010) and represents deep tier fodinichnial and chemichnial ethologies. Commonly, *Chondrites* itself is associated with anoxia (e.g. Bromley and Ekdale, 1984). Beds displaying more diverse ichnofaunal assemblages in the late Palaeocene of Zumaia

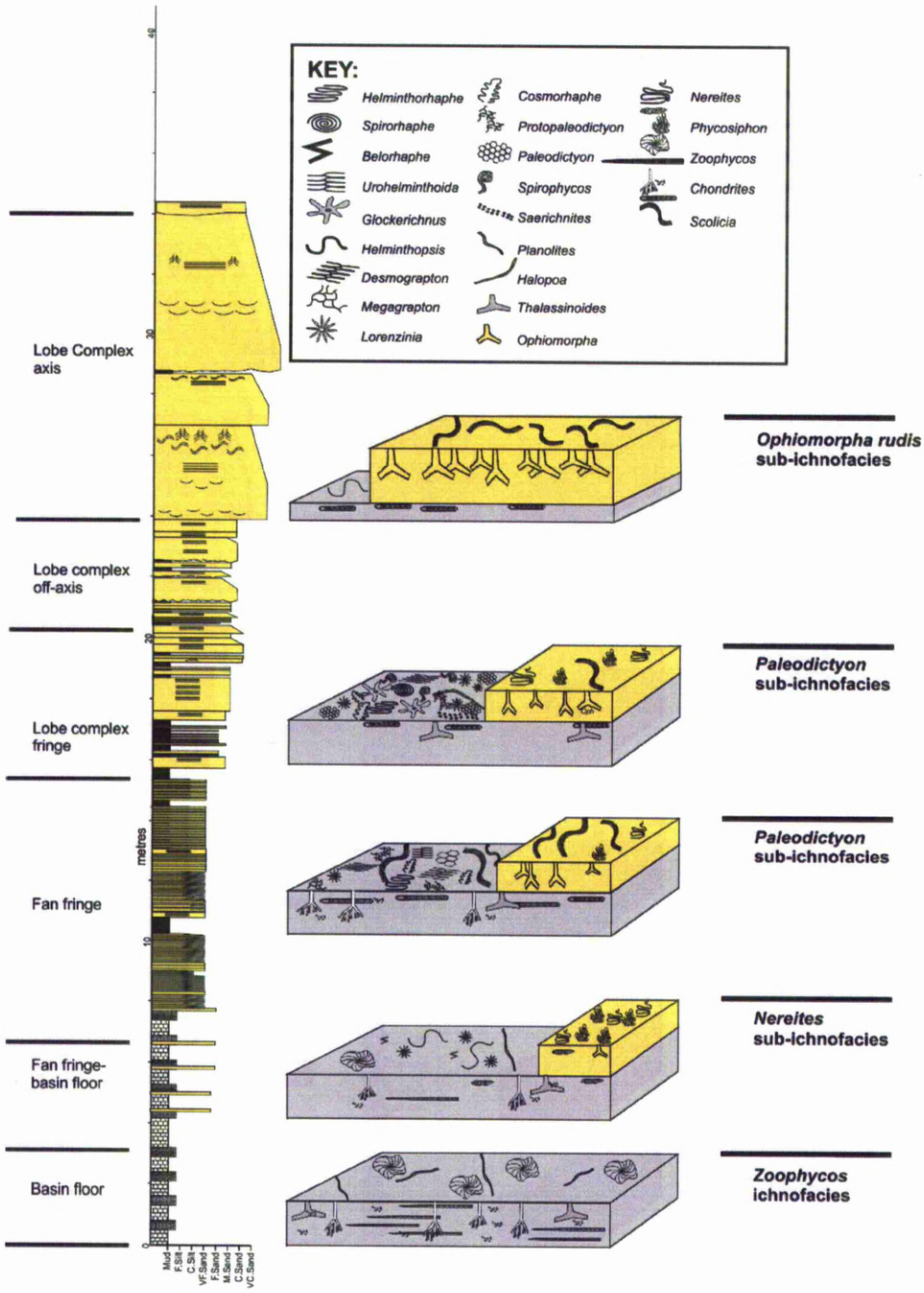

Fig. 5.9 Idealised sedimentary log displaying a progression from; distal carbonate basin floor deposits displaying typical *Zoophycos* ichnofacies, to lobe complex off-axis and lobe axis deposits displaying a typical thick bedded lobe complex trace fossil assemblage (or *Ophiomorpha rudis* sub-ichnofacies of Uchman, 2001).

are associated with input of calcareous turbidity currents (see also Gianetti and McCann, 2010) and probably represent opportunistic colonization of event beds (or r-selected ichnotaxa *sensu* Ekdale, 1985). The background (hemi) pelagic sediments are generally low ichnodiversity assemblages dominated by *Zoophycos* and *Chondrites*.

The external levee deposits at Orio (early Eocene) preserve a rich graphoglyptid assemblage (12 ichnotaxa) dominated by *Paleodictyon* but also preserve an unusually large amount of *Spirophycus bicornis*, occurring on nearly 50% of beds sampled. While not being a graphoglyptid, *Spirophycus bicornis* is probably a fodinichnial trace (see Uchman, 1998 for discussion) and occupies the same shallow tier and equilibrium community as the graphoglyptids. More detailed ichnological studies of levee systems may reveal this to be part of an ichnoguild (*sensu* Bromley 1996; Taylor *et al.*, 2003) that is diagnostic of (proximal) external levee deposits, at least of broadly contemporaneous ages. Kane *et al.*, (2007) record similar graphoglyptid rich assemblages in an Upper-Cretaceous-Paleocene levee system to this study but also record 'anomalous' components of the *Cruziana* and *Skolithos* ichnofacies overprinting the background *Nereites* assemblage. In fact, these elements (predominantly *Ophiomorpha* and *Thalassinoides*) can be considered normal components of deep sea trace fossil assemblages of at least Upper Cretaceous age and younger (see Tchoumatchenco and Uchman, 2001; Uchman, 2009). The shallow tier equilibrium community is overprinted by opportunistic associations of *Ophiomorpha* and *Thalassinoides* that rapidly colonize the coarser sand inputted into the levee and exploit nutrients within these event beds. Eventually, the equilibrium community re-establishes until the next turbidity current exhumes and casts them onto the sole of the next event deposit.

In lobe-related environments, similar colonization strategies are evident. Pre-depositional graphoglyptids are abundant in all but the most proximal lobe facies suggesting benthic conditions well suited to their trace makers. Thin-to-medium thickness beds (c.0.1-1m) in the lobe fringe environment of Getaria (early Eocene) preserve a rich graphoglyptid assemblage with 16 ichnotaxa identified at this one 30 m-thick section (20 graphoglyptid ichnotaxa were identified in total across all lobe fringe outcrops). It is probable that such an environment is taphonomically beneficial for shallow tier burrowers. Despite the turbidite thickness (~0.1 - 1m), the grain size range is narrow (fine-to-medium-grained sand) with fine sand predominating. Pelagic muddy units are usually in excess of 0.1m and commonly as thick as 0.3-0.4m, which allowed equilibrium communities (K-selected *sensu* Ekdale, 1985) to establish. Such communities are then preserved on the sole of the weakly erosive thick turbidite beds that exhume and cast the traces (e.g. Seilacher, 1977; Wetzel and Uchman, 2001; Uchman, 2003), rather than completely obliterating shallow tier burrows as a coarser grained, more erosive turbidity currents might. This implies both a strong grain size control and a dependence on pelagic muds thick enough to allow equilibrium communities to develop.

Commonly, post depositional *Ophiomorpha annulata* and *O. rudis* producers bioturbate turbidite beds in excess of 1m thickness in all lobe settings in the Basque basin. Epichnial surfaces of thicker turbidite beds are commonly intensely bioturbated by *Scolicia* trace makers, representing opportunistic colonization of newly deposited turbidites. However, *Scolicia strozzi* is a common component of the pre-depositional trace fossil communities representing shallow tier burrowers (including the graphoglyptids). This suggests that the echinoid trace makers of *Scolicia* were able to optimize food in both quiescent pelagic sedimentation and then able to exploit any nutrients transported into the basin via turbidity currents. It has been suggested that both *Scolicia* and

Ophiomorpha experience a peak in contribution to *Nereites* assemblages during the early Eocene (Uchman, 2004). This is apparently contrary to the oligotrophic conditions of the time as both are infaunal sediment feeders relying on nutrients within the sediment. *Ophiomorpha* burrow dimensions in early Eocene Basque country deposits can reach c.40-45mm diameter (*Ophiomorpha rudis* and *O.* isp.) inferring a large robust animal able to sustain itself on available nutrients within the sediment. One hypothesis is that *Ophiomorpha* developed an agrichnial strategy to harvest and break down cellulose based organic matter (e.g. Uchman, 2004). Whilst further work testing this hypothesis is required, Cummings and Hodgson (2011) discuss several examples of highly organized and systematic *Ophiomorpha* related trace fossils that seem to suggest an agrichnial feeding strategy.

5.5.4 Does age matter? Global ecological change as a control on trace fossil assemblages

In the Ainsa-Jaca basin, both Uchman (2001) and Heard and Pickering (2008) note decreasing agrichnia/graphoglyptids from the fan fringe to the distal basin floor. However, whilst the same trend is observed in this study, the Ainsa-Jaca basin still preserves rich graphoglyptid assemblages in the more distal basin floor. At Zumaia (Fig. 5.1), only a single graphoglyptid ichnotaxon (*Paleomeandron elegans*) was recorded in the distal basin floor. Gianetti and McCann (2010) recorded a similar low ichnodiversity assemblage to this study but also recorded a single occurrence of *Belorhaphe zickzack.* Gianetti and McCann (2010) observed abundant *Zoophycos* and *Chondrites* in the distal basin floor environment of the late Paleocene at Zumaia, consistent with this study. However, the latest Paleocene-earliest Eocene at Zumaia witnessed an increase in siliciclastic supply (the transitional zone of Winkler and Gawenda, 1999) and a concomitant increase in the number of graphoglyptids with three ichnotaxa identified (*Belorhaphe zickzack Lorenzinia plana* and *Lr. carpathica,* with *Lorenzinia* occurring

commonly). The increased frequency of siliciclastic (and increasingly rare calcareous) turbidite beds led to an environmental interpretation of fan fringe-basin plain transition eventually developing into a fan fringe environment approximately 90m above the Paleocene-Eocene boundary. The fan fringe environment records a dramatic increase in overall ichnodiversity with a total of 48 ichnotaxa identified, 15 of them being graphoglyptids (see Table 5.3).

Graphoglyptids are representative of well oxygenated, mildly oligotrophic conditions (e.g. Seilacher, 1977; Rodríguez-Tovar *et al.*, 2010). Bottom water warming associated with the PETM and continuing into the Early Eocene Climatic Optimum (EECO) likely led to oligotrophic conditions in the early Eocene in the Basque Basin. This is supported by foraminferal assemblages (e.g. Algeret *et al.*, 2009) that are dominated by opportunistic (r-selected) ichnotaxa adapted to low oxygen conditions in the lowermost Eocene returning to more oligotrophic conditions following this period. If trace fossils are to be reliably used as an additional tool in determining submarine fan environments of deposition, then close consideration of the palaeoecological conditions in each sub-environment is required. However, the need for this consideration in the Basque Basin is pertinent due to the presence of several key events affecting palaeoecological conditions that occur, most notably the K/T boundary and the PETM.

The lack of graphoglyptids on the soles of both siliciclastic and calcareous turbidite beds in the late Paleocene of the Basque Basin suggests a palaeoecological control rather than a purely taphonomic one. It is possible that the trace makers of the graphoglyptids are adapted to living in conditions with regular pulses of siliciclastic material, transporting in nutrients/organic matter that they are then able to exploit. An alternative hypothesis is that the same trace maker adopts

differing ethologies/feeding strategies when inhabiting carbonate-rich muds rather than siliciclastic-rich muds.

Siliciclastic turbidites in the late Paleocene of Zumaia are weakly bioturbated by low diversity assemblages. *Ophiomorpha annulata* occurs infrequently in pre-Eocene deposits at Zumaia but is one of the most common trace fossils in the early Eocene fan fringe facies (along with *Scolicia*). Both of these ichnotaxa represent r-selected strategists colonizing event beds. However, the frequency with which they occur combined with the wide range of dimensions suggests long term colonization of this environment rather than the doomed pioneer scenario *sensu* Follmi and Grimm (1990; see also Tchoumatchenco and Uchman, 2001; Uchman, 2009 for discussion). It is likely that palaeoecological changes brought about following the PETM created a more suitable environment for both *Ophiomorpha* and *Scolicia* producers. Most notably, an increase in refractory organic matter, inferred from benthic and planktontic foraminifera assemblages (e.g. Algeret *et al.*, 2009) would have benefitted *Ophiomorpha* trace makers. This would be particularly true if *Ophiomorpha* trace makers adapted an agrichnial strategy enabling break down and consumption of such material (Uchman, 2004; Cummings and Hodgson, 2011).

In summary, ethological characteristics of trace fossil assemblages are controlled by the environmental conditions in which the trace maker lived (e.g. Crimes and Fedonkin, 1994; Hagadorn and Bottjer, 1999; Orr, 2001). Tier preservation is almost completely dependent upon depth of erosion. Tier structure and 'ichnoguilds' may be consistent through both geological time and differing palaeogeographies (Taylor *et al.*, 2003; see also Bromley, 1996). However, such techniques should be treated with caution as this study reveals distinct differences in trace fossil assemblages from similar environments of deposition and grain-size range but of different ages in the same basin-fill. This is likely due to successions separated by periods of global

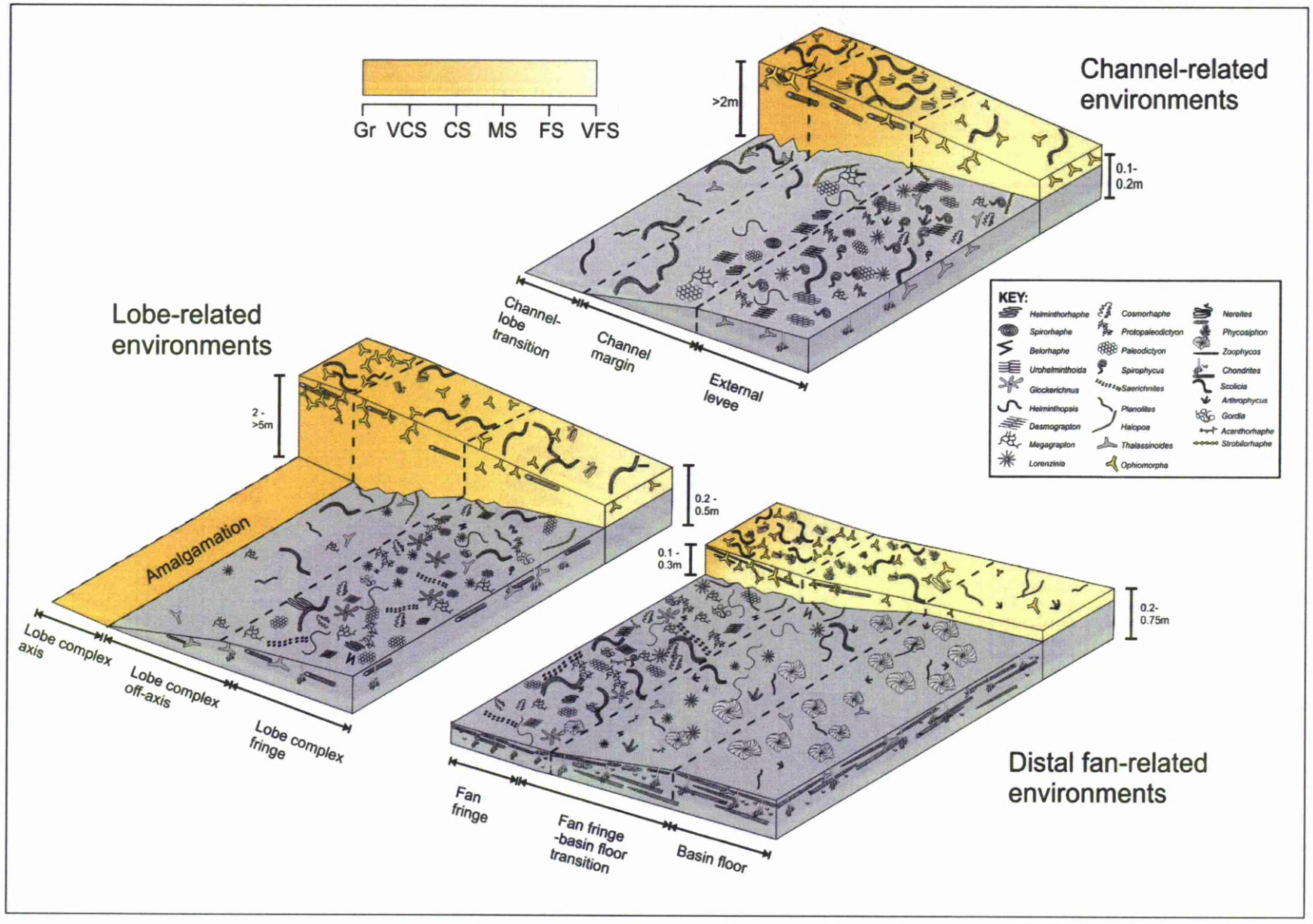

Fig. 5.10 Block diagrams from lobe related, channel related and distal fan related environments. Vertical scales approximate to typical bed thicknesses. Contact between sandstones (bold yellow grading to light yellow to indicate grain-size) and mudstones (grey) shows the relative levels of erosion and the different trace fossil assemblage that this variable preserves. Trace fossil assemblages show relative amounts of bioturbation and comprise typical (but not exhaustive) assemblages from each depositional environment.

environmental change that impacted benthic communities. Relying only on trace fossil assemblages to determine depositional environments based on the presence or absence of individual ichnotaxa is therefore an overly simplistic approach.

5.6 Conclusions

1. Previous workers (Seilacher, 1974; Uchman, 2001) have suggested that proximal-to-distal relationships within typical *Nereites* ichnofacies yield sufficient differences to assign sub-ichnofacies: the *Nereites* (mud-rich fan fringe-basin floor environments), the *Paleodictyon* (sand rich fan fringe environments) and the *Ophiomorpha rudis* (thick bedded channel and lobe related environments). Such sub-ichnofacies provide a useful, informal way of categorizing submarine fan trace fossil assemblages based on a general position (i.e. proximal-medial-distal) within a submarine fan system. However, all three of these sub-ichnofacies may be evident in a single stratigraphic succession (see Fig. 5.9), so are of limited value when attempting to interpret precise depositional environments.
2. If trace fossil assemblages are to be robustly used to discriminate between sub-environments within submarine fans, then detailed data concerning ichnodiversity, intensity and particularly ethologies of trace fossil assemblages needs to be compiled in conjunction with interpretation of depositional environment based on sedimentological criteria. Ichnodiversity as a quantitative measurement is reliant upon thorough taxonomy. However, the style of colonization (K-selected versus r-selected), the ethologies and tiering relationships of ichnotaxa preserved in a given environment is of greater importance than the presence or absence of specific ichnotaxon. Studies such as this and those of Heard and Pickering (2008), Knaust (2009) Monaco *et al.* (2010), and Philips *et*

al. (2011) should be supplemented by further studies where trace fossil assemblages are aligned to the specific environments of deposition in which they are preserved.

3. Where an ichnotaxon is repeatedly identified in an environment of deposition interpreted on the basis of sedimentary facies associations and stratigraphic context then the trace fossil could tentatively be used to constrain depositional environments (not just within the *Nereites* ichnofacies). However, there are dangers in taking this approach without considering the number of identifications (and confidence levels therein), the age, palaeolatitude, basin-type etc. However, in broadly contemporaneous basins then it is likely that 'ichnoguilds' of certain ichnotaxa (or at least of ethological groups) will be representative of a given depositional environment, even across periods of major environmental change (such as the PETM).

CHAPTER 6

AN INTEGRATED ICHNOLOGICAL AND GEOCHEMICAL ASSESSMENT OF THE EARLY PALAEOGENE HYPERTHERMAL EVENTS IN THE BASQUE COUNTRY, NORTHERN SPAIN

ABSTRACT

Here, ichnological changes are quantified and documented across several key Palaeogene environmental perturbations, the Danian-Selandian (D/S) transition, the mid-Paleocene biotic event (MPBE), the Palaeocene-Eocene Thermal Maximum (PETM) and the early Eocene climatic optimum (EECO), in the Basque Basin, northern Spain. Following the D/S transition, trace fossil assemblages are dominated by low diversity, deep-tier fodinichnial assemblages with *Zoophycos* and *Chondrites* being the dominant ichnogenera. Following the MPBE, *Thalassinoides* locally becomes more prevalent and *Zoophycos* occurrences decrease in frequency. Stressed conditions in the latest Palaeocene are inferred from low diversity assemblages with significant reductions in bioturbation intensity. Following the PETM, a gradual return to a 'normal' tiered community occurs but a significant change in the composition of trace fossil assemblages occurs. *Scolicia* and *Ophiomorpha* occurrences increase dramatically, approximately coincident with a dramatic increase in siliciclastic supply to the basin. However, diverse graphoglyptid dominated assemblages do no not appear until sedimentation becomes dominantly siliciclastic, approximately concurrent with the onset of the EECO. Increases in concentrations of the clay mineral kaolinite in the clay fraction of sediments deposited during the PETM and EECO are interpreted to represent increased terrigenous input into the basin (in the form of clay rich plumes),

driven by an enhanced weathering cycle associated with these hyperthermal events. Therefore, benthic palaeoecological changes are correlated with climatic changes on the continental hinterland.

6.1 INTRODUCTION

The greenhouse climate of the early Palaeogene was punctuated by several rapid high magnitude, yet transient episodes of global warming. These events are characterised by carbonate dissolution intervals, negative carbon isotope excursions (CIEs) and rapid evolutionary turnover and/or extinctions of marine microfauna (Alegret *et al.,* 2009). These hyperthermal events (Thomas and Zachos, 2000; Thomas *et al.*, 2000) include the Mid-Palaeocene Biotic Event (MPBE, Bernaola *et al.*, 2006a, 2007), the ELMO event (e.g. Lourens *et al.,* 2005), the X-event (e.g. Roehl *et al.*, 2005), the Palaeocene-Eocene Thermal Maximum (PETM, e.g. Kennet & Stott 1991; Koch *et al.* 1992; Dickens, 1995, 1997; Zachos *et al.*, 2001; Zachos *et al.*, 2005) and the early Eocene climatic optimum (EECO, Zachos *et al.,* 2001).

The PETM was the highest magnitude of these events and witnessed sea surface temperature increases of around 9-10°C at high latitudes and around 4-5°C at low latitudes, probably on a scale of 10^3 years (Kennet and Stott, 1991: Zachos *et al.*, 2003; Tripati and Elderfield, 2004; Zachos *et al.*, 2005). Deep ocean bottom waters also experienced increases of around 5°C (Zachos *et al.*, 2003; Tripati and Elderfield, 2004, 2005; Zachos *et al.*, 2005). A catastrophic release of 1400-2800gt of CH_4 from marine clathrates is now widely accepted to have caused the CIE (Dickens *et al.* 1995; Zachos *et al* 2005). However, there is still contention over the trigger mechanism of the methane release (e.g. Lourens *et al.,* 2005; Svensen *et al.*, 2010).

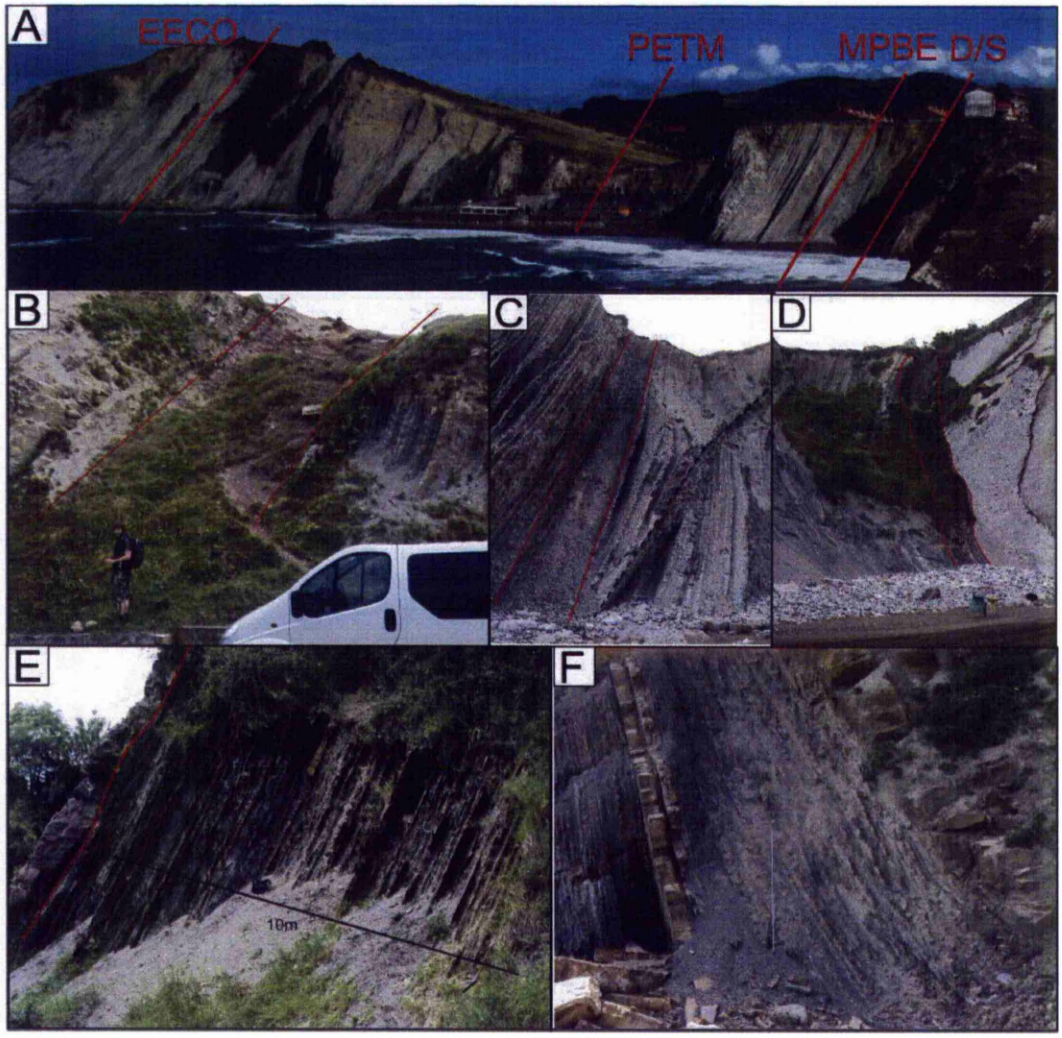

Fig. 6.1 Photo panel showing the stratigraphic position of Palaeogene hyperthermals in the Basque Basin. A.) Itzurun Beach, Zumaia, photographed from the Aitzgorri Headland. D/S = Danian-Selandian transition. MPBE = Mid-Palaeocene Biotic event. PETM = Palaeocene-Eocene Thermal Maximum. EECO = base of early Eocene climatic optimum. B.) Detail of the PETM interval. Note the carbonate rich (light-grey) sediments underlying and overlying the red clay carbonate dissolution interval that represents the main body of the PETM. C.) Detail of the MPBE. Note how this interval has been covered in scree so was not suitable for clay mineral sampling. D.) Detail of the D/S transition. This marks the base of the study interval at Zumaia. E.) PETM interval at Ermua (the 'SU' of

Schmitz *et al.*, 2001). F.) Clay rich interval at the base of a lobe complex of EECO age, Azkorri Sandstone, Gorrondatxe Beach.

The rapid nature of the CIE suggests that isotopically light CH^4 with a $\delta^{13}C$ of c.-60‰ was the source (Dickens *et al.* 1995, 1997; Zachos *et al.*, 2005). This mass input of isotopically light carbon into the carbon cycle led to rapid acidification of ocean waters leading to a rapid (<30 000 years) shoaling of the calcite compensation depth (CCD). The CCD shoaled by at least 2 km and took more than 100 000 years to recover to a normal state (Zachos *et al.* 2005). Shoaling of the CCD was coincident with the most significant benthic microfauna extinction event of the Cenozoic with around 30-50% of benthic foraminifera species becoming extinct (e.g. Thomas, 2007; Alegret *et al.*, 2009). Other biotic effects of the PETM include the *Apectodinium* Dinoflaggelate acme (e.g. Crouch *et al.* 2003), diversification of shallow water larger benthic foraminifera (e.g. Pujalte *et al.*, 2003), and the rapid evolutionary turnover of planktonic foraminifera (e.g. Kelly *et al.*, 1998) and calcareous nannoplankton (e.g. Aubry, 1998; Bralower, 2002). Biotic effects of the PETM were not confined to the marine realm. Rapid increases in temperature were on a global scale, affecting migration routes of fauna leading to dispersal and diversification of land mammals (e.g. Clyde & Gingerich 1998) and shifts in the relative abundance and latitudinal ranges of continental flora (e.g. Wing *et al.* 2003).

6.1.1 The Basque Basin as a natural ichnological laboratory

The Basque Basin preserves some of the best deep marine trace fossil assemblages in the world (e.g. Crimes, 1973, 1977; Leszczynski, 1991; Gianetti and McCann, 2010; Rodríguez-Tovar *et al.* 2010; Cummings and Hodgson, 2011a, 2011b; Rodríguez-Tovar *et al.* 2011), in a wide range of basinal and submarine fan related environments of deposition (e.g. Crimes, 1973, 1976; Van

Vliet, 1978, 2007; Hodgson and Wild, 2007; Cummings and Hodgson, 2011b). The Zumaia section provides an ideal natural laboratory to conduct an ichnological study across several key environmental perturbations, namely; the Danian-Selandian transition, the MPBE, the PETM and the EECO, due to the absence of major unconfirmities and its excellent preservation of trace fossils.

In spite of the extensive literature concerning the marine and terrestrial biotic effects associated with the PETM, one factor still remains elusive. Early Eocene deep-marine trace fossil assemblages comprise the highest diversity throughout the whole of the Phanerozoic (Uchman 2003, 2004). This is contrary to the stressed conditions suggested by the benthic extinction at the onset of the PETM. Also, the crustacean trace *Ophiomorpha*, generally associated with shallow marine conditions (e.g. Frey *et al.*, 1978) but a normal component of deep marine (or Nereites ichnofacies: Seilacher, 1967) trace fossil assemblages in Cretaceous-Miocene sediments, displays a distinct peak in abundance/occurrences during the early Eocene (e.g. Uchman, 2009; Cummings and Hodgson, 2011a). A dramatic increase in the diversity of the graphoglyptids (regular meander, star and net shaped trace fossils) also occurs during the early Eocene (Uchman, 2003). The inference that the graphoglyptids thrive in mildly oligotrophic benthic conditions (e.g. Seilacher, 1977a, 1977b; Tunis and Uchman, 1996; Uchman, 2003) seems to be at odds with robust organisms such as crustaceans thriving while utilising an infaunal feeding strategy.

Here, the response of benthic macrofauna to deep ocean palaeoecological changes driven by climate change and variability in weathering and erosion around the PETM (and several other major environmental perturbations) are considered. This study intends to:

- Analyse changes in ichnodiversity, bioturbation intensity, and occurrences of several environmentally sensitive trace fossils, across the PETM and several other major environmental perturbations during the early Palaeogene.
- Interpret weathering and sediment flux from the continental hinterland using a multi-proxy geochemical approach focusing on PETM clay mineral assemblages.
- Correlate the response of marine benthic macrofauna with changes in weathering and erosion on the continental hinterland and subsequent delivery of sediment to the deep marine Basque Basin associated with the PETM and other climatic/biotic events. .

6.2 GEOLOGICAL SETTING

In the late Cretaceous to early Eocene, the Basque Basin was an elongate deep marine trough with an approximate ESE-WNW orientation (Van Vliet, 1978, 2007). Sedimentation up to the latest Palaeocene was predominantly carbonate in nature and was dominated by alternations of pelagic micritic limestones and hemi-pelagic marlstones interbedded with calcareous turbidites sourced from collapse of pene-contemperaneous shallow-water carbonate platforms (Crimes, 1976; Pujalte *et al.*, 1995; Winkler and Gawenda, 1999). Siliciclastic sedimentation increased dramatically towards the end of the Palaeocene and into the early Eocene (termed the transitional system by Winkler and Gawenda, 1999), until sedimentation became almost exclusively siliciclastic into the early Eocene (NP11/NP12 biozone boundary, Winkler and Gawenda, 1999). Palaeoflow was dominantly axial (westward). Siliciclastic sediments were predominantly derived from the north and east with a subordinate supply from the southeast (Crimes, 1976; Van Vliet, 1978, 2007), leading to the development of a turbidite fan system ((Kruit *et al.*, 1972; Van Vliet, 1978).

The Zumaia section (UTM: 059919 4794322 – top Danian/base Selandian, see Figs. 6.1 and 6.2) records near continuous sedimentation from the late Cretaceous through to the early Eocene (e.g. Crimes, 1976; Winkler and Gawenda, 1999; Gawenda *et al.*, 1999). Sedimentary facies dominantly comprise distal basin plain-fan fringe facies (e.g. Van Vliet, 1978; Cummings and Hodgson, 2011b). The Zumaia section has one of the most widely studied PETM sections in the world (e.g. Canudo *et al.*, 1995; Schmitz *et al.*, 1997; Gawenda *et al.*, 1999; Dinarès-Turell *et al.*, 2002; Alegret *et al.*, 2009; Rodríguez-Tovar *et al.* 2011). The PETM is easily identifiable at Zumaia as it is represented by a c.5m thick siliciclastic red clay/marlstone that stands out prominently against the background (dominantly) light coloured carbonate sedimentation. The Zumaia section has also recently been awarded the global stratotype and section point (GSSP, e.g. Dinarès-Turell *et al.*, 2007; Bernaola *et al.*, 2009) for both the Danian-Selandian transition and the Selandian-Thanetian transition. Consummately it has well constrained biostratigraphy and lithostratigraphy, so provides an ideal natural laboratory for investigating benthic palaeoecological changes. Ermua (UTM: 0540759 4780681, Figs 6.1 and 6.2) is approximately 30km southwest of Zumaia. The PETM section at Ermua is also represented by a dissolution interval (or the siliciclastic unit 'SU' of Schmitz *et al.*, 2001). However, the interval is turbiditic and contains abundant, thin 1-5cm (calcareous) turbidites. As such, the section is greatly expanded compared to Zumaia (c.20m thick SU compared to c.4.5m at Zumaia) and affords higher resolution sampling on a temporal scale.

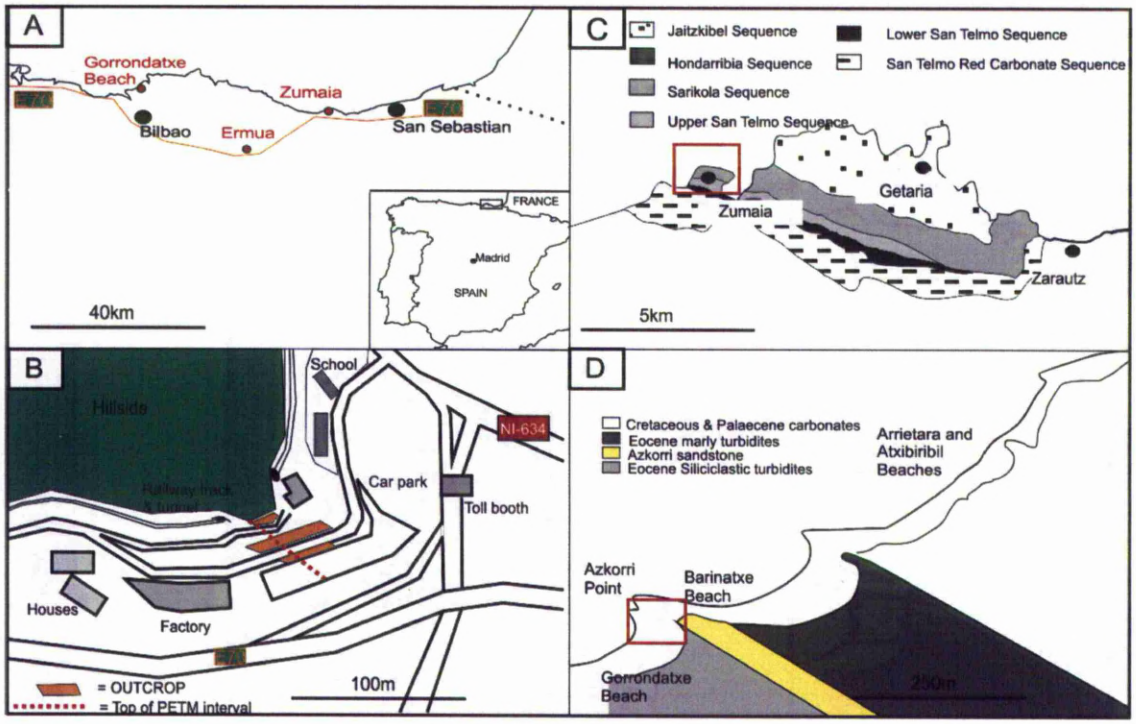

Fig. 6.2 A.) Map displaying localities relative to major urban centres. Inset shows position of the Basque Country on the coast of northern Spain. B.) Detailed map showing position of PETM outcrop at Ermua (see also, Schmitz *et al.*, 2001). C.) General geological map of the coastline around Zumaia (modified from Rosell *et al.*, 1985). Outcrop is located on main Itzurun Beach, Zumaia. D.) Simplified geological map of Sopelana area with Azkorri headland highlighted.

Schmitz *et al.* (2001) employed carbon isotope stratigraphy to constrain the onset of the CIE at Ermua and correlate it lithologically with Zumaia due to the presence of a green, glauconite rich limestone interval immediately beneath the SU at both localities. The Ermua section contains minor low concentration turbidites that did not reached the basin plain in Zumaia, plus carbonate slump beds in the late Palaeocene. This led Schmitz *et al.* (2001) to interpret Ermua as a base of slope apron depositional environment and therefore a more proximal expression of sedimentation at Zumaia. The Ermua section is a road/car park cut and has become considerably overgrown since 2001, with the base (lowermost 4m) of the SU now largely inaccessible.

Gorrondatxe Beach is located on the NE outskirts of Bilbao, on the western edge of the Basque Basin. The beach preserves over 600m of early-mid Eocene (including the Thanetian-Ypressian boundary) sediments (e.g. Bernaola *et al.*, 2006b; Rodríguez-Tovar *et al.*, 2010) deposited in a distal fan fringe environment by a mixture of hemipelagic carbonate and siliciclastic sedimentation and low concentration turbidity currents (e.g. Rodríguez-Tovar *et al.*, 2010; Cummings and Hodgson, 2011b). The Azkorri headland at the north eastern end of the beach (UTM: 0498860 4803277, Figs 6.1 & 6.2) preserves an excellent submarine fan lobe complex fringe (*sensu* Prélat *et al.*, 2009). This unit, known locally as the Azkorri sandstone falls within the NP13 biozone of Martini (1971). This places the succession within the upper portion of the EECO, which is defined as the $\delta^{18}O$ minima which persisted throughout the early Eocene from 53-c.49Ma (Zachos *et al.*, 2001; Hollis *et al.*, 2009). Thick mudstone units are preserved at the base of each lobe complex, providing an ideal sampling opportunity for EECO clays.

6.3 CLAY MINERALS AS A PALAEOCLIMATE PROXY

Sediments in modern oceans contain detrital clay mineral assemblages that are largely, but not solely governed by both climate and weathering patterns on the continental hinterland. As such, distribution of clay mineral assemblages are strongly latitude controlled. This so called 'zonal soil' theory (Biscay, 1965; Chamley, 1989, Thiry, 2000) forms the basis of using clay minerals as a palaeoclimate indicator. For example, illite and chlorite are thought to predominantly derive from physical erosion processes at high latitudes, whereas kaolinite forms due to hydrolysis of parent rock (generally Al-silicate rich) in well drained low latitude areas. Kaolinite is concentrated adjacent to humid, tropical-sub-tropical continental regions in modern oceans. (Millot, 1970; Robert and Chamley, 1991). Kaolinite-illite ratios are often used as a proxy for

climate/weathering processes (e.g. Ruffell and Worden, 2000; Ruffel *et al.*, 2002) because illite will predominate in areas dominated by mechanical erosion processes whereas kaolinite increases may signify an increase in chemical weathering and therefore humidity. When kaolinite is abundant in the detrital clay fraction in ancient sediments it may therefore be reasonably assumed that it was derived from a warm, humid hinterland. However, the interpretation of clay minerals as a palaeoclimate proxy is more complex than such simple assumptions.

Clay mineral formation is a result of many factors including parent material, the weathering regime/climate the parent material is exposed to, the environment of deposition in which the clay is subsequently deposited, and any diagenetic processes that may follow. Such processes are governed by factors such as pore water geochemistry and the burial history of the basin (Ruffell and Worden, 2000; Ruffel *et al.*, 2002). Quantifying these factors is a complicated process and often is overlooked. The value of using clay minerals as a high resolution palaeoclimate proxy is limited by the long timescales involved in the response of pedogenic processes to climate change (possibly as long as 10^6 yr; Thiry, 2000). However, as an accompaniment to traditional palaeoclimate proxies (e.g. Carbon and Oxygen isotopes) it can act as a powerful tool in the broad-scale interpretation of palaeoclimate regime changes (Ruffell and Worden, 2000, Ruffel *et al.*, 2002).

6.3.1 Kaolinite as a diagnostic indicator of the PETM

The extensive (2-5‰ in most oceanic settings) negative CIE that occurred globally at the Palaeocene-Eocene boundary is widely employed as a geochemical diagnostic tool in the

recognition of the onset of the PETM (e.g. Kennet & Stott 1991; Koch *et al.* 1992; Dickens, 1995, 1997; Schmitz *et* al., 2001; Zachos *et al.*, 2001; Zachos *et al.*, 2005). Commonly, a concomitant increase of kaolinite in the clay fraction of sediments is also reported at the onset of the CIE/earliest Eocene (e.g. Robert and Chamley, 1991; Robert and Kennet, 1994; Cramer *et al.,* 1999; Bolle and Adatte, 2000; Cramer and Kent, 2005; Harrington and Kemp, 2005; Dypvik *et al.,* 2011), and appears to be a (quasi)global diagnostic feature of the PETM. Previous studies in the Basque Basin have also identified this spike in kaolinite at the onset of the PETM (e.g. Bolle *et al.,* 1998; Knox, 1998; Gawenda *et al.*, 1999; Winkler and Gawenda, 1999). These authors interpreted this increase in kaolinite to represent the onset of warm humid conditions associated with the PETM. However, Schmitz *et al.* (2001) challenge this interpretation due to strong evidence of arid/semi-arid conditions in the Basque Basin at the PETM including prominent evaporites and caliche soil palaeosols and gypsum in coeval continental deposits (e.g. Schmitz and Pujalte, 2007) and a strongly evaporated freshwater shell $\delta^{18}O$ signature in the nearby Paris Basin. Conglomerate dominated braid plains in nearby continental strata (e.g. Eichenseer and Luterbacher, 1992, Schmitz and Pujalte, 2007) also seem to point to seasonally arid conditions with high magnitude storm events.

The PETM was a short term (<200 kyr) event an order of magnitude below that which Thiry (2000) suggested clay mineral assemblages may provide useful palaeoclimate information. Schmitz *et al* (2001) postulated that the increase in kaolinite associated with the onset of the PETM at Zumaia is actually the result of erosion of older kaolinite rich successions. This theory is plausible as the break-up of Gondwana likely redistributed land masses globally. Many of these land masses will have been enriched in kaolinite due to the long term prevailing warm

humid conditions throughout most of the Cretaceous (e.g. Thiry, 2000), allowing thick kaolinite regoliths to accumulate. The early Eocene witnessed one of the most significant long term inputs of sediment into the marine realm; the siderolithic discharge (Thiry, 2000; Schmitz, 2001). This period of sustained (Cretaceous-Eocene/Oligocene) detrital discharge saw ancient kaolinite profiles, largely developed during the Cretaceous on Alpine carbonate platforms, eroded and delivered to the marine realm throughout the western European region (Thiry, 2000). High magnitude storms associated with elevated temperatures at low to mid-latitudes may have enhanced such discharge events.

6.3.2 Spectral Gamma Ray data as a proxy for weathering in the continental hinterland

Myers (1987) suggested that Spectral Gamma Ray (SGR) data could tentatively be used as a palaeoclimate proxy. Concentrations of uranium (U; ppm), thorium (Th; ppm) and potassium (K; %) can be extracted from total gamma ray measurements. Potassium and uranium are more soluble than thorium (e.g. Myers, 1987; Parkinson, 1996; Ruffel and Worden, 2000), therefore, climatic/weathering conditions that favour the leaching of potassium and/or uranium may be detected in sedimentary rocks by analysing the relative abundances of the three discussed elements. Furthermore, it has been shown that Th/K ratios and Th/U ratios can be correlated with kaolinite to illite ratios (see Ruffell and Worden, 2000). Both potassium and uranium are preferentially leached from feldspars and muscovite during kaolinite formation. As such, elevated thorium and decreased uranium and potassium levels could reasonably be expected to result from similar climatic conditions and weathering regimes to those that would favour kaolinite formation.

6.4 METHODOLOGY

6.4.1 Sedimentology and ichnology

Detailed (cm-scale) sedimentary logs were constructed at Zumaia (c.280 m total thickness) and Ermua c.60m total thickness). Ermua has poor bedding plane exposure deeming it unsuitable for a detailed trace fossil analysis, and the lowermost PETM interval was too overgrown to note reliable sample depths when sampling for clays.

Trace fossils were identified to species level using Uchman's (1995, 1998) taxonomic classification system. The toponomy of each trace fossil assemblage was recorded using Martinsson's (1965, 1970) classification. Bioturbation intensity of each sampled bedding plane was calculated using a $0.2m^2$quadrat divided into a $2cm^2$ grid (bulk data capture method after Heard and Pickering, 2008). The number of squares containing bioturbation translates directly to a percentage value and to a bioturbation index (B.I. e.g. Droser and Bottjer, 1991; Taylor *et al,.* 2003) as subdivisions within the B.I. are largely based on semi-quantitative estimates of percentage bioturbation overprinting the original sedimentary fabric. Observations regarding cross-cutting relationships, burrow diameter etc were also noted. Ichnodiversity is defined by calculating the total number of ichnotaxa recorded in a given section. Total occurrences of individual environmentally sensitive trace fossils were also recorded.

6.4.2 Analytical methods

6.4.2.1 *X-Ray Diffraction*

Where possible, samples were collected at c. 50cm resolution, with key interval samples collected at c.30cm resolution. For consistency, siliciclastic mudstones were sampled where

possible. However, it was necessary to sample some carbonate rich mudstones as these predominate in pre- and post-PETM intervals.

Samples were initially hand ground and then mechanically ground for 10 minutes using a McCrone mill and agate mortars. Samples were then oven dried for 24hrs at 90°C. Traditionally, the <2 micron (clay) fraction is mechanically separated using a centrifuge but as samples were obtained from fine grained (siliciclastic claystone and micritic limestone/marlstone) intervals this proved to not enhance the resolution of XRD analysis. Whole rock XRD analysis also allowed calcite and quartz abundances to be accurately measured. Samples were analysed using a PANalytical X'pert Pro X-Ray Diffractometer with a copper X-ray tube used at 40kV and 40Ma. Quantitative measurements can be obtained by utilising the PANalytical XRD's Reitveld analysis function. However, this technique does not always successfully resolve the kaolinite 001 and chlorite 002 peaks. Results were therefore obtained semi-quantitatively using the instrument software. This allowed the kaolinite 001 and chlorite 002 peak (see Fig. 6.3) to be resolved accurately. Clay percentages reported herein are relative clay percents and not whole rock percents.

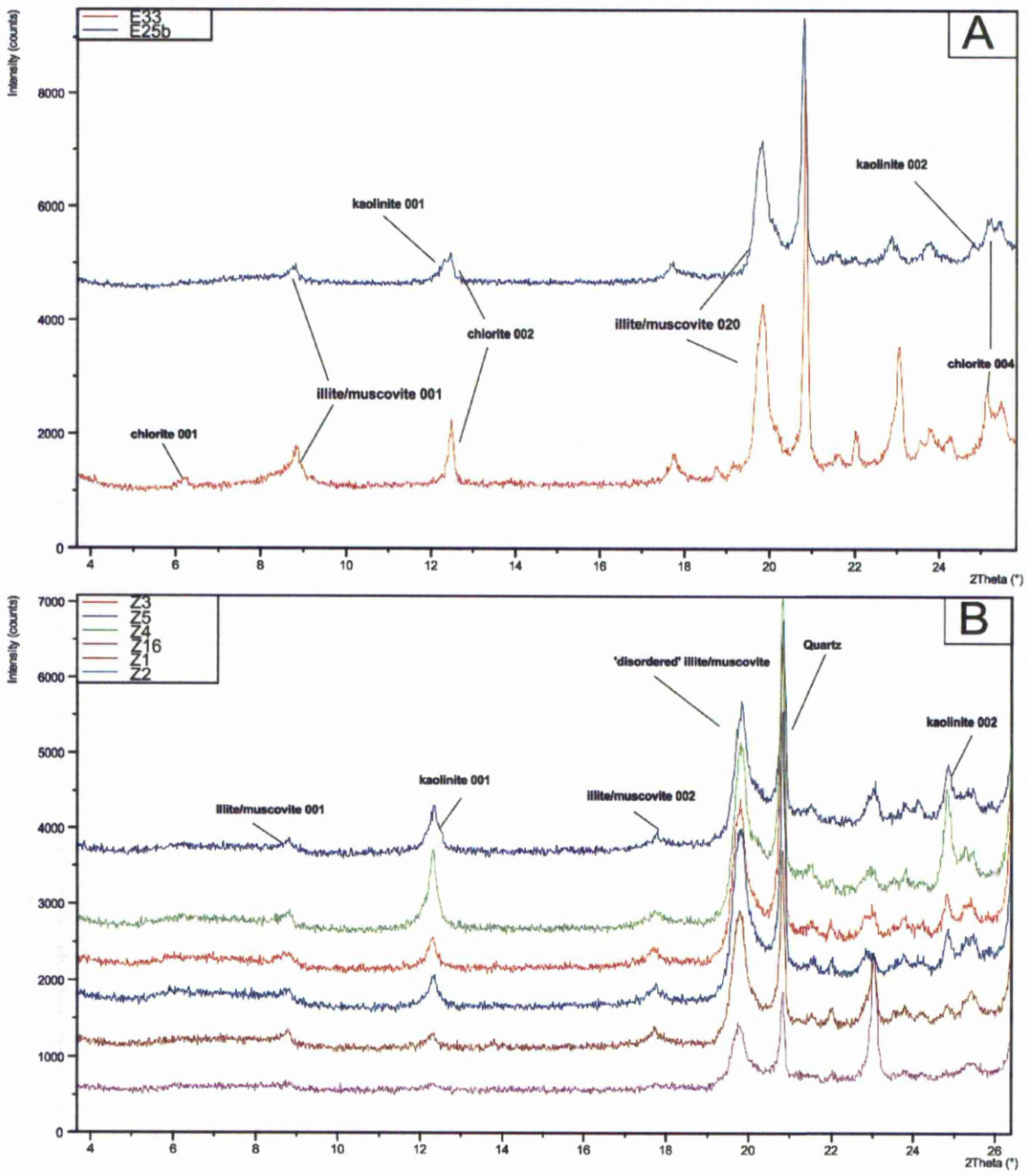

Fig. 6.3 A.) Selected XRD diffractograms from the Ermua section (see Fig. 5 for stratigraphic position of samples). Sample E25b (blue trace) contains both kaolinite and chlorite. The kaolinite 001 and chlorite 002 peaks are traditionally difficult to resolve due to them both being located at c. 12.3-12.5°2θ. This diffractogram clearly shows

both peaks, albeit with a slight overlap. However, the kaolinite 002 and chlorite 004 peak are resolved satisfactorily, allowing the instrument to (semi) quantify concentrations of each mineral. Sample E33 (red trace) contains chlorite but no kaolinite. Note the sharper peak at 25.2°2θ (chlorite 004) plus the better developed chlorite 001 peak at 6.2°2θ. B.) Selection of samples across the CIE interval at Zumaia. Note the dramatic increase in intensity of the kaolinite 001 peak between sample Z16 (latest Palaeocene carbonates) to samples Z1-Z4 (first four samples within the dissolution interval i.e. main body of the PETM). Both sets of diffractograms both display negligible illite 001 peaks at 9°2θ which is at odds with the high reported concentrations of illite/muscovite (upto 60% of whole rock fraction). Note the broad based, sharp peak at 19.5°2θ. This peak is interpreted to represent the 020 peak of disordered illite (see Moore and Reynolds, 1996). The large area of this peak accounts for the high 'illite' concentrations. Here, the mineral is referred to as 'disordered illite' *sensu* Moore and Reynolds (1996).

6.4.2.2 *Field based Spectral Gamma Ray*

Spectral Gamma Ray data were collected using an Exploranium GR-320 in assay mode (giving real time conversions into concentrations of potassium, uranium and thorium). Raw data was then converted into potassium (%) *versus* thorium (ppm) ratios and uranium *versus* thorium ratios. Converting the data from concentrations to ratios removes the diluting effect of variable calcite concentrations plus also minimises the effect of changing lithologies.

6.5 RESULTS

6.5.1 Disordered illite in Basque PETM/EECO assemblages

Illite is generally identified by its 001 peak at c.9°2θ (or 10Å) and its 003 peak at c.27°2θ (or 3 Å e.g. Gharrabi *et al.*, 1998; Hillier, 2003). Illite and muscovite can both be considered members of the mica group of minerals. The presence of illite versus muscovite is largely governed by parent material, weathering regime and subsequent post burial diagenesis (see Gharrabi *et al.*, 1998 for a review). All samples analysed in this study display low to negligible peaks at c.9°2θ (see Fig.

6.3). The PANanalytical Expert software continually identified muscovite as being the dominant clay mineral, at abundances much higher than the minor c.9°2θ peak would suggest. The minor peak at c.9°2θ suggests that; a) the main mineral phase is muscovite rather than illite, or b) the peak actually represents a poorly crystalline form of Illite (Gharrabi *et al.*, 1998).

It seems plausible that the mineral is in fact a poorly crystalline form of illite or possibly even a form of 'disordered' illite (*sensu* Moore and Reynolds, 1996) that has resulted from inter-layering of smectite. Several samples display a weak hump in the 6-9°2θ region, which is indicative of illite-smectite mixed layers. However, all of the samples display a strong, broad peak at c.19.5°2θ which is assigned to muscovite by the instrument software but which does not seem to be documented as a primary peak of either illite or muscovite in the literature. The large area of this peak accounts for the high illite/muscovite concentrations inferred from obtained XRD patterns. Moore and Reynolds (1996) assigned this peak as 'disordered illite 020'. Reynolds (1996) investigated the composition and XRD diffraction patterns of eleven different iilite-smectite mixed layer samples obtained from bentonites. Each of the samples displayed varying expandable illite inter-layers (between 19-100% expandability). XRD patterns for samples with 45-100% expandable illite inter-layers all display a similar broad peak at 19.5-20°2θ (Fig. 3 in Reynolds, 1996) as the samples discussed herein. The variability of XRD patterns of Reynolds' (1996) samples is due not to variations in the illite-smectite mixed layer but due to the presence of differing illite polytypes in each sample. The illite/muscovite in the samples analysed in this study are interpreted to represent such an illite polytype. However, this does not satisfactorily account for the very minor 10Å illite 001 peak. The mineral is here

referred to as disordered illite. See section 6 for discussion concerning the significance of this clay mineral.

6.5.2 Clay mineralogy Results

6.5.2.1 *Zumaia*

At Zumaia, the clay mineral assemblages across the PETM interval (i.e. latest Palaeocene to earliest Eocene) are dominated by disordered illite (from 63 to 100% (relative clay) see Fig. 6.4). Several samples also display a very minor illite/smectite mixed layer (not quantifiable, see Fig 6.3). Kaolinite increases slightly above the green glauconitic limestone that was deposited during the initial CIE (trace to 2%), however, at approximately 60 cm above the boundary between the green glauconitic limestone and the red siliciclastic clay, a distinct spike in kaolinite occurs (37%) and remains elevated into the CIE recovery interval (34 to 30%, see Fig. 6.4). The disappearance of kaolinite is coincident with the lithological transition from clays/clayey marls to more carbonate rich marlstones towards the end of the CIE recovery interval, where disordered illite is the only clay mineral present.

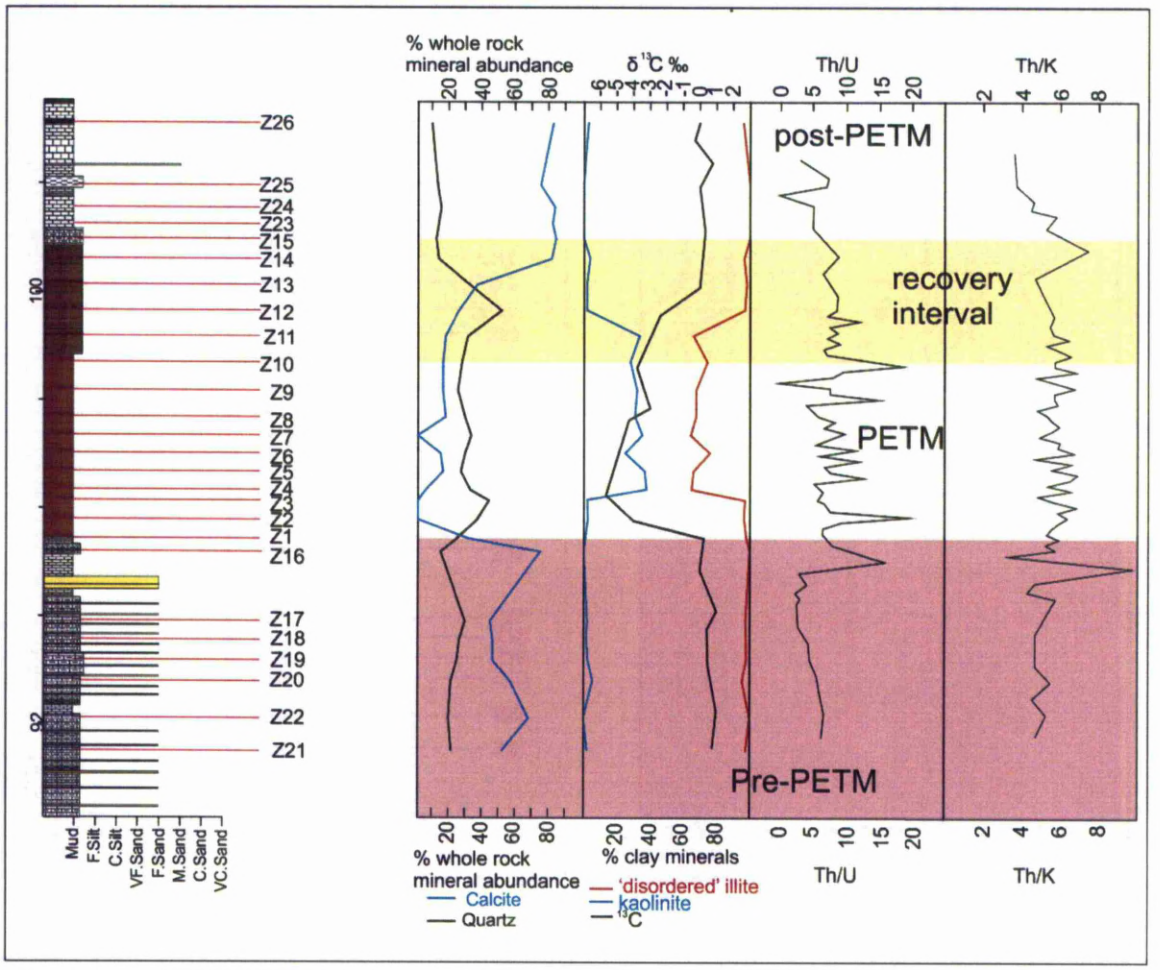

Fig. 6.4 Geochemical data from the Zumaia PETM section. Quartz and calcite concentrations are relative to whole rock percentages. Disordered illite and kaolinite are relative to total clay per cent. $\delta^{13}C$ generalised from Schmitz *et al.* (2001).

6.5.2.2 *Ermua*

At Ermua, the clay mineral assemblages are more dynamic. As with Zumaia, disordered illite is the dominant clay mineral (76 to 100%, Fig. 6.5). The PETM onset interval is not accessible due to heavy vegetation cover. Unlike Zumaia, the PETM at Ermua is turbiditic and thus offers an expanded section (c.20m of PETM stratigraphy vs c.5m at Zumaia). Kaolinite is almost

omnipresent (8 to 19%, see Fig. 6.5) throughout the PETM interval although it is locally absent. The main difference with Zumaia is that kaolinite commonly co-occurs with chlorite (8 to 13%, see Fig. 6.5). Similarly to Zumaia, kaolinite disappears following the CIE recovery and the return to a carbonate sedimentation regime, when disordered illite is the dominant clay mineral, although chlorite is also locally significant (8% - 10%, see Figs. 6.3 and 6.5).

6.5.2.3 *Gorrondatxe*

Clay mineral assemblages at Gorrondatxe are also dominated by disordered illite (77-100%, see Fig. 6.6), with kaolinite being the only other detectable clay above trace levels (10-23%, see Fig. 6.6). A sharp increase in carbonate content at sample location G7 is coincident with kaolinite disappearing. Disordered illite increases to 100% of the clay fraction but absolute concentrations (whole rock) reduce from 49% in sample G6 to 33% in sample G7.

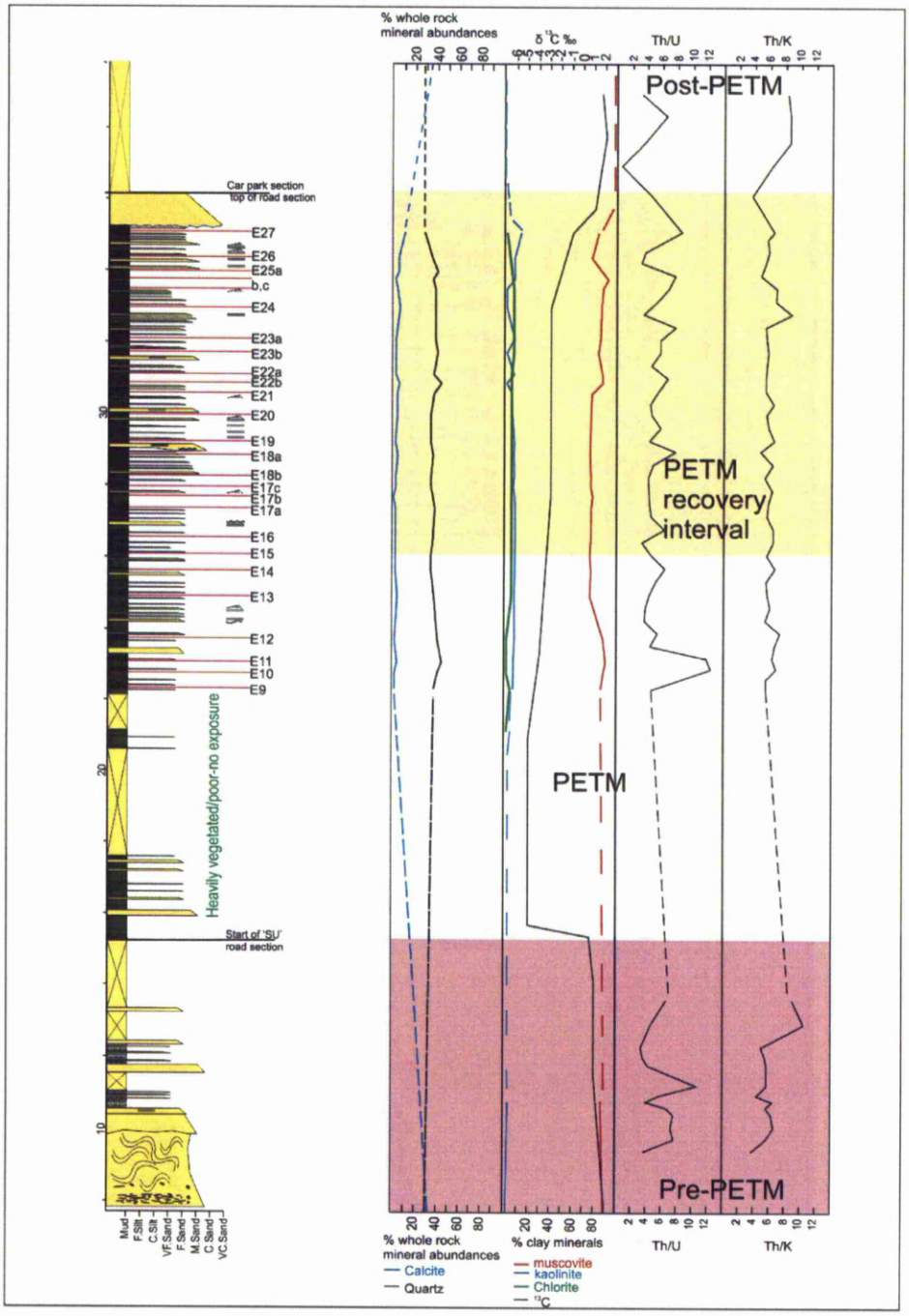

Fig. 6.5 Geochemical data from the Ermua PETM section. Quartz and calcite concentrations are relative to whole rock percentages. Disordered illite and kaolinite are relative to total clay per cent. $\delta^{13}C$ generalised from Schmitz *et al.* (2001).

6.5.3 Spectral Gamma Ray signatures across the PETM

At Zumaia, a spike in both Th/U and Th/K levels is observed in the green, glauconite rich limestone interval that marks the latest Palaeocene and the onset of the CIE. Th/U and Th/K levels remain elevated compared to pre-PETM levels throughout the main excursion/carbonate dissolution interval. Values begin to reduce as sedimentation transforms from siliciclastic clays to more carbonate rich marls. Th/U levels display three more distinct positive spikes following the onset of the PETM but Th/K levels appear less dynamic. Th/U levels also display a prominent negative spike immediately before the resumption of carbonate sedimentation (i.e. the recovery interval, see Fig. 6.4).

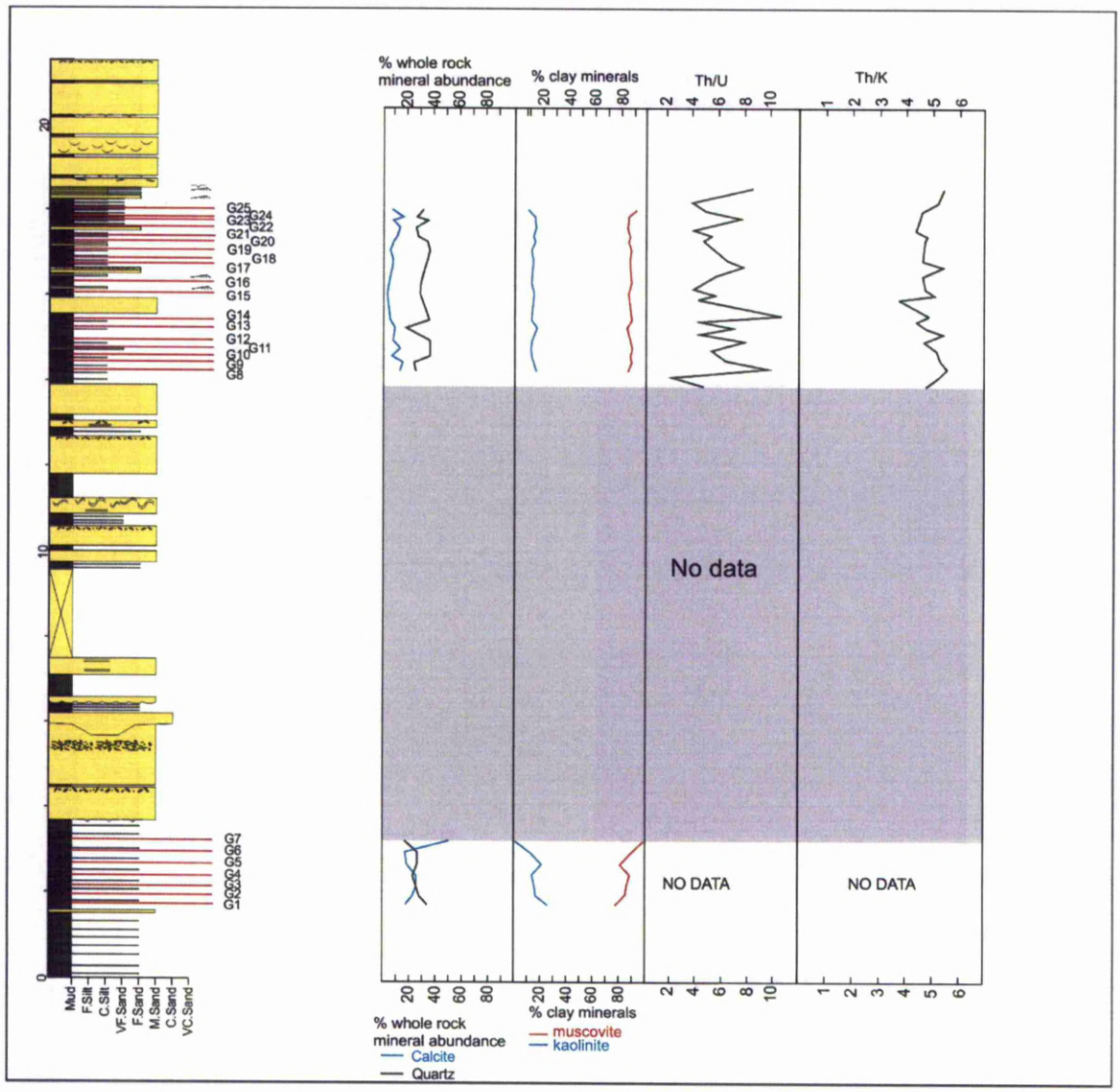

Fig. 6.6 Geochemical data from Gorrondatxe EECO section. Quartz and calcite concentrations are relative to whole rock percentages. Disordered illite and kaolinite are relative to total clay per cent. Note; EECO represents a prolonged climatic period so is not marked onto geochem curves as the whole interval falls within the EECO.

The onset of the CIE at Ermua is obscured by heavy vegetation cover so no accurate measurements could be taken in the lower most c.3-4m of the PETM. However, a prominent Th/U positive spike occurs approximately 5m above the onset of the PETM. No correlative spike

is evident in the Th/K curve. Throughout the PETM, Th/U and Th/K levels stay within a similar range to pre-PETM values. Both Th/U and Th/K values actually increase following the return to 'normal' conditions, marked by a 1m thick high-concentration turbidite at the top of the PETM interval (see Fig. 6.5).

Mean Th/U values at Zumaia during the PETM interval (8.17) are considerably higher than mean values recorded at Gorrondatxe (5.39) which is representative of the EECO. This trend is also mirrored in Th/K values with a mean value of 5.67 during the PETM at Zumaia compared to 4.93 at Gorrondatxe (see Figs 6.4 and 6.6). Ermua displays a generally low mean value for Th/U (5.94) during the PETM. The Th/K mean (6.11) value during the PETM however, is the highest recorded.

6.5.4 Ichnology

Recent work has established a strong environment of deposition control on trace fossil assemblages in the Basque Basin (Cummings and Hodgson, 2011b, see also Crimes, 1973, 1977). The Zumaia section however, is dominated by the most distal basinal and fan related facies (see Figs 6.8 to 6.10, see Chapter 5 for detailed discussion on depositional environments in the Basque Basin), meaning that the depositional environment control on trace fossils is minimised. However, across the narrow range of depositional environments preserved at Zumaia, a wide range of lithologies are present and display distinctly different trace fossil assemblages. Previous work in the Basque Basin (e.g. Crimes, 1973, 1977; Gianetti and McCann, 2010) has illustrated the powerful effect lithology has on trace fossil assemblages. However, this study aims to emphasise that such changes in lithology and benthic palaeoecological changes are intrinsic to broad scale climatic changes on the continental hinterland and associated changes in sediment supply to the deep marine basin.

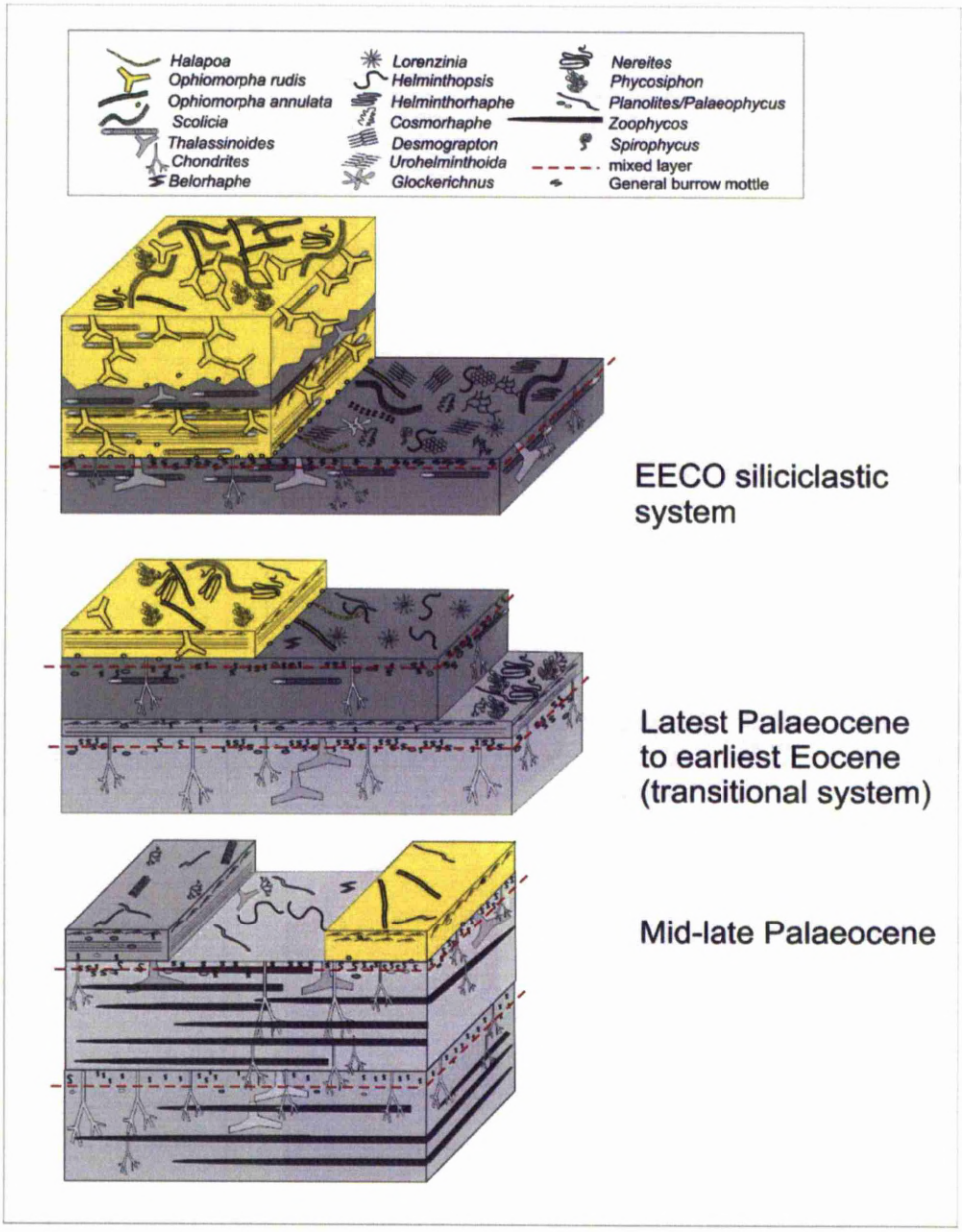

Fig. 6.7 Block digrams displaying trace fossil assemblages including relative abundances and depth of penetration (i.e. tiering) of various taxa including those listed as environmentally sensitive taxa (i.e. *Zoophycos, Ophiomorpha, Scolicia* and the graphoglyptids). Red dashed line marks the limit of the mixed layer. Only the deepest penetrating traces are likely to be preserved in the historical layer and transitional zone. In EECO assemblages, diverse graphoglyptid assemblages have a low preservation potential unless cast onto the soles of turbidity currents. In the

mid to late Palaeocene block diagram, the calcareous turbidite (dark grey) is representative of stratigraphy up to the MPBE. The siliciclastic turbidite (yellow) is representative of stratigraphy up to the latest Palaeocene.

Below is a summary of occurrences of key environmental indicator trace fossils (*Zoophycos, Ophiomorpha, Scolicia* and the graphoglyptids; see discussion, plus Fig. 6.11) and their tiering and colonisation styles (see also Fig. 6.7). These data are tied down to stratigraphic positions(and detailed oldest to youngest) relative to key environmental perturbations such as the Danian-Selandian transition, the MPBE and the PETM (see Fig. 6.1 and Figs. 6.7 – 6.10). The EECO represents a prolonged period of elevated yet stable temperatures compared to shorter term events such as the PETM. Zachos *et al.* (2001) defined the EECO as persisting from 53- c.49Ma. As such, this period at Zumaia spans the upper half of Winkler and Gawenda's (1999) transitional system and persists throughout all of the siliciclastic section investigated in the present study (Fig. 6.1).

6.5.4.1 *Ichnology of the Danian-Selandian transition to the MPBE*

Trace fossil assemblages preserved in the Danian-Selandian transition-MPBE interval are dominantly low diverse assemblages dominated by deep-tier fodinichnia. *Zoophycos brianteus* and *Z. Insignis* occur frequently. *Chondrites intricatus* is also abundant. Only a single graphoglyptid (*Paleomeandron elegans*) was recorded in this interval. The only other pre-depositional trace fossils evident represent cubichnia (*Bergaueria prantli* and *Mammillichnus aggeris*) with less than five recorded occurrences of each taxa. Indeterminate hypichnial mounds possibly resulting from resting echinoids are evident although *Scolicia* is absent. Shallow tier fodinichnia (predominantly *Palaeophycus tubularis* and *Planolites beverleyensis*) constitute the only other commonly occurring ichnotaxa with less common but significant *Thalassinoides*

suevicus also being evident. *Ophiomorpha* occurrences are limited to two occurrences of *O. recta*. Fig. 6.7 displays a tiering model for this interval and Fig. 6.8a displays quantitative ichnological data from a representative section of Danian-Selandian to MPBE stratigraphy at Zumaia.

6.5.4.2 Ichnology of the MPBE to the PETM

Trace fossil assemblages in this interval are similar to those recorded in the D/S-MPBE interval. *Zoophycos insignis* and *Chondrites intricatus* represent the most commonly occurring ichnotaxa. *Thalassinoides* (*Th. suevicus* and *Th.* isp.) is also locally abundant. An increase in the occurrence of shallow tier fodinichnia is noted. No graphoglyptids were recorded in this interval but *Helminthopsis hieroglyphica* and *H. tenuis*, here interpreted as pre-depositional shallow tier pascichnia (grazing traces) are commonly occurring (i.e. 5-10 recorded occurrences) ichnotaxa. The first recorded occurrence of *Scolicia* is recorded in this interval, in the form of *S. plana* and *S.* isp. However, these ichnotaxa only record low to moderate levels of bioturbation. *Ophiomorpha* occurrences increase slightly with two recorded occurrences of *Ophiomorpha annulata* and the first recorded occurrence of *O. rudis*. The increase in frequency of *Ophiomorpha* is concomitant with an increase in the frequency of siliciclastic turbidites. Fig. 6.7 displays a tiering model for this interval and Fig. 6.8b displays quantitative ichnodata from a representative section of MPBE –latest Palaeocene stratigraphy at Zumaia.

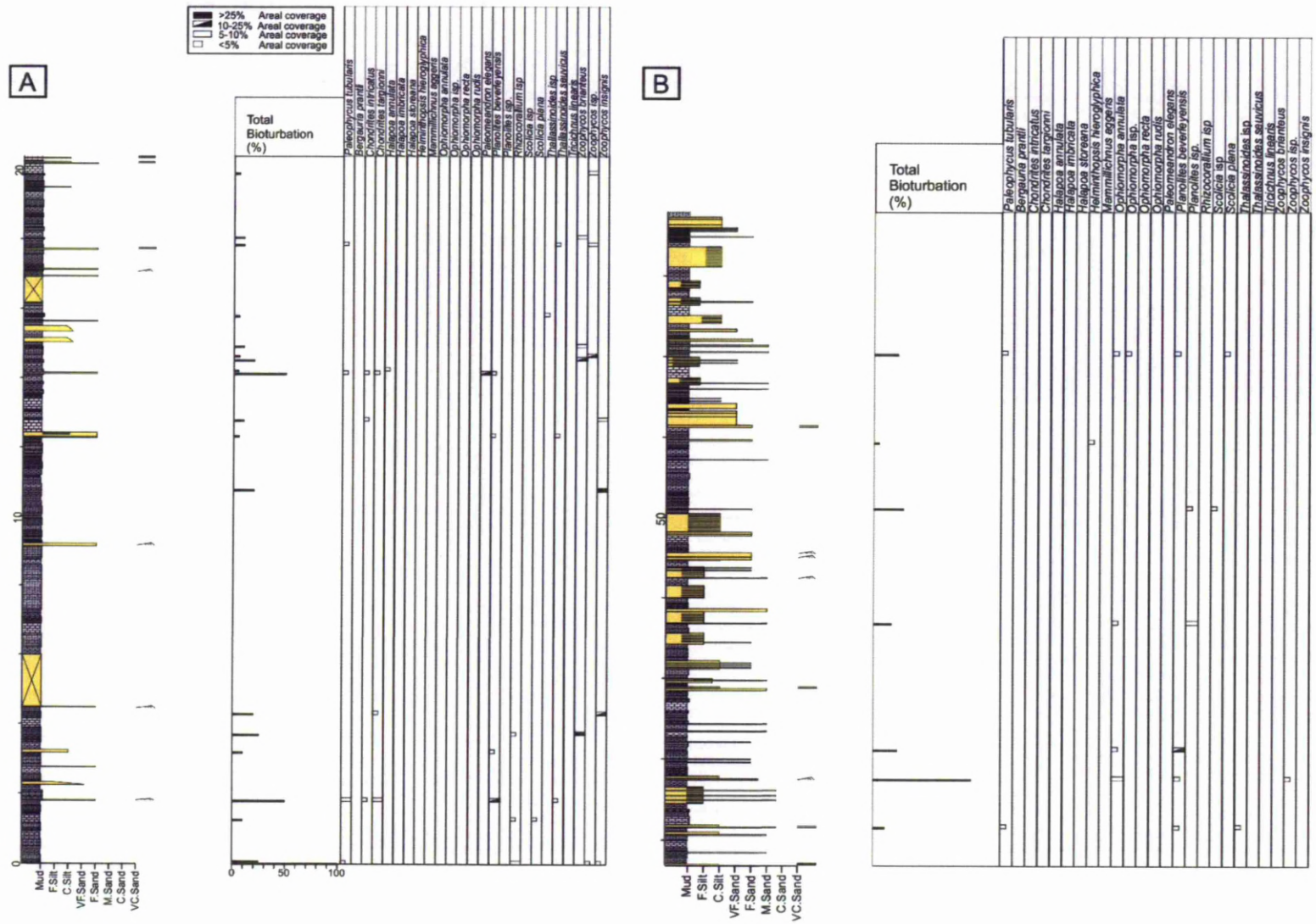

Fig. 6.8 Quantitative ichnological data from; A.) D/S transition to the MPBE. B.) MPBE to latest Palaeocene. Data capture/presentation method after Heard and Pickering (2008).

6.5.4.3 Latest Palaeocene - PETM recovery interval trace fossil assemblages

The latest Palaeocene witnesses a reduction in *Zoophycos* occurrences with only sporadic *Z. insignis*. The last recorded occurrence of *Zoophycos* occurs in a marlstone in the lowermost metre of the PETM marlstone recovery interval. *Planolites* is the most commonly occurring ichnotaxa in this interval with the chemichnia *Chondrites intricatus* and *Trichichnus linearis*, plus *Thalassinoides suevicus* the only other commonly occurring ichnotaxa. Isolated occurrences of *Scolicia plana* were noted. A decrease in bioturbation is recorded in the latest Palaeocene although it is difficult to ascertain whether this is primarily due to poor bedding plane exposure. No bioturbation is recorded in the PETM interval itself although the PETM is represented by a semi consolidated claystone that offers no bedding plane exposure.

Rodríguez-Tovar *et al.* (2011) provide a high resolution ichnological analysis across this key interval that utilise some polished cross sections of substrate. Their observations support a decrease in bioturbation in the latest Palaeocene with a complete lack of bioturbation coincident with the onset of the CIE (and the associated benthic extinction event). They note a gradual recovery to a normal tiered community. Here, it is noted that trace fossil assemblages in the recovery interval and earliest Eocene are still very low diversity and also display very few signs of coherent bioturbation suggesting inhospitable conditions for macrofauna. See Fig. 6.9 for high resolution ichnological data across this key interval.

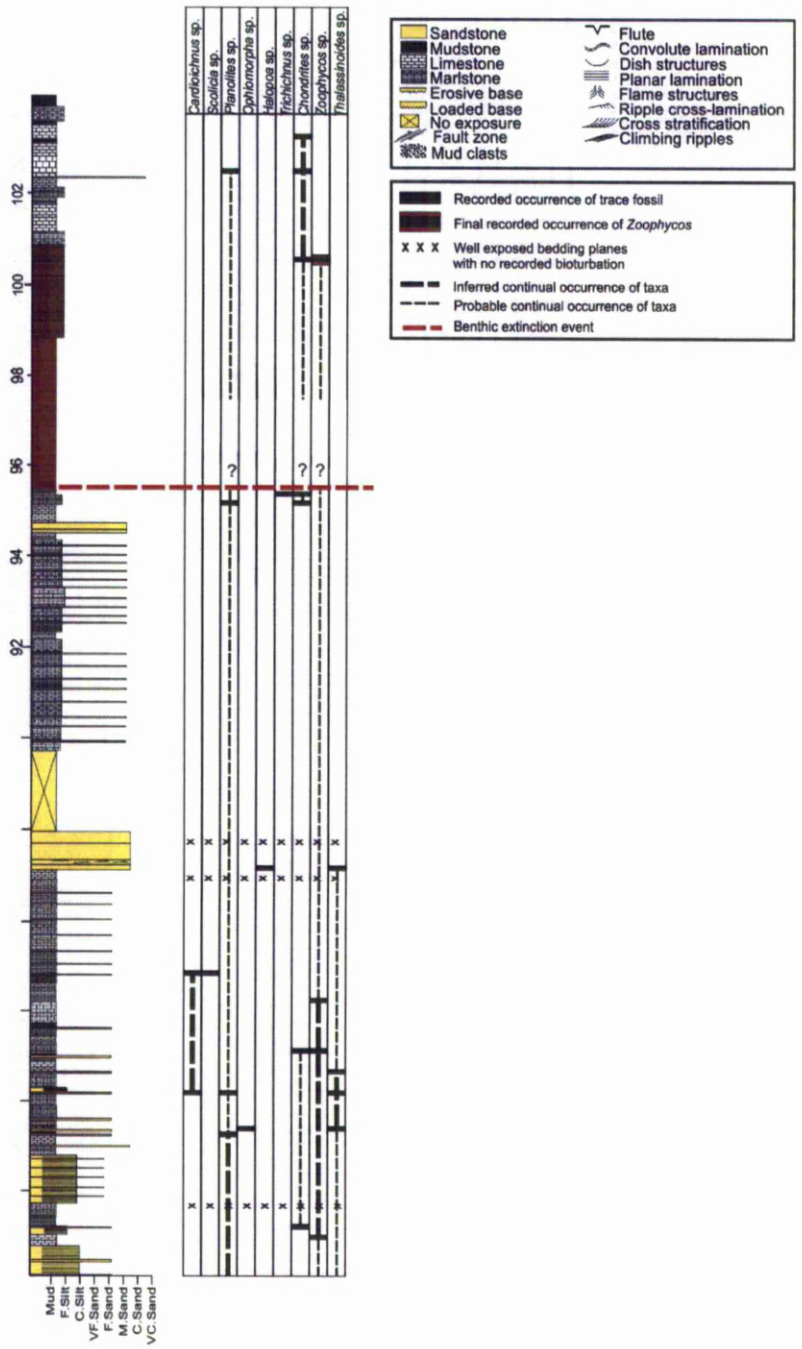

Fig 6.9 High resolution sedimentary and ichnological log across PETM interval showing actual recorded occurrences of trace fossil taxa and inferred and probable continued occurrences of recorded taxa. Benthic extinction event equivalent to onset of PETM.

6.5.4.4 Early Eocene 'transitional system' trace fossil assemblages

The transitional system (*sensu* Winkler and Gawenda, 1999) preserves an increase in diversity to similar levels prior to the onset of the PETM. However, there is an extreme bias towards diverse assemblages associated with siliciclastic turbidite beds over limestone/marl beds. The increase in siliciclastic sedimentation is coincident with a dramatic increase in occurrences of *Ophiomorpha annulata* (widely described as *Granularia*, see Uchman, 1998 for discussion). Monospecific assemblages of *O. annulata* often result in individual bed bioturbation intensities in excess of 40% bioturbation, usually on hypichnial surfaces. *Scolicia* is still comparatively rare. However, the first recorded occurrence of *S. strozzi* is noted which is of particular importance as *S. strozzi* is a pre-depositional form of *Scolicia* (commonly referred to as *Taphrohelminthopsis/Taphrohelminthoida*, see Uchman, 1995, 1998 for discussion) that essentially represents a washed out cast of an echinoid burrow. This suggests that the echinoid trace maker was able to survive in the background hemipelagic equilibrium community (or K-selected community, *sensu* Ekdale, 1985). Notwithstanding the increase in siliciclastic supply, the only graphoglyptids recorded are *Lorenzinia* (*L. plana* and *L. carpathica*) and *Belorhaphe zickzack* (see also Cummings and Hodgson, 2011b). However, shallow tier pascichnia such as *Helminthopsis abeli, Nereites irregularis* and *Phycosiphon incertum* are relatively common, with *Nereites irregularis* routinely contributing monospecific, intensely bioturbated assemblages on very fine sand to silt grade epichnial surfaces that probably represent dilute tails of turbidity currents (or Bouma Td divisions). Fig. 6.7 displays tiering model for this interval. Figure 6.10a displays quantitative ichnological data from a representative section of post PETM 'transitional system' stratigraphy

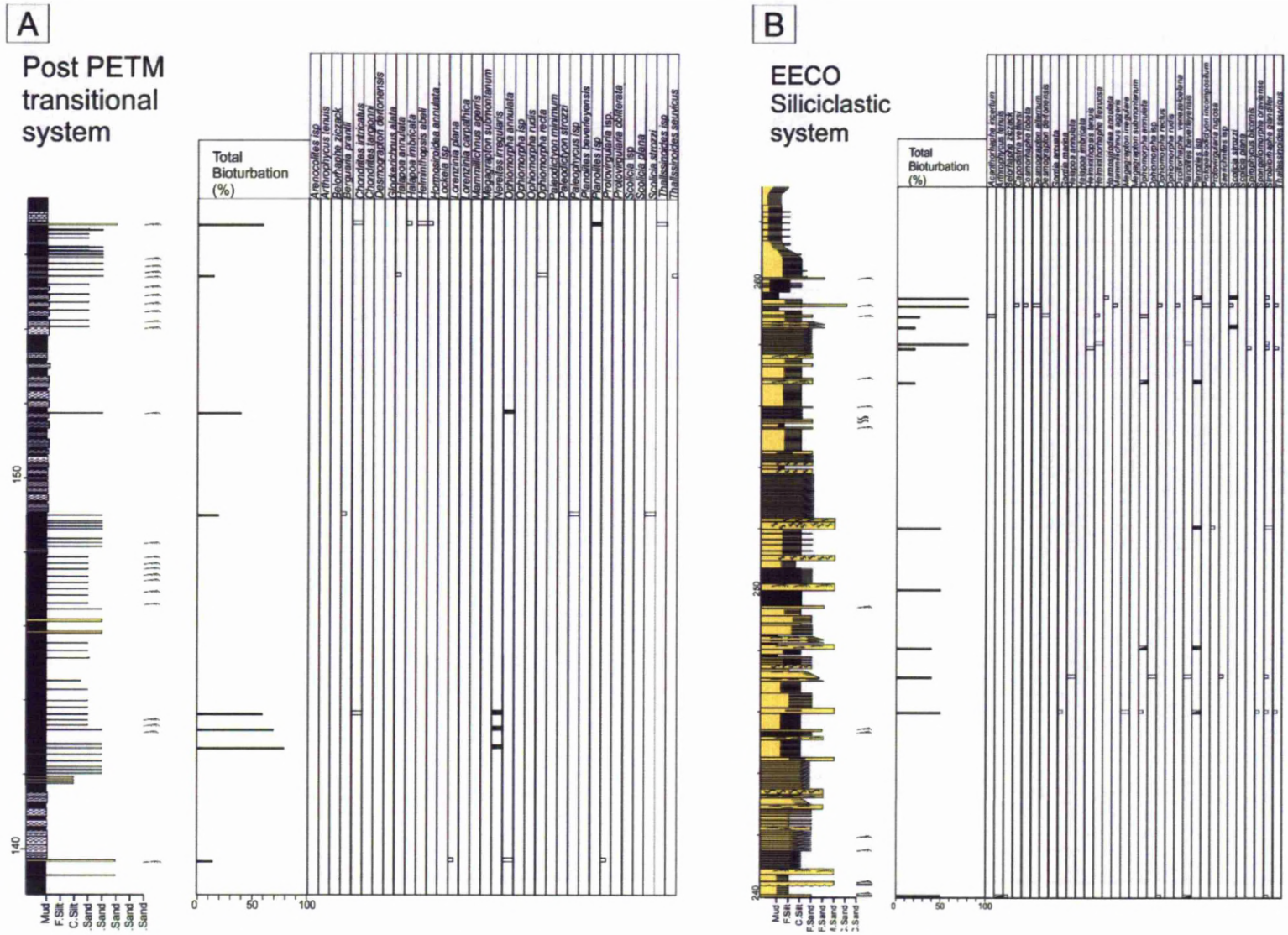

Fig. 6.10 Quantitative ichnological data from; A.) early Eocene 'transitional system' of Winkler and Gawenda (1999) B.) Early Eocene 'siliciclastic system' of Winkler and Gawenda (1999). Note; This section of stratigraphy is approximately equivalent to the EECO. Data capture/presentation method after Heard and Pickering (2008).

6.5.4.5 Early Eocene siliciclastic trace fossil assemblages

The transition to dominantly siliciclastic sedimentation approx 85 m above the PETM witnesses a dramatic overall increase in ichnodiversity, both on a broad scale and on a bed by bed basis. The most notable change is an influx of graphoglyptids with over 15 taxa being identified in this section. Graphoglyptids were recorded on 35% of all beds sampled and contribute significantly to the overall increase in ichnodiversity. However, *Ophiomorpha* occurrences also increase dramatically and are recorded on 61 % of beds sampled. *Ophiomorpha annulata* is one of the most frequently occurring ichnotaxa throughout the section and can be found in highly to intensely bioturbated monospecific assemblages and also as a post depositional opportunistic community that overprints the pre-depositional graphoglyptid dominated assemblages that have been cast onto the soles of turbidites. *Ophiomorpha rudis* also increases dramatically in both frequency and its contribution to overall bioturbation intensity levels.

Scolicia witnesses a dramatic increase in both the frequency of its occurrence and the levels of bioturbation *Scolicia's* echinoid trace makers were able to achieve. Pre-depositional *Scolicia strozzi* occurs frequently, again suggesting that its echinoid trace maker was able thrive in the background quiescent, hemipelagic conditions. However, post-depositional *Scolicia plana* (and to a lesser extent *S. prisca*) frequently contribute to intensely bioturbated beds on both epichnial surfaces and hypichnial surfaces (in *Subphyllochorda* preservation, *sensu* Uchman, 1995). *Zoophycos* is absent in early Eocene siliciclastic sediments at Zumaia. Fig. 6.7 displays tiering model for this interval. Fig. 6.10b displays quantitative ichnological data from a representative section of early Eocene siliciclastic system/EECO stratigraphy.

6.6 DISCUSSION

6.6.1 Palaeoclimatic signal in Basque Basin clay mineral assemblages

The globally widespread increase in kaolinite within the clay fraction of PETM/early Eocene sediments (e.g. Robert and Chamley, 1991; Robert and Kennet, 1994; Cramer *et al.,* 1999; Bolle and Adatte, 2000; Cramer and Kent, 2005; Harrington and Kemp, 2005; Dypvik *et al.,* 2011) is here shown to occur in the Basque Basin. However, previous studies analysing clays in the Basque Basin (e.g. Bolle *et* al., 1998; Knox, 1998; Gawenda *et al.*, 1999; Winkler and Gawenda, 1999) have largely been limited to single locality studies. The Ermua and Zumaia sections are approximately 30km apart. Schmitz *et al* (2001) interpreted Ermua to represent a proximal base of slope apron depositional environment with Zumaia representing a basin plain expression of the same depositional system. Here, it is shown that the two localities have distinctly different clay mineral assemblages which may in part be due to the differeing depositional settings. Both localities preserve clay mineral assemblages that display elevated kaolinite throughout the PETM. However, the PETM clay fraction at Ermua also contains significant chlorite (see also, Bolle *et al.,* 1998), which is absent at Zumaia.

A interpreted proximal base of slope setting for Ermua (Schmitz *et al.*, 2001) is supported here due to significant carbonate breccia slump beds in the upper Palaeocene that probably resulted from either unstable slope failures or possibly even large scale failures of the contemporaneous shallow water carbonate platform. However, the presence of thin turbidites throughout the PETM interval at Ermua indicate that turbidity currents were able to reach this area. Zumaia's higher concentrations of kaolinite compared to Ermua maybe due to an influx of chlorite-rich sediment

via turbidity currents. This would have diluted kaolinite concentrations in the clay fraction, meaning the PETM kaolinite spike is less evident (but still present) at Ermua.

Bolle *et al.* (1998) infer that the presence of chlorite during the PETM at Ermua records increased mechanical erosion on the hinterland, due to prevailingly arid climatic conditions. They propose that kaolinite in the same sediments is a climatic artefact of warm humid conditions, but that the kaolinite was reworked and transported by ocean currents in to the basin. Multiple provenance sources for clays in turbiditic settings is not an unlikely scenario. However, if the chlorite was an inherited signal from the prevailing climatic conditions on the hinterland, then it would perhaps be reasonable to expect chlorite to be detected in hemipelagic sediments (such as those at Zumaia).

Winkler and Gawenda (1999) suggested that clays analysed from the Zumaia section display a very low diagentic overprint, thereby providing a direct palaeoclimate signal. This is based primarily on the presence of kaolinite which is subject to illitization under even moderate diagenetic conditions (c. 2500m burial depth, e.g. Lanson *et al.*, 2002). Winkler and Gawenda's (1999) study also revealed high variance of illite crystallinity which is indicative of inheritance from source rocks of mixed metamorphic grade (i.e. the illite is detrital rather than authigenic). As such, they interpret the clay assemblages to provide a direct palaeoclimatic signal, inferring the PETM kaolinite spike to represent increased warmth and humidity.

The unusual composition of illite which is present in all analysed samples suggests that some diagenetic overprinting has occurred. This mineral was most likely derived detritally as illite that was mechanically eroded from metamorphic rocks located on the continental hinterland and subject to minor/moderate diagenetic modification upon burial. However the presence of

kaolinite in many of the samples suggests only moderate burial. This is further supported by the fact that the whole of the Palaeogene sequence in the Basque Basin is only c. 2000m thick (e.g. Winkler and Gawenda, 1999; Bernaola *et al.*, 2006b) and was uplifted during the main Alpine orogeny.

Schmitz *et al.* (2001) provide strong evidence that the Basque Basin hinterland was predominantly arid during the PETM. Lack of vegetation cover, combined with increasingly steep coastal gradients due to the incipient Pyrenees will have provided an easily erodible landscape. Schmitz and Pujalte (2007) presented evidence that the local hinterland was also subject to extreme seasonal precipitation which will have further enhanced delivery of terrestrially-derived material to the deep ocean basin. The breakup of Gondwana redistributed land masses globally, many of which will have been enriched in kaolinite that was inherited from the prevailing warm humid conditions at equatorial to mid-latitudes throughout the Cretaceous (Thiry, 2000). However, it is not clear whether increased seasonality, as proposed by Schmitz and Pujalte (2007) may have resulted in periods of humidity sufficient to generate kaolinite via pedogenic processes. It seems unlikely that a true palaeoclimate signal can be derived from kaolinite generated during seasonally humid periods without clay mineral assemblages providing any evidence of the prevailing arid conditions such as palygorskite or sepiolite. However, both of these minerals have been recorded during the PETM within the Tethyan realm at several localities (e.g. Caravaca, southern Spain (Adatte and Lu, 1995), Italian Apennines (Calvacante *et al.*, 2011)).

The PETM was one of a series of hyperthermal events (Thomas and Zachos, 2000; Thomas *et al.*, 2000) that also included include the Mid-Palaeocene Biotic Event (MPBE, Bernaola *et al.*, 2006a, 2007), the ELMO event (e.g. Lourens *et al.*, 2005) and the X-event (e.g. Roehl *et al.*,

2005). Lourens *et al.* (2005) provide evidence that these events may in fact have been astronomically paced. The early Eocene also experienced a prolonged period of elevated yet stable climatic conditions known as the early Eocene climatic optimum (EECO, Zachos *et al.*, 2001). These extreme climatic events will have fundamentally affected the delivery of terrestrially-derived material to the marine realm and will have contributed significantly to the siderolithic discharge event that witnessed one of the most significant and prolonged input of sediment into the deep marine realm throughout the whole of the Phanerozoic (e.g. Thiry, 2000). Major discharge events associated with these hyperthermal events will have had profound effects on the deep marine realm. Notwithstanding the prevailing high global sea levels in the early Eocene (e.g. Haq *et al.*, 1987), active turbidite systems were common on a global scale, further increasing the delivery of terrigenous material to the deep marine realm.

The kaolinite increase associated with the PETM is therefore interpreted to primarily represent a symptom of a global scale increase in sediment supply to the oceans that drove evolutionary changes in benthic communities. The primary mechanism for this is probably increased delivery of refractory organic matter to the deep-marine realm. Furthermore, throughout all of the studied sections referred to herein, increases in kaolinite coincide with dramatic reductions in calcite concentrations (see Figs. 6.4 to 6.6). Increases in calcite are usually coincident with not only drastic reductions in kaolinite concentrations, but also with reductions in the amount of clay recorded in the whole rock fraction. Such intervals are usually characterised by pure disordered illite clay assemblages. Therefore, kaolinite increases most probably provide a proxy for general increases in terrigeneous derived sediment to deep ocean settings. Sections devoid of kaolinite either represent increased carbonate productivity in the ocean, decreasing sediment supply from the hinterland, or a combination of these two factors. The most satisfactory explanation for the

seemingly global distribution of kaolinite in PETM deep sea sediments is therefore reworking of older kaolinite-rich regolith from land masses that were redistributed latitudinally following on from the post-Cretaceous break up of Gondwana (Thiry, 2000; Schmitz *et al.*, 2001), possibly with a subordinate supply transported into marine basins by mechanisms such as oceanic currents and wind.

6.6.2 Spectral Gamma Ray response to the PETM

The SGR signatures across the PETM and those obtained in the EECO (Gorrondatxe section) reveal an even more ambiguous picture than the clay mineral profiles. Dypvik *et al.* (2011) record a negative spike in Th/U values at the PETM, preserved in cores obtained from Svalbard. This negative spike is coincident with deposition of laminated, pyrite rich clays. They infer this to represent a period of dysoxia/hypoxia and propose that the conditions were stimulated by a flooding event associated with climatic changes brought about by the PETM.

The abrupt transition from carbonate to siliciclastic muds recorded at Zumaia may possibly also represent a maximum flooding surface. However, it could also be associated with carbonate dissolution associated with shoaling of the CCD (see Zachos *et al.*, 2005) or a combination of both. However, contrary to the negative Th/U spike observed by Dypvik *et al.* (2011), Th/U values display a prominent positive spike and remain elevated throughout the PETM at Zumaia. The onset of the CIE at Zumaia actually occurs in a green, glauconite rich, limestone interval that immediately and sharply underlies the main siliciclastic red clay interval that represents the main body of the PETM. Glauconite is typically associated with dysoxic conditions/maximum flooding surfaces and usually results in reduced thorium in SGR profiles (e.g. Hasselbro, 1996).

No such reduction in Th/U and Th/K ratios or in individual thorium concentrations is observed at Zumaia.

Hasselbo (1996) recognises a clay mineralogical control on Th/K ratios in Palaeogene to Quaternary sediments cored in New Jersey, USA (IODP leg 150). Low Th/K ratios are shown to correspond to illite rich clay mineral assemblages, with increased Th/K ratios corresponding with increasing kaolinite concentrations. These observations are supported here (see also Ruffel et al., 2002). It appears that kaolinite concentrations are the primary driver of variations in both Th/K and Th/U ratios in Basque Basin SGR profiles. Ultimately, this also appears to be driven by dominantly terrigenous derived sedimentation regimes over pelagic carbonate sedimentation (and therefore ocean surface layer productivity).

6.6.3 Ichological changes across environmental perturbations

Giannetti and McCann (2010) noted a strong lithological, and therefore substrate control on late Palaeocene trace fossil assemblages at Zumaia. *Zoophycos* dominated assemblages are subdivided into the *Zoophycos brianteus* and the *Z. insignis* assemblage. The former is interpreted to represent comparatively nutrient/organic-rich sediments deposited on a firmground sea floor with the more lobate *Z. insignis* representing another firmground assemblage but in a more nutrient/organic matter starved setting. Diverse assemblages assigned to their *Planolites beverleyensis* assemblage are associated with equilibrium communities developing in softground intervals overlying calcareous turbidites. This increase in diversity is most likely due to a combination of well oxygenated waters and increased refractory organic matter being transported to the deep basin via the turbidity currents.

Monotonous series of micritic limestones and marly mudstones predominantly display low diversity ichnofabrics dominated by deep-tier *Zoophycos* and *Chondrites.* The *Zoophycos-Chondrites* ichnoguild (see Bromley, 1996; Taylor *et al.*, 2003) has been repeatedly documented in such successions and is due to a combination of a low oxygen tolerance of their tracemakers and a specialised feeding strategy that in the case of *Chondrites,* includes a chemosymbiotic (or chemichnial) feeding strategy, possibly linked to utilising sulphate reducing bacteria (e.g. Seilacher, 1990; Bromley, 1996; Uchman, 2010). The trophic strategy of *Zoophycos* and even its tracemaker still remains enigmatic, however the deep-tier nature of *Zoophycos* means it has the ability to penetrate down into more consolidated sediments from an overlying softground/soupground assemblage. Of palaeoenvironmental significance is that trace fossil diversity and distribution appears to be little affected by the environmental perturbations associated with the MPBE, possibly with the exception of *Zoophycos insignis* becoming less abundant following the MPBE with *Z. brianteus* being the dominant taxa.

Graphoglyptids are exceptionally rare throughout the Palaeocene at Zumaia despite an increase in siliciclastic turbidites that provide taphonomically beneficial conditions for the graphoglyptids (see Seilacher, 1977a, 1977b; Uchman, 2003). Leszczynski (1991) notes that nutrient-rich carbonate beds at Zumaia are often intensely bioturbated, as evidenced by their mottled fabric. Biogenic mixing may therefore have destroyed the delicate open graphoglyptid burrows, meaning that siliciclastic turbidites that eroded into underlying carbonate muds were unable to exhume and cast graphoglyptid burrows as they were obliterated by intense bioturbation prior to emplacement of the turbidite. Alternatively, the lack of graphoglyptids could be a true ethological response by deep marine macrofauna, in that agrichnial (microbe cultivating) feeding

strategies are not beneficial during times of high carbonate productivity due to sufficient conventional food resources on the sea floor.

The sporadic distribution of *Ophiomorpha* in Palaeocene sediments is perhaps due to a lack of terrigenous derived plant material and other refractory organic matter that *Ophiomorpha* trace makers appeared to develop the ability to exploit in Palaeogene deep-marine settings (e.g. Uchman, 2004; Cummings and Hodgson, 2011a). The calcareous turbidites that predominate in the mid to late Palaeocene seemingly did not contain exploitable food sources for *Ophiomorpha's* crustacean trace maker. *Scolicia* is also exceptionally rare in the Palaeocene of Zumaia, although does start to increase in frequency towards the latest Palaeocene.

Rodríguez-Tovar *et al.*(2011) conducted a high resolution ichnological investigation across the PETM interval itself and note a rapid decline in bioturbation intensity and ichnodiversity at the onset of the PETM, comparable with the benthic extinction event witnessed by benthic microfauna (e.g. Alegret *et al.*, 2009). Their study extracted beds and polished surfaces to reveal traces in cross section. This allowed them higher resolution of investigation across this key interval. However, broader scale observations noted here support their findings. The uppermost Palaeocene witnesses a steady decrease in ichnodiversity with only sporadic chemichnia (*Chondrites intricatus* and *Trichichnus linearis*) and local *Planolites* observed in the uppermost 2m of the Palaeocene. Due to the lack of bedding plane exposure, no syn-PETM data was captured but a gradual return to a tiered but slightly impoverished community, equivalent to that in the uppermost 5m of the Palaeocene was noted.

It appears that the increase in terrigenous discharge evidenced by the kaolinite spike (see section 5.1.1 and 6.1) throughout the PETM did not provide any new, exploitable food sources for

benthic macrofauna in the Basque Basin. The decrease/disappearance of bioturbation following the initial CIE suggests that the benthic extinction event that microfauna communities experienced (e.g. Thomas, 2007; Alegret, 2009) was caused by inhospitable conditions that also affected macrofauna. This suggests that carbonate dissolution associated with acidification of ocean water (e.g. Zachos *et al.*, 2005) was not the primary trigger of the extinction event (see also Alegret *et al.*, 2009). Fundamental changes in sediment supply and nutrient availability, combined with reduced oxygenation at the sea floor seems a far more likely scenario.

6.6.4 The PETM as a maximum flooding surface?

The transition from limestone/marlstone to siliciclastic red clay at Zumaia is very sharp and may actually represent a maximum flooding surface. A eustatic control on sea level during a greenhouse world is controversial. However, some sequence stratigraphic studies (e.g. Miller *et al.*, 2005) suggest a significant eustatic control on global sea level during the early Cenozoic. The PETM represents one of the most significant global warming events of the whole of the Phanerozoic, and the most significant of the Cenozoic. A rise in sea level associated with this event almost seems certain. Dypvik *et al.* (2011) correlated the onset of the PETM in Svalbard with a pyrite-rich laminated clay interval that they interpret as both a maximum flooding surface and a period of hypoxia. Speijer and Morsi (2002) also propose a c. 20m sea level rise in the Tethys realm associated with the PETM. Thermal expansion of sea water caused by temperature rises associated with the PETM may have triggered a sea level rise of up to 5m without any glacio-eustatic influence (Hanley *et al.*, 2011 and refs therein). Poorly oxygenated benthic conditions associated with such a sea level rise (assuming a minor glacio-eustatic influence) may have been a significant factor in contributing to both the benthic micofauna extinction event and the severe reduction/disappearance in bioturbation at the onset of the PETM in the Basque Basin.

However, the basin will have also been sand starved during such a sea level rise and this substrate change may have also fundamentally affected benthic communities (particularly infaunal communities).

The transitional system (e.g. Gawenda *et al.*, 1999; Winkler and Gawenda, 1999) at Zumaia consists of predominantly siliciclastic turbidites deposited into a background hemipelagic, marl dominated setting with subordinate pelagic limestones. Ichnodiversity increases dramatically, both compared to the earliest Eocene and to most of the Palaeocene. Graphoglyptid diversity is comparatively low with *Lorenzinia* representing the only commonly occurring graphoglyptid taxa. However, shallow tier pascichnia become extremely common with *Nereites irregularis* being the dominant taxa with *Phycosiphon incertum* (which is sometimes considered mid-tier, e.g. Leszczynski, 1991) also abundant. Occurrences of *Scolicia* also increase dramatically with pre-depositional *S. strozzi* and post depositional *S. plana* and *S. prisca* occurring commonly. This suggests that the echinoid trace maker of *Scolicia* was able to adapt to changing benthic conditions as its pre- and post-depositional origin suggests it was able to survive as part of the background equilibrium (or K-selected, *sensu* Ekdale, 1985) community and the post-depositional opportunistic (or r-selected, *sensu* Ekdale, 1985) community. *Ophiomorpha* occurrences also increase significantly with diminutive *Ophiomorpha annulata* (often referred to as *Granularia*, see Uchman, 1998 for discussion/taxonomy) moderately to locally intensely bioturbating hypichnial surfaces of turbidites.

Further into the Eocene, sedimentation becomes almost exclusively siliciclastic in nature and a marked increase in diversity of trace fossils occurs. This is largely due to both abundant and diverse graphoglyptid assemblages combined with post-depositional, opportunistic assemblages that are dominated by *Ophiomorpha annulata,* with *O. rudis* becoming common on thicker

(>30cm) turbidites, plus localised instances of beds displaying close to 100% bioturbation that preserve mono-specific *Scolicia* assemblages.

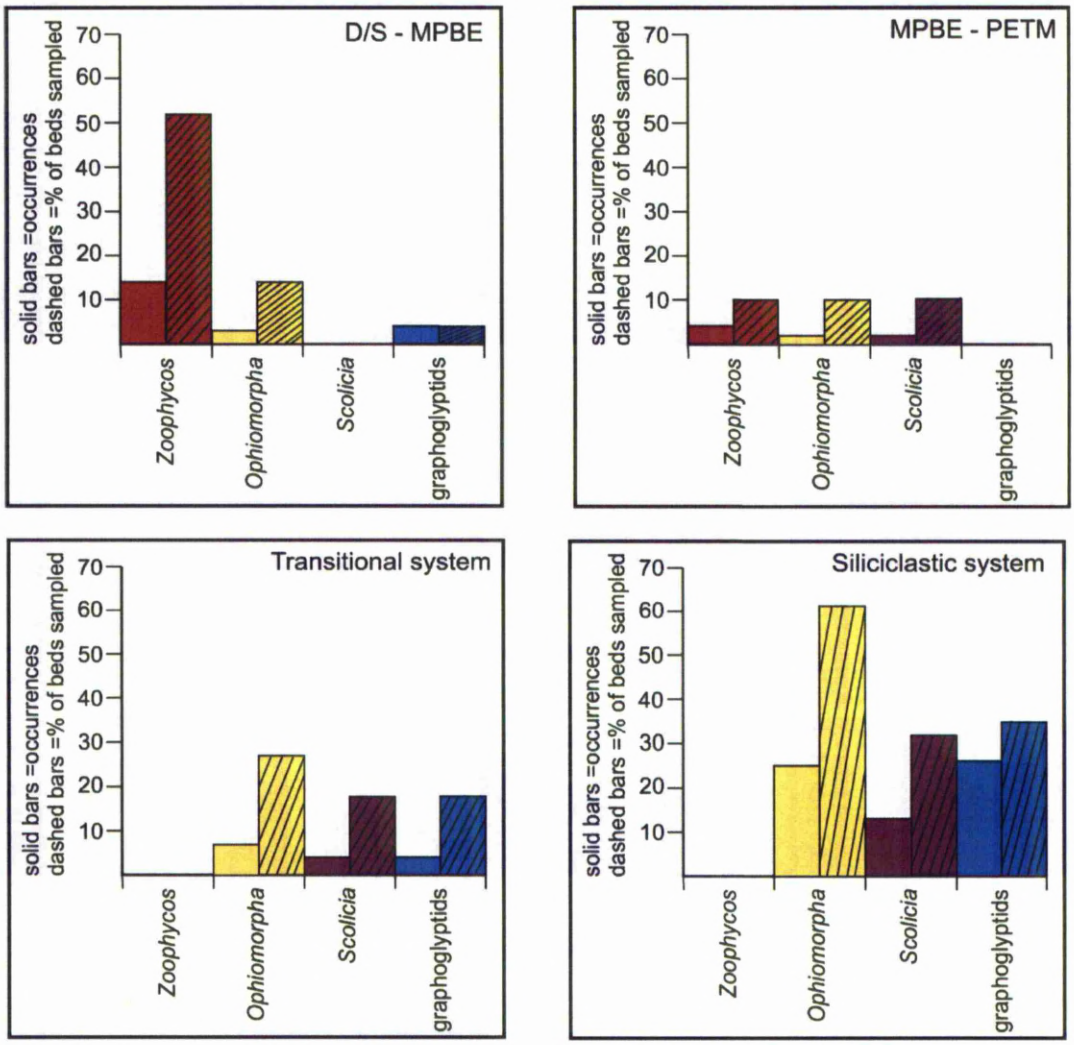

Fig 6.11 Bar chart displaying occurrences of 'environmental indicator' taxa during the D/S to MPBE, MPBE to PETM, early Eocene transitional system and early Eocene siliciclastic system. Solid bars = actual recorded occurrences of taxa. Recorded occurrences relate to actual occurrences on a single bedding plane and do not account for multiple occurrences (i.e. intense bioturbation) of the same taxa on the same bedding plane. Dashed bars = percent of bedding planes sampled preserving each group of trace fossils.

While it may appear that the influx of terrigenous material associated with the PETM did not aid colonisation of the deep sea floor in the short term (<100 Ka), the long term (>100Ka) delivery of such material allowed benthic communities to both adapt and exploit this increase in refractory organic matter and terrigenous derived material associated with the siderolithic discharge. Elevated kaolinite concentrations at Gorrondatxe (which is of EECO age) suggests that input of such material to the deep ocean basin continued until at least the latest early Eocene/mid Eocene.

6.6.5 Oligotrophy as a driver of ichnological change?

It is widely believed that the graphoglyptids represent agrichnia (see Seilacher, 1977a, 1977b; Uchman, 2003 for discussion) that essentially cultivate microbes to feed on in their burrow systems, compensating for the relative lack of conventional nutrients at 1000s of metres water depth. Graphoglyptid-rich assemblages are therefore often interpreted to represent mildly oligotrophic bottom conditions. Uchman (2004) speculated that *Scolicia* burrow systems may actually feed on graphoglyptid burrow systems, essentially hunting the microbe gardens of the graphoglyptids. While this may be a difficult hypothesis to test, *Scolicia* and the graphoglyptids do have an oligotrophic connection.

The graphoglyptids adapt to oligotrophic conditions by cultivating/farming microbes in their burrow systems. The spatangoid echinoids (*Scolicia's* tracemaker, e.g. Ward and Lewis 1975; Frey and Seilacher 1980; Smith and Crimes 1983; Uchman 1998) also have an adaptation to oligotrophy. The spatangoids feed selectively on fine organic detritus rather than inefficiently mass ingesting sediment (Smith and Jeffery, 1998; Smith *et al.*, 1999). In the Basque Basin, the PETM witnessed an enhanced weathering cycle and increased erosion rates on the continental

hinterland (Schmitz and Pujalte, 2003). Coupled with increased seasonal precipitation (Schmitz and Pujalte, 2007), this will no doubt have increased concentrations of refractory organic matter reaching the marine realm (Schmitz and Pujalte 2003, 2007; Algeret *et al.* 2009). The spatangoids were perfectly adapted to rapidly fluctuating environmental conditions compared to other regular and irregular echinoids that were hit hard at the K/T boundary. Most echinoids at the larval stage are planktotrophic and rely on a steady influx of phytodetritus. The non plankotrophic feeding strategy of the Spatangoids means they may be less susceptible to rapidly fluctuating environmental conditions. (e.g. Smith and Jeffery, 1998).

The amount of phytodetritus reaching the seafloor is strongly influenced by both seasonality and surface productivity. Enhanced seasonality associated with the PETM may have limited planktotrophic taxa that survived the K/T event, leading to the spatangoids (and *Scolica*) establishing their niche in the deep oceans by capitalizing on loss of competition from other echinoids. Rapidly fluctuating benthic conditions associated with terrigenous discharge throughout the early Eocene (evidenced here by variations in clay mineral assemblages and variations in carbonate productivity) also seems to have benefitted *Scolicia's* echinoid trace makers.

The selective feeding strategy utilized by the spatangoids is suited to mildly oligotrophic conditions. Boersma *et al.* (1998) suggested a reduction in oceanic mixing in response to the PETM, leading to increased oligotrophy throughout the water column. Nannofossil assemblages in PETM strata support this theory (e.g. Brawoler 2002; Tremolada and Brawoler 2004), as do some foraminifera studies (e.g. Kelly *et al.* 1998; Kelly, 2002). Other studies suggest that successful foraminifera in the earliest Eocene were those adapted to rapidly fluctuating environmental conditions, such as buliminids (e.g. Ernst *et al.*, 2006). It seems that the

proliferation of both *Scolicia* and the graphoglyptids is therefore inherently linked to benthic food supply although there is clearly a strong lithological control as both are almost exclusively preserved in siliciclastic turbidite successions in the Basque Basin. However, this lithological control is intrinsically linked to delivery of terrigenous derived material, which in turn has a strong control exerted by climatic conditions in the continental hinterland. However, these major climatic changes were also coincident with the onset of the Pyrenean orogeny, which in itself will have greatly increased clastic sediment supply to the basin.

6.7 CONCLUSIONS

1. Clay mineral assemblages preserved at two localities (Zumaia and Ermua) in the deep marine Basque Basin record an influx of kaolinite coincident with the onset of the PETM. Kaolinite concentrations remain elevated throughout the PETM until the PETM recovery interval when disordered illite dominated clay assemblages are preserved. This spike in kaolinite is interpreted to represent an increase in erosion and discharge rates of clay-rich flows (with limited sand supply) from the continental hinterland during a sea-level highstand. The kaolinite influx does not record a direct climatically controlled pedogenic signal. Clay minerals analysed at a section of EECO age (Gorrondatxe) also display significant kaolinite concentrations, indicating prolonged terrigeneous input into the basin.
2. Sections with high calcite concentrations are generally devoid of kaolinite and are interpreted to represent periods of high carbonate productivity and low terrigenous input. SGR signatures in the Basque Basin appear to be predominantly controlled by illite/kaolinite ratios where low Th/K and Th/U ratios are prevalent in intervals with low

to absent kaolinite with increases in Th/K and Th/U being coincident with elevated kaolinite concentrations.

3. The PETM was one of a series of hyperthermal events that occurred throughout the Palaeogene, meaning that extreme erosion and discharge events may potentially have fundamentally affected delivery of terrigenous derived materials to the deep-marine realm. Lithological changes recorded in the Basque Basin's rock record were driven by changes in sediment supply (as well as surface ocean productivity) which drove benthic ecological changes recorded by deep-marine trace fossil communities.
4. Predominantly low diversity, deep tier fodinichnia dominated assemblages prevail throughout the Palaeocene, seemingly remaining unaffected by benthic environmental changes associated with the MPBE. Such assemblages are associated with periods of high carbonate productivity and low terrigenous input. The benthic microfauna extinction event that occurred at the onset of the PETM is also recorded in deep-marine trace fossil assemblages with a rapid decline in ichnodiversity and bioturbation intensity at the PETM, coincident with severe depletion of carbonate at the sea floor. Post PETM trace fossil assemblages display a gradual recovery to a tiered, moderately diverse community similar to pre-PETM assemblages but lacking *Zoophycos*.
5. Diverse graphoglyptid dominated assemblages do not appear until sedimentation becomes almost exclusively siliciclastic in nature, well into the early Eocene. The transition to a fully siliciclastic system is approximately concomitant with the early stages of the EECO. *Scolicia* occurrences increase dramatically and appear to be intrinsically linked to mildly oligotrophic conditions that also benefitted the graphoglyptids. However, occurrences of both *Scolicia* and graphoglyptids are limited to absent in siliciclastic

sediments in the Palaeocene, suggesting that early Eocene assemblages are not solely governed by taphonomical processes.

6. Post PETM increases in occurrences of *Ophiomorpha* appear contrary to the oligotrophic conditions suggested by graphoglyptid dominated assemblages. However, post-depositional *Ophiomorpha* represent opportunistic taxa that utilised refractory organic matter and/or terriginous plant material to compensate for the relative lack of conventional nutrients.

CHAPTER 7

CONCLUSIONS

7.1 RESPONSES TO KEY RESEARCH QUESTIONS

This study set out to execute a multidisciplinary approach in the investigation of the effects of the PETM in the benthic realm in the deep-marine Basque Basin, northern Spain. This approach also required an investigation into the effectiveness of utilising ichnology as a supplementary tool in the identification of environments of deposition within submarine fan systems. It also became clear that the PETM was one a series of 'hyperthermal' events (Thomas and Zachos, 2000; Thomas *et al.*, 2000) that punctuated the 'background' greenhouse climate of the early Palaeogene. As such, the effects of these events in the benthic realm were also to be investigated.

To effectively assess these issues a number of key research questions were outlined in chapter 1. Responses to these key research questions are detailed below:

Question 1: ***How do trace fossil assemblages respond to severe environmental perturbations such as the PETM in terms of;***

i.) Changes in abundances and diversity?

ii.) Changes in the contribution of 'key environmental indicator' taxa to deep marine trace fossil assemblages?

iii.) Changes in tiering patterns?

Chapter 6 provides a synthesis of the impact of several early Palaeogene hyperthermal events on deep-marine trace fossil assemblages. Effects of these hyperthermals are summarised below:

The Mid-Palaeocene Biotic Event (MPBE) witnessed significant evolutionary turnover of benthic microfauna (e.g. Bernaola, 2006a, 2007) but appears to have had comparatively little effect on benthic macrofauna communities. The most notable ichnological change is a reduction in occurrences of *Zoophycos*. This is interpreted to represent a slight increase in benthic oxygenation levels, possibly associated with increased input of siliciclastic turbidity currents into the basin. Turbidites deposited in late Palaeocene sediments (post-MPBE) preserve slightly more diverse assemblages than pre-MPBE turbidites. However, simple fodinichnia/pascichnia such as *Planolites, Palaeophycus* and less common *Helminthopsis* predominate over very rare agrichnial graphoglyptids. Occurrences of *Ophiomorpha* are limited to rare *O. recta* with *O. annulata* becoming increasingly common towards the late Palaeocene, approximately concurrent with increases in siliciclastic turbidite supply.

Perhaps as a precursor to abundant *Ophiomorpha* preserved in the early Eocene, *Thalassinoides* occurrences are locally abundant in post MPBE sediments. Benthic conditions were becoming increasingly conducive for the crustacean trace makers of both *Ophiomorpha* and *Thalassinoides* as the Palaeocene progressed. This suggests that lithology exerted a strong control on occurrences of both taxa. *Thalassinoides* predominates in carbonate mudstone (marlstone and micritic limestone) units with *Ophiomorpha* limited to siliciclastic turbidites. However, occurrences of *Ophiomorpha* in late Palaeocene sediments are largely restricted to low population densities compared to intensely bioturbated *Ophiomorpha* fabrics preserved in early Eocene siliciclastic successions.

Both pre- and post-MPBE trace fossil assemblages are characterised by predominantly low diversity, deep tier fodinichnial dominated assemblages with the *Chondrites-Zoophycos* ichnoguild (*sensu* Bromley, 1996) being particularly prevalent.

The Palaeocene Eocene Thermal Maximum (PETM) witnessed the most significant benthic extinction event of the whole of the Cenozoic with up to 50% of benthic foraminifera taxa becoming extinct (e.g. Thomas, 2007; Alegret *et al.*, 2009). However, the effect of this event on benthic macrofauna communities has largely been poorly constrained. However, Rodríguez-Tovar *et al.* (2011) show that the event significantly affected trace fossil communities in the Basque Basin, with an apparent concomitant extinction event affecting trace fossil communities as the one that affected microfauna. This implies unfavourable conditions for trace making macrofauna (see chapter 6 for discussion).

The results presented herein support the results of Rodríguez-Tovar *et al.* (2011). However, the results presented herein constitute a temporal scale two orders of magnitude (>10Ma compared to c. 200ka) higher than that investigated by Rodríguez-Tovar *et al.* (2010). Uchman (2004) provides evidence that the early Eocene witnessed the highest deep-marine trace fossil diversity of the whole Phanerozoic which seems to be at odds with a significant benthic extinction event at the PETM. Both this study and that of Rodríguez-Tovar *et al.* (2011) suggest a return to a 'normal' tiered community following the PETM. However, sediments directly overlying the main body of the PETM preserve very low diversity and low population density assemblages suggesting a slow recovery of the benthic realm to 'normal' conditions.

Ophiomorpha, plus the echinoid trace *Scolicia,* become increasingly abundant following the PETM but are largely restricted to siliciclastic turbidites. Graphoglyptid occurrences are still comparatively rare in earliest Eocene sediments, with *Lorenzinia* being the only commonly occurring graphoglyptid. Some authors (e.g. Seilacher, 1977a, 1977b; Uchman, 2003; Rodríguez-Tovar *et al.*, 2010) have suggested that graphoglyptid rich assemblages may be indicative of mildly oligotrophic benthic conditions. Shallow tier and surface grazing traces such

as *Nereites, Phycosiphon* and *Helminthopsis* are relatively common in trace fossil assemblages in the early Eocene 'transitional system' suggesting relatively abundant food at the sea floor. This seems to support the hypothesis that graphoglyptids predominate in relatively nutrient poor (oligotrophic) settings. The majority of mudstone inter-beds are marlstone with micritic limestones also commonly occurring. The carbonate nature of hemipelagic sediments suggests high surface productivity which seems to have contributed conventional/exploitable nutrients for infauna. The absence of *Zoophycos* in these sediments is rather enigmatic. A plausible hypothesis is that the influx of siliciclastic turbidites in the earliest Eocene brought well oxygenated bottom waters into the basin. This increase in oxygenation allowed a more diverse macrofauna to thrive in the basin, creating competition for the (unknown) *Zoophycos* trace maker.

The early Eocene Climatic optimum (EECO) seems to have had the most profound effect on trace fossil assemblages in the Basque Basin. Graphoglyptids become exceptionally common with 16 different graphoglyptid taxa identified, some of which occur commonly. *Ophiomorpha* occurrences increase dramatically. Pre-depositional, graphoglyptid dominated assemblages can often be seen to be cross cut by intensely bioturbate, post depositional *Ophiomorpha* assemblages. As such, two distinct communities are preserved:

1. A background equilibrium (or K-selected *sensu* Ekdale, 1985) community composed of diverse shallow tier graphoglyptid dominated assemblages that display low individual population densities.

2. Deep tier, post depositional assemblages dominated by *Ophiomorpha annulata,* with common *O. rudis.* This post depositional community represents opportunistic (or r-

selected *sensu* Ekdale, 1985) taxa that rapidly colonised event beds (i.e. turbidites) and exploited whatever nutrients/food was available. This community can be seen to cross cut the pre-depositional community that is preserved on the sole of the casting turbidite.

Scolicia occurrences also increase dramatically in EECO sediments. Many bedding planes displaying near complete bioturbation preserve mono-specific *Scolicia* assemblages. However, *Scolicia* dominated beds rarely preserve *Ophiomorpha,* suggesting that crustaceans and echinoids may have occupied different ecological niches in the deep marine realm.

The dramatic increase in trace fossil diversity, graphoglyptid occurrences, plus *Ophiomorpha* and *Scolicia* occurrences is coincident with the basin becoming a siliciclastic dominated system (versus mixed siliciclastic – carbonate deposition). This may suggest that lithology is the primary control on trace fossil diversity. However, whilst it is true that siliciclastic turbidites are much less common in Palaeocene sediments, where present, they lack significant bioturbation attributable to *Ophiomorpha, Scolicia* or graphoglyptids. This suggests that the transition from mixed carbonate-siliciclastic sedimentation to dominantly siliciclastic sedimentation represents a fundamental ecological as well as sedimentological change in the benthic realm. This change was driven by changes in sediment supply which is intrinsically linked to changes in weathering and erosion in the continental hinterland. However, it should be noted that the incipient Pyrenean orogeny was also progressing during the Eocene, meaning that this will also have fundamentally affected the delivery of siliciclastic sediments into the Basque Basin.

An observation that remains enigmatic is the disappearance of *Zoophycos* at Zumaia following the PETM. This suggests a lithological control as *Zoophycos* occurs exclusively in carbonate sediments during the Palaeocene at Zumaia.. It is likely that *Zoophycos* is adapted to thriving in

monotonous sedimentation regimes that experience low to negligible input of organic matter from the shallow marine/terrestrial realm. The input of siliciclastic turbidites into the basin perhaps led to increased competition from organisms adapted to exploiting such material, forcing the *Zoophycos* trace maker out into more distal environmental settings. This in turn may have allowed the graphoglyptids to successfully colonise the background pelagic muds.

Perhaps the most important conclusion to draw from this key research question is that trace fossil assemblages are dynamic and diverse in space and time. However, their response to environmental perturbations seems to be gradual rather than rapid, with the exception of the disappearance of bioturbation at the onset of the PETM. The PETM and the EECO have the most notable effect on trace fossil diversity, ethology and tiering relationships in the Basque Basin. However, these major environmental perturbations are broadly contemporaneous with significant changes in sedimentation regimes, most notably, significant increases in siliciclastic sediment supply. The PETM is broadly contemporaneous with Winkler and Gawenda's (1999) 'transitional system' of mixed carbonate and siliciclastic sedimentation at Zumaia (versus the predominantly carbonate nature of sediments throughout the mid- to late Palaeocene), and the EECO is broadly contemporaneous with the onset of the 'siliciclastic system'. As such, it is difficult to quantify the precise effects of these environmental perturbations. Trace fossils are largely responding to changes in sediment supply, which in part are driven by climatic changes on the continental hinterland (see also, chapter 6) and are therefore intrinsically linked to these hyperthermal events. However, the incipient Pyrenean orogeny will also have fundamentally affected both the delivery rates and types of sediment delivered into the basin.

Question 2: ***How do trace making organisms respond ethologically in response to palaeoecological changes?***

Chapter 4 provides a detailed investigation into several traces that are interpreted to be morphologically related to *Ophiomorpha* group trace fossils (i.e. *Ophiomorpha, Spongeliomorpha* and *Thalassinoides*). However, these traces all display regular polygonal/hexagonal morphologies that are more typical of agrichnial trace fossils than domichnial/fodinichnial trace fossils such as *Ophiomorpha* and *Thalassinoides.* All of the discussed specimens share morphological and taxonomic features with *Ophiomorpha* group trace fossils (e.g. 120° branches, swellings at bifurcation points and locally, irregularly distributed granules in the wall structure). The burrow systems were constructed post-depositionally at the sand:mud interface (i.e. hypichnial surfaces) at the base of decimetre-thick turbidites. All of the burrow systems are interpreted to represent open burrow networks (i.e. they maintained an open connection to the sea floor) that facilitated irrigation of the burrow network. This may have aided trapping of organic material within the burrow network that will have eventually been broken down by microbes.

It has been postulated previously that *Ophiomorpha's* crustacean trace maker may have been able to exploit an increase in terrigeneous derived, cellulose based plant matter. Typically, however, marine invertebrates are unable to break down such material (e.g. Kent Barnes *et al.*, 1991). Uchman (2004, 2009) postulated that crustaceans may have developed the ability to break down such material by cultivating microbes in their burrow systems, providing an exploitable food source. The three *Ophiomorpha* group morphotypes discussed in chapter 4 provide some of the first examples of *Ophiomorpha* group trace fossils that display characteristics of agrichnial burrow networks:

i.) Regular, polygonal, 3-dimensional networked burrow systems allowing frequent revisiting of different parts of the burrow network.

ii.) An open connection to the sea floor encouraging irrigation of the network by oxygenated water and also facilitating the trapping of organic matter transported by bottom (and possibly turbidity) currents.

Figure 4.8 shows an apparent correlation between the radiation of angiosperms and occurrences of *Ophiomorpha* in deep marine settings. *Ophiomorpha* may have been able to exploit an increase in angiosperm derived plant detritus by exploiting increased influx of terrestrially derived organic matter associated with enhanced runoff, due to climatic changes associated with the early Eocene hyperthermal events such as the PETM. However, exploiting this material will have necessitated *Ophiomorpha's* trace maker adapting new trophic strategies such as microbe cultivation. The irrigated, polygonal networked burrows of the three morphotypes discussed in chapter 4 are interpreted to represent an increasingly organised trophic strategy, culminating in the development of an agrichnial feeding strategy. This adaptation is inferred to be in response to significant changes in food supply/availability in the benthic realm. Changes in food supply/availability are interpreted to have been driven by changes in sediment supply, in response to climatic changes on the hinterland. As such, the three discussed *Ophiomorpha* group morphotypes represent a direct ethological response to global climatic changes.

Question 3: ***Is it possible to utilise trace fossil assemblages as a diagnostic tool in discriminating between sub-environments within submarine fans?***

Recent work has shown that a detailed ichnological analysis can provide a powerful supplementary tool in the diagnosis of sub-environments with submarine fan settings (e.g. Heard

and Pickering, 2008, Monaco *et al.*, 2010, Philips *et al.*, 2011). Previous work has suggested that the use of sub-ichnofacies (see chapter 5) can be used to characterise environments within a submarine fan setting (e.g. Seilacher, 1974; Uchman, 2001; Heard and Pickering, 2008). This study shows that the use of sub-ichnofacies provides a useful, informal way of determining a general proximal to distal, axis to off axis position within a submarine fan system. However, the style of colonization (K-selected versus r-selected), the ethologies and tiering relationships of ichnotaxa preserved in a given environment is of greater importance than the presence or absence of specific ichnotaxon. Studies such as this and those of Heard and Pickering (2008), Knaust (2009) Monaco *et al.* (2010), and Philips *et al.* (2011) should be supplemented by further studies where trace fossil assemblages are aligned to the specific environments of deposition in which they are preserved. Moreover, the environments of deposition interpreted in such studies need to be explicitly documented and supplemented with evidence (photographs, sedimentary logs etc).

In broadly contemporaneous basins then it is likely that 'ichnoguilds' of certain ichnotaxa (or at least of ethological groups) will be representative of a given depositional environment. However, care should be taken when the stratigraphic position of outcrops in study areas are punctuated by major environmental perturbations such as the PETM.

Question 4*: Is it possible to determine if the large influx of kaolinite during the PETM was the result of climatically influenced pedogenetic processes on the continental hinterland or was the kaolinite derived from erosion of older regolith?*

A key geochemical feature of the PETM is a prominent spike in the abundance of the clay mineral kaolinite. This has frequently been ascribed to an increase in warmth and humidity at the PETM. However, it still remains unclear whether the kaolinite spike represents a true climatic

signal or represents erosion of older kaolinite rich regolith delivered to the deep marine realm. The PETM interval at Zumaia and Ermua is preserved as a clay dominated carbonate dissolution interval (or the siliciclastic unit (SU) of Schmitz *et al.,* 1997, 2001) that records a dramatic increase in kaolinite concentrations following the onset of the PETM. Kaolinite concentrations remain elevated throughout the PETM until the PETM recovery interval when disordered illite dominated clay assemblages are preserved. This spike in kaolinite is interpreted to represent an increase in erosion and discharge rates of clay-rich flows (with limited sand supply) from the continental hinterland during a sea-level highstand. The kaolinite influx does not appear to record a direct climatically controlled pedogenetic signal. Therefore, the preferred mechanism for delivery of the kaolinite is erosion of older kaolinite rich regolith.

EECO clay mineral assemblages (preserved at Gorrondatxe) also display elevated kaolinite concentrations compared to Palaeocene assemblages. This seems to infer that enhanced terrigenous input into the basin was not restricted to short term transient events such as the PETM but also persisted over more prolonged periods such as the EECO. However, kaolinite concentrations are significantly higher during the PETM. This reflects the high magnitude of terrigenous input associated with the PETM.

SGR data obtained from Ermua, Zumaia and Gorrondatxe support the hypothesis that Th/K ratios and Th/U ratios can be correlated with kaolinite to illite ratios (e.g. Myers, 1987; Parkinson, 1996; Ruffel and Worden, 2000). However, the SGR data set does not shed light on the question of whether or not the kaolinite/illite assemblages are derived from climatically driven pedogenic processes. Elevated thorium and decreased uranium and potassium levels could reasonably be expected to result from similar climatic conditions and weathering regimes to those that favour kaolinite formation. However, this kaolinite may potentially have been

delivered to the basin much later than its formation due to erosion of older regolith. As such, it seems that the SGR signature in the Basque Basin is largely an artefact of this erosion.

Question 5: ***Can changes in terrestrially derived sediment supply be tied with palaeoecological effects in deep marine trace fossil assemblages through analysis of changes in the composition and abundance of clay mineral assemblages?***

Kaolinite enriched sections are interpreted to represent periods of high terrigenous input, particularly of clay-grade material. Sections with high calcite concentrations are generally devoid of kaolinite and are interpreted to represent periods of high carbonate productivity and low terrigenous input.

Predominantly low diversity, deep tier fodinichnia dominated assemblages prevail throughout the Palaeocene. Such assemblages are associated with periods of high carbonate productivity and low terrigenous input. The benthic microfauna extinction event that occurred at the onset of the PETM is recorded in deep-marine trace fossil assemblages with a rapid decline in ichnodiversity and bioturbation intensity at the PETM, coincident with severe depletion of carbonate at the sea floor.

Diverse graphoglyptid dominated assemblages do not appear until sedimentation becomes almost exclusively siliciclastic in nature, well into the early Eocene. The transition to a fully siliciclastic system is approximately concomitant with the early stages of the EECO, which preserves kaolinite rich clay assemblages. Occurrences of *Ophiomorpha* and *Scolicia* also increase dramatically following the PETM and peak in the EECO. It is interpreted here that this major change in trace fossil assemblages is driven by prolonged terrigenous input into the basin that

diluted carbonate content in the benthic realm and affected both the quantity and types of food available to benthic infauna.

Ichnological variations cannot be directly correlated with changes in the composition and abundances of clay mineralogical assemblages. However, such changes in clay composition are driven by broader scale climatic changes in the continental hinterland. These changes fundamentally affected sediment delivery to the deep basin which is reflected not only in lithological changes but also in trace fossil diversity, abundances, ethology and tiering patterns.

7.2 GENERAL CONCLUSIONS

This study represents one of the first attempts to constrain the effect of the early Palaeogene hyperthermal events (with a focus on the PETM) on deep-marine benthic macrofauna communities (preserved as trace fossil assemblages). The results emphasise that trace fossil assemblages respond to environmental perturbations in a dynamic non-linear manner. To fully assess the response of trace fossil communities to such environmental perturbations requires an understanding of other factors that may influence the types of assemblages preserved.

An implication of this study is that taphonomy appears to be secondary to actual palaeoecological conditions in determining trace fossil communities. For example, pre-depositional graphoglyptid communities seem to thrive in the Basque Basin during the EECO, most likely as a result of well oxygenated, mildly oligotrophic benthic conditions. They are exclusively preserved on the soles of siliciclastic turbidites. However, while siliciclastic turbidites are much less frequent in the Palaeocene, they are not uncommon. Graphoglyptids are exceptionally rare in such deposits. This implies a fundamental palaeoecological change following the PETM, albeit the response is not immediate. This differs from previous hypotheses

that suggested graphoglyptids were taphonomically biased towards siliciclastic turbidites versus marly turbidites (e.g. Uchman, 1995).

Broad-scale lithological changes are shown to have a dramatic effect on the trace fossil communities preserved. *Zoophycos* disappears following the PETM at Zumaia. This disappearance is approximately concurrent with the most dramatic decrease in carbonate sedimentation noted throughout the whole of the Zumaia succession (i.e. Danian to late Ypressian). *Ophiomorpha* and *Scolicia* occurrences increase dramatically as siliciclastic sedimentation increases. However, these broad-scale changes in sedimentation regime (carbonate versus siliciclastic) are coincident with major environmental perturbations. The PETM and EECO display the most dramatic effect on ichnological assemblages. These major environmental events are approximately coincident with the 'transitional system' and the 'siliciclastic system' of Winkler and Gawenda (1999). As such, major lithological/sedimentological changes are shown to be inherently tied to changes in climate in the continental realm. However, the effect of tectonics is more difficult to quantify. The ongoing (local) uplift of the Pyrenees throughout the early Eocene most likely accentuated the (global) effects of these major environmental perturbations.

This study highlights the power of ichnology as a supplementary tool in high resolution, deep-water sedimentology. By explicitly documenting depositional environments and quantifying their trace fossil assemblages, this study has generated a model that is exportable to deep marine basins of a similar age (i.e. late Mesozoic to early Cenozoic). However, one of the most important aspects is that of utilising ethology as a tool to support interpretation of depositional environments. Although it is true that most trace fossil taxa have a wide stratigraphic range, this study has highlighted that their occurrences through geological time are not always limited to

specific oceanic realms (e.g. bathymetic 'windows') and therefore environments of deposition. However, ethologies are governed by an organisms response to changes in environmental parameters that are at least passively controlled by the environment of deposition. As such, in submarine fan settings, analysing ethologies of trace fossil assemblages (without necessarily identifying specific taxa) can be a powerful tool. It is likely that this approach can be exported to older (i.e. Mesozoic and older) successions.

The punctuation of the early Palaeogene's background greenhouse climate by extreme 'hyperthermal' events may call into question the exportability of the results of this study to settings of a different age, due to the unique effect of hinterland climate on sediment supply. Climatically driven changes in sediment supply have been shown to have significant palaeoecological effects in the deep marine realm. However, this study has also shown that in the Basque Basin, broad-scale lithological changes are coincident with major environmental perturbations. As such, the hyperthermal events of the early Palaeogene acted as a trigger mechanism for fundamental changes in sediment supply into the basin. These changes in sediment supply contributed to and accentuated the wide range of submarine fan sub-environments preserved in the Basque Basin. As such, the Basque Basin preserves an ideal natural laboratory for investigating the control that depositional environment exerts on trace fossil assemblages in deep marine settings.

Ratios of pre- versus post-depositional trace fossils are shown to be strongly controlled by relative proximal to distal and axis to off-axis positions within a submarine fan setting. Arguably it is the pre-depositional assemblages that provide the key to interpreting sub-environments of a submarine fan. Pre-depositional trace fossils are exhumed by erosive turbidity currents. As such, the depth of erosion of turbidity currents determines the depth of tier (and therefore trace fossil

taxa) that may be exposed. The depth of erosion by a turbidity current is largely determined by the environment of deposition it is preserved in. To utilise this technique effectively it is critical that environments of deposition are not interpreted on a locality by locality basis. Environmental interpretations should acknowledge the highly dynamic nature of turbidite depositional systems. Characterising environments of deposition using terms such as 'lobe complex axis, lobe complex off-axis and lobe complex fringe' in distributive systems (*sensu* Prélat *et al.*, 2009) or channel axis, off axis, margin, internal levee, external levee (Hodgson *et al.*, 2011) is preferred to more general terms such as 'medial lobe' or channel complex. By using this nomenclature/terminology, single localities can be sub-divided at m-scale resolution, offering a much greater accuracy in data capture.

7.3 SUGGESTIONS FOR FURTHER RESEARCH

This study has shown that a detailed ichnological analysis is a powerful supplementary tool in both high resolution sedimentary environmental interpretation and in palaeoecological reconstructions across environmental perturbations. However, there are a number of areas in which ichnology would benefit enormously from an increased level of understanding.

7.3.1 Core based environmental interpretation utilising ichnology

Until recently, most deep-marine ichnological research has been biased towards taxonomical investigation. Detailed taxonomical monographs such as those produced by Uchman (1995, 1998, 2001) are invaluable to provide a robust taxonomic framework by which to constrain correct identification of trace fossils. However, environmental interpretations in such monographs are usually limited. In recent years, a concerted effort has been made to utilise ichnology as a high resolution, powerful tool in the interpretation of depositional environments

in deep-marine settings. Notable examples of such work include Heard and Pickering (2008), Monaco *et al.* (2010), Phillips *et al.* (2011) and Cummings and Hodgson (2011b). However, all of these studies have been outcrop based. Subsurface (i.e. core based) studies utilising ichnology as a supplementary tool in environmental interpretation of deep-marine settings are still limited (with the exception of Knaust, 2009b). However, Heard (2008) has unpublished work on ichnofacies analysis from core and outcrop in the same stratigraphic succession. Further studies such as this are recommended. Chapter 2.2.8 details the different techniques and limitations of core based versus outcrop based ichnological studies.

Given that most taxonomical work is based on bedding plane expression of trace fossils, identification of trace fossils on core cuts is biased toward vertical and large burrows, and limited by the lack of material to compare to in the literature. The two dimensional nature of core also limits the morphological expression of trace fossils, limiting the amount of taxonomical data available to the ichnologist. The vast diversity of traces such as the graphoglyptids is therefore lost in core as they express themselves generally as unlined traces with a differing infill to the host sediment (personal observation). Essentially, this is identical to the core expression of *Planolites* (see Pemberton and Frey, 1982 for discussion) limiting the use of the most diverse, and in some settings, abundant trace fossil taxa encountered in deep marine settings. As such, an important step in deep marine ichnology is to improve the database of identifiable trace fossils in core. Techniques such as X-ray radiography (e.g. Wetzel, 2008) could improve the 2-dimensional appearance of 3-dimensional structures. Once we have a more robust framework for identifying deep-marine trace fossils in core, then similar studies to this, and those listed above, should be conducted on core datasets to carefully begin to document the types of trace fossils prevalent in certain depositional environments of particular ages. Then, the exportability of any

findings can be tested. This would be of particular value for the hydrocarbon industry where the limited lateral extent of core can make environmental interpretations challenging even for experienced geologists.

7.3.2 Collaboration between neoichnologists and palaeoichnologists

A better understanding of colonisation of modern sediments in the deep-marine realm would greatly enhance our understanding of ancient sedimentary successions. Many common deep-marine trace fossils (e.g. *Zoophycos*) still have no affinity to a trace maker. This in some ways limits the ethological interpretation of such traces.

The inference that the graphoglyptids represent agrichnia is largely based on Seilacher's (1977a) observations on regularity of burrow morphology combined with their maintenance of an open burrow network to facilitate trapping of organic matter and irrigation of the burrow network. The archetypal graphoglyptid (and therefore agrichnia) is *Paleodictyon.* The origin of this trace has recently been questioned by Rona *et al.* (2009), who suggest that *Paleodictyon* may not represents a trace fossil, rather it is a form of hexactinellid sponge, due to the presence of sponge DNA in the network. Such challenges to traditional ichnological fundamentals are necessary if ichnology is to progress as a relevant discipline in geology.

This study details three morphotypes of *Ophiomorpha*-related trace fossils that mimic *Paleodictyon*-type, 3-dimensional hexagonal networks. The 120° branches, swelling at bifurcation points, and reinforcement of the burrow walls with granulated sediment ally the traces with crustacean burrows. This demonstrates that burrowing organisms are able to construct polygonal/hexagonal burrow networks. However, the work by Rona *et al.* (2009) is still

of value as it attempts to unify and/or disprove palaeoichnological techniques and theory with those of neoichnology.

7.3.3 Constraining the PETM kaolinite spike

The seemingly global spike in concentrations of the clay mineral kaolinite at the onset of the PETM seems to be a key diagnostic feature of the PETM (e.g. Robert and Chamley, 1991; Robert and Kennet, 1994; Cramer *et al.,* 1999; Bolle and Adatte, 2000; Cramer and Kent, 2005; Harrington and Kemp, 2005; Dypvik *et al.,* 2011). This study proposed that this spike in kaolinite was due to erosion of older kaolinite enriched regolith (see also Thiry, 2000; Schmitz *et al.*, 2001). As such, kaolinite concentrations were treated as a proxy data set for increased erosion and delivery of terrigenous derived material into the deep Basque Basin. Analysis of spectral gamma ray (SGR) data was employed to attempt to constrain whether the kaolinite was a climatically driven pedogenic product or whether it was in fact due to erosion of older, kaolinite enriched regolith that had been redistributed globally following the break-up of Gondwana (e.g. Thiry, 2000). SGR signatures in the Basque Basin appear to be predominantly controlled by illite/kaolinite ratios where low Th/K and Th/U ratios are prevalent in intervals with low to absent kaolinite with increases in Th/K and Th/U being coincident with elevated kaolinite concentrations. However, it is not possible to confidently state whether or not SGR signatures reflect weathering and prevailing climate in the continental hinterland or whether they have been inherited from the same, older eroded material that delivered kaolinite into the basin.

The PETM is also marked by a global rise in eustatic sea-level (e.g. Speijer and Morsi,2002; Miller *et al.,* 2005; Hanley *et al.*, 2011) so the influx of kaolinite occurs in the background of flooded continental shelves and reduced coarse-grained sediment supply. Increased

sedimentation rates in deep basinal settings during sea-level highstands seem contrary to basic sequence stratigraphic principles. However, the hinterland of the Basque Basin was tectonically active during the PETM and the effect of this on the contemporaneous shelf is unknown. It is likely that uplift of the incipient Pyrenees will have generated steep coastal gradients that may have also resulted in the generation of a very narrow shelf. Increased terrigenous input into the basin may have resulted from high magnitude storms/flooding events associated with the elevated temperatures of the PETM.

An influx of rapidly deposited clay grade sediment during the PETM may therefore have been triggered by fluvial input across a very narrow continental shelf during times of high magnitude storms and associated high discharge rates from fluvial systems. This may have been further exacerbated by increased erosion associated with both increased coastal gradients and a climatically induced reduction in perennial vegetation cover (e.g. REF here!!!). High sedimentation rates in deep-marine settings during the current global sea-level highstand have been reported from active submarine canyons in California, USA. Mullenbach *et al.* (2004) report increased terrigenous input into the Eel Canyon at depths of up to 900m during winter flooding events between 1998 -2000. Furthermore, sedimentation in the canyon comprises a high proportion of clay grade sediment. This highlights the possibility that high sedimentation rates in deep basinal settings can result in thick accumulations of fine grained sediments and need not necessarily comprise sand grade sediment delivered by typical turbidity currents/gravity flows.

Clay mineral results obtained from core samples taken from ODP leg 174ax (onshore New Jersey) display a prominent kaolinite spike following the onset of the PETM (see fig. 7.1). These sediments were deposited in a shallow marine (shelfal) setting at a slightly different palaeolatitude, sourced from differing parent material and deposited much closer landward than

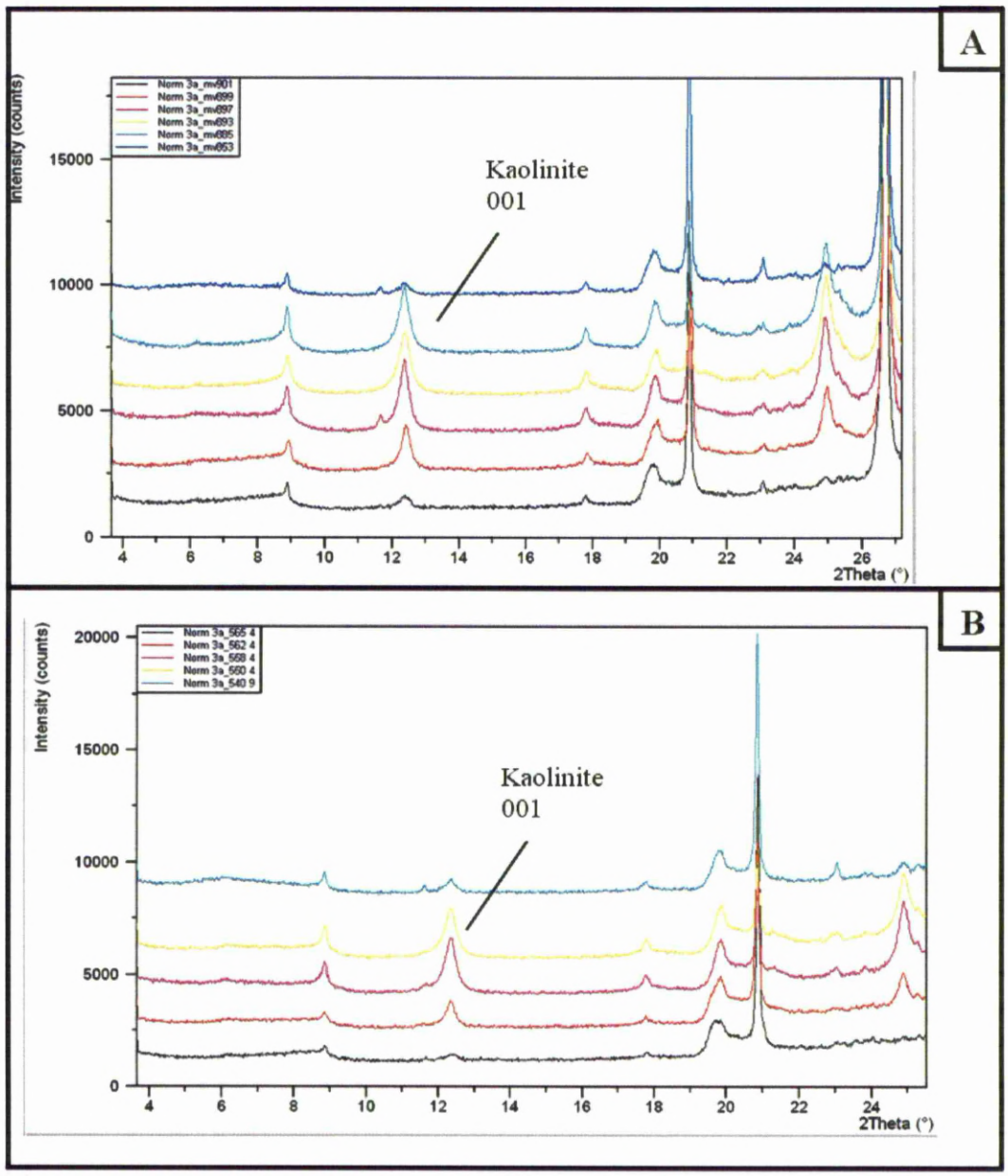

Fig. 7.1 XRD diffractograms obtained from analysis of core samples from ODP Leg 174AX, onshore New Jersey, USA. A,.) Samples taken from the Millville core. MV901 and MV899 are samples taken from the latest Palaeocene (901 and 899 being depth of core in feet). The Palaeocene Eocene boundary is placed somewhere between samples MV899 and MV897 (Miller *et al.*, 1999). Note the dramatic increase in intensity of the kaolinite 001 peak. However, it should be noted that kaolinite has increased significantly in the latest Palaeocene (MV899) sample. .Note how kaolinite has returned to 'backgound' levels by MV853 which is outside of the main CIE/PETM event. B.) Similar patterns are recorded at the Ancora site. The CIE excursion occurs between samples 562 and 558.

sediments deposited in the deep marine Basque Basin. The dominant clay mineral in pre- and post PETM sediments is a smectite-illite mixed layer mineral. However, just as with the Basque Basin, kaolinite increases dramatically at the onset of the PETM and persists throughout the main body of the event. Given that sediments in the two basins were deposited on opposing margins of the Atlantic Ocean under different climatic conditions and experienced different burial histories following deposition, this suggests a common mechanism led to the influx of kaolinite into the ocean at the onset of the PETM. Redistribution of kaolinite enriched land masses following the break-up of Gondwana, followed by significant episodes of erosion associated with an enhanced weathering cycle (due to the PETM) is a plausible explanation (see also Thiry, 2000). However, this problem warrants further investigation. There are many cored intervals of the PETM (e.g. North Sea, Gulf of Mexico, ODP Legs) and outcrop examples from different basins (e.g. Egypt, Svaalbard, Austria) that could be analysed together to understand the global controls on kaolinite influx at the PETM.

Although SGR data proved to be somewhat inconclusive in this study, it is recommended that SGR data be used where possible. A multi-proxy approach, conducted at several locations may uncover trends between SGR signatures and clay mineral assemblages that may reveal a more robust palaeoclimate signal. These results should also be supplemented by oxygen and carbon isotope data to further reinforce any interpretations.

CHAPTER 8

REFERENCES

Adatte T. & Lu G. (1995) Clay mineral correlation across the Paleocene-Eocene boundary: evidence for global turnover from western to eastern Tethys. GSA Ann. Meet. New Orleans, USA, Abstract p. 405.

Alegret, L., Ortiz, S., Orue-Etxebarria, X., Bernaola, G., Baceta, J.I., Monechi, S., Apellaniz, E., Pujalte, V., 2009. The Paleocene-Eocene Thermal Maximum: New data on microfossil turnover at the Zumaia section, Spain. Palaios 24, 318-328.

Alonso-Zarza, A.M. et al. 2002. The Tertiary, in, (ed) Moreno, T., The Geology of Spain. Geological Society London. p. 293-334.

Amy, L.A., Talling, P.J., 2006. Bed geometry used to test recognition criteria of turbidites and (sandy) debrites. Sedimentary Geology 179, 163-174.

Angori, E., Bernaola, G., Monechi, S., 2006. Calcareous nannofossil assemblages and their response to the Paleocene-Eocene Thermal Maximum at different latitudes: ODP site 690 and Tethyan sections, in (eds), Monechi, S., Coccioni, R., Rampino, M.R., Large Ecosystem Perturbations: Causes and consequences. Geological Society of America Special Paper 424, p. 69-86.

Apellaniz, E., Baceta, J.I., Bernaola, G., Núñez-Betelu, K., Orue-Etxebarria, X., Payros, A., Pujalte, V., Robin, E., Rocchia, R., 1997. Analysis of uppermost Cretaceous-lowermost Tertiary hemipelagic successions in the Basque country (Western Pyrenees): evidence of a sudden extinction of more than half planktic foraminifer species at the K/T boundary. Bull. Soc. Geol. France 168, 783-793.

Apellaniz, E., Lamolda, M.A., Orue-Etxebarria, X., 1983. Posición estratigráfica de las "Calizas del Danés", País Vasco. Revista española de Micropaleontología 15, 447-455.

Arenillas, I., Arz, J.A., Molina, E., 1998. El límite Cretácico-Terciario en Zumaia, Osinaga y Musquiz (Pirineos): control bioestratigráfico y cuantitativo de hiatos con foraminíferos planctónicos. Rev. Soc. Geol España 11, 127-138.

Aubry, M.-P., 1998. Early Paleogene calcareous nannoplankton evolution: A tale of climatic amelioration, in: Aubry, M.P., Lucas, S., Berggren, W.A., Late Paleocene and Early Eocene Climatic and Biotic Evolution, Columbia Univ. Press, New York, p. 158–203.

Ausich, W.I., Bottjer, D.J., 1982. Tiering in suspension-feeding communities on soft substrata throughout the Phanerozoic. Science 9, 173-174.

Azpeitia M.F., 1933. Datos para el studio paleontólogico del Flysch de la Costa Cantábrica y de algunos otros puntos de España. Boletín. Instituto Geológico y Minero de España. 53, 1-65.

Baceta, J.I., Pujalte, V., Dinarès-Turell, J., Payros, A., Orue-Etxebarria, X., Bernaola, G., 2000. The Paleocene-Eocene boundary interval in the Zumaia section (Gipuzkoa, Basque basin): magnetostratigraphy and high-resolution lithostratigraphy. Rev. Soc. Geol. España 13, 375-391.

Baceta, J. I., Pujalte, V., Serra-Kiel, J., Robador, A., Orue-Etxebarria, X., 2004. El Maastrichtiense final, Paleoceno e Ilerdiense inferior de la Cordillera Pirenaica. In: J.A. Vera (Ed.), Geología de España. Sociedad Geológica de España- Instituto Geológico y Minero de España, Madrid, p. 308-313.

Beckmann, J.P., 1960. Distribution of benthic foraminifera at the Cretaceous- Tertiary boundary of Trinidad (West Indies), *in* Report of the 21st session, Norden, v. 5: Copenhagen, International Geological Congress, p. 57–69.

Berggren, W.A., Kent, D.V., Swisher, C.C.III., Aubry, M.P., 1995. A revised Cenozoic geochronology and chronostratigraphy, in, (eds) Berggren, W.A., Kent, D.V., Aubry, M.P. Hardenbol, J., Geochronology, time scales and global stratigraphic correlations. S.E.P.M. special publication 54, 129-212.

Bernaola, G., Baceta, J.I., Orue-Etxebarria, X., Alegret, L., Martín-Rubio, M., Arostegui, J., Dinarès-Turell, J., 2006a. The mid Paleocene biotic event, in: Bernaola, G *et al.*, (eds)., The Paleocene and lower Eocene of the Zumaia section (Basque Basin): Post conference field trip guidebook, Climate & Bioata of the Early Paleogene: Bilbao, Spain, p. 49–51.

Bernaola, G., Orue-Etxebarria, X., Payros, A., Dinarès-Turrel, J., Tosquella, J., Apellaniz, E., Caballero, F., 2006b. Biomagnetostratigraphic analysis of the Gorrondatxe section (Basque Country, western Pyrenees): Its significance for the definition of the Ypressian/Lutetian boundary stratotype. Neues Jarbruch fü r Geologie und Paläontologie Abhandlungen 241, 67-109.

Bernaola, G., Baceta, J.I., Orue-Etxebarria, X., Alegret, L., Martín-Rubio, M., Arostegui, J., Dinarès-Turell, J., 2007. Evidence of an abrupt environmental disruption during the mid-Paleocene biotic event (Zumaia section, western Pyrenees). Geological Society of America Bulletin 119, 785-795.

Bernaola, G., Martín-Rubio, M., Baceta, J.I., 2009. New high resolution calcareous nannofossil analysis across the Danian/Selandian transition at the Zumaia section: comparison with South Tethys and Danish sections. Geologica Acta 7, 79-92.

Billings, E., 1862. New species in fossils from the different parts of the lower, Middle and Upper Silurian rocks of Canada, in: Palaeozoic Fossils, volume 1 1861-1865. Geological Survey of Canada, Dawson Brothers, Montreal, p. 96-168.

Billings, E., 1866. Catalogues of the Silurian fossils. Geological Survey of Canada, Dawson Brothers, Montreal, pp. 93.

Biscay, P.E., 1965. Mineralogy and sedimentation of recent deep-sea clay in the Atlantic Ocean and adjacent seas and oceans. Geological Society of America Bulletin 76, 803-832.

Boersma, A., Premoli Silva, I., and Hallock, P., 1998. Trophic models for well-mixed and poorly mixed warm oceans across the Paleocene/Eocene epoch boundary. In: Aubry, M.P., Lucas, S.G., and Berggren, W.A. (Eds.), Late Paleocene–Early Eocene Biotic and Climatic Events in the Marine and Terrestrial Records, New York (Columbia Univ. Press), 204–213.

Bolle, M.P., Addatte, T. 2000. Palaeocene-early Eocene climatic evolution in the Tethyan realm: clay mineral evidence. Clay Minerals 36, 249-261.

Bolle, M.P., Adatte, T., Keller, G., von Salis, K., Hunziker, J., 1998. Biostratigraphy, mineralogy and geochemistry of the Trabakua Pass and Ermua sections in Spain. Eclogae Geologicae Helvetiae 91, 1-25.

Bottjer, D.J., Drosser, M.L., Jabonski, D., 1987. Bathymetric trends in the history of trace fossils, in: Bottjer, D.J., (ed), New Concepts in the use of Biogenic Sedimentary Structures for Paleoenvironmental Interpretation: Society of Economic Paleontologists and Mineralogists, Los Angeles, p. 57-65.

Bottjer, D.J., Drosser, M.L. Jabonski, D., 1988. Palaeoenvironmental trends in the history of trace fossils. Nature 333, 252-255.

Bowen, G.J., Beerling, D.J., Koch, P., Zachos, J.C., Quattelbaum, T., 2004. A humid climate state during the Palaeocene-Eocene thermal maximum. Nature 432, 495–499.

Bowen, G. J., Clyde, W. C., Koch, P. L., Ting, S., Alroy, J., Tsubamoto, T., Wang, Y., Wang, Y., 2002 Mammalian dispersal at the Paleocene/Eocene boundary, Science 295, 2062– 2065.

Bralower, T.J., 2002. Evidence of surface water oligotrophy during the Paleocene-Eocene thermal maximum: Nannofossil assemblage data from Ocean Drilling Program Site 690, Maud Rise, Weddell Sea. Paleoceanography 17, 1023.

Bromley, R.G., 1996. Trace Fossils: Biology, Taphonomy and Applications, 2nd edition: Chapman and Hall, London, 361 pp.

Bromley, R.G., Ekdale, A.A., 1984. *Chondrites*: a trace fossil indicator of anoxia in sediment. Science 224, 872-874.

Bromley, R.G., Ekdale, A.A., 1986. Composite ichnofabrics and tiering of burrows. Geological Magazine 123, 59-65.

Brongniart, A.T., 1823. Observations sur les Fucoids. Société d'Hist Natur. Paris. Mémoir. 1, 301-320.

Brongniart, A.T., 1828. Histoire des végétaux fossils ou recherches botaniques et géologiques sur les végétaux renfermés dans les diverses couches du globe. Volume 1. G. Dufour and E. d'Ocagne, Paris. pp. 136.

Buatois, L.A., Mangano, M.G., Sylvester, Z., 2001. A diverse deep-marine ichnofauna from the Eocene Tarcau Sandstone of the Eastern Carpathians, Romania. Ichnos 8, 23-62.

Cadée, G.C., Goldring, R., 2007. The Wadden Sea, Cradle of Invertebrate Ichnology, in (ed) Miller III, W., Trace Fossils: Concepts, Problems, Prospects, Elsevier, Oxford. p. 3-13.

Canudo, J.I., Keller, G., Molina, E., Ortiz, N., 1995. Planktic foraminiferal turnover and $\delta^{13}C$ isotopes across the Paleocene-Eocene transition at Caravaca and Zumaya, Spain. Palaeogeography, Palaeoclimatology, Palaeoecology 114, 75-100.

Cavalcante F., Belviso, C., Bentivenga, M., Fiore, S., Prosser, G., 2011. Occurrence of palygorskite and sepiolite in upper Paleocene–middle Eocene marine deep sediments of the Lagonegro Basin (Southern Apennines—Italy): Paleoenvironmental and provenance inferences. Sedimentary Geology 233, 42–52.

Chamberlain, C.K., 1971. Morphology and ethology of trace fossils from the Ouachita Mountains, Southeast Oklahoma. Journal of Paleontology 45, 212-246.

Chamley, H., 1989. Clay Sedimentology. Springer, Berlin, 623pp.

Clyde, W. C., Gingerich, P. D., 1998. Mammalian community response to the latest Paleocene thermal maximum: An isotaphonomic study in the northern Bighorn Basin, Wyoming, Geology, 26, 1011 –1014.

Cramer, B.S., Aubry, M.P., Miller, K.G., Olsson, R.K., Wright, J.D., Kent, D.V. 1999. An exceptional chronologic, isotopic, and clay mineralogic record of the latest Paleocene thermal maximum, Bass River, NJ, ODP 174AX. Geological Society of France, Bulletin. 170, 883-897.

Cramer, B.S., Kent, D.V. 2005. Bolide summer: The Paleocene/Eocene thermal maximum as a response to an extraterrestrial trigger. Palaeogeography, Palaeoclimatology, Palaeoecology 224, 144– 166.

Crimes, T.P., 1973. From limestones to distal turbidites: a facies and trace fossil analysis of the Zumaya flysch (Paleocene-Eocene), North Spain. Sedimentology 20, 105-131.

Crimes, T.P., 1976. Sand fans, turbidites, slumps and the origin of the Bay of Biscay: A facies analysis of the Guipuzcoan Flysch. Palaeogeography, Palaeoclimatology, Palaeoecology 19, 1-15.

Crimes, T.P., 1977. Trace fossils of an Eocene deep-sea sand fan, northern Spain, in: Crimes, T.P., Harper, J.C., (eds.), Trace Fossils 2. Geological Journal Special Issue 9, p. 71-90.

Crimes, P.T. and Anderson, M.M., 1985. Trace Fossils from Late Precambrian-Early Cambrian strata of Southeastern Newfoundland, Canada: temporal and environmental implications. Journal of Paleontololgy 59, 310-343.

Crimes, T.P., Fedonkin, M.A., 1994. Evolution and dispersal of deep sea traces. PALAIOS, 9, 74-83.

Crouch, E., Brinkhuis, H., Visscher, H., Addatte, T., Bolle, M.P., 2003. Late Paleocene-early Eocene dinoflagellate cyst records from the Tethys: Further observations on the global distribution of *Apectodinium.* In: Wing, S.L., Gingerich, P.D., Schmitz, B., Thomas, E., (Eds), Causes and Consequences of Globally Warm Climates in the Early Paleogene: The Geological Society of America, Special Paper 369.

Crouch E.M., Dickens, G.R., Brinkhuis, H., Aubry, M.P., Hollis, C.J., Rogers, K.M., Visscher, H., 2003. The Apectodinium acme and terrestrial discharge during the Paleocene-Eocene thermal maximum: new palynological, geochemical and calcareous nannoplankton observations at Tawanui, New Zealand. Palaeogeography, Palaeoclimatology, Palaeoecology 194, 387-403.

Crouch, E.M., Heilmann-Clausen, C., Brinkhuis, H., Morgans, H.E.G., Rogers, K.M., Egger, H., Schmitz, B., 2001. Global dinoflagellate event associated with the late Paleocene thermal maximum. Geology 29, 315–318.

Cummings, J.P., Hodgson, D.M., 2011a. An agrichnial feeding strategy for deep-marine Paleogene *Ophiomorpha.* PALAIOS 26, 212-224. DOI: 10.2110/palo.2010.p10-098r

Cummings, J.P., Hodgson, D.M., 2011b. Assessing controls on the distribution of ichnotaxa in submarine fan related environments, the Basque Basin, northern Spain. Sedimentary Geology, 239, 162-187. DOI 10.1016/j.sedgeo.2011.06.009

Das Gupta, K., Pickering, K.T. 2008. Petrography and temporal changes in petrofacies of deep marine Ainsa-Jaca Basin sandstones. Sedimentology 55, 1083-1114.

De Gibert, J.M., 1996, A new decapod burrow system from the NW Mediterranean Pliocene: Revista Española de Paleontologìa 11, 251-254.

De Gibert, J.M., Kyungwan, J., Martinell, J., 1999, Ethologic and ontogenic significance of the Pliocene trace fossil *Sinusichnus sinuosis* from the northwestern Mediterranean. Lethaia 32, 31-40.

De Gibert, J.M., Netto, R.G., Tognoli, F.M.W., Grangeiro, M.E., 2006, Commensal worm traces and possible juvenile thalassinidean burrows associated with *Ophiomorpha nodosa*, Pleistocene, southern Brazil. Palaeogeography, Palaeoclimatology, Palaeoecology 230, 70-84.

De Stefani, C., 1895. Apercu géologique et description paléontologique de I'lle de Karpathos, in, (eds) De Stefani, C., Forsythe Major, C.J., Barbey, W. Karpathos. Etude géologique, paléontologique et botanique. G, Bridel, Lousanne, p. 1-28.

Dickens, G.R., 1999. Carbon cycle: The blast in the past. Nature 401, 752-755.

Dickens, G.R., O'Neil, J.R., Rea, D.K., & Owen, R.M., 1995. Dissociation of oceanic methane hydrate as a cause of the carbon isotope excursion at the end of the Paleocene. Paleooceanography 10, 965-971.

Dickens, G.R., Castillo, M.M., Walker, J.C.G., 1997. A blast of gas in the latest Paleocene: Simulating first order effects of massive dissociation of oceanic methane hydrate. Geology 25, 259-262.

Dinarès-Turell, J., Baceta, G., X., Pujalte, V., Orue-Etxebarria, J.I., Bernaola, 2002. Magnetostratigraphic and cyclostratigraphic calibration of a prospective Palaeocene/Eocene stratotype at Zumaia (Basque Basin, northern Spain). Terra Nova 14, 371–378.

Dinarès-Turell, J., Baceta, J.I., Bernaola, G., Orue-Etxebarria, X., Pujalte, V., 2007. Closing the Mid-Palaeocene gap: Toward a complete astronomically tuned Palaeocene Epoch and Selandian and Thanetian GSSPs at Zumaia (Basque Basin, W Pyrenees). Earth and Planetary Science Letters, 262, 450-467.

Droser, M.L., Bottjer, D.J., 1991. Trace fossils and ichnofabric in leg 119 cores: Proceedings of the Ocean Drilling Program, Scientific Results 119, 635-641.

Droser, M.L., Bottjer, D.J., 1993. Trends and patterns of Phanerozoic ichnofabrics. Annual Review of Earth and Planetary Science Letters 21, 205-225.

Dypvik, H., Riber, L., Burca, F., Rüther, D., Jargvoll, D., Nagy, J., Jochmann, M., 2011. The Paleocene–Eocene thermal maximum (PETM) in Svalbard — clay mineral and geochemical signals. Palaeogeography, Palaeoclimatology, Palaeoecology 302, 156–169.

Egger, H., Homayoun, M., & Schnabel, W., 2002. Tectonic and climatic control of Paleogene sedimentation in the Rhenodanubian Flysch basin (Eastern Alps, Austria). Sedimentary Geology 153, 247-262.

Ehrenberg, K., 1944. Ergänzende Bemerkungen zu den seinerzeit aus dem Miozän von Burgschleinitz beschrieben Gangkernen und Bauten dekapoder Krebse: Paläeontologische Zeitschrift 23, 345-359.

Eichenseer, H., Luterbacher, H., 1992. The Marine Paleogene of the Tremp region (NE Spain) – depositional sequences, facies history, biostratigraphy and controlling factors. Facies 27, 119-152.

Ekdale, A.A., 1985. Palaeoecology of the marine endobenthos. Palaeogeography, Palaeoclimatology, Palaeoecology 50, 63-81.

Ekdale, A.A., Bromley, R.G., 2003. Paleoethologic interpretation of complex *Thalassinoides* in shallow marine limestones, Lower Ordivician, southern Sweden: Palaeogeography, Palaeoclimatology, Palaeoecology 192, 221-227.

Emmons, E., 1844. The Taconic system based on observations in New York, Massachusetts, Maine, Vermont and Rhode Island. Caroll and Cook, Albany. pp. 63.

Ernst, S.R., Guasti, E., Dupuis, C., Speijer, R.P., 2006. Environmental perturbation in the southern Tethys across the Paleocene/Eocene boundary (Dababiya, Egypt): Foraminiferal and clay mineral records. Marine Micropaleontology, 89–111.

Fischer-Ooster, C., 1858. Die fossilen Fucoiden der Schweizer Alpen, nebst Erörterungen über deren geologisches Alter. Huber, Bern. pp. 72.

Föllmi, K.B., Grimm, K.A., 1990. Doomed Pioneers: gravity flow deposition and bioturbation in marine oxygen-deficient environments. Geology 18, 1069-1072.

Frey, R.W., 1970. Trace fossils of the Fort Heys Limestone Member, Niobrara Chalk (Upper Cretaceous), west central Kansas. University of Kansas Paleontology Contr. 53, 1-41.

Frey, R.W., Howard, J.D., Pryor, W.A., 1978. *Ophiomorpha*: its morphologic, taxonomic and environmental significance. Palaeogeography, Palaeoclimatology, Palaeoecology 23, 199-223.

Frey, R.W., Pemberton, S.G., 1985. Biogenic structures in outcrops and cores: Approaches to Ichnology. Bulletin of Canadian Petroleum Geology 33, 72-115.

Frey, R.W., Pemberton, S.G., Saunders, T.D., 1990. Ichnofacies and bathymetry: A passive relationship. Journal of Paleontology 64, 155-158.

Frey, R.W. Seilacher, A. 1980. Uniformity in marine invertebrate ichnology. Lethaia 13, 183-207.

Füchs, T., 1895. Studien über fucoiden und hieroglyphen. Denkschr Akad Wiss Wien Math-Naturwiss Kl. 62, 369-448.

Gabelli, L. De., 1900. Sopra un interessante impronta medusoidae. Il Pensiero Aristotelico della Scienza Moderna 1, 74-78.

Gawenda, P., Winkler, W., Schmitz, B., Adatte, T., 1999. Climate and bioproductivity control on carbonate turbidite sedimentation (Paleocene to earliest Eocene, Gulf of Biscay, Zumaia, Spain). Journal of Sedimentary Research 69, 1253-1261.

Gharrabi, M., Velde, B., Sagon, J.P. 1998. The Transformation Of Illite To Muscovite In Pelitic Rocks: Constraints From X-Ray Diffraction. Clays and Clay Minerals 46, 79-88.

Gianetti, A., McCann, T., 2010. The Upper Paleocene of the Zumaya Section (Northern Spain): review of the ichnological content and preliminary palaeoecological interpretation. Ichnos 17, 137-161.

Gingerich, P.D., 2003. Mammalian response to climate change at the Paleocene-Eocene boundary: Polecat Bench record in the northern Bighorn Basin, Wyoming, in (eds), Wing, S.L., Gingerich, P.D., Schmitz, B., Thomas, E., Causes and consequences of globally warm climates of the Paleogene: Geological Society of America Special Paper 369, p 463-478.

Hagadorn, J.W., Bottjer, D.J., 1999. Restriction of a characteristic late Neoproterozoic biotope: suspect microbial structures and trace fossils at the Vendian-Cambrian transition. PALAIOS 14, 73-85.

Haldeman, S. S., 1840. Supplement to Number One of "A monograph of the Limniades, or freshwater univalve shells of North America." Containing descriptions of apparently new animals in different classes, and the names and characters of the subgenera, in: Paludina and Anculosa. J. Dobson, Philadelphia.

Hall, J., 1847. Paleontology of New York. Volume 1. C. Van Benthuysen, Albany. pp. 338.

Hall, J., 1852. Paleontology of New York. Volume 2. C. Van Benthuysen, Albany. pp. 362.

Hanisch, J., 1974. Der Tiefsee-Diapir Zarauz (N-Spanien) im Spiegel von Sedimentation und Tektonic des Kreide/Tertiär Flyschs. Geol. Jahbr. 11, 101-142.

Hanley, L., Crouch, E.M. Pancost, R.D., 2011. A New Zealand record of sea level rise and environmental change during the Paleocene–Eocene Thermal Maximum. Palaeogeography, Palaeoclimatology, Palaeoecology 305, 185-200.

Häntzschel, W., 1975. Trace fossils and problematica, in, (Ed) Teichert, C., Treatise on invertebrate paleontology. Geological Society of America and Kansas University Press.

Haq, B.U., Hardenbol, J., Vail, P.R., 1987, Chronology of Fluctuating Sea Levels since the Triassic. Science 235, 1156-1167.

Harrington, G.J., Kemp, S.J., 2005. US Gulf Coast vegetation dynamics during the latest Palaeocene. Palaeogeography, Palaeoclimatology, Palaeoecology 167, 1-21.

Hasselbo, S.P., 1996. Spectral Gamma-Ray logs in relation to clay mineralogy and sequence stratigraphy, Cenozoic of the Atlantic margin, offshore New Jersey, in: Mountain, G.S., Miller, K.G., Blum, P., Poag, C.W., and Twichell, D.C. (Eds.), Proceedings of the Ocean Drilling Program, Scientific Results 150, 411-422.

Haughton, P.D.W., Barker, S.P., McCaffrey, W.D., 2003. 'Linked' debrites in sand-rich turbidite systems – origin and significance. Sedimentology 50, 459-482.

Haughton P.D., Davis, C., McCaffrey, W.D., Barker, S., 2009. Hybrid sediment gravity flow deposits – Classification, origin and significance. Marine and Petroleum Geology 26, 1900-1918.

Hillier, S., 2003. Quantitative analysis of clay and other minerals in sandstones by X-ray powder diffraction (XRPD). Blackwell.

Heard, T., Pickering, K.T., 2008. Trace fossils as diagnostic indicators of deep-marine environments, Middle Eocene Ainsa - Jaca basin, Spanish Pyrenees. Sedimentology 55, 809-844.

Heer, O. 1877. Flora fossilis helvetiae. Vorweltliche flora der Schweiz. J. Wurster and Comp. Zürich. pp. 182.

Hodgson, D.M., 2009. Distribution and origin of hybrid beds in sand-rich submarine fans of the Tanqua depocentre, Karoo Basin, South Africa. Marine and Petroleum Geology 26, 1940-1956.

Hodgson, D.M., Di Celma, C., Brunt, R., Flint S.S., 2011. Submarine Slope Degradation and Aggradation and the Stratigraphic Evolution of Channel-Levee Systems. Journal of the Geological Society 168, 625-628.

Hodgson, D.M., Wild, R.J., 2007. Facies, bed geometries and evidence for strong bottom currents in the deep-water Eocene Guipuzcoa Basin, NW Spain, in: Nilsen, T., Shew, R., Stefans, G. and Studlick, J., (eds.), Atlas of Deepwater Outcrops. American Association of Petroleum Geologists, ST56, CD-ROM.

Hollis, C.J., Handley, L., Crouch, E.M., Morgans, H.E.G., Baker, J.A., Creech, J., Collins, K.S., Gibbs, S.J., Huber, M., Schouten, S., Zachos, J.C., Pancost, R.D., 2009. Tropical sea temperatures in the high-latitude South Pacific during the Eocene. Geology 37, 99-102.

Howard, J.D., Frey, R.W., 1984. Characteristic trace fossils in nearshore to offshore sequences, Upper Cretaceous of East Central Utah: Canadian Journal of Earth Science 21, 200-219.

Kane, I., Hodgson, D.M., 2011. Submarine channel levees: nomenclature and criteria to differentiate subenvironments. Exhumed examples from the Rosario Fm. (Upper Cretaceous) of Baja California, Mexico, and the Laingsburg Fm. (Permian), Karoo Basin, S. Africa. Marine and Petroleum Geology 28, 807-823.

Kane, I.J., Kneller, B.C., Dykstra, M., Kassem, A., McCaffrey, W.D., 2007. Anatomy of a submarine channel-levee: An example from Upper Cretaceous slope sediments, Rosario Formation, Baja California, Mexico. Marine and Petroleum Geology 24, 540-563.

Katz, M.E., Cramer, B.S., Mountain, G.S., Katz, S., Miller, K.G., 2001. Uncorking the bottle: What triggered the Paleocene/Eocene thermal maximum methane release? Paleoceanography 16, 549–562.

Kelly, D.C., 2002. Response of Antarctic (ODP Site 690) planktonic foraminifera to the Paleocene–Eocene thermal maximum: Faunal evidence for ocean/climate change. Paleooceanography, 17, 1071.

Kelly, D.C., Bralower, T.J., Zachos, J.C., 1998. Evolutionary consequences of the latest Paleocene thermal maximum for tropical planktonic foraminifera: Palaeogeography, Palaeoclimatology, Palaeoecology 141, 139–161.

Kelly, D.C., Zachos, J.C., Bralower, T.J., Schellenberg, S.A., 2005. Enhanced terrestrial weathering/runoff and surface-ocean carbonate production during the recovery stages of the Paleocene-Eocene Thermal Maximum. Paleoceanography 20, PA4023 (1-11).

Kennett, J.P., and Stott, L.D., 1991. Abrupt deep-sea warming, palaeoceanographic changes and benthic extinctions at the end of the Paleocene. Nature 353, 225-229.

Kent, D.V., Cramer, B., Lanci, L., Wang, D., Wright, J., Van der Voo, R., 2003. A case for a comet impact trigger for the Paleocene/Eocene Thermal maximum and carbon isotope excursion. Earth and Planetary Science Letters 211, 13–26.

Kent Barnes, R.S., Callow, P., Olive, P.J.W., Golding, D.W., Spicer, J.I., 1991, The Invertebrates: a synthesis, Blackwell Publishing, Oxford, U.K. p.216.

Kern, J.P., 1980. Origin of trace fossils in Polish Carpathian flysch. Lethaia 13, 347-362.

Kerne, P.J., Warme, J.E., 1974, Trace fossils and bathymetry of the Upper Cretaceous Point Loma Formation, San Diego, California: Geological Society of America Bulletin 85, 893-900.

Knaust, D., 2009a. Ichnology as a tool in carbonate reservoir characterization: A case study from the Permian – Triassic Khuff Formation in the Middle East. GeoArabia 14, 17-38.

Knaust, D., 2009b. Characterisation of a Campanian deep-sea fan system in the Norwegian Sea by means of ichnofabrics. Marine and Petroleum Geology 26, 1199-1211.

Knox, R.W., 1998. Kaolinite influx within Paleocene/Eocene boundary strata of western Europe. Newsl. Stratigr. 36, 49-53.

Koch, P.L., Clyde, W.C., Hepple, R.P., Fogel, M.L., Wing, S.L., Zachos, J.C., 2003. Carbon and oxygen isotope records from paleosols spanning the Paleocene-Eocene boundary, Bighorn Basin, Wyoming, in (eds) Wing, S.L., Gingerich, P.D., Schmitz, B., Thomas, E., Causes and consequences of globally warm climates of the Paleogene: Geological Society of America Special Paper 369, p. 49–64.

Koch, P.L., Zachos, J.C., Gingerich, P.D., 1992. Correlation between isotope records in marine and continental carbon reservoirs near the Palaeocene-Eocene boundary: Nature 358, 319–322.

Kruit, C., Brouwer, J., Ealey, P., 1972. A deepwater sand fan in the Eocene Bay Of Biscay. Nature Physical Science 240, 59-61.

Książkiewicz, M., 1958. Stratigraphy of the Magura Series in the Średni Beskid Carpathians. Inst. Geol. Biul. 153, 43-96.

Książkiewicz, M., 1968. On some problematic organic traces from the flysch of the Polish Carpathians, Part 3. Rocznik Polskiego Towarzystwa Geologicznego 38, 3-17.

Książkiewicz, M., 1970. Observations on the ichnofauna of the Polish Carpathians, in: Crimes, T.P., Harper, J., (eds.), Trace Fossils. Geological Journal Special Issue 3, pp. 283-322.

Książkiewicz, M., 1977, Trace fossils in the flysch of the Polish Carpathians. Palaeontologica Polonica 36, 1-208.

Kuhnt, W., Kaminski, M.A., 1993. Changes in the community structure of deep water agglutinated foraminifers across the K/T boundary in the Basque Basin, northern Spain. Rivista Española de Micropaleontologia 25, 57-92.

Lamolda, M.A., Mathey, B., Wiedmann, J., 1988. Field-guide excursion to the Cretaceous-Tertiary boundary section at Zumaya (Northern Spain), in, (eds) M.A. Lamolda, E.G. Kauffman And O.H. Walliser. Paleontology and Evolution: Extinction Events. 2nd International Conference on Global Bioevents, Bilbao, Revista de Paleontología, nº extraordinario, 141-155.

Lamolda, M.A., Gorostidi, A., 1992. Nannofossil stratigraphic record in upper Maastrichtian-Lowermost Danian at Zumaya. Mem. Ist. Geol. Miner. Univ. Padova 43, 149-161.

Lamolda, M.A., Orue-Etxebarria, X., Proto-Decima, F., 1983. The Cretaceous-Tertiary boundary in Sopelena (Biscay, Basque Country). Zitteliana 10, 663-670.

Lanson, B., Beaufort, D., Berger, G., Bauer, A., Cassagnabere, A., Meunier, A., 2002. Authigenic kaolin and illitic minerals during burial diagenesis of sandstones: a review. Clay Minerals 37, 1-22.

Leszcyznski, S., 1991. Trace fossil tiering in flysch sediments: examples from the Guipuzcoan flysch (Cretaceous-Paleogene), northern Spain. Palaeogeography, Palaeoclimatology, Palaeoecology 88, 167-184.

Lidgard, S., Crane, P.R., 1988. Quantitative analyses of the early angiosperm radiation: Nature 331, 344-346.

Lourens, J.L., Sluijs, A., Kroon, D., Zachos, J.C., Thomas, E., Röhl, U., Bowles, J., Raffi , I., 2005. Astronomical pacing of late Paleocene to early Eocene global warming events. Nature 435, 1083–1087.

Lundgren, B., 1891. Studier ofver fossilforande losa block: Geologiska Föreningens i Stockholm Förhandlingar 13, 111-121.

MacEachern, J.A., Bann, K.L., Pemberton, S.G., Gingras, M.K., 2007. The Ichnofacies Paradigm: High Resolution Paleoenvironmental Interpretation of the Rock Record, in: MacEachern, J.A., Bann, K.L., Pemberton, S.G., Gingras, M.K., (eds.), Applied Ichnology. SEPM Short course Notes 52, p. 27-64.

MacLeay, W.S., 1839. Note on the Annelida, in: Murchinson, R.I. (Ed.). The Silurian System, Part II, organic remains. J. Murray, London. p. 699-701.

Martinsson, A., 1965. Aspects of a middle Cambrian thanatotope on Öland. Geologiska Foreningens I Stockholme: Forhandlingar 87, 171-230.

Martinsson, A., 1970. Toponomy of trace fossils, in: Crimes, T.P., Harper, J.C., (eds.), Trace Fossils. Geological Journal Special Issue 3. p. 323-330.

Martini, E., 1971. Standard Tertiary and Quaternary calcareous nannoplankton zonation. Proceedings of the 2nd plankton conference (Roma), 749-785.

Massalongo, A., 1855. Zoophycos, novum genus plantorum fossilium, Antonelli, Verona, pp. 52.

McCoy, F., 1850. On some genera and species of Silurian Radiata in the collection of the University of Cambridge. Annual Magazine of Natural History, Series 2, 6, 270-290.

Meneghini, G., 1850. *Paleodictyon,* in: Savi, P., and Meneghini, G., (Eds.). Osservazioni stratigrafiche e paleontologicke concernati la geologie della Toscana e dei paesi limitrofi (Appendix to R.R. Murchinson, Memoria sulla struttura geol. delle Alpi). Firenze. p. 246-528.

Miller, W, III., 1991. Paleoecology of graphoglyptids: Ichnos 1, 305-312.

Miller, K.G., Kominz, M.A., Browning, J.V., Wright J.D., Mountain, G.S., Katz, M.E., Sugarman, P.J., Cramer, B.S., Christie-Blick, N., Pekar, S.F., 2005. The Phanerozoic record of sea level change: Science 310, 1293-1298.

Miller, K.G., Sugarman, P.J. Browning, J.V., et al. 1999. Proceedings of the Ocean Drilling Program, Initial Reports Volume 174AX, 1-65.

Miller, M.F., Smail, S.E., 1997. A semiquantitative field method for evaluating bioturbation on bedding planes. Palaios 12, 391-396.

Millot, G., 1970. Geology of Clays. Springer, New York, NY. 425 pp.

Monaco, P., Milighetti, M. Checconi, A., 2010. Ichnocoenoses in the Oligocene to Miocene foredeep basins (Northern Apennines, central Italy) and their relation to turbidite deposition. Acta Geologica Polonica, 60, 53-70.

Monaco, P., Caracuel, J., Gianetti, A., Soria, J.M., Yébenes, A., 2007. *Thalassinoides* and *Ophiomorpha* as cross-facies trace fossils of crustaceans from shallow-to-deep-water environments: Mesozoic and Tertiary examples from Italy and Spain. 3rd Symposium on decapods Mesozoic and Cenozoic crustaceans, Milan. p. 79-82.

Moore, D.M., Reynolds, 1996. X-Ray Diffraction and the identification of clay minerals (2nd edition). New York, Oxford university Press.

Mount, J.F., Ward, P., 1986. Origin of limestone/marl alternations in the upper Maastrichtian of Zumaya, Spain. Journal of Sedimentary Petrology 56, 228-236.

Mullenbach, B.L., Nittrouer, C.A., Puig, P., Orange, D.L., 2004. Sediment deposition in a modern submarine canyon: Eel Canyon, northern California. Marine Geology 211, 101 – 119.

Myers, K.J., 1987. Onshore Outcrop Gamma-Ray Spectroscopy as a Tool in Sedimentological Studies. Unpubl. Ph.D Thesis, Univ. London.

Nathorst, A.G., 1873. Om några förmodade växtfossiler. Kongliga Svenska Vetenskaps-Akademiens Handlingar 9, 25-52.

Nathorst, A.G., 1881. Om spar af evertebrerade djur m. m. Och deras paleontologiska betydelse. Kongliga Svenska Vetenskaps-Akademiens Handlingar 18, 1-104.

Nicholson, H.A., 1873. Contributions to the study of the errant annelids of the older Palaeozoic rock. Proceedings of the Royal Society London 21, 288-290.

Orr, P.J., 2001. Colonization of the deep marine environment during the early Phanerozoic: the ichnofaunal record. Geological Journal 36, 265-278.

Orue-Etxebarria, X. (1983): Los foraminíferos planctónicos del Paleógeno del Sinclinorio de Bizkaia (corte Sopelana-Punta Galea): Parte 1. Kobie 13, 175-249.

Orue-Etxebarria, X., Apellaniz, E., Bacetta, J.I., Coccioni, R., Di Leo, R., Dinares-Turrell, J., Galeotti, S., Monechi, S., Nunez-Betelu, K., Pares, J.M., Payros, A., Pujalte, V., Samso, J.M., Serra-Kiel, J., Schmitz, B., Tosquella, J., 1996. Physical and Biostratigraphic analysis of two prospective Paleocene-Eocene boundary stratotypes in the intermediate-deep water Basque basin, western Pyrenees: The Trabakua Pass and Ermua sections. Neues Jahrbuch für Geologie und Paläontologie 201, 179-242.

Osgood, R.G., 1975. The history of invertebrate ichnology, in, (ed) Frey, R.W., The study of trace fossils. Springer-Verlag, New York. p. 3-12.

Ott, J.A., Fuchs, B., Fuchs, R., Malasek, A., 1976, Observations on the biology of *Callianassa stebingi* Borrodaille and *Upogebia litoralis* Risso and their effect upon the sediment: Senckenbergiana Maritima 8, 61-79.

Parkinson, D.N., 1996. Gamma-ray spectrometry as a tool for stratigraphical interpretation: examples from the western European Lower Jurassic. In: Hesselbo, S.P., Parkinson, D.N. (Eds.), Sequence Stratigraphy in British Geology. Geological Society Special Publication 103, 231–255.

Payros, A., Bernaola, G., Orue-Etxebarria, X., Tosquella, J., Apellaniz, E., 2007. Reassessment of the early-middle Eocene biomagnetochronology based on evidence from the Gorrondatxe section (Basque Country, Western Pyrenees). Lethaia 40, 183-195.

Pemberton, S.G., Frey, R.W., 1982. Trace fossil nomenclature and the *Planolites-Palaeophycus* dilemma. Journal of Palaeontology 56, 843-881.

Pemberton, S.G., Frey, R.W., Ranger, M.J., MacEachern, J., 1992. The conceptual framework of ichnology, in: Pemberton, S.G., (ed.), Applications of Ichnology to Petroleum Exploration. SEPM Core Workshop 17, Tulsa, USA, p. 1-32.

Pemberton, S.G., Zhou, Z., MacEachern, J., 2001. Modern ecological interpretation of opportunistic r-selected trace fossils and equilibrium K-selected trace fossils. Acta Palaeontologica Sinica 40, 134-142.

Peruzzi, D.G., 1880. Osservazioni sui generi *Paleodictyon* e *Paleomeandron* dei trreni cretacei ed eocenici dell' Appennino sett. E centrale. Atti della Società Toscana di Scienze Naturali Residente in Pisa 5, 3-8.

Pickerill, R.K., 1982. Glockerichnus, a new name for the trace fossil ichnogenus Glockeria Książkiewicz, 1968. Journal of Paleontology 56, 816.

Pickering, K.T., Corregidor, J., 2000. 3D reservoir scale study of Eocene confined submarine fans, South Central Spanish Pyrenees, in: (eds) Weimer. P., Slatt. R.M., Coleman. J., Rosen, N.C., Nelson, H., Bouma, A.H., Styzen, M.J., and Lawrence. D.T., Deep water reservoirs of the world: Gulf Coast Section. SEPM Foundation 20th Annual Bob F. Perkins Research Conference, p. 776-781.

Pickering, K.T. Corregidor, J., 2005. Mass-transport complexes (MTCs) and tectonic control on basin-floor submarine fans, Middle Eocene, South Central Spanish Pyrenees. Journal of Sedimentary Research 75, 761-783.

Phillips, C., McIllroy, D., Elliot, T., 2011. Ichnological characterization of Eocene/Oligocene turbidites from the Grès d'Annot Basin, French Alps, SE France. Palaeogeography, Palaeoclimatology, Palaeoecology 300, 67-83.

Plaziat, J.C., 1981. Late Cretaceous to Late Eocene paleogeographic evolution of southwest Europe. Palaeogeography, Palaeoclimatology, Palaeoecology 36, 263-320.

Prantl, F., 1945. Two new problematic trails from the Ordovician of Bohemia (in Czech, English summary). Akadémie Tchéque Sci. Bull. Intern. Cl. Sci. Math. Nat. Méd 46, 49-59.

Prélat, A., Hodgson, D.M., Flint, S.S., 2009. Evolution, architecture and hierarchy of distributary deep-water deposits: a high-resolution outcrop investigation from the Permian
Karoo Basin, South Africa. Sedimentology 56, 2132–2154. doi:10.1111/j.1365-3091.2009.01073.x

Pujalte, V., Bacetta, J.I., Dinares-Turell, J., Orue-Etxebarria, X., Pares, J.P., Payros, A., 1995. Biostratigraphic and magnetostratigraphic intercalibration of latest Cretaceous and Paleocene depositional sequences from the Basque Basin, western Pyrenees, Spain. Earth and Planetary Science Letters 136, 17-30.

Pujalte, V., Baceta, J.I., Orue-Etxebarria, X., Payros, A., 1998. Paleocene strata of the Basque Country, western Pyrenees, northern Spain, in: Graciansky, P.C., Hardenbol, J., Jacquin, T., Vail, P.R., (eds.), Mesozoic and Cenozoic Sequence Stratigraphy of European Basins: SEPM Special Publications 60, p. 311-325.

Pujalte, V., Robles, S., Orue-Etxebarria, X., Bacetta, J.I., Payros, A., Larruzea, I.F., 2000. Uppermost Cretaceous-middle Eocene strata of the Basque-Cantabrian region and Western Pyrenees: A sequence stratigraphic perspective: Revista Sociedad Geológica España, v. 13, p. 191-211.

Pujalte, V., Orue-Etxebarria, X., Schmitz, B., Tosquella, J., Baceta, J.I., Payros, A., Bernaola, G., Caballero, F., Apellaniz, E., 2003. Basal Ilerdian (earliest Eocene) turnover of larger foraminifera: Age constraints based on calcareous plankton and $\delta^{13}C$ isotopic profiles from new southern Pyrenean sections (Spain), in: Wing, S.L., Gingerich, P.D., Schmitz, B., Thomas, E., (Eds), Causes and Consequences of Globally Warm Climates in the Early Paleogene: The Geological Society of America, Special Paper 369.

Quatrefages, De M.A., 1849. Note sur la *Scolicia prisca* A. de Q. annélide fossile de la Craie. Annales des Sciences Naturelles, 3 série, Zoologie 12, 265-266.

Rieth, A., 1932. Neue Funde spongeliomorpher Fucoiden aus dem Jura Schwabens. Geologie Paläontologie Abhandlung 19, 257-294.

Robert, C., Chamley, H., 1991. Development of early Eocene warm climates, as inferred
from clay mineral variations in oceanic sediments. Palaeogeography, Palaeoclimatology, Palaeoecology 89, 315-331.

Robert, C., Kennett, J.P., 1994. Antarctic subtropical humid episode at the Paleocene Eocene boundary: Clay-mineral evidence. Geology 22, 211-214.

Rodríguez-Tovar, F.J., Uchman, A., 2004. Trace fossils after the K–T boundary event from the Agost section, SE Spain. Geological Magazine 141, 429-440.

Rodríguez-Tovar, F.J., Uchman, A., 2006. Ichnological analysis of the Cretaceous–Palaeogene boundary interval at the Caravaca section, SE Spain. Palaeogeography, Palaeoclimatology, Palaeoecology 242, 313–325.

Rodríguez-Tovar, F.J., Uchman, A., Alegret, L., Molina, E., 2011. Impact of the Paleocene–Eocene Thermal Maximum on the macrobenthic community: Ichnological record from the Zumaia section, northern Spain. Marine Geology 282, 178-187.

Rodríguez-Tovar, F.J., Uchman, A., Payros, A., Orue-Etxebarria, X., Apellaniz, E., Molina, E., 2010. Sea level dynamics and palaeoecological factors affecting trace fossil distribution in Eocene turbiditic deposits (Gorrondatxe section, N Spain). Palaeogeography, Palaeoclimatology, Palaeoecology 285, 50-65.

Roggenthen, W.M., 1976. Magnetic stratigraphy of the Paleocene. A comparision between Spain and Italy. Mem. Soc. Geol. Italia 15, 73-82.

Röhl, U., Westerhold, T., Monechi, S., Thomas, E., Zachos, J.C., Donner, B., 2005. The third and final Early Eocene thermal maximum: Characteristics, timing, and mechanisms of the "X" event: Geological Society of America Abstracts with Programs 37, p. 264.

Romein, A., 1979, Lineages in early Paleogene nannoplankton: Utrecht Micropal. Bull., 22, 18-22.

Rona, P.A., Seilacher, A., De Vargas, C., Gooday, A.J., Bernhard, J.M., Bowser, S., Vetriani, C., Wirsen, C.O., Mullineaux, L., Sherrell, R., Grassle, J.F., Low, S., Lutz, R.A., 2009, *Paleodictyon nodosum*: A living fossil on the deep-sea floor: Deep-Sea Research II, v. 56, p. 1700-1712.

Rosell, J., Remacha, E., Zamorano, M., Gabaldon, V., 1985. Estratigrafía de la Cuenca turbidítica de Guipúzcoa. Comparación con la Cuenca turbidítica prepirenaica central. Boletin Geológico y Minero 96, 471-482.

Ruffel, A., Worden, R., 2000. Palaeoclimate analysis using spectral gamma-ray data from the Aptian (Cretaceous) of southern England and southern France. Palaeogeography, Palaeoclimatology, Palaeoecology 155, 265–283.

Ruffel, A., McKinley, J.M., Worden, R.H., 2002. Comparison of clay mineral Stratigraphy to other proxy palaeoclimate indicators in the Mesozoic of NW Europe. Philosophical Transactions of the Royal Society London 360, 675-693.

Sacco, F., 1886. Impronte organiche dei terreni terziari del Piemonte. Atti Reale Accad. Sci. Torino 21, 297-348.

Sacco, F., 1888. Note di Paleoicnologia Italiana. Atti Soc. Ital. Sci. Nat. 31, 151-192.

Salter, J.W., 1857. On annellide burrows and surface markings from the Cambrian rocks of the Longmynd. No. 2. Quarterly Journal of the Geological Society of London 13, 199-206.

Saporta, G., 1887. Nouveaux documents relatifs aux organismes problematiques : Bulletin. Société Géologique de France, Serie 3. 15, 286-302.

Savi, P., and Meneghini, G.G., 1850. Osservazioni stratigrafische e paleontologische concernati la geologia della Toscana e dei paesi limitrofi. Appendix in: Memoria sulla struttura geologica delle Alpi, degli Apennini e dei Carpazi. R.I. Murchison Stemparia granucale, Firenze.

Schäfer, F.X., 1928. *Hormosiroidea florentina* n.g., n. sp., ein *Fuchs* aus der Kreide der Umbegung von Florenz. Paläontologishe Zeitscrift. 10, 212-215.

Schafhäutl, K.E. 1851. Geognostische Untersuchungen des südbayerischen Alpengebirges. Literarisch-artistische Anstalt, München, pp. 208.

Schmitz, B., Asaro, F., Molina, E., Monechi, S., von Salis, K., Speijer, R.P., 1997. High-resolution iridium, $\delta^{13}C$, $\delta^{18}0$, foraminifera and nannofossil profiles across the latest Paleocene benthic extinction event at Zumaya, Spain. Palaeogeography, Palaeoclimatology, Palaeoecology 133, 49-68.

Schmitz, B., Molina, E., Von Salis, K., 1998. The Zumaya section in Spain: a possible global stratotype section for the Selandian and Thanetian stages. Newsletters on Stratigraphy 36 35-42.

Schmitz, B., Peucker-Ehrenbrink, B., Heilmann-Clausen, C., Aberg, G., Asaro, F., Lee, C.T., 2004. Basaltic explosive volcanism, but no comet impact at the Paleocene-Eocene boundary: High resolution chemical and isotope records from Egypt, Spain and Denmark. Earth and Planetary Science Letters 225, 1–17.

Schmitz, B. Pujalte, V. 2003. Sea level, humidity, and lad erosion records across the initial Eocene thermal maximum from a continental-marine transect in northern Spain. Geology 31, 689-692.

Schmitz, B., Pujalte, V., 2007. Abrupt increase in seasonal extreme precipitation at the Paleocene-Eocene boundary. Geology 35, 215-218.

Schmitz, B., Pujalte, V., Núñez-Betelu, K, 2001. Climate and sea-level perturbations during the Initial Eocene Thermal Maximum: evidence from siliciclastic units in the Basque Basin (Ermua, Zumaia and Trabakua Pass), northern Spain. Palaeogeography, Palaeoclimatology, Palaeoecology 165, 299–320.

Seilacher, A., 1964. Sedimentological classification and nomenclature of trace fossils. Sedimentology 3, 253-256.

Seilacher, A. 1967. Bathymetry of trace fossils. Marine Geology 5, 413-428.

Seilacher, A., 1974. Flysch trace fossils: evaluation of behavioural diversity in the deep sea. Neues Jarbruch für Geologie und Paläontologie Monatshefte 4, 233-245.

Seilacher, A., 1977a. Evolution of trace fossil communities in the deep sea, in: Hallam, A. (ed.), Patterns of Evolution: Elsevier, Amsterdam, p. 359-376.

Seilacher, A., 1977b, Pattern analysis of *Paleodictyon* and related trace fossils, in: Crimes, T.P., Harper, J.C., (eds)., Trace Fossils 2: Geological Journal Special Publication 9, p. 289-334.

Seilacher, A., 1990. Aberrations in bivalve evolution related to photo- and chemosymbiosis . Historical Biology 3, 289-311.

Simpson, S., 1957. On the trace fossil *Chondrites*. Quarterly Journal of the Geological Society of London 112, 475-499.

Smith, A.B. Crimes, T.P. 1983. Trace fossils formed by heart urchins – a study of *Scolicia* and related traces. Lethaia 16, 79-92.

Smith, A.B., Gallemi, J., Jeffery, C.H., Ernst, G., Ward, P.D., 1999. Late Cretaceous-early Tertiary ecinoids from northern Spain: implications for the Cretaceous-Tertiary extinction event. Bulletin of the Natural History Museum London 55, 81-137.

Smith, A.B., Jeffery, C.H., 1998. Selectivity of extinction amongst sea urchins at the end of the Cretaceous period. Nature 392, 69-71.

Smith, A.G., Smith, D.G., Funnel, B.M., 1994. Atlas of Mesozoic and Cenozoic coastlines: Cambridge University Press, UK, p. 31-32.

Speijer, R.P., Morsi, A.M.M., 2002. Ostracod turnover and sea level changes associated with the Paleocene Eocene thermal maximum. Geology 30, 23-26.
Svarda, C.E., 2007. Taphonomy of trace fossils, in: Miller III, W ., (ed.), Trace Fossils: Concepts, Problems, Prospects. Elsevier, Amsterdam, The Netherlands, p. 92-107.

Speijer, R.P., Wagner, T., 2002. Sea-level changes and black shales associated with the late Paleocene thermal maximum (LPTM): Organic geochemical and micropaleontologic evidence from the southern Tethyan margin (Egypt-Israel), in (eds) Koeberl, C., and MacLeod, K., Catastrophic events and mass extinctions: Impacts and beyond. Geological Society of America Special Paper 356, p. 533–550.

Squinabol, S., 1890. Alghae und Pseudoalghae fossili ilatiane. Atti. Soc. Ling. Sci. Nat. Geogr. 1, 29-49 166-199.

Sternberg, G.K., 1833. Versuch einer geognostisch, botanischen Darstellung der Flora der Vorvwelt. IV Heft. Brenck, C.E. Regensburg. pp. 48.

Stoll, H. M., Shimizu, N., Archer, D., Ziveri, P., 2007. Coccolithophore productivity response to greenhouse event of the Paleocene-Eocene Thermal Maximum. Earth and Planetary Science Letters, 258, 192–206.

Svensen, H., Planke, S., Corfu, F., 2010. Zircon dating ties NE Atlantic sill emplacement to initial Eocene global warming: Journal of the Geological Society of London 167, 433-436.

Svensen, H., Planke, S., Malthe-Sorenssen, A., Jamtveit, B., Myklebust, R., Rasmussen-Eidem, T., and Rey, S.S., 2004, Release of methane from a volcanic basin as a mechanism for initial Eocene global warming: Nature 429, 542–545.

Taylor, A.M., Goldring, R., 1993. Description and analysis of bioturbation and ichnofabric. Journal of the Geological Society of London 150, 141-148.

Taylor, A.M., Goldring, R., Gowland, S., 2003. Analysis and application of ichnofabrics. Earth-Science Reviews 60, 227-25.

Tchoumatchenco, P., Uchman, A., 2001. The oldest deep sea *Ophiomorpha* and *Scolicia* and associated trace fossils from the Upper Jurassic-Lower Cretaceous deep-water turbidite deposits of SW Bulgaria. Palaeogeography, Palaeoclimatology, Palaeoecology 169, 85-99.

Ten Kate, W.G., Sprenger, A., 1993. Orbital cyclicities above and below the Cretaceous/Paleogene boundary at Zumaya (N Spain), Agost and Relleu (SE Spain). Sedimentary Geology 87, 69-101.

Thiry, M. 2000. Palaeoclimatic interpretation of clay minerals in marine deposits: an outlook from the continental origin. Earth Science Reviews 49, 201–222.

Thomas, E., 1989. Development of Cenozoic deep-sea benthic foraminiferal faunas in Antarctic waters: Geological Society [London] Special Publication 47, 283-296.

Thomas, E., 1990b, Late Cretaceous–early Eocene mass extinctions in the deep sea, in (eds) Sharpton, V.L., and Ward, P.D., Global catastrophes in earth history. Geological Society of America Special Publication 247, p. 481–495.

Thomas, E., 1998, The biogeography of the late Paleocene benthic foraminiferal extinction, in (eds) Aubry, M.P, Lucas, S.G., and Berggren, W.A., Late Paleocene-early Eocene biotic and climatic events in the marine and terrestrial records: New York, Columbia University Press, p. 214–243.

Thomas, E., 2007. Cenozoic mass extinctions in the deep sea: What perturbs the largest habitat on Earth? The Geological Society of America Special Paper 424, 1-23.

Thomas, E., Zachos, J.C., 2000, Was the late Paleocene thermal maximum a unique event?: GFF 122, p. 169–170.

Thomas, E., Zachos, J.C., Bralower, T.J., 2000, Deep-sea environments on a warm Earth: Latest Paleocene–early Eocene, in: Huber, B.T, MacLeod, K.G., and Wing, S.L., (eds)., Warm climates in earth history: Cambridge, UK, Cambridge University Press, p. 132–160.

Thomas, E., Brinkhuis, H., Huber, M., and Röhl, U., 2006, An ocean view of the early Cenozoic Greenhouse World. Oceanography (Special Volume on Ocean Drilling), 19, 63-72.

Torfstein, A., Winckler, G., Tripati, A., 2009. Productivity feedback did not terminate did not terminate the Paleocene-Eocene Thermal Maximum (PETM). Climate of the Past Discussions 5, 2391-2410.

Torell, O.M., 1870. Petrifacta Suecana Formationis Cambricae. Lunds University. 6, 1-14.

Tremolada, F., Bralower, T.J., 2004. Nannofossil assemblage fluctuations during the Paleocene-Eocene Thermal Maximum at Sites 213 (Indian Ocean) and 401(North Atlantic Ocean): Palaeoceanographic implications. Marine Micropaleontology 52, 107–116,

Tripati, A., and Elderfield, H., 2004, Abrupt hydrographic changes in the equatorial Pacific and subtropical Atlantic from foraminiferal Mg/Ca indicate greenhouse origin for the thermal maximum at the Paleocene/Eocene boundary: Geochemistry, Geophysics, Geosystems 5.

Tripati, A., Elderfield, H., 2005. Deep-sea temperature and circulation changes at the Paleocene-Eocene Thermal Maximum: Science 308, 1894-1898.

Tunis, G., Uchman, A., 1996a. Trace fossils and changes in Cretaceous-Eocene flysch deposits of the Julian Prealps Italy and Slovenia: consequences of regional and world-wide changes. Ichnos 4, 169-190.

Tunis, G., Uchman, A., 1996b. Ichnology of Eocene flysch deposits of the Istria Peninsula, Croatia and Slovenia. Ichnos 5, 1-22.

Tunis, G., Uchman, A., 1998. Ichnology of Eocene flysch deposits in the Carnian pre-Alps (north-eastern Italy). Gortania 20, 41-58.

Uchman, A. 1992. An opportunistic trace fossil assemblage from the flysch of the Inoceramian beds (Campanian-Palaeocene), Bystrica Zone of the Magura Nappe, Carpathians, Poland. Cretaceous Research 13, 539-547.

Uchman, A., 1995. Taxonomy and palaeocology of flysch trace fossils: The Marnoso-arenacea Formation and associated facies, Miocene, Northern Apennines, Italy. Beringeria 15, 3-115.

Uchman, A., 1998. Taxonomy and ethology of flysch trace fossils: A revision of the Marian Książkiewicz collection and studies of complementary materials. Annales Societatis Geologorum Poloniae 68, 105-218.

Uchman, A., 1999. Ichnology of the Rhenodanubian Flysch Lower Cretaceous-Eocene in Austria and Germany. Beringeria 25, 67-173.

Uchman, A., 2001. Eocene flysch trace fossils from the Hecho Group of the Pyrenees, northern Spain. Beringeria 28, 3-41.

Uchman, A., 2003. Trends in diversity, frequency and complexity of graphoglyptid trace fossils: evolutionary and palaeoenvironmental aspects. Palaeogeography, Palaeoclimatology, Palaeoecology 192, 123-142.

Uchman, A., 2004. Phanerozoic history of deep sea trace fossils, in: McIlroy, D., (ed.), The Application of Ichnology to Palaeoenvironmental and Stratigraphical Analysis. Geological Society (London) Special Publication 228, p. 125-139.

Uchman, A., 2007a. Deep sea trace fossils from mixed carbonate-siliciclastic flysch of the Monte Antola formation (Late Campanian-Maastrichtian), North Apennines, Italy. Cretaceous Research 28, 980-1004.

Uchman, A., 2007b. Trace fossils of the Pagliaro formation (Paleocene) in the North Appenines, Italy. Beringeria 37, 217-237.

Uchman, A., 2007c. Deep-Sea Ichnology: Development of Major Concepts, in (Ed), Miller III, W., Trace Fossils: Concepts, Problems, Prospects, Elsevier, Oxford, UK, p. 248-268.

Uchman, A., 2009. The *Ophiomorpha rudis* ichnosubfacies of the *Nereites* ichnofacies: Characteristics and constraints. Palaeogeography, Palaeoclimatology, Palaeoecology 276, 107-119.

Uchman, A., 2010. A new ichnogenus *Skolichnus* for *Chondrites hoernesii* Ettingshausen, 1863, a deep-sea radial trace fossil from the Upper Cretaceous of the Polish Flysch Carpathians: Its taxonomy and palaeoecological interpretation as a deep-tier chemichnion. Cretaceous Research 31, 515-523.

Uchman, A., and Demircan, H., 1999. Trace fossils of Miocene deep-sea fan fringe deposits from the Cingöz Formation, southern Turkey. Annales Societatis Geologorum Poloniae 69, 125-153.

Uchman, A. and Wetzel, A., 2011, Deep-Sea ichnology: the relationships between depositional environment and endobenthic organisms, in: Hüneke, H. and Mulder, T. (eds.), Developments in Sedimentology: Deep-Sea Sediments,Elsevier,63,517-556.

Van Vliet, A., 1978. Early Tertiary deepwater fan deposits of Guipuzcoa, Northern Spain, in: Stanley, J.S., Kelling, G., (eds.), Sedimentation in Submarine Canyons, Fans, and Trenches: Dowden, Hutchinson and Ross, Pennsylvania, USA, p. 190-209.

Van Vliet, A., 2007. Submarine Fans and Associated Sediments of the Tertiary Coastal Range of Guipúzcoa, Spain, in: Nilsen, T.H., Shew, R.D., Steffens, G.S., Studlick, J.R.J., (eds.), Atlas of Deep-Water Outcrops. AAPG Studies in Geology 56 (and Shell International Exploration and Production), p. 341-347.

Verges, J., Millan, H., Roca, E., Munoz, J.A., Marzo, M., Cires, J., Bezerner, T.D., Zoetemeijer, R., Cloetingh, S., 1995. Eastern Pyrenees and related foreland basins: Pre-, syn-, and post collisional crustal scale cross-sections. Marine and Petroleum Geology 12, 893-915.

Vialov, O.S., 1962. Problematica of the Beacon Sandstone at Beacon Height, West Antarctica. New Zealand Journal of Geology and Geography 5, 718-732.

Vialov, O.S., 1971. The rare Mesozoic problematica from Pamir and Caucasus. Paleontologica Sbornik. 7, 85-93.

Vialov, O.S., Golev, B.T., 1965. O drobnom podrazdieleni gruppy Paleodictyonidae. Byulletin Moskovskovo Obshczhestva Ispityvania Prirody, Odtiel Gieologii 40, 93-114.

Von Hillebrandt, A., 1962, Das Palaeozaen und seine Foraminiferenfauna im Becken von Reichenhall und Salzburg: Bayerische Akademie der Wissenschaften, Mathematisch-Naturwissenschaftliche Klasse, Abhandlungen. Neue Folge, 108 -182

Von Hillebrandt, A., 1965. Foraminiferen-Stratigraphie im Alttertiär von Zumaya (Prov. Guipuzcoa, NW Spanien) und ein Vergleich mit anderen Tethys-Gebieten. Abh. Königl. Bayer. Akad. Wissench. München 123, 1-63.

Ward, D.M. Lewis, D.W. 1975. Paleoenvironmental implications of storm scoured ichnofossiliferous mid-Tertiary limestones, Waihao District, South Canterbury, New Zealand. New Zealand Journal of Geology and Geophysics 18, 881-908.

Ward, P., Kennedy, K.G., 1993. Maastrichtian ammonites from the Biscay region (France, Spain). Jour. Paleontology 67, 1-58.

Ward, P., Kennedy, K.G., McLeod, K.G., Mount, J., 1991. End-Cretaceous molluscan extinction patterns in the Bay of Biscay K/T boundary sections: two different patterns. Geology 19, 14-81.

Wetzel, A., 1991. Ecologic interpretation of deep-sea trace fossil communities. Palaeogeogaphy Palaeoclimatology Palaeoecology 85, 47-69.

Wetzel, A., 2000. Giant *Paleodictyon* in Eocene Flysch: Palaeogeography, Palaeoclimatology, Palaeoecology 160, 171-178.

Wetzel, A., 2008. Recent bioturbation in the deep south china sea: a uniformitarian ichnologic approach. PALAIOS 23, 601-615.

Wetzel, A., Bromley, R.G., 1996. Re-evaluation of ichnogenus *Helminthopsis* Heer 1877 – a new look at the type material. Palaeontology 39, 1-19.

Wetzel, A., Uchman, A., 1998. Deep-sea benthic food content recorded by ichnofabrics: A conceptual model based on observations from Paleogene Flysch, Carpathians, Poland. Palaios 13, 533-546.

Wetzel, A., Uchman, A., 2001. Sequential colonization of muddy turbidites in the Eocene Beloveza Formation, Carpathians, Poland: Palaeogeography, Palaeoclimatology, Palaeoecology 168, 171-186.

Wetzel, A., Blechschmidt, I., Uchman, A., Matter, A., 2007. A highly diverse ichnofauna in Late Triassic deep-sea fan deposits of Oman. Palaios 22, 567-576.

Wiedmann, J., 1988. The Basque coastal sections of the K/T boundary: a key to understanding "mass extinction" in the fossil record, in: (eds) Lamolda, M.A., Kauffman, E.C., Walliser, O., Paleontology and evolution: Extinction events. Rev. Esp. Paleontología, p. 127-140.

Wing, S.L., Harrington, G.J., Bowen, G.J., Koch, P.L., 2003. Floral change during the initial Eocene Thermal Maximum in the Powder River Basin, Wyoming, in: Wing, S.L., Gingerich, P.D., Schmitz, B., Thomas, E., (Eds), Causes and Consequences of Globally Warm Climates in the Early Paleogene: The Geological Society of America, Special Paper 369.

Wing, S.L., Harrington, G.J., Smith, F.A., Bloch, J.I., Boyer, D.M., Freeman, K.H., 2005. Transient floral change and rapid global warming at the Paleocene-Eocene boundary. Science 310, 993-996.

Winkler, W., Gawenda, P., 1999. Distinguishing climatic and tectonic forcing of turbidite sedimentation, and the bearing on turbidite bed scaling: Paleocene-Eocene of northern Spain. Journal of the Geological Society London 156, 791-800.

Zachos, J., Pagani, M., Sloan, L., Thomas, E., Billups, K., 2001. Trends, rhythms and aberrations in global climate; 65Ma to present. Science 292, 686-693.

Zachos, J.C., Röhl, U., Schellenberg, S.A., Sluijs, A., Hodell, D.A., Kelly, D.C., Thomas, E., Nicolo, M., Raffi, I., Lourens, L.J., Mccarren, H., Kroon, D., 2005. Rapid acidification of the ocean during the Paleocene-Eocene Thermal Maximum. Science 308, 1611-1615.

Zachos, J.C., Wara, M.W., Bohaty, S., Delaney, M.L., Petrizzo, M.R., Brill, A., Bralower, T.J., Premoli-Silva, I., 2003, A transient rise in tropical sea surface temperature during the Paleocene-Eocene Thermal Maximum. Science, 302, 1551–1554.

Zenker, J.C., 1836. Historich-topoghrafisches Taschenbuch von Jena und seiner Umgebung besonders in seiner naturewissen-schaftlicher und medicinischer Beziehung. pp. 338.

Zuber, R., 1910. Eine fossile Meduse aus dem Kreideflysch der ostgalizischen Karpathen. Verh. Geol. Reichsanst 1910, 57.

Appendix 1

Taxonomy table listing discussed specimens, the corresponding plate number (see appendix 2), type specimen (holotype) reference, and their morphological groupings

Taxa	Plate (appendix 2)	Type specimen reference	Morphological group (after Uchman 1998)	Ethology
Acanthorhaphe		**Książkiewicz 1970**	**BWM**	**agrichnia**
Acanthorhaphe delicatula	4	Książkiewicz 1977		agrichnia
Acanthorhaphe incerta	4	Książkiewicz 1970		agrichnia
Arenicolites		**Salter 1857**	**Simple and branched**	**Domichnia**
Arenicolites isp.	1	-		Domichnia/fodinichnia
Arthrophycus		**Hall 1852**	**Simple and branched**	**Fodinichnia**
Arthrophycus strictus	1	Książkiewicz 1977		Fodinichnia
Arthrophycus tenuis	1	Książkiewicz 1977		Fodinichnia
Beaconites		**Vialov 1962**	**Simple and branched**	**Fodinichnia**
cf. *Beaconites capronus*	2	Howard and Frey 1984		Fodinichnia
Belocosmorhaphe		**Uchman 1998**	**BWM**	**agrichnia**
Belocosmorhaphe aculeata	3	Uchman 1998		agrichnia
Belorhaphe		**Fuchs 1895**	**BWM**	**agrichnia**
Belorhaphe zickzack	4	Heer 1877		agrichnia
Bergaueria		**Pranti 1945**	**Circular and elliptical**	**Cubichnia**
Bergaueria pranti	2	Książkiewicz 1977		Cubichnia
Chondrohaphe		**Seilacher 1977**	**Radial**	**agrichnia**
?*Chondrohaphe* isp.	3	-		agrichnia
Cardiolchnus		**Smith and Crimes 1983**	**Circular and elliptical**	**Cubichnia**
Cardiolchnus planus	2	Smith and Crimes 1983		Cubichnia
Chondrites		**Sternberg 1833**	**Simple and branched**	**Chemichnia**
Chondrites intricatus	3	Brongniart 1823		Chemichnia
Chondrites targionni	3	Brongniart 1828		Chemichnia
Cosmorhaphe		**Fuchs 1895**	**Winding and meandering**	**agrichnia**
Cosmorhaphe lobata	3	Fuchs 1895		agrichnia
Desmograpton		**Fuchs 1895**	**BWM**	**agrichnia**
Desmograpton alternum	5	Książkiewicz 1977		agrichnia
Desmograpton dertonensis	5	Sacco 1888		agrichnia
Fascichnium		**Książkiewicz 1968**	**Radial**	**Pascichnia**
Fascichnium extentum	5	Książkiewicz 1968		Pascichnia
Glockerichnus		**Pickerill 1982**	**Radial**	**agrichnia**
Glockerichnus alata	5	Seilacher 1977b		agrichnia
Glockerichnus glockeri	5	Książkiewicz 1968		agrichnia
Gordia		**Emmons 1844**	**Winding and meandering**	**Pascichnia**
Gordia marina	5	Emmons 1844		Pascichnia
Halopoe		**Torell 1870**	**Simple and branched**	**Pascichnia**
Halopoe annulata	6	Książkiewicz 1977		Pascichnia
Halopoe imbricata	6	Torell 1870		Pascichnia
Helminthopsis		**Heer 1877**	**Winding and meandering**	**Pascichnia**
Helminthopsis abeli	6	Książkiewicz 1977		Pascichnia
Helminthopsis granulata	6	Książkiewicz 1968		Pascichnia
Helminthopsis tenuis	6	Książkiewicz 1968		Pascichnia
Helminthopsis hyroglyphica	6	Wetzel and Bromley 1996		Pascichnia
Helminthorhaphe		**Seilacher 1977**	**Winding and meandering**	**agrichnia**
Helminthorhaphe flexuosa	5	Uchman 1995		agrichnia
Helminthorhaphe miocenica	5	Uchman 1995		agrichnia
Hormosiroidea		**Schaffer 1928**	**Simple and branched**	**Calichnia**
Hormosiroidea annulata	5	Vialov 1971		Calichnia
Lorenzinia		**Gabelli 1900**	**Radial**	**agrichnia**
Lorenzinia carpathica	4	Zuber 1910		agrichnia
Lorenzinia plana	4	Książkiewicz 1968		agrichnia
Mammillichnus		**Chamberlain 1971**	**Circular and elliptical**	**?Cubichnia**
Mammillichnus aggeris	2	Chamberlain 1971		**?Cubichnia**
Megagrapton		**Książkiewicz 1968**	**Networks**	**agrichnia**
Megagrapton irregulare	3	Książkiewicz 1968		agrichnia
Megagrapton submontanum	3	Azpeitia Moros 1933		agrichnia
Nereites		**Macleay 1839**	**Winding and meandering**	**Pascichnia**
Nereites irregularis	3	Schaufhäutl 1851		Pascichnia
Ophiomorpha		**Lundgren 1891**	**Simple and branched**	**Domichnia**
Ophiomorpha annulata	1	Książkiewicz 1977		Domichnia/pascichnia
Ophiomorpha nodis	1	Książkiewicz 1977		Domichnia/?agrichnia
Ophiomorpha recta	1	Fischer-Ooster 1858		Domichnia
Oscillorhaphe		**Seilacher 1977b**	**BWM**	**agrichnia**
Oscillorhaphe venzelaelana	4	Seilacher 1977b		agrichnia
Paleodictyon		**Meneghini 1850**	**Networks**	**agrichnia**
Paleodictyon gomezi	6	Azpeitia Moros 1933		agrichnia
Paleodictyon latum	6	Vialov and Golev 1965		agrichnia
Paleodictyon majus	6	Meneghini 1850		agrichnia
Paleodictyon minimum	6	Sacco 1888		agrichnia
Paleodictyon miocenicum	6	Sacco 1886		agrichnia
Paleodictyon strozzi	6	Meneghini 1850		agrichnia
Paleomeandron		**Peruzzi 1880**	**BWM**	**agrichnia**
Paleomeandron elegans	4	Peruzzi 1880		agrichnia
Paleomeandron robustum	4	Książkiewicz 1968		agrichnia
Paleophycus		**Hall 1847**	**Simple and branched**	**Domichnia/?Praedichnia**
Paleophycus tubularis	1	Hall 1847		**Domichnia/?Praedichnia**
Planolites		**Nicholson 1873**	**Simple and branched**	**Fodinichnia/Pascichnia**
Planolites beverleyensis	1	Billings 1862		Fodinichnia/Pascichnia
Phycosiphon		**Fischer-Ooster 1858**	**Spreiten**	**Pascichnia**
Phycosiphon incertum	2	Fischer-Ooster 1858		Pascichnia
Protovirgularia		**McCoy 1850**	**Winding and meandering**	**Pascichnia**
Protovirgularia obliterata	5	Książkiewicz 1977		Pascichnia
Protopaleodictyon		**Książkiewicz 1958**	**BWM**	**agrichnia**
Protopaleodictyon incompositum	4	Książkiewicz 1958		agrichnia
Rhizocorallium		**Zenker 1836**	**Spreiten**	**Fodinichnia**
Rhizocorallium jenense	2	Zenker 1836		Fodinichnia
Saerichnites		**Billings 1866**	**Simple and branched**	**?Domichnia**
Saerichnites isp.	5	-		?Domichnia
Saerichnites canadensis	5	Crimes and Anderson 1985		?Domichnia/?agrichnia
Scalicia		**de Quatrefages 1849**	**Winding and meandering**	**Pascichnia**
Scalicia plana	2	Książkiewicz 1970		Pascichnia
Scalicia prisca	2	de Quatrefages 1849		Pascichnia
Scalicia strozzi	2	Savi and Meneghini 1850		Pascichnia
Scalicia vertabralis	2	Książkiewicz 1977		Pascichnia
Skolithos		**Haldeman 1840**	**Simple and branched**	**Domichnia**
?*Skolithos* isp.	2	-		Domichnia
Spirorhaphe		**Fuchs 1895**	**Spiral**	**agrichnia**
Spirorhaphe involuta	3	De Stefani 1895		agrichnia
Spirophycus		**Heer 1877**	**Spiral**	**Fodinichnia**
Spirophycus bicornis	4	Heer 1877		Fodinichnia
Spirophycus involitimus	4	Sacco 1888		Fodinichnia
Spongeliomorpha		**de Saporta 1887**	**Simple and branched**	**Fodinichnia**
Spongeliomorpha cravierense	1	Książkiewicz 1977		Fodinichnia
Spongeliomorpha slumbricoides	1	Azpeitia Moros 1933		Fodinichnia
Strobilorhaphe		**Książkiewicz 1968**	**Simple and branched**	**Pasichnia/fodinichnia**
Strobilorhaphe clavatus	6	Książkiewicz 1968		Pasichnia/fodinichnia
Strobilorhaphe glandifer	6	Książkiewicz 1977		Fodinichnia/?calichnia
Taenidium		**Heer 1877**	**Winding and meandering**	**Pascichnia**
Taenidium isp.	2	-		Pascichnia
Thalassinoides		**Ehrenberg 1944**	**Simple and branched**	**Fodinichnia**
Thalassinoides suevicus	1	Rieth 1932		Fodinichnia
Trichichnus		**Frey 1970**	**Simple and branched**	**Chemichnia**
Trichichnus linearis	2	Frey 1970		Chemichnia
Urohelminthoida		**Sacco 1888**	**BWM**	**agrichnia**
Urohelminthoida dertonensis	4	Sacco 1888		agrichnia
Zoophycos		**Massalongo 1855**	**Spreiten**	**Fodinichnia**
Zoophycos brianteus	3	Massalongo 1855		Fodinichnia
Zoophycos insignis	3	Squinabol 1890		Fodinichnia

Note BWM= branched, winding and meandering

APPENDIX 2

PLATES

Captions:

Plate 1: A. *Ophiomorpha recta* hypichnial full-relief. B. & C. *Ophiomorpha annulata* hypichnial/exichnial full-relief. D. *Ophiomorpha rudis (Or)* and *Spongeliomorpha slumbricoides (Sp)* exichnial full-relief. E. *Ophiomorpha rudis* hypichnial and exichnial full-reliefs. F. *Spongeliomorpha oraviense* hypichnial full-relief. G. *Thalassinoides suevicus* epichnial full-relief. H. *Arenicolites* isp. endichnial full-relief. I. *Planolites beverleyensis* epichnial full-relief. J. *Arthrophycus strictus* epichnial full-relief. K. *Arthrophycus tenuis* hypichnial full-relief. L. *Paleophycus tubularis (Pa)* and *Thalassinoides* isp. *(Th)* hypichnial full-reliefs.

Plate 2: A. *Mammillichnis aggeris* hypichnial mound (semi-relief). B. *Bergaueria prantli* hypichnial mound (semi-relief). C. *Rhizocorralium irregulare* endichnial full-relief. D. *Scolicia plana* hypichnial full-relief. E. *Scolicia strozzi* hypichnial semi-relief. F. *Scolicia prisca* epichnial full-relief. G. *Scolicia vertebralis* epichnial full-relief. H. *Cardioichnus planus* hypichnial semi-relief. I. *Skolithos* isp. *(Sk)* Endichnial full-relief. Note; may potentially be paired vertical burrows (i.e. *Arenicolites, Ar*) but too densely packed to fully discern. J. *Taenidium* isp. Epichnial full-relief (may possibly be preservational variant of *Scolicia* isp.). K. *Beaconites capronus (Bc)* and *Phycosiphon incertum (Ph)* epichnial full-reliefs. L. *Trichichnus linearis* endichnial full-relief.

Plate 3: A. *Zoophycos brianteus* endichnial full-relief. B. *Zoophycos insignis* endichnial full-relief. C. *Zoophycos ?insignis, Spirophyton* type endichnial full-relief. D. *Nereites irregularis* epichnial full-relief. E. *Chondrites targionii* epichnial full-relief (geological hammer for scale). F. *Chondrites intricatus* epichnial full-relief. G. *Cosmorhaphe lobata* hypichnial semi-relief. H. *Spirohaphe involuta (Sr)* hypichnial semi-relief cross cut by *Ophiomorpha annulata (Oa)* hypichnial full-relief. I. *?Chondrohaphe* isp. hypichnial full-relief. J. *Belocosmorhaphe aculeata* hypichnial semi-relief. Note; specimen is less meandering than typical *Belocosmorhaphe* (see Uchman, 1998 for discussion and taxonomy) so may potentially be a form of *Belorhaphe* isp. K. *Megagrapton submontanum* hypichnial semi-relief. L. *Megagrapton irregulare* hypichnial semi-relief.

Plate 4: A. *Protopaleodictyon incompositum* hypichnial full-relief. B. *Spirophycus involutissimus* hypichnial semi-relief. Upper specimen (arrowed) seems to be gradational with *Helminthopsis*. C. *Spirophycus bicornis* hypichnial semi-relief. D. *Lorenzinia carpathica* hypichnial semi-relief. E. *Lorenzinia plana* hypichnial semi-relief. F. *Belorhaphe zickzack* hypichnial semi-relief. G. *Paleomeandron elegans* hypichnial semi-relief. H. *Paleomeandron robustum* hypichnial full-relief. I. *Oscillorhaphe venezoelana* hypichnial semi-relief. J. *Urohelminthoida dertonensis* hypichnial semi-relief. K. *Acanthorhaphe delicatula* hypichnial semi-relief. L. *Acanthorhaphe incerta* hypichnial semi-relief.

Plate 5: A. *Desmograpton dertonensis* hypichnial semi-relief. B. *Desmograpton alternum* hypichnial semi-relief. C. *Glockerichnus alata* hypichnial semi-relief. D. *Glockerichnus glockeri* hypichnial semi-relief. E. *Helminthorhaphe flexuosa* hypichnial semi-relief. F. *Helminthorhaphe miocenica* hypichnial semi-relief. G. *Hormosiroidea annulata* hypichnial full-relief. H. *Gordia marina* epichnial full-relief. I. *Fascichnium extentum* hypichnial semi-relief. J. *Saerichnites canadensis* hypichnial full-relief. K. *Saerichnites* isp. hypichnial semi-relief. L. *Protovirgularia obliterata* hypichnial full-relief.

Plate 6: A.) *Halopoa annulata* hypichnial full-relief. B & C.) *Halopoa imbricata* hypichnial full-relief. D.) *Strobilorhaphe clavatus* hypichnial full-relief. E.) *Strobilorhaphe glandifer* hypichnial full-relief. F.) *Helminthopsis hieroglyphica* hypichnial semi-relief. G.) *Helminthopsis tenuis* hypichnial semi-relief. H.) *Helminthopsis abeli* hypichnial semi-relief. I.) *Helminthopsis granulata (He)* hypichnial semi-relief and *Ophiomorpha annulata (Oa)* hypichnial full-relief. J.) *Paleodictyon latum* hypichnial semi-relief. K.) *Paleodictyon majus* hypichnial semi-relief. L.) *Paleodictyon minimum* hypichnial semi-relief. M.) *Paleodictyon miocenicum* hypichnial semi-relief. N.) *Paleodictyon strozzi* hypichnial semi-relief. O.) *Paleodictyon gomezi* (very large partially preserved specimen) hypichnial semi-relief. Note; see Uchman, 1995 for taxonomical discussion of *Paleodictyon*.

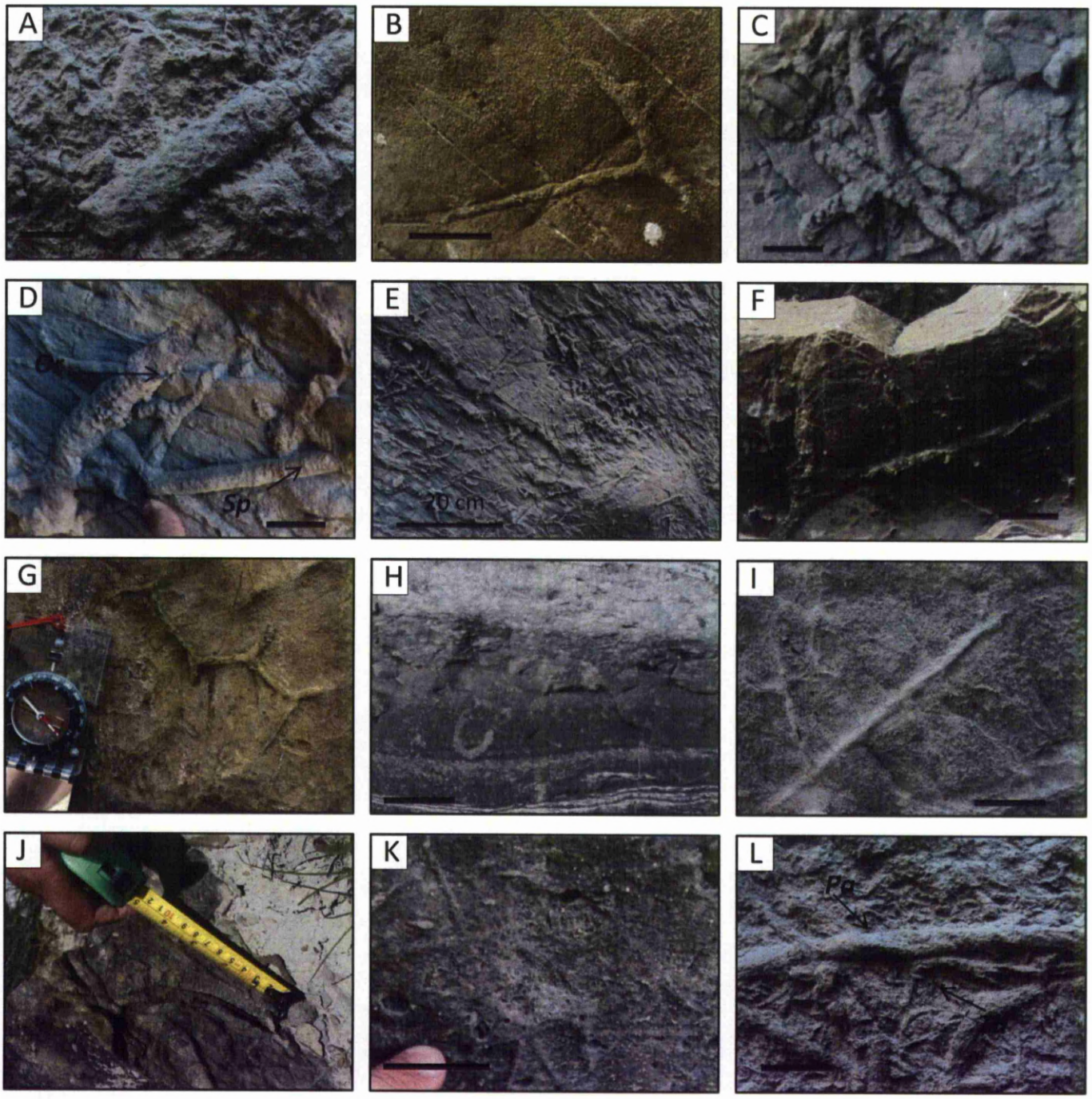

Plate 1

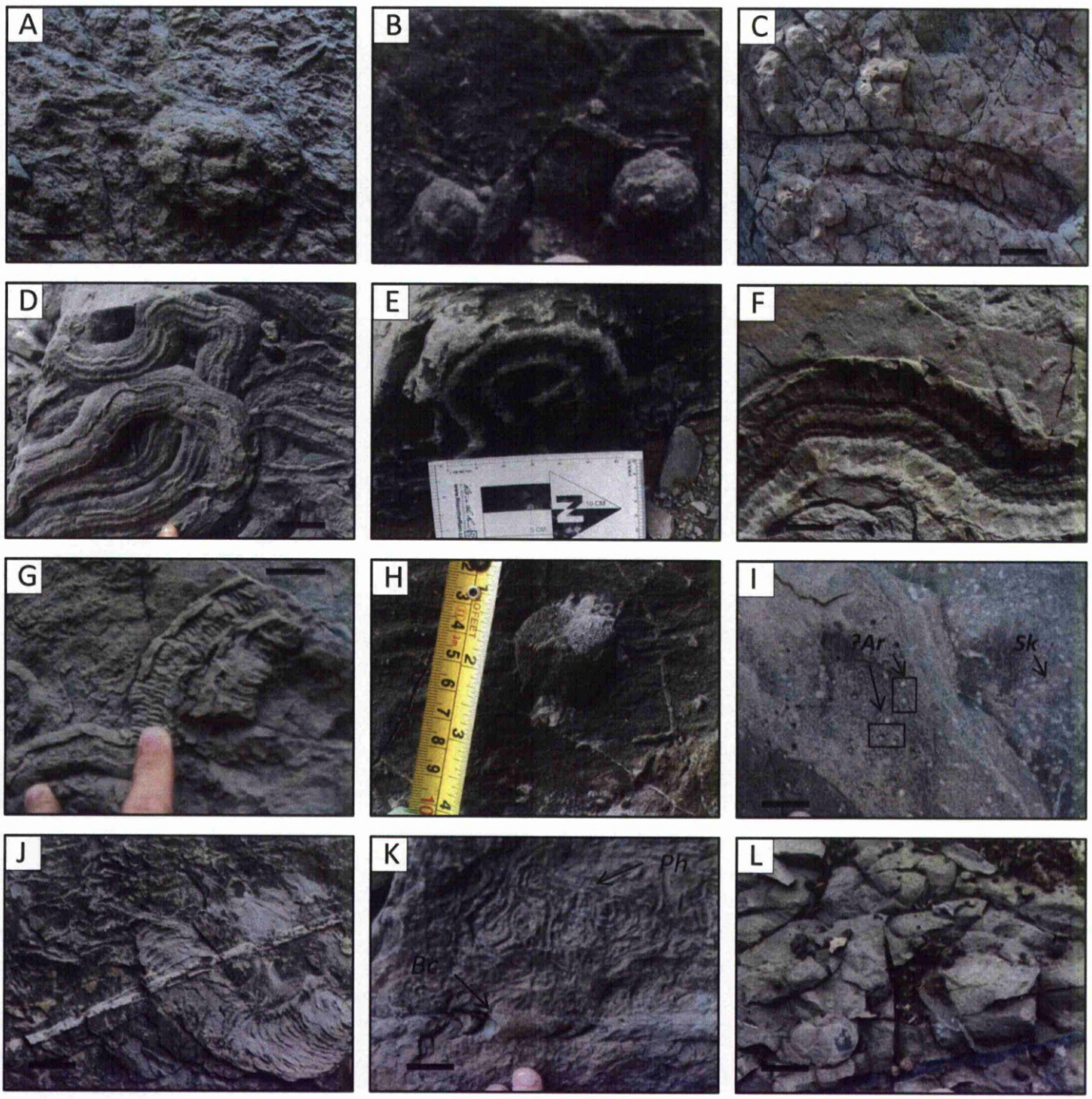

Plate 2

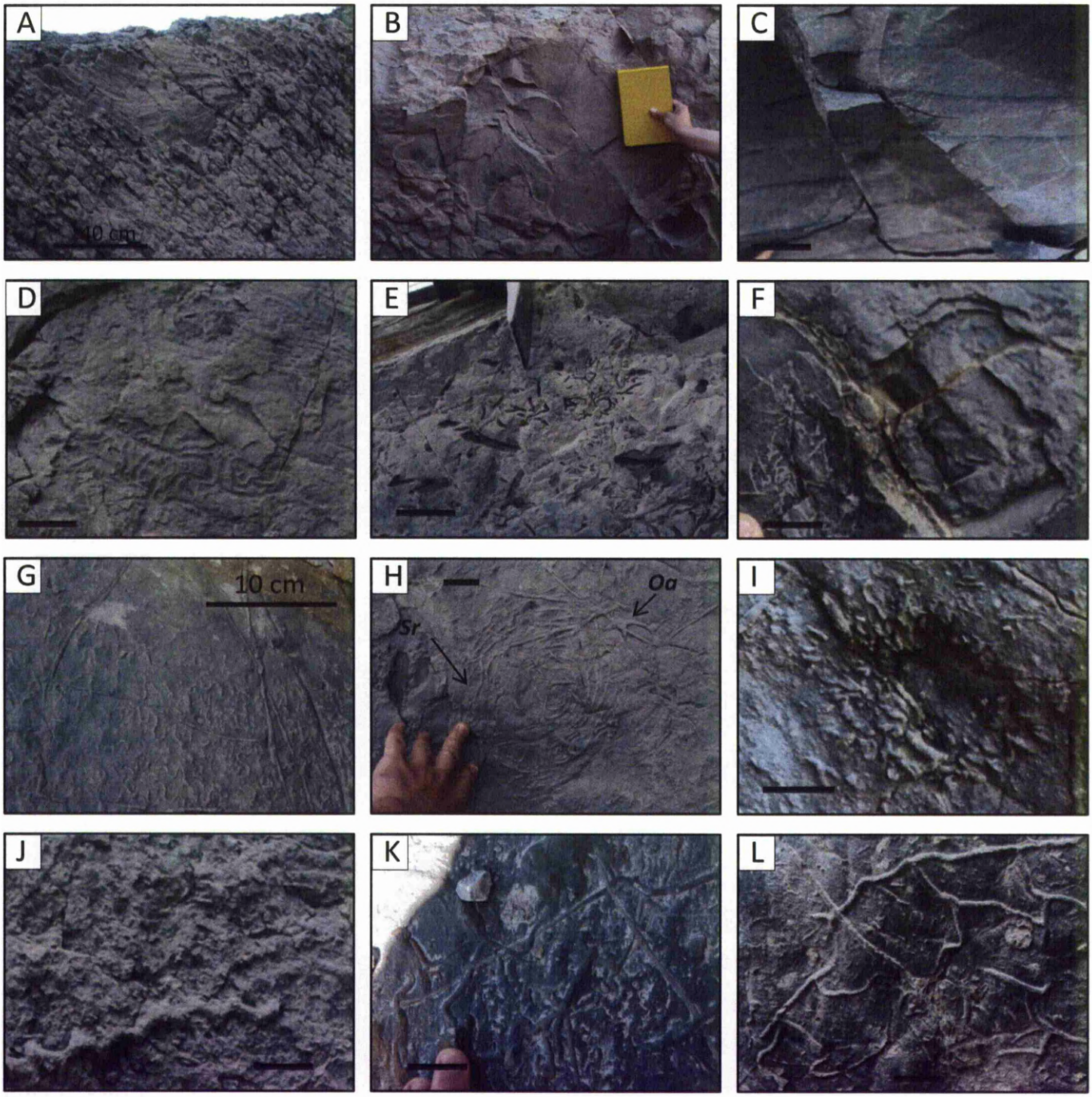

Plate 3

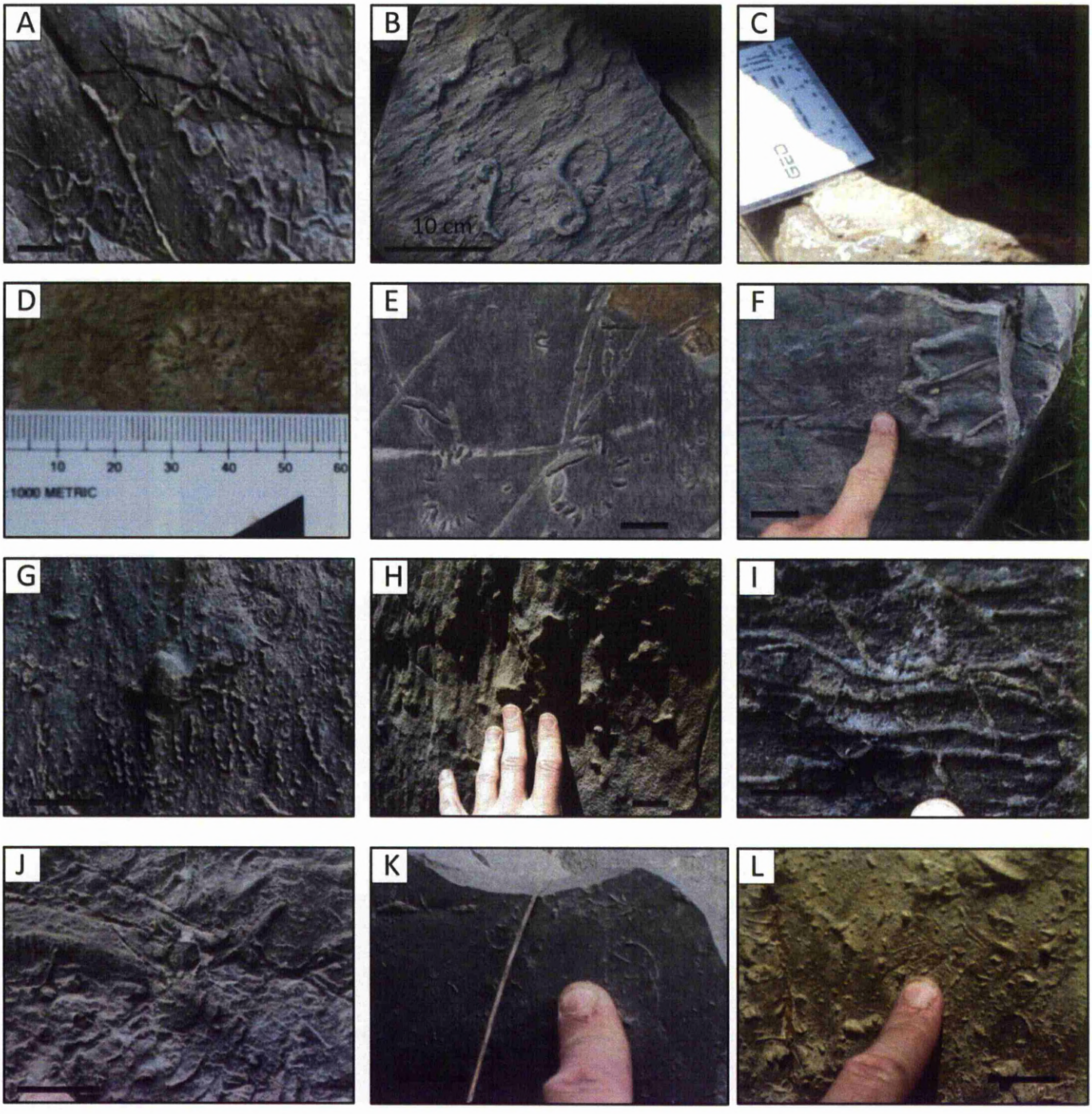

Plate 4

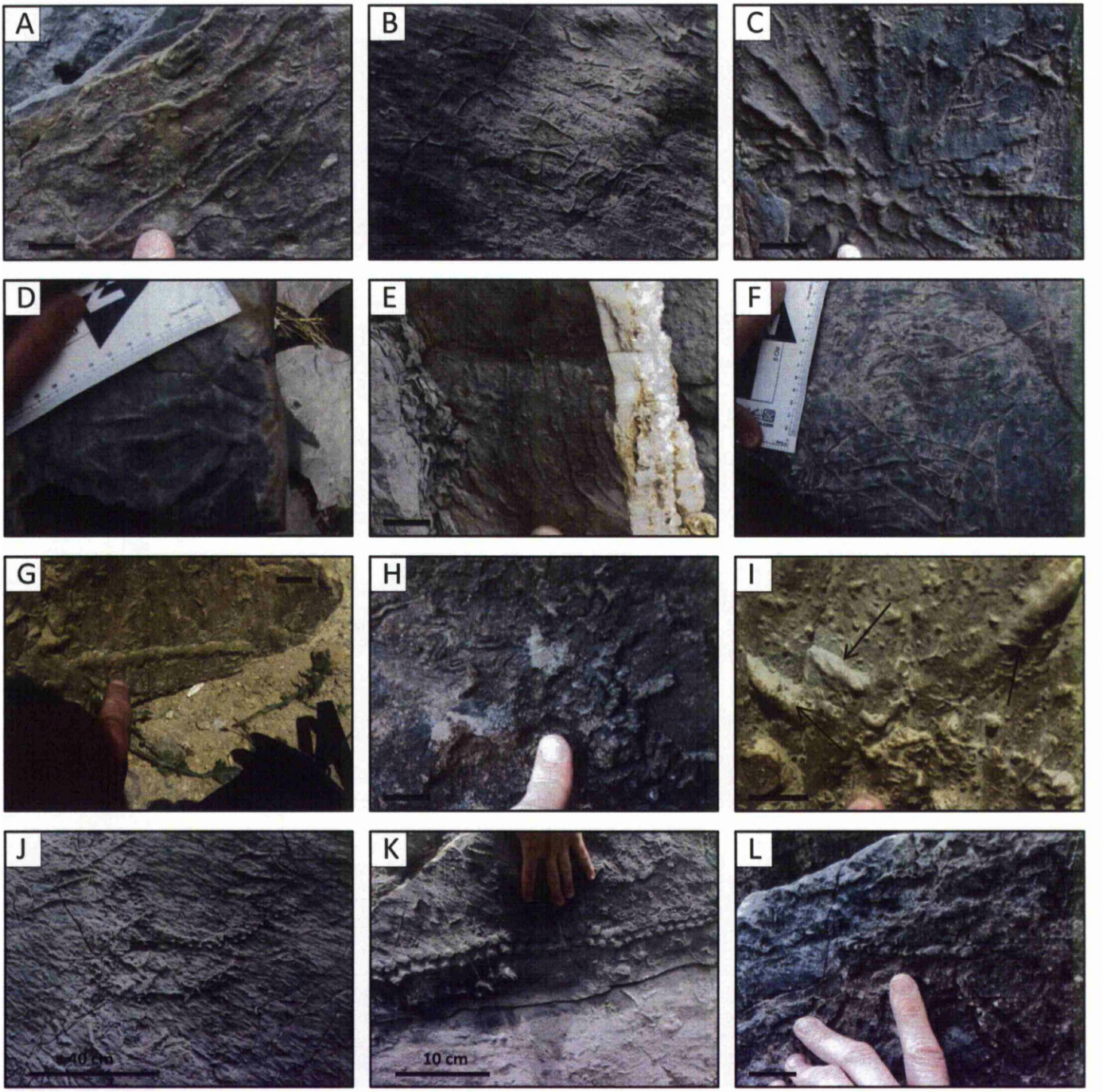

Plate 5

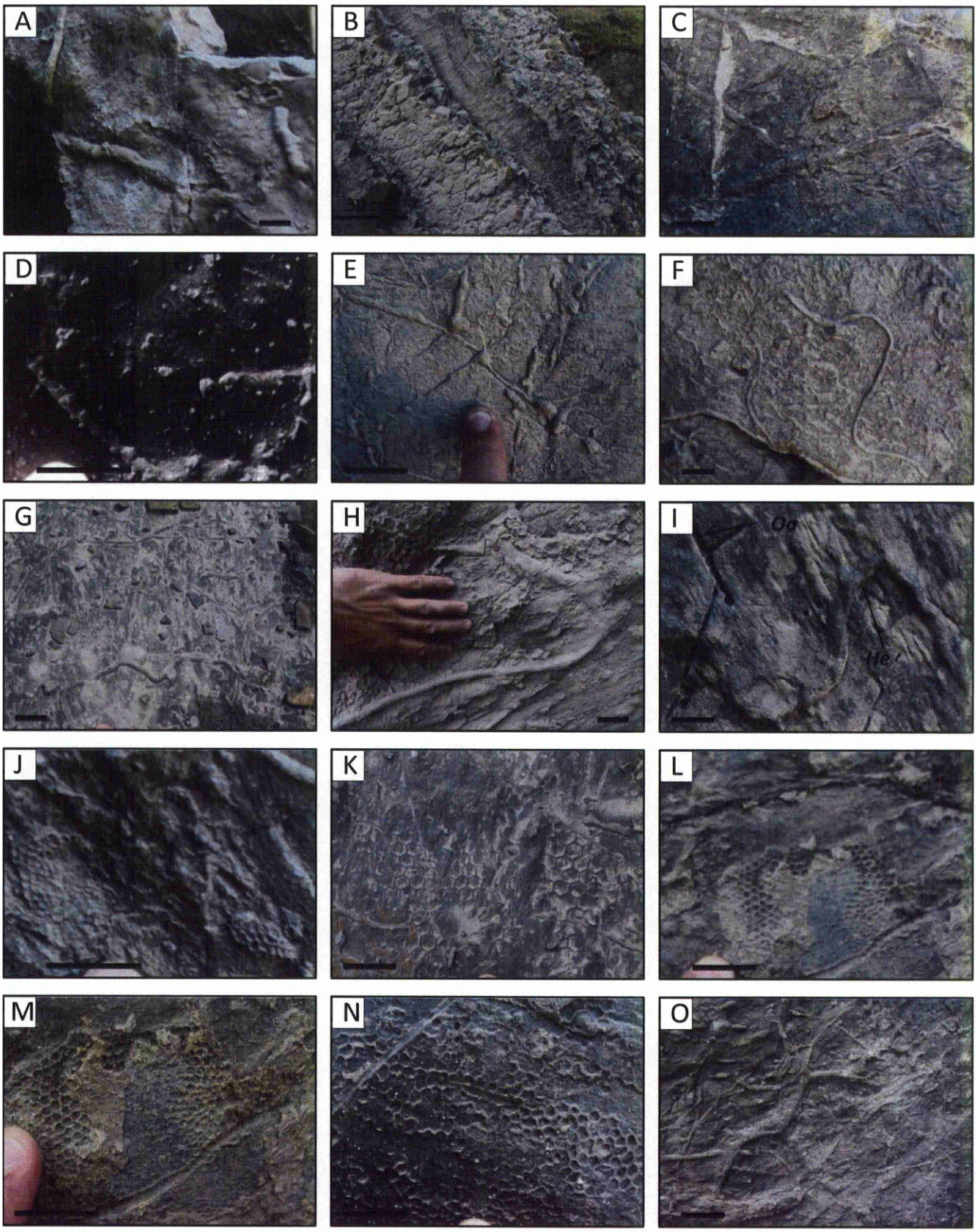

Plate 6

APPENDIX 3

SEDIMENTARY LOGS AND ICHNODATA

Zumaia (Itzurun Beach)
Log Z1 (0-30m)

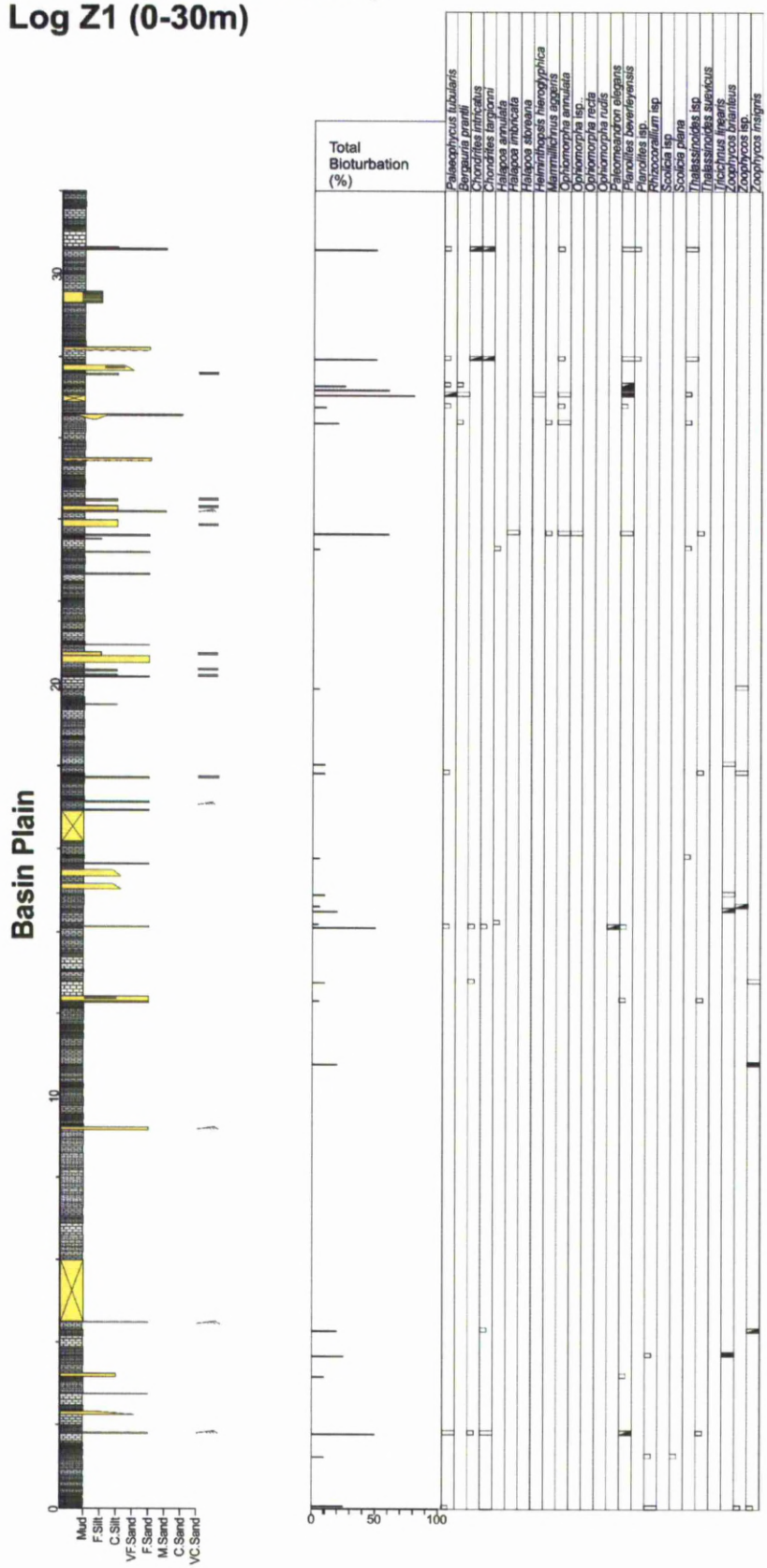

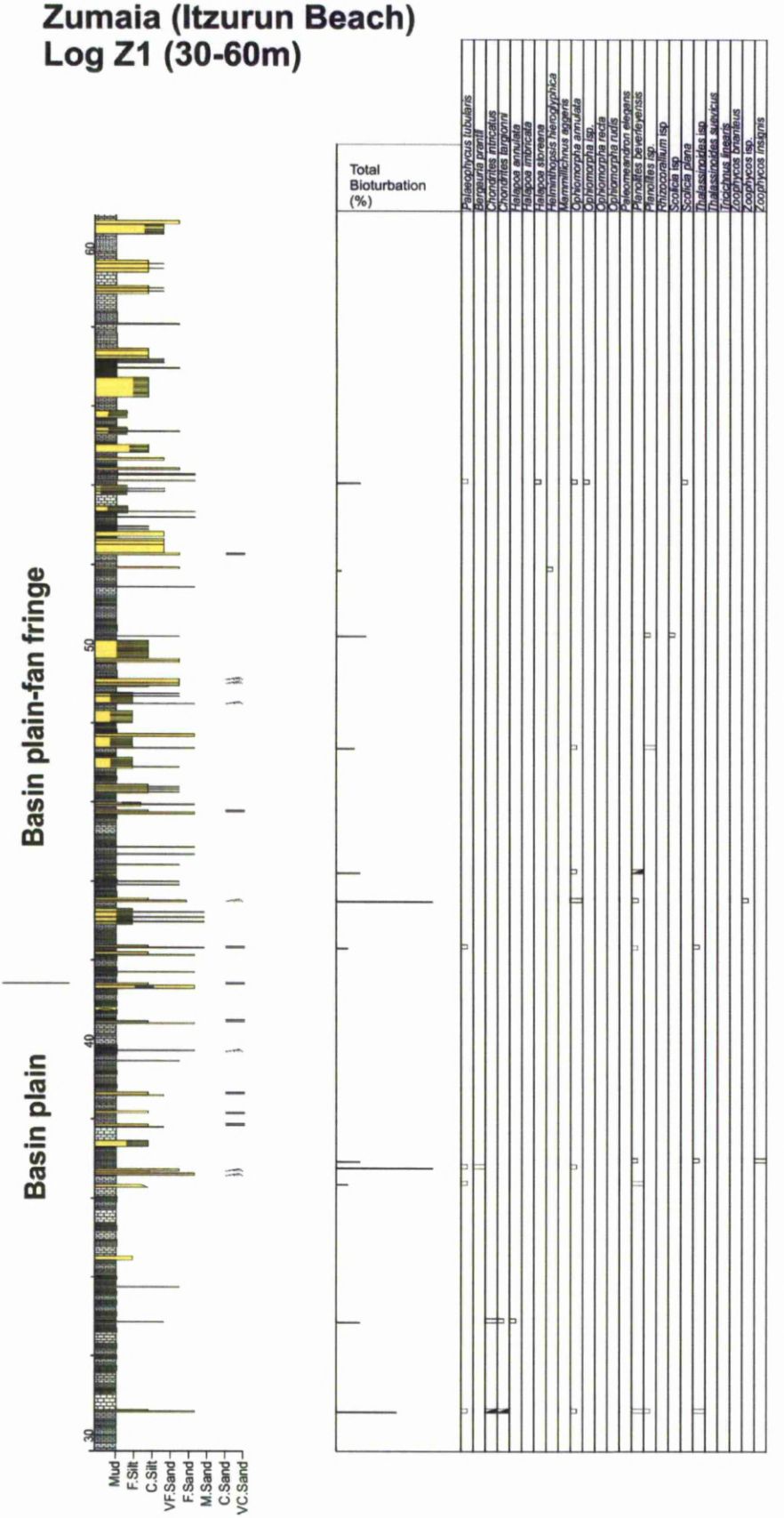
Zumaia (Itzurun Beach)
Log Z1 (30-60m)
Basin plain
Basin plain-fan fringe
30
40
50
60
Mud
F.Silt
C.Silt
VF.Sand
F.Sand
M.Sand
C.Sand
VC.Sand
Total Bioturbation (%)
Palaeophycus tubularis
Bergauria prantl
Chondrites intricatus
Chondrites targionii
Halopoa annulata
Halopoa imbricata
Halopoa sinuosa
Helminthopsis hieroglyphica
Mammilichnus segens
Ophiomorpha annulata
Ophiomorpha isp.
Ophiomorpha nodosa
Ophiomorpha rudis
Paleodictyon elegans
Parahaentzschelinia isp
Phycodes isp
Rhizocorallium isp
Scalicia isp
Scolicia plana
Thalassinoides isp
Thalassinoides suevicus
Zoophycos brianti
Zoophycos isp
Zoophycos insigns

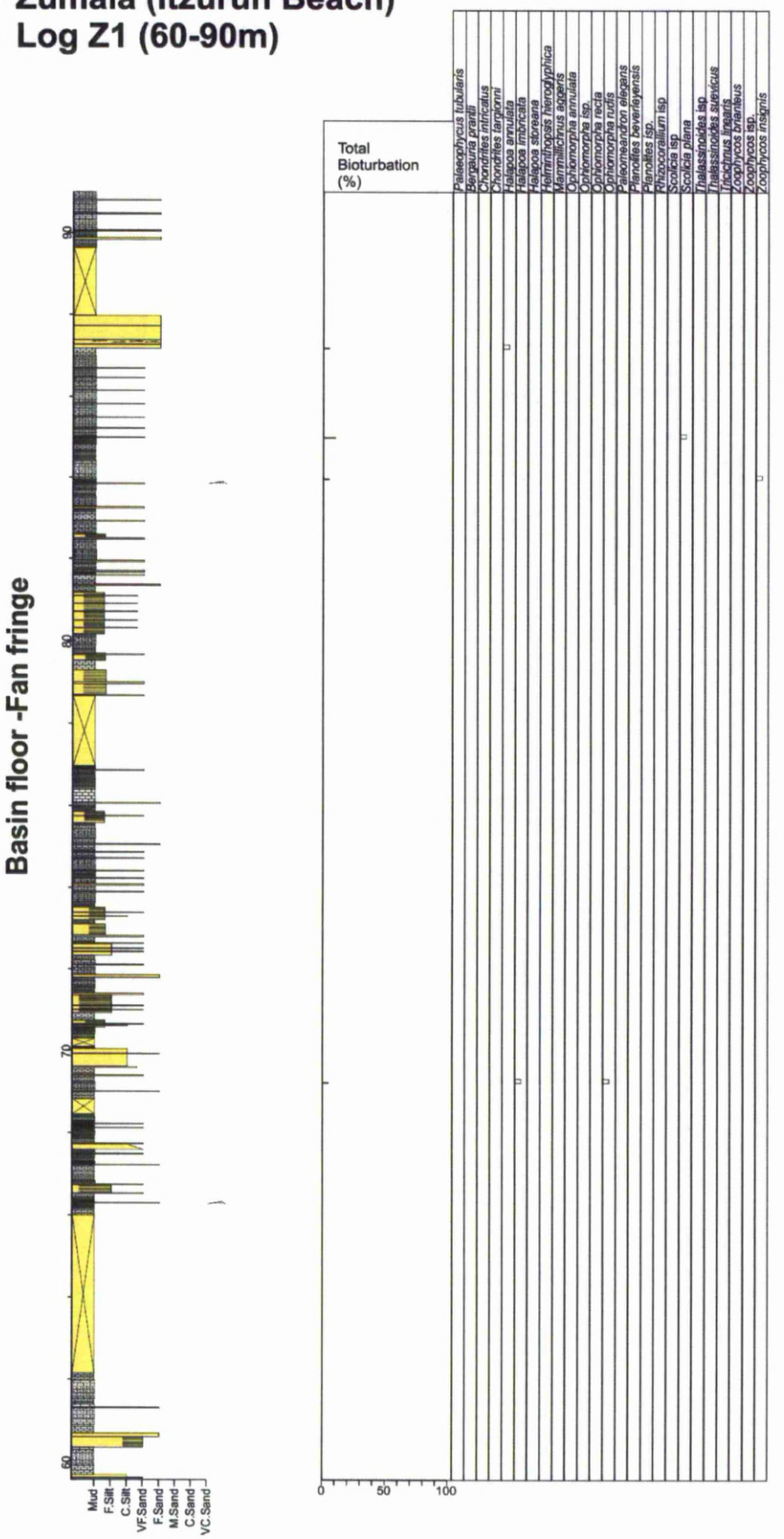
Zumaia (Itzurun Beach)
Log Z1 (60-90m)
Basin floor -Fan fringe
90
80
70
60
Mud
F.Silt
C.Silt
VF.Sand
F.Sand
M.Sand
C.Sand
VC.Sand
Total Bioturbation (%)
Palaeophycus tubularis
Bergaunia pratti
Chondrites intricatus
Chondrites targionni
Halopoa annulata
Halopoa imbricata
Halopoa stroeana
Helminthopsis hieroglyphica
Mammillichnus squiers
Ophiomorpha annulata
Ophiomorpha isp.
Ophiomorpha recta
Ophiomorpha rudis
Paleomeandron elegans
Planolites beverleyensis
Planolites isp.
Rhizocorallium isp.
Scolicia isp.
Scolicia plana
Thalassinoides isp.
Thalassinoides suevicus
Trichichnus linearis
Zoophycos briarleus
Zoophycos isp.
Zoophycos insignis
0
50
100

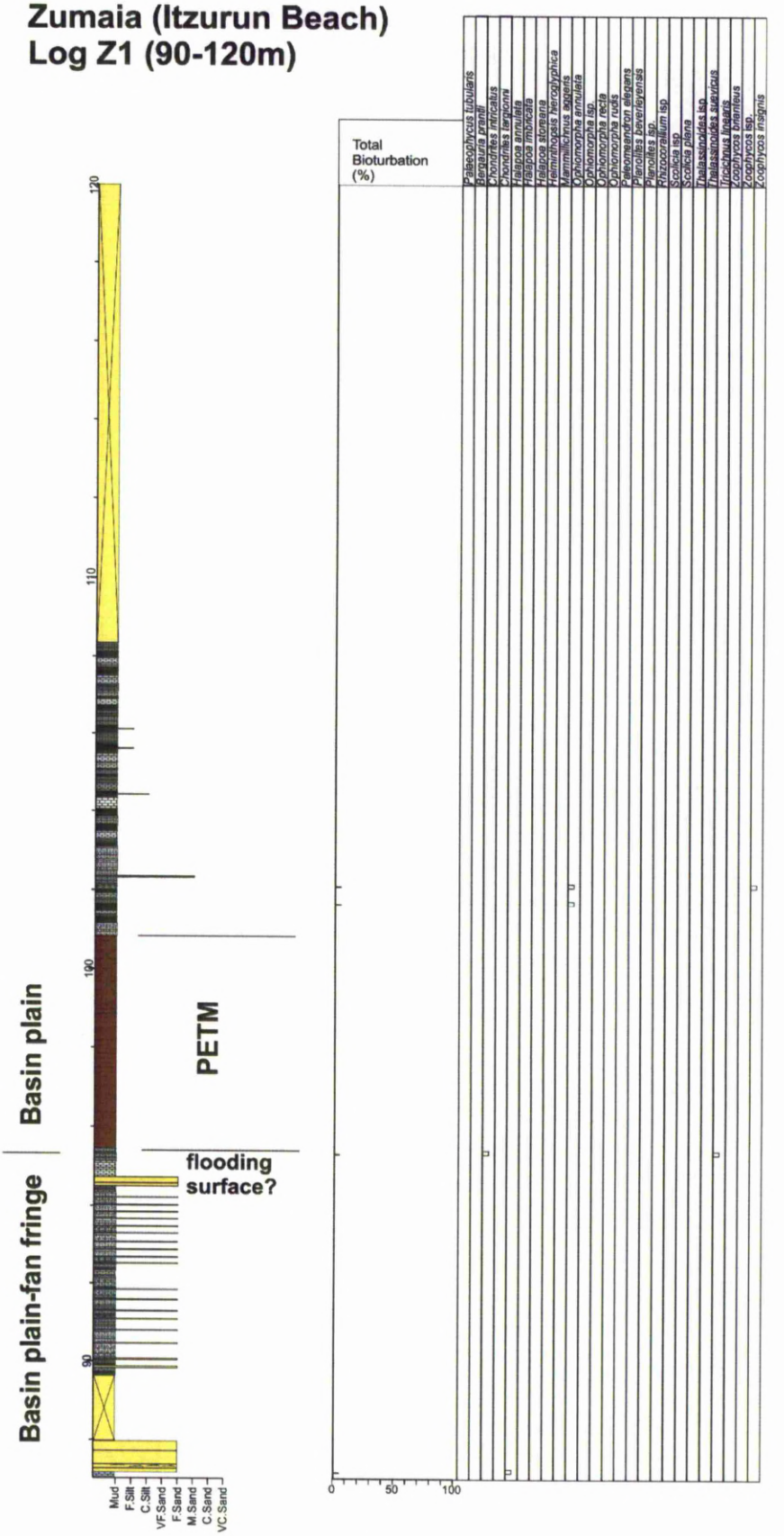
Zumaia (Itzurun Beach)
Log Z1 (90-120m)
Basin plain-fan fringe
Basin plain
PETM
flooding surface?
Total Bioturbation (%)
Palaeophycus tubularis
Bergauria prantli
Chondrites intricatus
Chondrites targionni
Halopoa annulata
Halopoa imbricata
Halopoa stomaria
Helminthopsis hieroglyphica
Mammilichnus sagens
Ophiomorpha annulata
Ophiomorpha isp.
Ophiomorpha recta
Ophiomorpha rudis
Phoebichnion elegans
Planolites beverleyensis
Planolites isp.
Rhizocorallium isp.
Scolicia isp.
Scolicia plana
Thalassinoides isp.
Thalassinoides suevicus
Uriichnus linearis
Zoophycos bimarleus
Zoophycos isp.
Zoophycos insignis
120
110
100
90
Mud
F.Silt
C.Silt
VF.Sand
F.Sand
M.Sand
C.Sand
VC.Sand
0
50
100

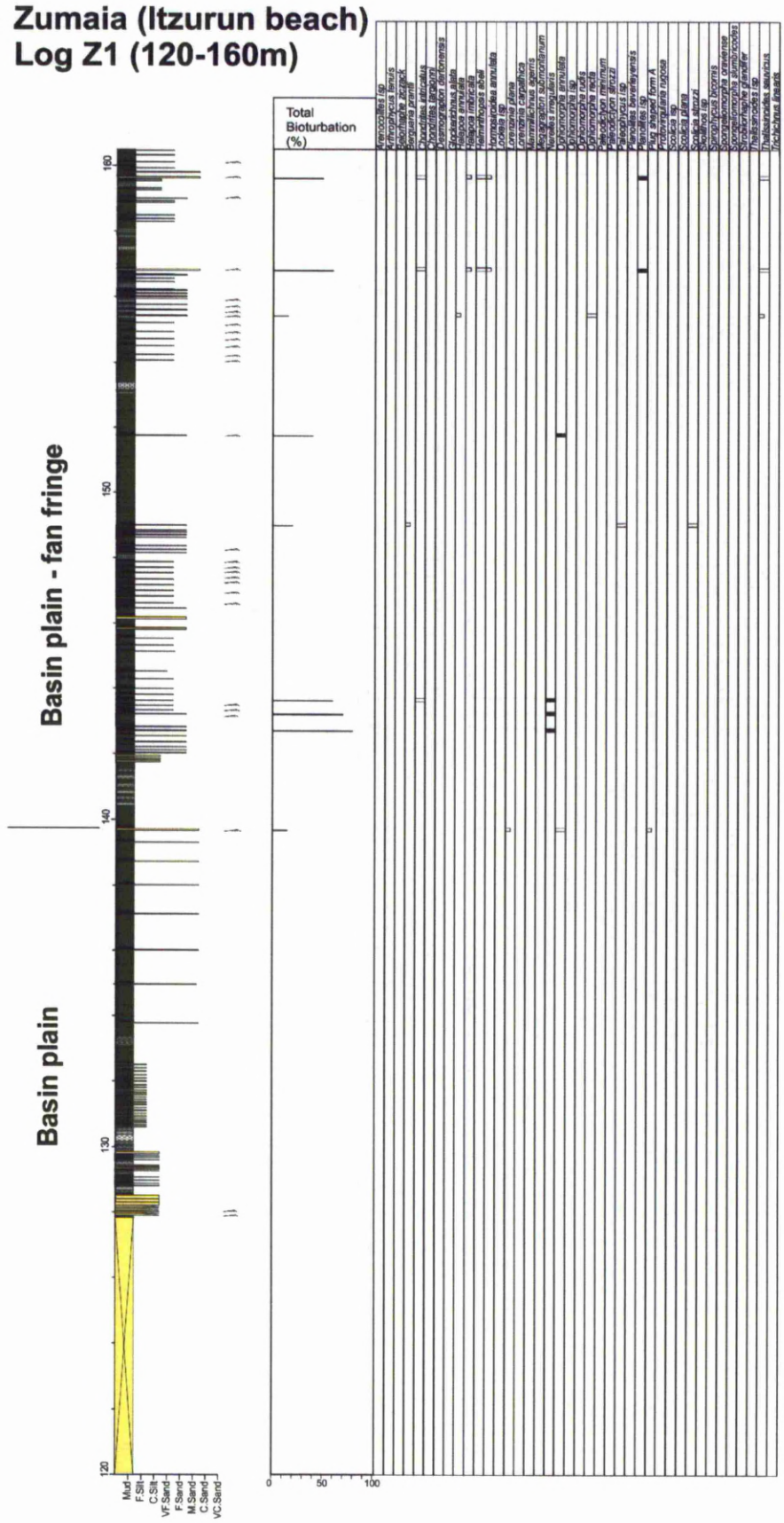
Zumaia (Itzurun beach)
Log Z1 (120-160m)
Basin plain - fan fringe
Basin plain
Total Bioturbation (%)
Mud
F.Silt
C.Silt
VF.Sand
F.Sand
M.Sand
C.Sand
VC.Sand

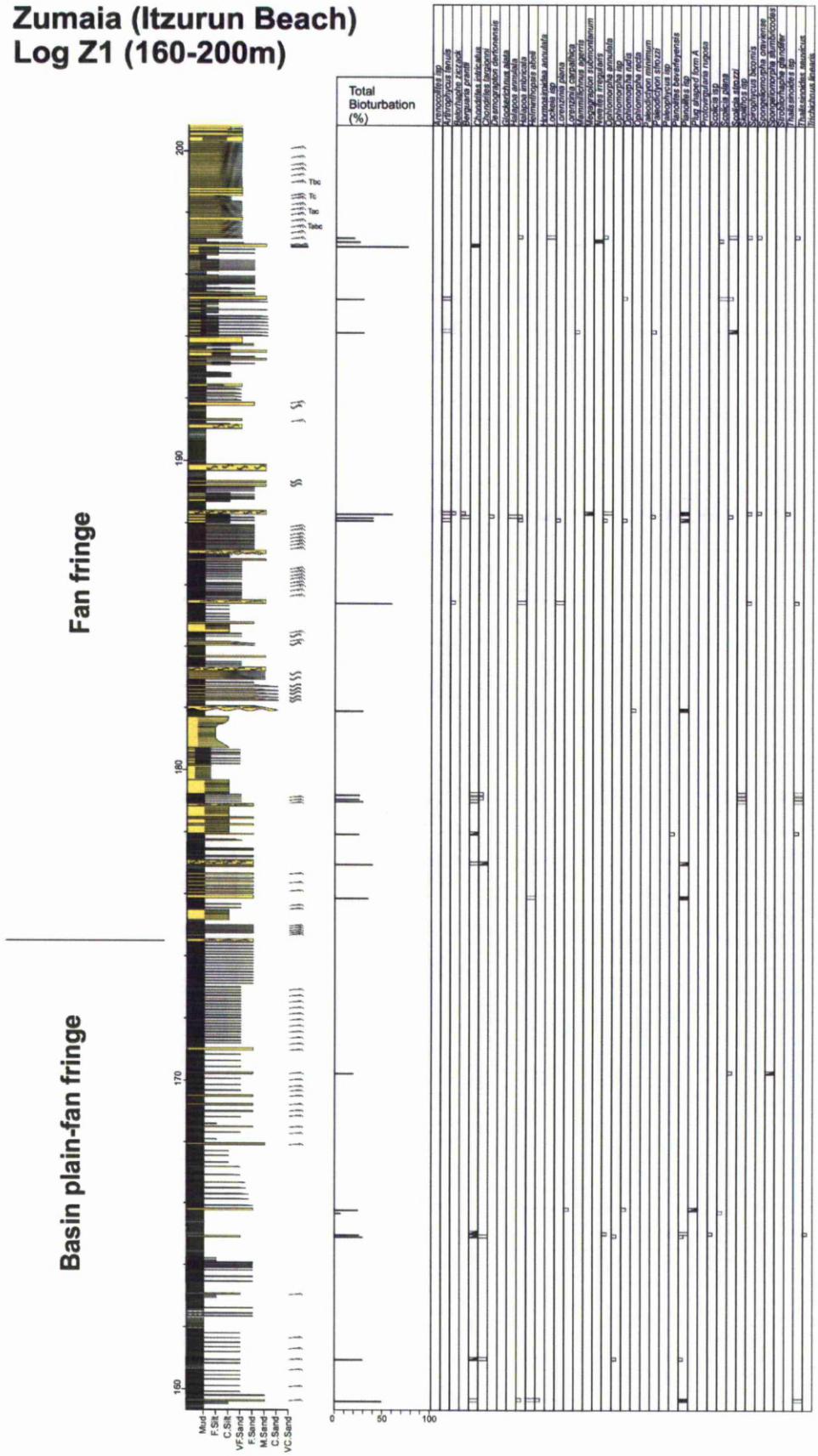
Zumaia (Itzurun Beach)
Log Z1 (160-200m)
Fan fringe
Basin plain-fan fringe
Total Bioturbation (%)
Tbc
Tc
Tac
Tabc
Mud
F.Silt
C.Silt
VF.Sand
F.Sand
M.Sand
C.Sand
VC.Sand
160
170
180
190
200
0
50
100
Ammodiscus sp.
Ammosphaeroidina pseudopauciloculata
Bathysiphon zickzack
Bergueria pralli
Chondrites intricatus
Chondrites targionii
Dictyodora liebeana
Glockerichnus isp.
Halopoa imbricata
Hormosinella distans
Lockeia isp.
Lorenzinia carpatica
Lorenzinia gigantea
Megagrapton irregulare
Nereites irregularis
Oichnomorpha annulata
Oichnomorpha isp.
Oichnomorpha maeandrica
Paleodictyon minimum
Paleodictyon strozzi
Paleophycus isp.
Paleophycus tubularis
Phycodes isp.
Plug shaped form A
Protovirgularia rugosa
Scolicia isp.
Scolicia plana
Spirophyton isp.
Spirophycus bicornis
Squamodermichnus wrangelli
Subphyllochorda isp.
Taenidium isp.
Thalassinoides isp.
Thalassinoides suevicus
Trichichnus linearis

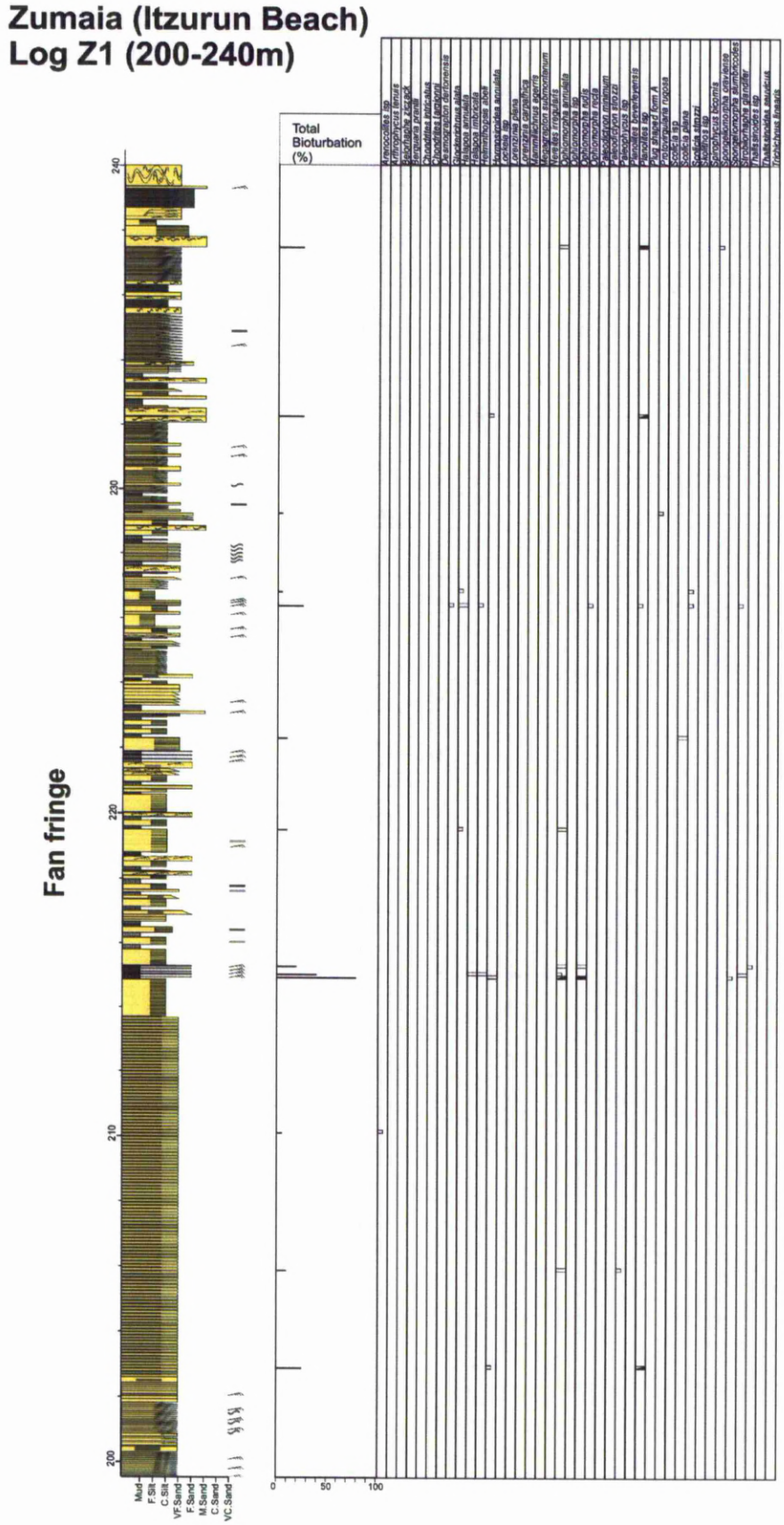
Zumaia (Itzurun Beach)
Log Z1 (200-240m)
Fan fringe
Total Bioturbation (%)
240
230
220
210
200
0
50
100
Mud
F.Silt
C.Silt
VF.Sand
F.Sand
M.Sand
C.Sand
VC.Sand
Amiocolites sp
Arthrophycus alnus
Asterosoma isp
Bergaueria pirumi
Chondrites arbuscula
Chondrites intricatus
Chondrites targionii
Cylindrichnus concentricus
Halopoa imbricata
Helicodromites sinuatus
Helminthopsis abeli
Lorenzinia carpathica
Lorenzinia isp
Megagrapton irregulare
Nereites missouriensis
Ophiomorpha annulata
Ophiomorpha isp
Ophiomorpha nodosa
Paleodictyon majori
Paleodictyon strozzi
Palaeophycus isp
Phycodes isp
Planolites beverleyensis
Scalarituba missouriensis
Scolicia isp
Scolicia plana
Spirophyton isp
Spirorhaphe graecilenta
Taenidium isp
Thalassinoides paradoxicus
Trichichnus linearis

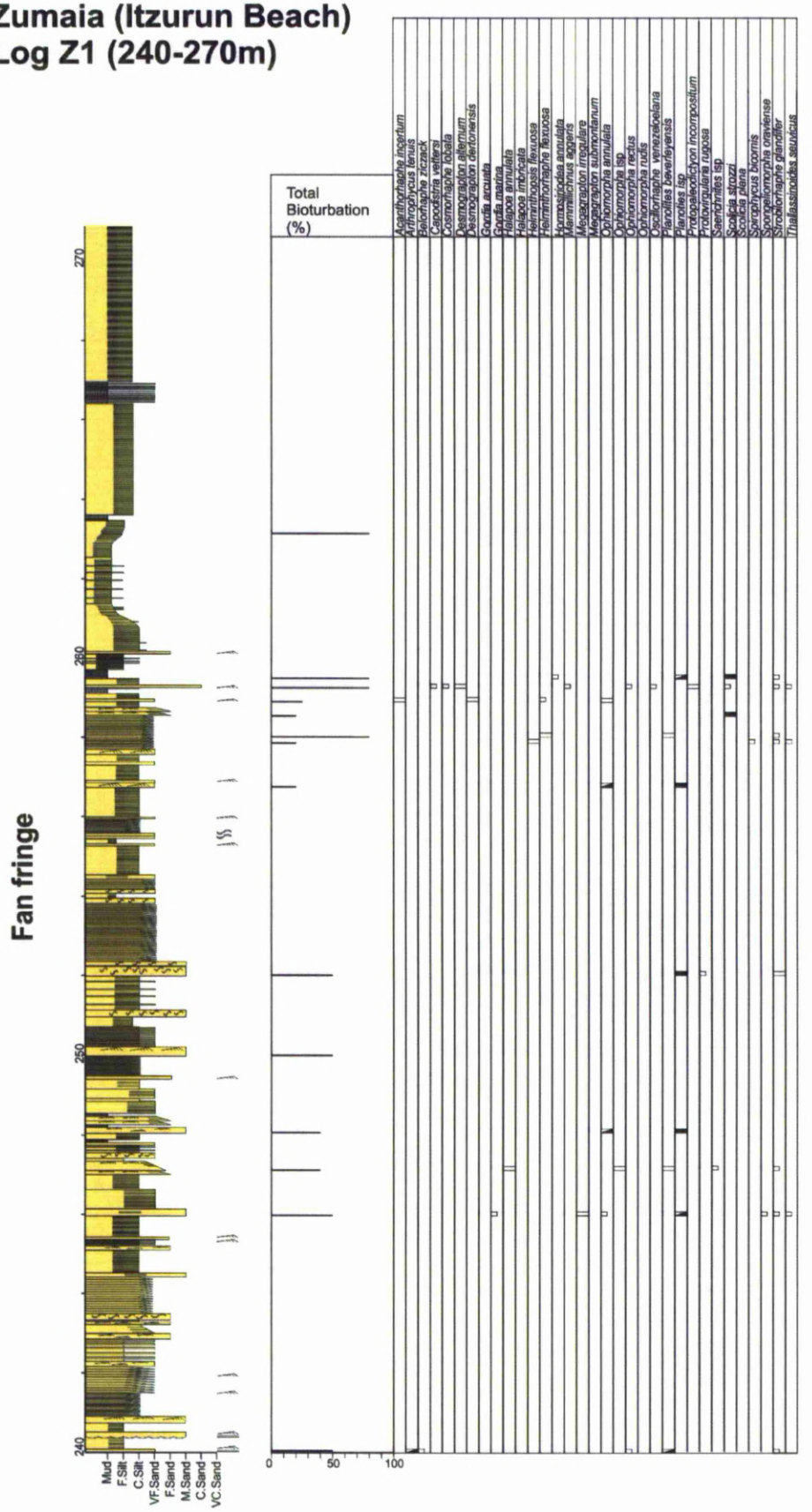
Zumaia (Itzurun Beach)
Log Z1 (240-270m)
Fan fringe
Total Bioturbation (%)
Agaricorhaphe incertum
Arthrophycus tenuis
Belorhaphe zickzack
Capodistria vetfera
Cosmorhaphe lobata
Desmograption alternum
Desmograption dertonensis
Gordia acuata
Gordia marina
Halapoa annulata
Halapoa imbricata
Helminthoida flexuosa
Helminthorhaphe flexuosa
Hormosiroidea annulata
Mammillichnus aggeris
Megagraption irregulare
Megagraption submontanum
Ophiomorpha annulata
Ophiomorpha isp.
Ophiomorpha rectus
Ophiomorpha nudis
Oscillorhaphe venezuelana
Planolites beverleyensis
Planolites isp.
Protopaleodictyon incompositum
Protovirgularia rugosa
Saerichnites isp.
Scolicia strozzi
Scolicia plana
Spirophycus bicornis
Spongeliomorpha oraviense
Strobilorhaphe glandifer
Thalassinoides seuvicus
270
260
250
240
Mud
F.Silt
C.Silt
VF.Sand
F.Sand
M.Sand
C.Sand
VC.Sand
0
50
100

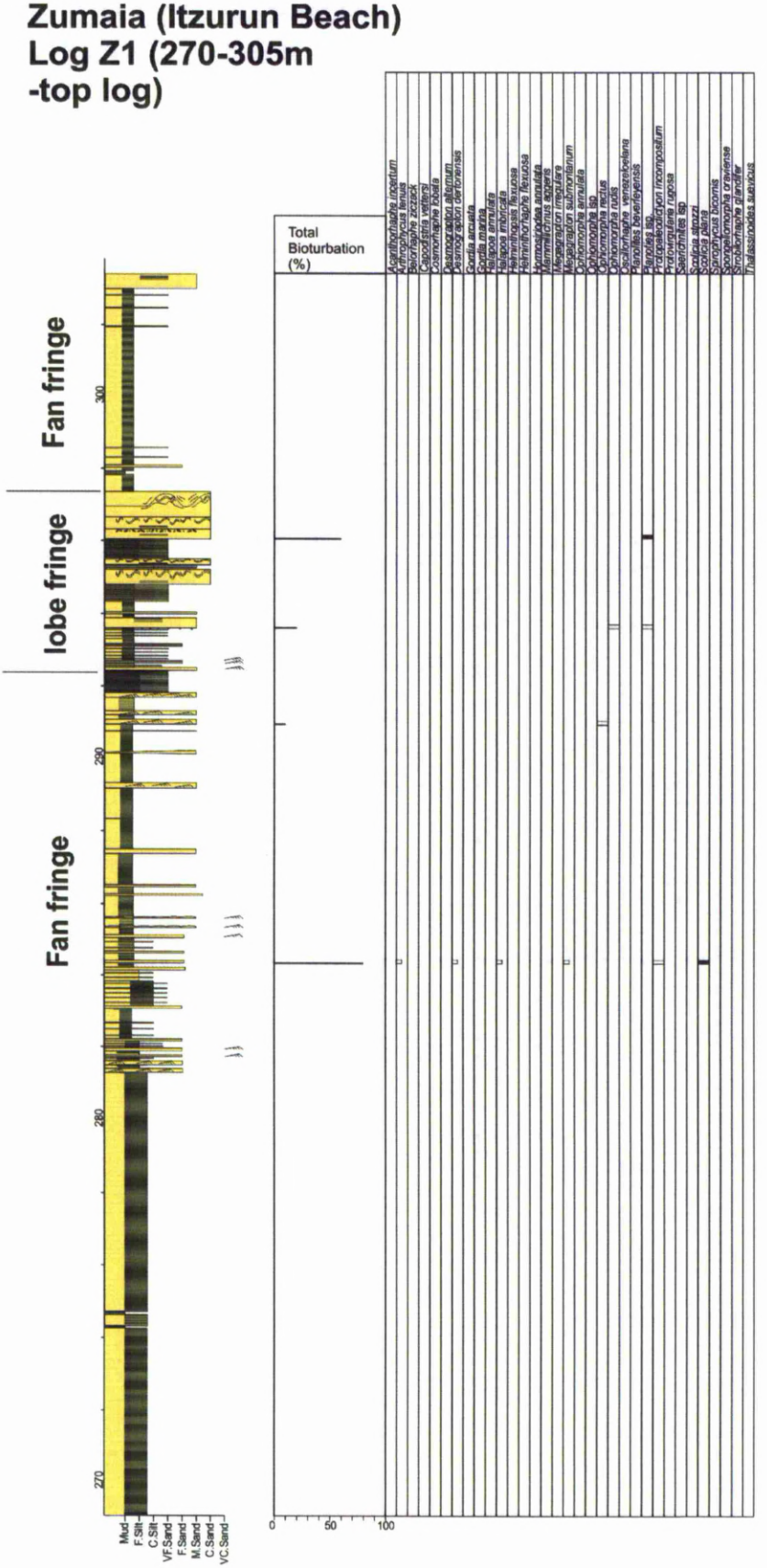
Zumaia (Itzurun Beach)
Log Z1 (270-305m
-top log)
Fan fringe
lobe fringe
Fan fringe
300
290
280
270
Mud
F.Silt
C.Silt
VF.Sand
F.Sand
M.Sand
C.Sand
VC.Sand
Total
Bioturbation
(%)
0
50
100
Agerhorhaphe incertum
Arthrophycus tenuis
Bayerlaphe zezzeck
Capodistria vetteri
Cosmorhaphe bocala
Cosmorhaphe torquatum
Desmograpton dertonensis
Gordia arcuata
Gordia marina
Halopoa annulata
Halopoa imbricata
Helminthopsis flexuosa
Helminthopsis tenuissa
Mammilichnus isperis
Megagraplon irregulare
Megagraplon submorlanum
Ophiomorpha annulata
Ophiomorpha isp.
Ophiomorpha nodosa
Ophiomorpha rudis
Oscillorhaphe venezolelana
Ranolites bayerleyensis
Rhenoleg isp.
Protopaleodictyon incompositum
Protovirgularia rugosa
Saerichnites isp
Scolicia plana
Scolicia strozzi
Spirophycus bicornis
Spongeliomorpha oravense
Strictorhaphe glandifer
Thalassinoides suevicus

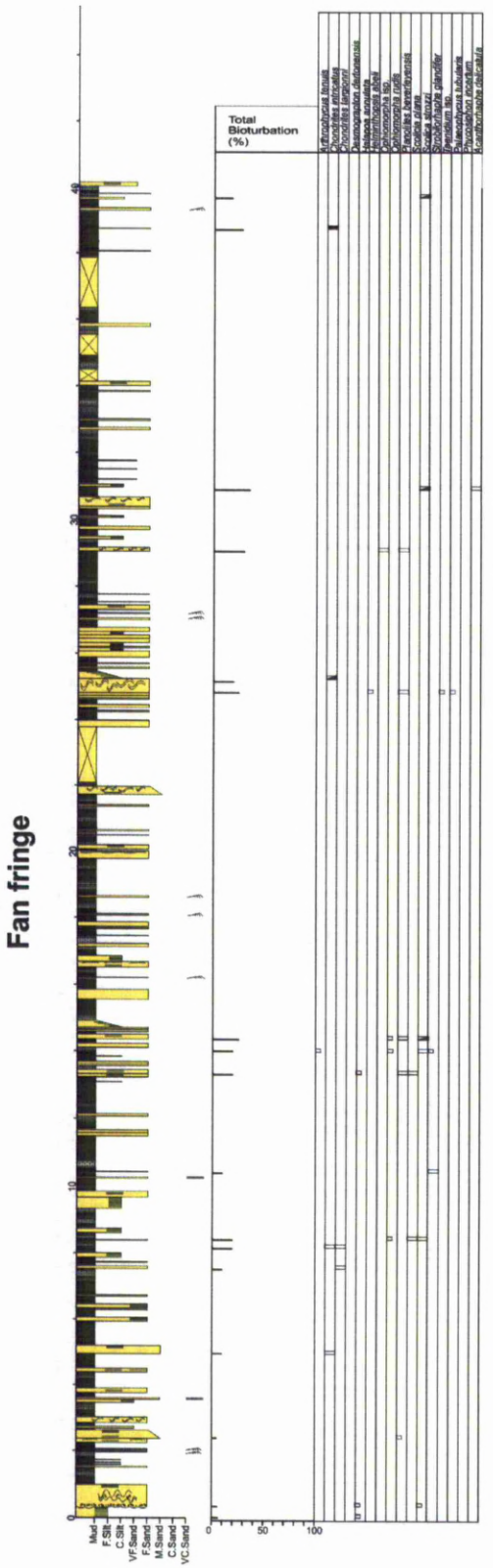

Gorrondatxe Beach (main beach)
Log G1

Gorrondatxe (Azkorri Sst.)
Log G2

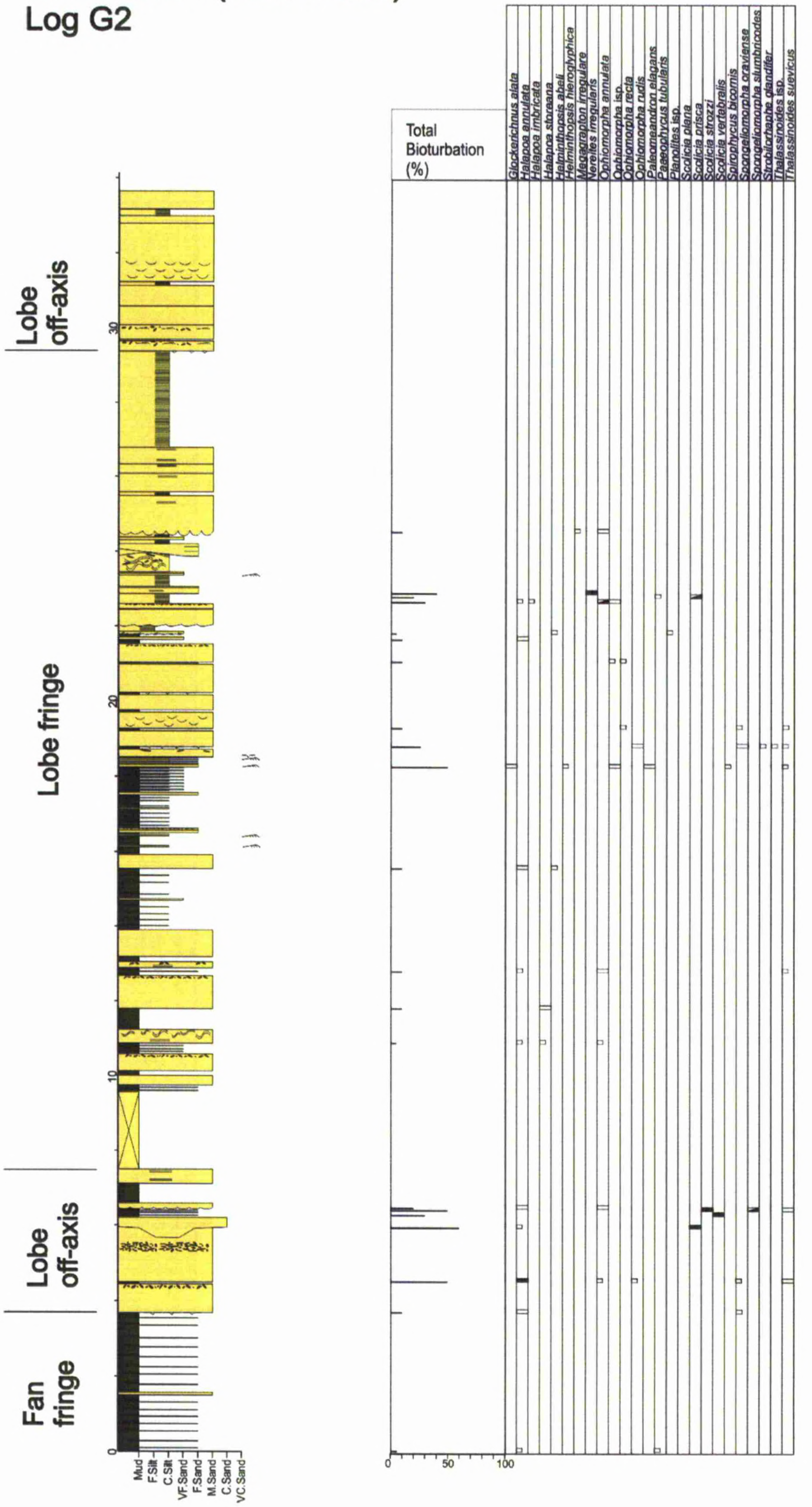

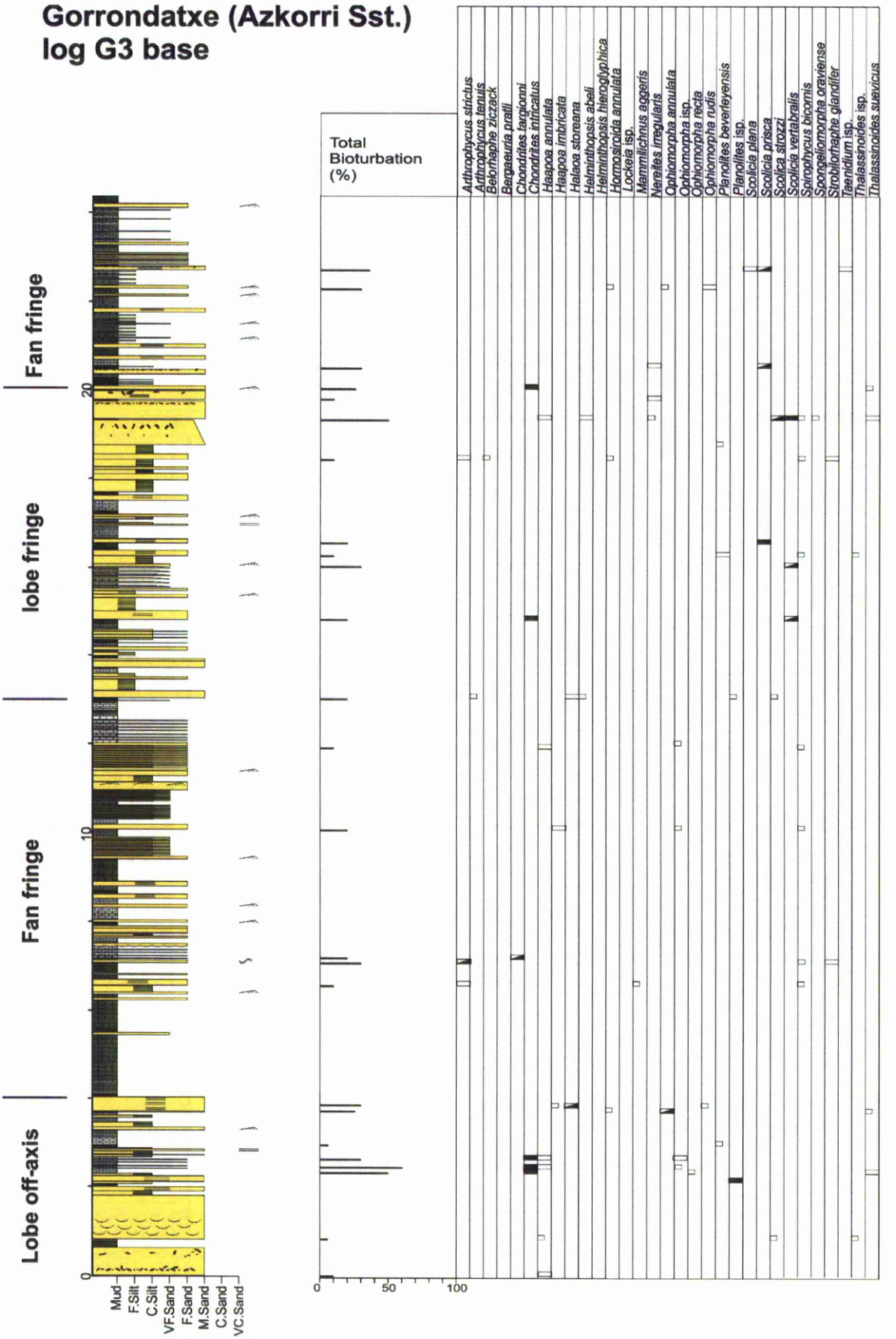
Gorrondatxe (Azkorri Sst.)
log G3 base
Lobe off-axis
Fan fringe
lobe fringe
Fan fringe
Mud
F.Silt
C.Silt
VF.Sand
F.Sand
M.Sand
C.Sand
VC.Sand
0
10
20
Total Bioturbation (%)
0
50
100
Arthrophycus stirctus
Arthrophycus tenuis
Belorhaphe zickzack
Bergaeuria pralli
Chondrites targionni
Chondrites intricatus
Haapoa annulata
Haapoa imbricata
Halcoa storeana
Helminthopsis abeli
Helminthopsis hieroglyphica
Hormosirolida annulata
Lockeia isp.
Mammilichnus aggeris
Nereites irregularis
Ophiomorpha annulata
Ophiomorpha isp.
Ophiomorpha recta
Ophiomorpha rudis
Planolites beverleyensis
Planolites isp.
Scolicia plana
Scolicia prisca
Scolicia strozzi
Scolicia vertabralis
Spirophycus bicornis
Spongeliomorpha oravíense
Strobilorhaphe glandifer
Taenidium isp.
Thalassinoides isp.
Thalassinoides suevicus

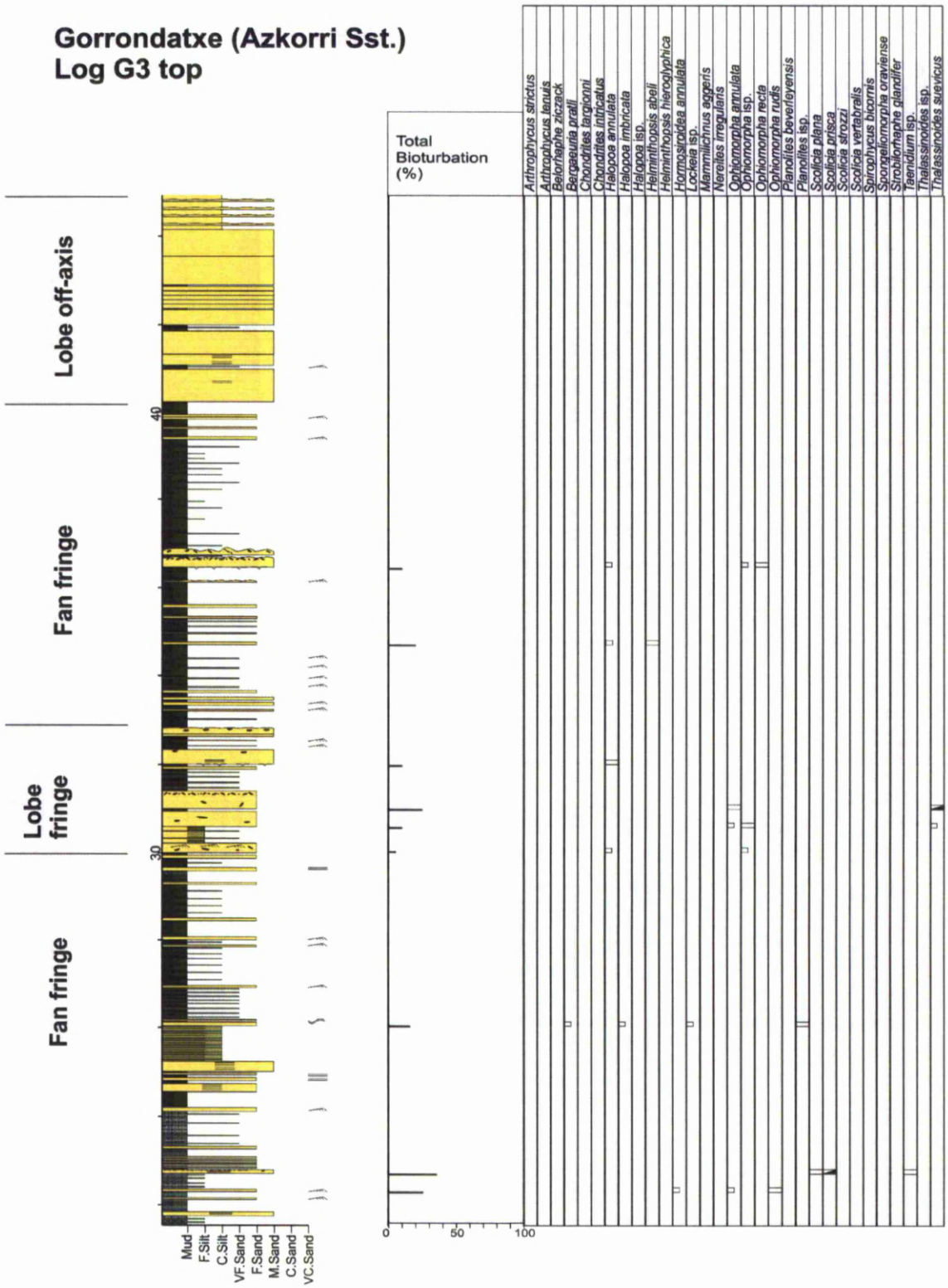
Gorrondatxe (Azkorri Sst.)
Log G3 top
Lobe off-axis
Fan fringe
Lobe fringe
Fan fringe
40
30
Mud
F.Silt
C.Silt
VF.Sand
F.Sand
M.Sand
C.Sand
VC.Sand
Total Bioturbation (%)
0
50
100
Arthrophycus stinctus
Arthrophycus tenuis
Belorhaphe zickzack
Bergaeunia praitl
Chondrites targionni
Chondrites intricatus
Halopoa annulata
Halopoa imbricata
Halopoa isp.
Helminthopsis abeli
Helminthopsis hieroglyphica
Hormosiroidea annulata
Lockeia isp.
Mammilichnus aggeris
Neroites irregularis
Ophiomorpha annulata
Ophiomorpha isp.
Ophiomorpha recta
Ophiomorpha rudis
Planolites beverleyensis
Planolites isp.
Scolicia plana
Scolicia prisca
Scolicia strozzi
Scolicia vertebralis
Spirophycus bicornis
Spirorhaphe graviense
Strobilorhaphe glandifer
Taenidium isp.
Thalassinoides isp.
Thalassinoides suevicus

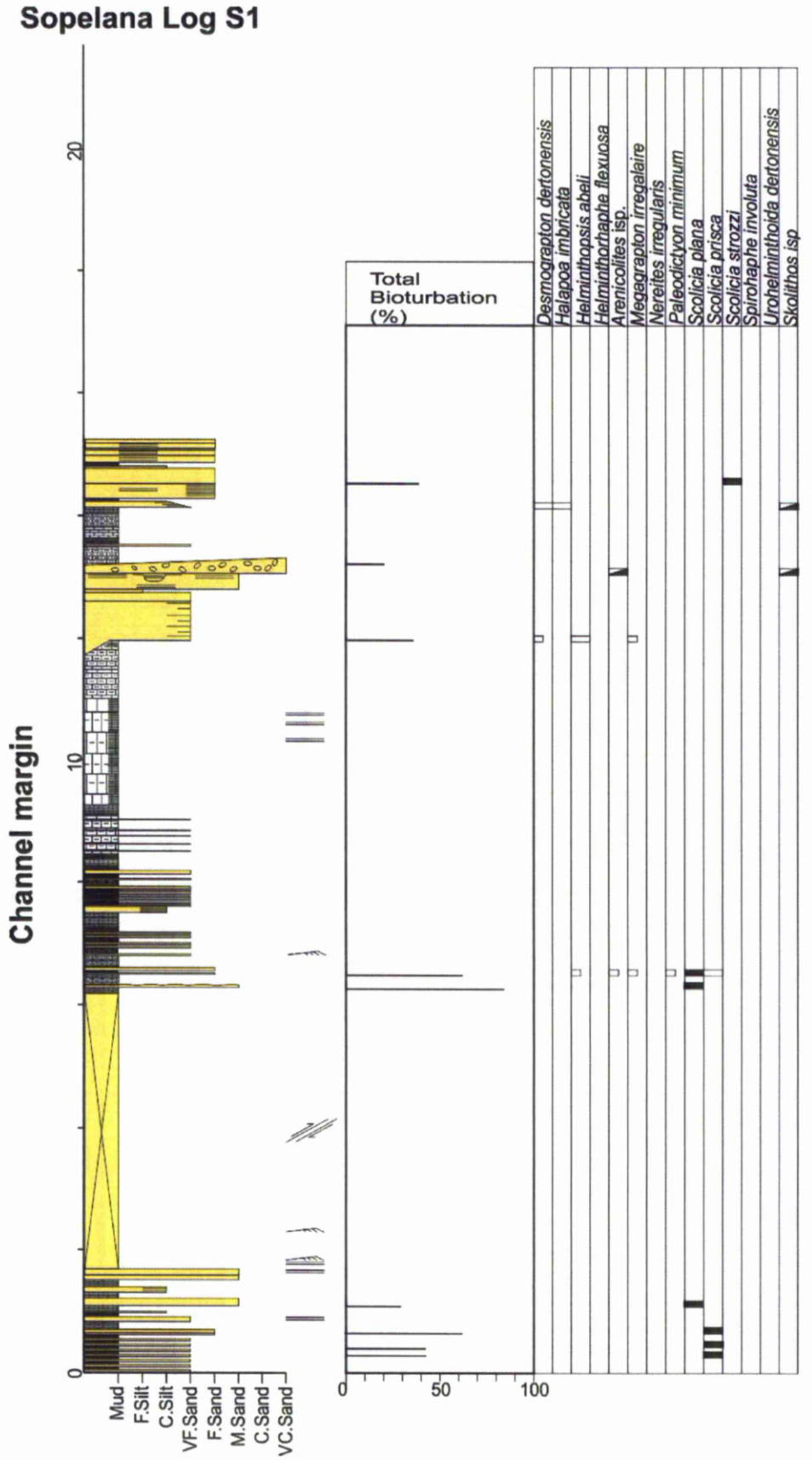
Sopelana Log S1
Channel margin
0
10
20
Mud
F.Silt
C.Silt
VF.Sand
F.Sand
M.Sand
C.Sand
VC.Sand
Total Bioturbation (%)
0
50
100
Desmograpton dertonensis
Halapoa imbricata
Helminthopsis abeli
Helminthorhaphe flexuosa
Arenicolites isp.
Megagrapton irregalaire
Nereites irregularis
Paleodictyon minimum
Scolicia plana
Scolicia prisca
Scolicia strozzi
Spirohaphe involuta
Urohelmintoida dertonensis
Skolithos isp

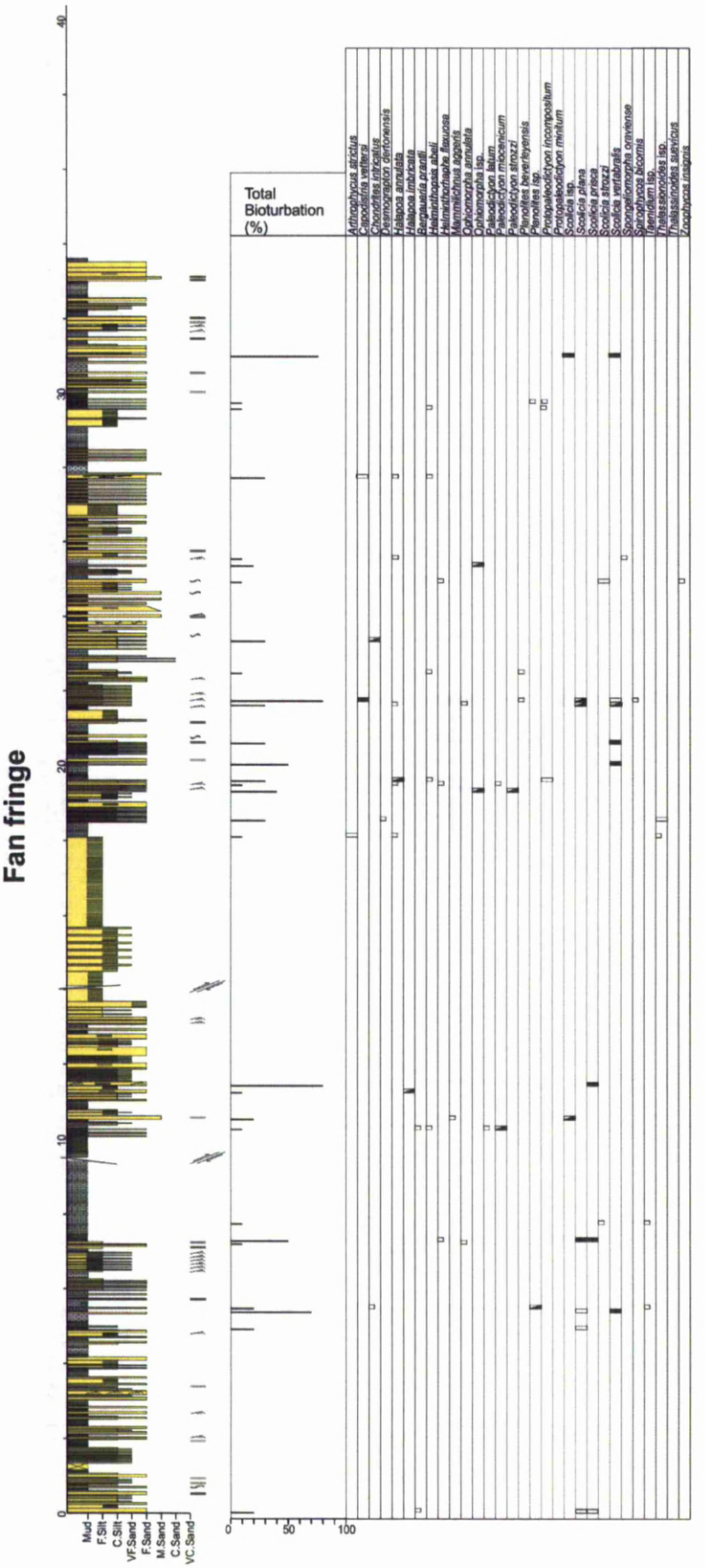

Sopelana Log S2

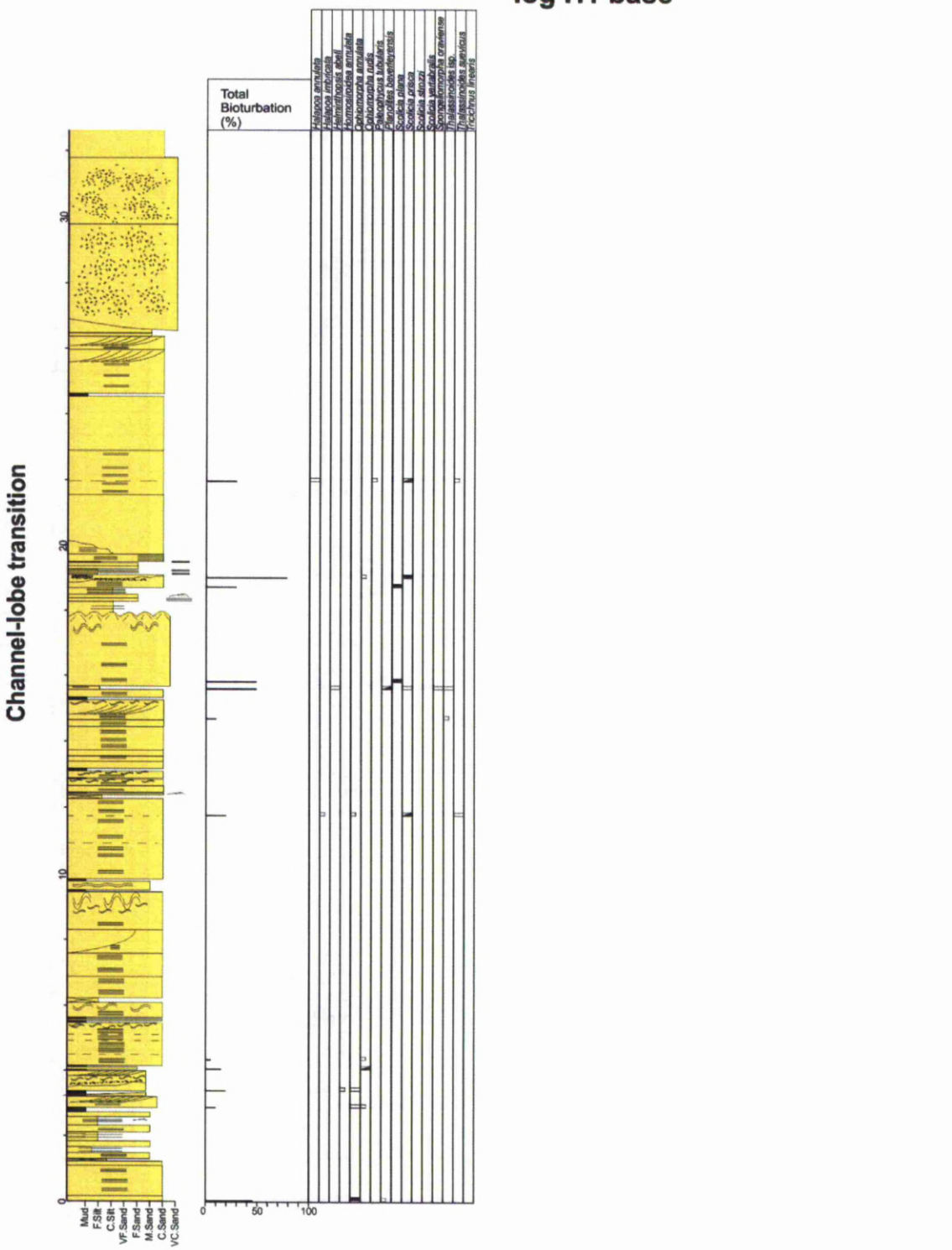
Hondaribbia (lighthouse section)
log H1 base
Channel-lobe transition
Total Bioturbation (%)
Halopa annulata
Halopa imbricata
Helminthopsis abeli
Homalohalopa annulata
Orthomorpha annulata
Orthomorpha nuda
Paleocortina bifaria
Paradiles bicentrisensis
Scolicia cf. plana
Scolicia plana
Scolicia strozzi
Scolicia vertebralis
Spongeliomorpha cravense
Thalassinoides isp.
Thalassinoides suevicus
Trichichnus linearis
Mud
F.Silt
C.Silt
VF.Sand
F.Sand
M.Sand
C.Sand
VC.Sand
0
10
20
30
0
50
100

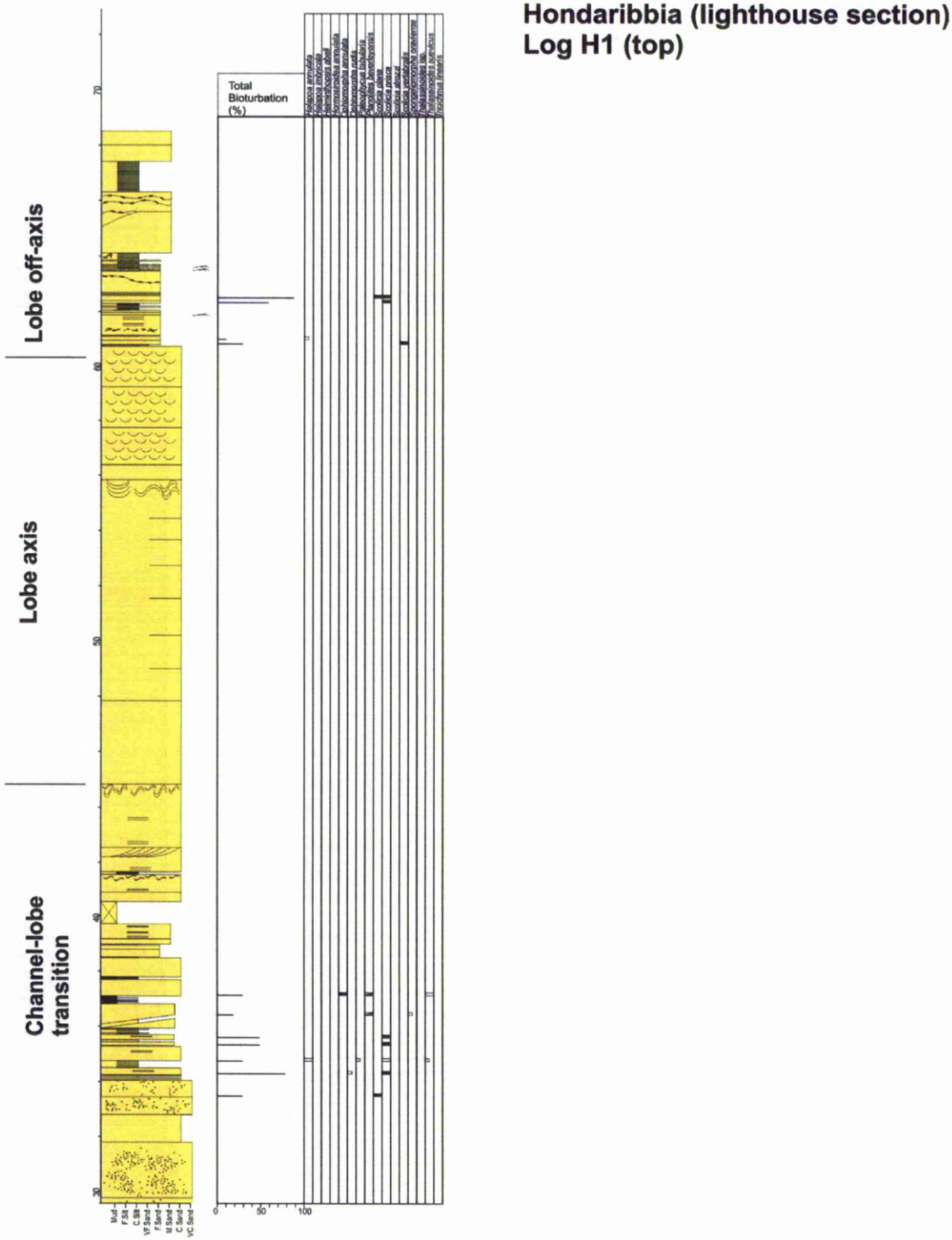

Appendix 3b Sed logs only (see appendix 3c for ichnodata)

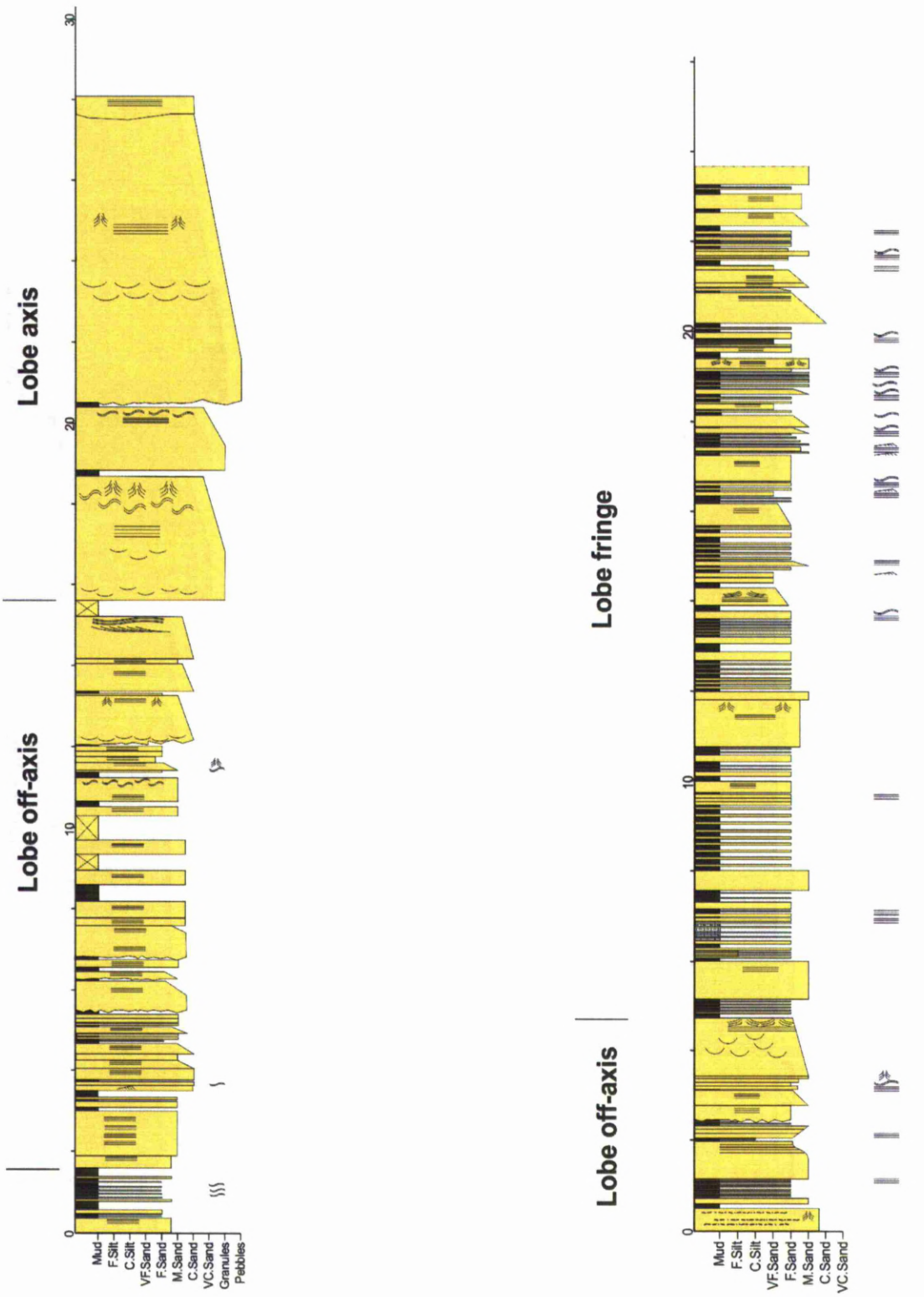
Pasaia Harbour
Log P1
Lobe axis
Lobe off-axis
0
10
20
30
Mud
F.Silt
C.Silt
VF.Sand
F.Sand
M.Sand
C.Sand
VC.Sand
Granules
Pebbles
Illurgita Senotia
Log IS1
Lobe fringe
Lobe off-axis
0
10
20
Mud
F.Silt
C.Silt
VF.Sand
F.Sand
M.Sand
C.Sand
VC.Sand

Orio log O1
western side of harbour entrance

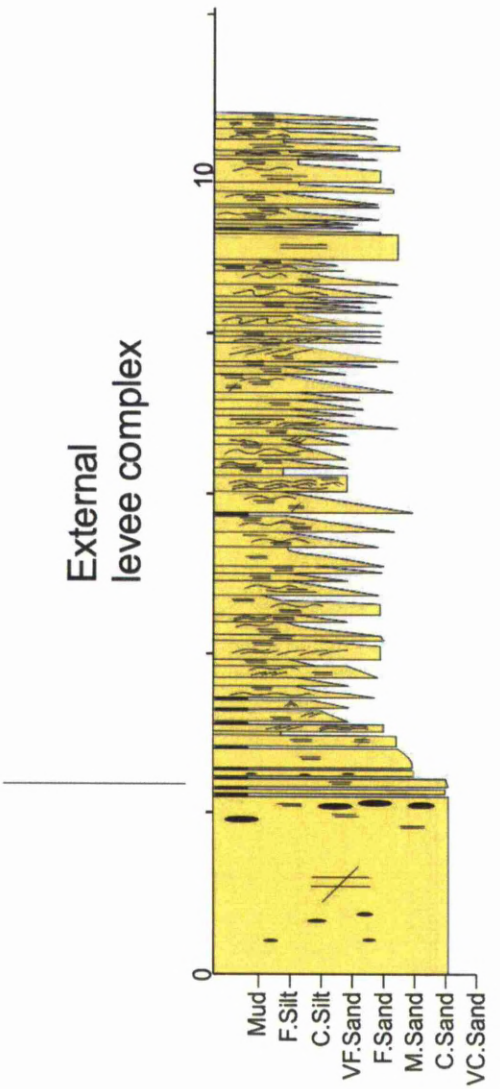

Appendix 3c raw trace fossil data

external levee

Orio Ichnolog O1			
Bed number	*Ichnogenera & species*	Position	Abundance (%) (Bold figure = BT index)
1	*Oph annulata*	ep	25
	Oph rudis	ep	20
	Oph rudis	ep	xl
	Th isp		10
			65
2	*Pl beverleyensis*	hyp	5
	Pal minimum	hyp	5
	v small bedding plane		5
3	*Oph annulata*	hyp	10
	pl beverleyensis	hyp	5
	Strob glandifer	hyp	5
			15
4	*?Helicolithus sampelas*	hyp	5
	Strabilorhaphe glandifer	hyp	5
	Protopal incompositum	hyp	5
	Oscillorhaphe venezoalana	hyp	5
	Small bedding plane-prob much more diverse		20
5	Meandering trackway	hyp	5
	Pl beverleyensis	hyp	10
	poor bedding plane exposure		10
6	*Desmograpton dertonensis*	hyp	5
	Cosmorhaphe lobata	hyp	5
	Pl beverleyensis	hyp	5
	Meandering trackway	hyp	5
	oblique/oblit	hyp	5
			10
7	*Oph annulata*	hyp	5
	oblique/oblit	hyp	10
	Helicolithus type trackways	hyp	5
	Belocosmorhaphe aculeata	hyp	5
	Paleomeandron rude	hyp	5
	poorly preserved graphoglyptids	hyp	5
			20
8	*Spirophyton bicornis*	hyp	5
	Helminthopsis tenuis	hyp	5
	Oph annulata	hyp	10
	Paleomeandron rude	hyp	5
			25
9	*Oph annulata*	hyp	10
	Ch intricatus	hyp	5
	Lorenzinia plana	hyp	5
			10
	No bedding planes exposed between9 &10		
10	*Spiro bicornis*	hyp	10
	Oph annulata	ex	5
	Helminthopsis granulata	hyp	5
	Paleodictyon minimum	hyp	5
			20
11	*Paleodictyon majus*	hyp	10
	Paleodictyon strozzi	hyp	5
	Oph annulata	hyp	5
			10
	No bedding planes exposed between11&12		
12	*Oph annulata*	hyp	15
	Oph rudis	hyp	10
			25
13	*Oph annulata*	hyp	20
	Oph rudis	hyp	15
	Spiro bicornis	hyp	5
			35
14	*Strob glandifer*	hyp	5
	Oph annulata	hyp	10
			10
15	*Oph annulata*	hyp	15
			15
16	*Oph annulata*	hyp	10
			10
17	*Spiro bicornis*	hyp	25
	Strobilorhaphe clavatus	hyp	5
	Sc strozzi	hyp	10
	Spong slumbricoides	hyp	10
	Oscillorhaphe venezoalana	hyp	5
			55
18	*Spiro bicornis*	hyp	5
	Strob clavatus	hyp	5
	Helicolithus type traces	hyp	5
			10
19	*Paleomeandron robustum*	hyp	5
	Oscillorhaphe venezoala	hyp	5
	Oph isp	end	5
	Strob clavatus	hyp	5
	Arth. Striatus	hyp	10
			25
20	*Sc strozzi*	hyp	25
	Helminthopsis abeli	hyp	5
	Hormo annulata	hyp	5
	Oph annulata	hyp	10
	Th sewicus	hyp	5
	Arthroplycus isp	hyp	5
			50

Lobe-off axis

Lobe fringe

Ichnolog IS1 (Illurilla Senotta)			
Bed	Taxa	preservation	Bioturbation intensity
1	*Oph. Annulata*	hyp	10
			10
2	oblique burrows *(prob Oph. Annulata)* cross cutting flutes	hyp	5
	Th. Sewicus	hyp	5
			5
3	*Oph annulata*	hyp	15
	Paleomeandron robustum	hyp	5
	Th. Sewicus	hyp	5
	Unknown trace	hyp	5
	Oph. Annulata	ep	15
	Oph. Rudis	ep	10
			15
	No bedding planes exposed in thin bedded muddy package		
4	*Oph. Annulata*	hyp	15
	Oph. Annulata (upto 100% in places 2091)	ep	25
	Gordia marina 2091	ep	5
	Pl. Isp	ep	5
	Phycosiphon incertum	ep	15
			40
5	*Sc. Plana*	ep	10
	Ne. Irregularis		15
	Oph. Annulata		25
			40
	Oph. Annulata	hyp	10
	Hormo. Annulata	hyp	5
	Partially preserved graphoglyptids plus Helicolithus type (??) trace		40
			40
6	*Hormo. Annulata*	hyp	10
	Ne. Irregularis	ep	30
			30
	Ne. Irregularis occurs at similar levels on all silt topped beds		
7	*Oph. isp.*	ex	5
	Oph annulata	ep	25
	Oph rudis	ep	10
			80
	Beddding planes v. Poorly exposed between 7 and 8		
8	*Hormosiroidea annulata*	hyp	5
	Th. Sewicus	hyp	10
	Belorhaphe zigzack	hyp	10
	Th. Sewicus	ep	10
	Oph. Annulata	ep	10
	Ne. Irregularis	ep	25
			90
9	*Phycosiphon incertum*	ep	25
	Beaconites capranus	ep	5
			70
10	*Ne. Irregularis*		25
	Oph. Annulata	ep	25
			40
11	*Sc. Prisca*	ep	10
			10
12	*Oph. Rudis*	ep	20
	Ne. Irregularis	ep	25
	Sc. Prisca	ep	5
	Oph isp.	ep	5
			30
13	*Halopoa Annulata*	ep	10
			10
14	*Hormo. Annulata*	hyp	10
	Protopal. Incompositum	hyp	10
	Pal. Minimum	hyp	5
	Oph. Annulata	hyp	20
	Capodistria vettersi	hyp	10
	organised type? *Th sucvicus*	hyp	10
			40
15	*Oph. Annulata*	ep	25
	Desmograpton alternum	hyp	5
			30
16	*Spiro. Bicornis*	hyp	5
	Th. Isp.	hyp	5
	Oph. Annulata	hyp	10
	Helminthopsis annulata	hyp	5
	Oph. rudis	ep	25
			70
17	*Oph. Rudis*	ep	20
	Sc. Prisca	ep	5
	Strob glandifer	hyp	5
	Protovirgularia obliterata	ep	5
			25
18	*Oph annulata*	hyp	25
			50
19	*Saerichnites isp*	hyp	10
	Oph annulata	hyp	10
	Ha annulata	hyp	5
	Sc. Strozzi	hyp	5
			25
20	*Saerichnites canadiensis*	hyp	10
21	*Saerichnites isp*	hyp	15
	Oph annulata	hyp	20
	Th sewicus	hyp	10
			65

	Pasaia Harbour Ichnolog P1			
Env. Of deposition	Bed number	*Ichnogenera & species*	Position	Abundance (%) (Bold figure = BT index)
lobe fringe	1	*Oph annulata*	ep	15
				15
	2	*Oph annulata*	hyp	25
		Spiro bicornis	hyp	10
		Helminthopsis granulata	hyp	5
				70
	3	*Hormo annulata*	hyp	5
		Oph annulata	hyp	10
		Strob glandifer	hyp	5
		Paleomeandron rude	hyp	5
		Poorly preserved graphoglyptids	hyp	30
		Lorenzinia plana	hyp	5
				50
lobe off-axis	4	*Oph annulata*	hyp/end	15
				15
	5	*Oph annulata*	hyp/end	15
		Oph rudis	ep	25
				40
	7	*Oph annulata*	hyp	10
		Oph rudis	hyp	30
				40
	8	*Sc strozzi*	hyp	10
		Oph annulata	hyp/end	20
				30
	9	*Oph annulata*	end	10
				10
	10	*Oph annulata*	hyp/end	10
				10
Lobe -axis	11	*Oph annulata (inc vertical examples)*	ep	20
				20
	12	*Hormo annulata*	hyp/end	5
		Th sewicus	hyp	10
		Lorenzinia carpathica	hyp	10
		Fasichnium extentum	hyp	10
		Lorenzinia plana	hyp	5
		Acanthorhaphe incerta	hyp	5
				50

	San Sebastian Ichnolog SS1			
Environment of deposition	Bed number	*Ichnogenera & species*	Position	Abundance (%) (Bold figure = BT index)
Lobe off axis	1	*Oph annulata*	hyp	10
				10
	2	*Spong xbmbricolas*	ep	5
		Oph annulata	ep	10
				15
	3	*Oph annulata*	ep	20
				20
Fan fringe	4	*Sc strozzi*	hyp	10
		Lorenzinia type mounds	hyp	5
		Sc praeca	ep	5
				10
	5	*Oph annulata*	hyp	10
				10
	6	*Oph annulata*	hyp	5
				5
	7	*Hormo annulata*	hyp	5
		Cardioichnus planus	hyp	5
				5
	8	*Pilbeerleyensis*	hyp	5
		Large, poorly preserved burrow-Sc?	hyp	5
		Obliquebit	hyp	10
				10
	9	*Helminthopsis tenuis*	hyp	5
		Hormo annulata	hyp	5
		Lorenzinia type mounds	hyp	10
				10
	10	*Helminthopsis tenuis*	hyp	5
		Paleomeandron rude	hyp	5
		Hormithichnus or plug shape (or echinoid rest trace??)	hyp	10
		Th sewicus	hyp	5
		Lorenzinia poorly preserved or trackway?	hyp	20
		Oph annulata	hyp	5
				40
	11	*Oph annulata*	hyp	10
		Helminthopsis abeli	hyp	5
		Strob glandifer	hyp	5
		Bichordates-Sc. isp	hyp	5
				10
	12	*Lorenzinia carpathica*	hyp	5
		Oph annulata	hyp	10
		Cardioichnus planus	hyp	5
		Th sewicus	hyp	5
		Ha imbricata	hyp	10
				25
	13	*Cosmorhaphe lobata*	hyp	5
				5
Lobe off axis	14	*Oph annulata*	hyp	10
		Oph annulata	ep	10
				10
		No bedding planes between 14 -15		
	15	*Sc strozzi*	hyp	10
		Oph annulata	hyp	10
		Th sewicus	hyp	5
		Oph annulata	ep	10
				30
	16	*Sc strozzi*	hyp	10
		Helminthopsis tenuis	hyp	10
		Strob glandifer	hyp	5
		Sc praeca	ep	20
				30
	17	*?Lophoctenium ramosum*	ep	20
		Oph annulata	ep	10
				30
	18	*Oph rudis*	ep	10
				10
	19	*Helminthopsis granulata*	hyp	5
		Oph annulata	hyp	10
		Sc praeca	ep	20
		Spiro bicornis	hyp	5
				30
lobe fringe	20	*Oph annulata*	hyp	10
		Arth tenuis	hyp	10
				20
	21	*Paleomeandron rude*	hyp	5
		Urohelminthoida dertonensis	hyp	5
		Oph annulata	hyp	5
		No bedding planes between 21&22		**5**
	22	*Helminthopsis tenuis*	hyp	5
		Paleomeandron robustum	hyp	5
		Oph annulata	hyp	10
		Strob glandifer	hyp	5
				10
		Section of poor bedding plane exposure		
	23	*Oph annulata*	hyp	10
				10
	24	*Th sewicus*	hyp	5
		Oph annulata	hyp	5
				5
	25	*Oph annulata*	hyp	5
		Oph rudis	hyp	5
		Belorhaphe zickzac	hyp	5
		Helminthopsis tenuis	hyp	5
				5
	Ichnolog SS2-slightly further up the beach. Better representati			
	1	*Oph annulata*	hyp	10
				10
	2	*Oph annulata*	hyp	10
		Th sewicus	hyp	10
				20
	3	*Oph annulata*	hyp/ex	20
		Th sp	hyp/ex	10
				30
	4	*Th sp*	hyp	10
		Oph rudis	ex	10
		larger Oph rudis	ex	5
				20
	5	*Oph annulata*	hyp	10
				10
	6	*Oph rudis*	hyp	25
		Hormo annulata	hyp	5
		Oph annulata	hyp	10
				40
	7	*Oph rudis*	hyp/ex	25
				60
	8	*Oph rudis hyp*		25
				40
	9	*Oph rudis*	ex	25
		Glockenthinus alata	hyp	5
				30

	Ichnolog Ge1 Getaria road section.			
environment of deposition	Bed number	*Ichnogenera & species*	Position	Abundance (%) (Bold figure = BT index)
Lobe fringe	1	*Oph annulata*	ep	15
		Oph rudis	ep	15
				30
	2	*Oph annulata*	hyp	25
				60
	3	*Helminthopsis tenuis*	hyp	5
		Pl heverleyensis	hyp	10
		Paleomeandron elegans		5
				10
	4	*Lockeia/rest trace*	hyp	5
		Pl heverleyensis	hyp	10
		Helminthopsis tenuis	hyp	5
				20
	5	*Sc strozzi*	hyp	5
		Pal strozzi	hyp	5
		Desmograpton dertonensis	hyp	5
		Oph annulata	hyp	10
				25
	6	*Pal latum*	hyp	5
		Oph annulata	hyp	10
				10
	7	*Sc strozzi*	hyp	10
		Oph annulata	hyp	10
				20
	8	*Sc strozzi*	hyp	5
		Oph annulata	hyp	10
				15
	9	*Oph annulata*	hyp	15
		Cosmorhaphe lobata	hyp	25
		Spirorhaphe involuta	hyp	5
				60
	10	*Sc vertabralis*	ep	25
				80
	11	*Lorenzinia carpathica*	hyp	10
		Acanthorhaphe denticulata	hyp	5
		Megagrapton submontanum	hyp	5
		Helminthopsis abeli	hyp	10
				25
	12	*Ch intricatus*	ep	25
		Oph annulata	ep	15
				50
	13	*Lorenzinia carpathica*	hyp	10
		dense vertical burrows (?Skolithos or ?Arenicolites	ep	10
		Strob glandifer	hyp	5
		Spiro bicornis	hyp	5
				25
	14	*Helminth tenuis*	hyp	5
		Pal eodictyon gomezi	hyp	25
		Helminthopsis tenuis	hyp	5
		Megagrapton irregulare	hyp	20
		Paleomeandron rude	hyp	5
		Lorenzinia carpathica	hyp	10
		Oph rudis? Very pelleted	hyp	5
		Protovirgularia obliterata	hyp	15
				70
	15	*Oph annulata*	hyp	20
		Oph rudis	hyp	10
				30
	16	*Oph annulata*	hyp	25
	17	*Oph annulata*	hyp	25
		Lorenzinia plana	hyp	10
				40
	18	*Oph annulata*	hyp	25
		Thalassinoides suevicus	hyp	5
		Spirophycos biornis	hyp	5
				35
	19	*Sc strozzi*	hyp	10
		Lorenzinia carpathica	hyp	20
		Lorenzinia plana	hyp	10
		Megagrapton irregulare	hyp	25
				60
	20	*Helminthorhaphe flexuosa*	hyp	5
		Oph annulata	hyp	10
		Oph rudis	hyp	5
		Glockerichnus glockeri	hyp	5
		Lorenzinia plana in various preservational states		10
		Arthrophycos isp	hyp	15
				40

APPENDIX 4 RAW CLAY MINERAL DATA

Zumaia PETM section

Sample	Disordered illite	Kaolinite	Quartz	Calcite	Disordered illite (as % clay fraction)	Kaolinite (as % clay fraction)
Z1	43.1	0.1	24.3	32	99.77	0.23
Z2	62.2	1	37	0	98.42	1.58
Z3	56.6	0.1	43	0	99.82	0.18
Z4	39.4	23.4	32.3	4	62.74	37.26
Z5	33.6	17.8	29	16	65.37	34.63
Z6	39	12.6	29.9	14.7	75.58	24.42
Z7	43.2	21.6	34	0	66.67	33.33
Z8	36.3	15.9	30	17	69.54	30.46
Z9	32.5	14.1	26	16	69.74	30.26
Z10	39.8	14.8	29.1	15.5	72.89	27.11
Z11	33.4	14.5	31	17.8	69.73	30.27
Z12	22.2	0.1	51	26	99.55	0.45
Z13	27.4	0.1	33	38	99.64	0.36
Z14	6.4	0.1	13.2	80.4	98.46	1.54
Z15	4.2	0	12	83.8	100.00	0.00
Z16	11.1	0	15	75	100.00	0.00
Z17	34.1	0.1	29.5	36.4	99.71	0.29
Z18	25	0.1	27	48	99.60	0.40
Z19	27.1	0.1	25	48	99.63	0.37
Z20	20	1	21	56	95.24	4.76
Z21	28	0.1	21	51	99.64	0.36
Z22	10.5	0	20	69	100.00	0.00
Z23	4.9	0	13	82	100.00	0.00
Z24	1.3	0	15	84	100.00	0.00
Z25	10.6	0	13	76	100.00	0.00
Z26	6.2	0.1	10	84	98.41	1.59

Ermua PETM section

Sample	Quartz	Disordered illite	Calcite	Kaolinite	chlorite (chlinochlor)	Disordered illite (as % of total clay)	kaolinite (as % of total clay)	Chlorite (as % of total clay)
E9	38	51	1	6	5	82.26	9.68	8.06
E10	40	53	1	6	0	89.83	10.17	0.00
E11	44	49	2	5	0	90.74	9.26	0.00
E12	40	53	1	6	0	89.83	10.17	0.00
E13	38	46	3	7	6	77.97	11.86	10.17
E14	34	50	2	8	6	78.13	12.50	9.38
E15	34	50	2	8	7	76.92	12.31	10.77
E16	35	49	2	8	6	77.78	12.70	9.52
E17a	36	49	2	8	6	77.78	12.70	9.52
E17b	35	51	1	7	6	79.69	10.94	9.38
E17c	34	49	2	8	6	77.78	12.70	9.52
E18a	33	49	2	8	7	76.56	12.50	10.94
E18b	36	46	3	8	7	75.41	13.11	11.48
E19	33	50	2	8	7	76.92	12.31	10.77
E20	34	48	3	7	7	77.42	11.29	11.29
E21	38	47	3	7	6	78.33	11.67	10.00
E22a	42	48	4	0	6	88.89	0.00	11.11
E22b	37	47	2	7	6	78.33	11.67	10.00
E23a	40	53	2	0	6	89.83	0.00	10.17
E23b	39	49	2	6	5	81.67	10.00	8.33
E24	39	49	6	0	7	87.50	0.00	12.50
E25a	39	52	3	0	6	89.66	0.00	10.34
E25b	37	49	2	7	5	80.33	11.48	8.20
E25c	40	51	4	0	5	91.07	0.00	8.93
E26	34	47	5	8	6	77.05	13.11	9.84
E27	29	49	10	11	0	81.67	18.33	0.00
E28	25	36	38	0	0	100.00	0.00	0.00
E29	35	46	19	0	0	100.00	0.00	0.00
E30	31	44	22	0	4	91.67	0.00	8.33
E31	25	35	36	0	4	89.74	0.00	10.26
E32	23	34	39	0	4	89.47	0.00	10.53
E33	34	47	14	0	5	90.38	0.00	9.62
E34	27	41	28	0	4	91.11	0.00	8.89
E35	24	35	36	0	4	89.74	0.00	10.26
E36	29	36	31	0	4	90.00	0.00	10.00
E40	28	38	34	0	0	100.00	0.00	0.00
E41	17	0	83	0	0	0.00	0.00	0.00
E42	21	31	45	0	3	91.18	0.00	8.82
E43	28	38	33	0	0	100.00	0.00	0.00
E44	27	38	31	0	4	90.48	0.00	9.52
E45	25	32	44	0	0	100.00	0.00	0.00

Gorrondatxe EECO section

Sample	Disordered illite	Kaolinite	Quartz	Calcite	Disordered illite (as % clay fraction)	Kaolinite (as % clay fraction)
G1	40	12	33	16	76.92	23.08
G2	40	8	29	22	83.33	16.67
G3	41	7	26	25	85.42	14.58
G4	41	6	23	25	87.23	12.77
G5	44	11	27	18	80.00	20.00
G6	49	6	27	17	89.09	10.91
G7	33	0	17	50	100.00	0.00
G8	55	9	24	12	85.94	14.06
G9	55	7	23	14	88.71	11.29
G10	51	7	34	7	87.93	12.07
G11	47	6	34	11	88.68	11.32
G12	50	7	34	8	87.72	12.28
G13	61	11	19	9	84.72	15.28
G14	54	7	34	5	88.52	11.48
G15	59	9	28	3	86.76	13.24
G16	59	8	29	4	88.06	11.94
G17	54	8	31	6	87.10	12.90
G18	54	8	32	6	87.10	12.90
G19	55	7	33	4	88.71	11.29
G20	52	8	32	7	86.67	13.33
G21	54	8	26	10	87.10	12.90
G22	49	8	25	11	85.96	14.04
G23	51	8	32	8	86.44	13.56
G24	52	8	26	13	86.67	13.33
G25	55	6	30	8	90.16	9.84